PhD degree in Systems Medicine (curriculum in Molecular Oncology)

European School of Molecular Medicine (SEMM),

University of Milan

Settore disciplinare: BIO/11

The polo-like kinase Cdc5 and the Cdk-counteracting phosphatase Cdc14 play distinct roles in the resolution of DNA linkages in mitosis

Alice Finardi

European Institute of Oncology, Milan

Matricola n. 12076

Supervisor: Dr. Rosella Visintin

European Institute of Oncology, Milan

PhD coordinator: Prof. Saverio Minucci

Anno accademico 2020-2021

Table of contents

List of abbreviations

5-FOA	5-fluoroorotic acid
AID	auxin-inducible degron
APC/C	anaphase promoting complex or cyclosome
ARS	autonomously replicating sequence
as	analog-sensitive
ATP	adenosine triphosphate
BFB	breakage-fusion-bridge
bp	base pair
Cdk	cyclin-dependent kinase
ChIP	chromatin immunoprecipitation
CPC	chromosomal passenger complex
DAPI	4',6-diamidino-2-phenylindole
DNA	deoxyribonucleic acid
dsDNA	double stranded DNA
DSB	double strand break
EC	error correction
FEAR	Cdc14 early anaphase release
IF	indirect immunofluorescence
IP	immunoprecipitation
HU	hydroxyurea
HR	homologous recombination
JM	joint molecule
KT	kinetochore
LRI	late-replication intermediate
LTR	long terminal repeat
MAP	microtubules-associated protein
MCC	mitotic checkpoint complex
MEN	mitotic exit network
NEM	N-ethylmaleimide
O/N	over-night
PTM	post-translational modification

rDNA	ribosomal DNA
RENT	regulator of nucleolar silencing and telophase complex
SAC	spindle assembly checkpoint
SCI	sister chromatid intertwine
SDS	sodium dodecyl sulfate
SIM	SUMO-interacting motif
SMC	structural maintenance of chromosomes
SN	supernatant
SPB	spindle pole body
ssDNA	single stranded DNA
SSE	structure-selective endonuclease
STUbL	SUMO-targeting ubiquitin ligase
SUMO	small ubiquitin-like modifier
tRNA	transfer ribonucleic acid
ts	thermosensitive
UFB	ultra-fine DNA bridge
WT	wild-type

Figures index

Tables index

Abstract

During mitosis, the newly duplicated genetic material, organized in pairs of sister chromatids, is distributed between the daughter cells by the spindle machinery, in a process called chromosome segregation. Errors in this process can compromise genome integrity. Faithful chromosome segregation requires the removal of all sorts of cohesion between sister chromatids. Although the main contributors of sister chromatid cohesion are cohesin complexes, which are cleaved at anaphase onset, another source of cohesion is represented by DNA linkages, also called Sister Chromatid Intertwines (SCIs). These linkages comprise unreplicated segments, recombination intermediates, and double-stranded catenanes. If not properly removed, SCIs can break during cell division causing DNA damage and jeopardizing genome stability. Although most DNA linkages are removed before mitosis, their complete resolution only occurs concomitantly with chromosome segregation, in a process whose regulation is still poorly understood.

In this thesis, to investigate the mechanisms of SCI resolution during mitosis, we exploited the unique phenotype of *S. cerevisiae* cells lacking the activities of the polo-like kinase Cdc5 and the Cdk-counteracting phosphatase Cdc14. These cells arrest after cohesin cleavage, with short bipolar spindles and undivided nuclei, because impaired in spindle elongation. Evidence suggests that *cdc5 cdc14* cells are also impaired in sister chromatid separation, due to the presence of unresolved SCIs, and previous work in our laboratory revealed that these linkages mainly consist of DNA catenanes. Here, we found that both Cdc14 and Cdc5 contribute to the resolution of DNA linkages, with different functions. Cdc14 is mainly involved in nucleolar segregation and processing of recombination intermediates, while Cdc5 seems to act through a more generalized mechanism and promote the removal of DNA catenanes. At the molecular level, Cdc14 acts through its known substrate Yen1. On the other hand, we found that Cdc5 controls post-translational modification of the decatenating enzyme Top2 during mitosis, particularly conjugation with small ubiquitin-like modifier (SUMO) and, possibly, also phosphorylation. The polo-like kinase is known to inactivate the SUMO protease Ulp2 in metaphase, thus increasing SUMOylation of Ulp2 substrates, like Top2. Since the decatenation defect of *cdc5* cells correlates with a dysregulation of the SUMO pathway and this pathway is known to regulate sister chromatid cohesion, we speculate that the hyperactivation of Ulp2 may be the reason behind the

sister chromatid separation defect of *cdc5* cells. Taken together, our findings integrate the current knowledge of the mechanisms of sister chromatid separation and allow us to propose a model that foresees Cdc5 and Cdc14 coordinating cohesin cleavage and spindle elongation with the removal of DNA intertwines.

1. Introduction

1.1. Consequences of faulty mitosis

"Felix qui potuit rerum cognoscere causas
atque metus omnis et inexorabile fatum
subiecit pedibus."

Virgilio, Georgica

In order to multiply and form tissues and organs, cells must generate copies of themselves. The series of events that lead to the division of a cell into two identical daughters is termed the cell cycle and it includes the duplication of the genetic material, packaged in chromosomes, and its correct repartition between the daughter cells, which is carried out by the mitotic spindle. Genome duplication occurs during S (Synthesis) phase, while the process through which the newly duplicated genetic material is distributed among the daughter cells is called mitosis.

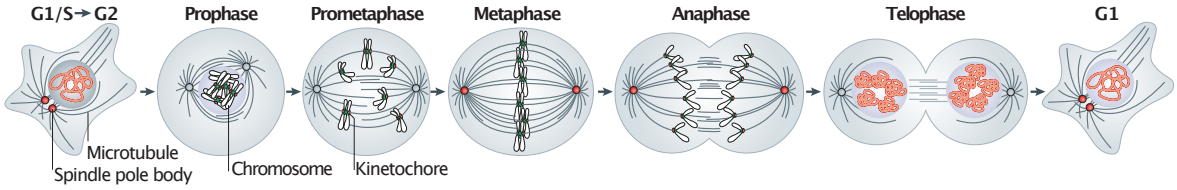

Figure 1.1. Overview of mitosis
Modified from (Sivakumar and Gorbsky, 2015).

Despite being a continuous process, mitosis is conventionally divided into prophase, prometaphase, metaphase, anaphase, and telophase (**Figure 1.1**). During prophase, chromosome condensation occurs and the microtubule-organizing centers, called spindle pole bodies (SPBs) in budding yeast and centrosomes in higher eukaryotes, move to the opposite poles of the cell and begin to assemble the mitotic spindle. During prometaphase, which is only observed in vertebrate cells, the nuclear envelope breaks down and the spindle microtubules start to contact the chromosomes. Instead, in the budding yeast *Saccharomyces cerevisiae*, the model organism used in this thesis, the nuclear envelope remains intact throughout the mitosis, SPBs are embedded in the nuclear membrane and the spindle assembles inside the nucleus. In metaphase, all chromosomes are attached to the mitotic spindle with bipolar orientation (**Figure 1.2**), meaning that each sister of a pair is in contact with microtubules emanating from opposite spindle poles. After this phase is complete, anaphase begins, sister chromatids separate and move towards the opposite

poles of the cell by spindle elongation. Finally, during telophase, the spindle disassembles, chromosomes start to decondense and, in vertebrate cells, the nuclear envelope reassembles around the two separated nuclear masses. The last step of cell division is the physical separation of mother and daughter cells through a process termed cytokinesis.

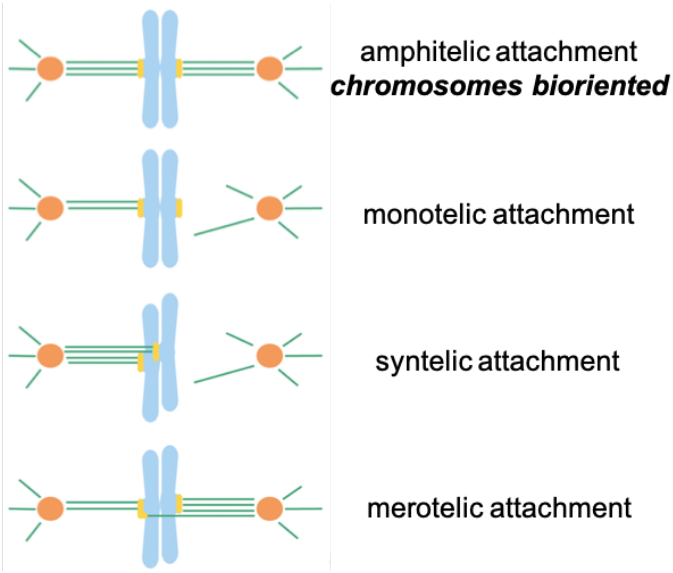

Figure 1.2. Types of kinetochore-microtubule attachments
Modified from (Kelly and Funabiki, 2009).

Errors in mitosis can cause an incorrect transmission of the genetic material to the daughter cells and jeopardize genome integrity with disastrous consequences (Ganem and Pellman, 2012). Genomic instability is associated with many diseases and is an important driver of tumorigenesis (Negrini et al., 2010; Sansregret and Swanton, 2017).

Faulty mitosis can threaten genome stability in many ways. For example, if one or more chromosomes are incorrectly segregated, daughter cells will inherit an abnormal set of chromosomes, leading to a condition known as aneuploidy. Notably, the fact that an imbalanced karyotype is a common feature of cancer cells was first observed more than a hundred years ago (Boveri, 2008), and we now know that about 90% of solid tumors are aneuploid (Taylor et al., 2018). Alternatively, lagging chromosomes can be trapped and damaged at the cleavage site during cytokinesis, or they can fail to be incorporated into the nucleus, giving rise to micronuclei (Santaguida and Amon, 2015). Another source of genome instability in mitosis is the failure to resolve DNA entanglements between sister chromatids, also called sister chromatid intertwines (SCIs). These structures normally arise as a consequence of DNA replication/repair and must be completely removed to allow the separation of the sister chromatids and faithful chromosome segregation. Unresolved DNA

linkages can hinder cell division, leading to tetraploidy, or break during cytokinesis, driving genome instability in the next cell cycle (Finardi et al., 2020).

1.2. Post-translational modifications drive mitotic progression

> *"Does the existence of such order imply the existence of control mechanisms that enforce order? […] If, for example, replicated chromosomes are essential substrates for mitosis, then the dependence is due to substrate-product order; alternatively, if the dependence is due to an inhibitor of mitosis produced in response to unreplicated chromosomes, then we would say the dependence is due to control."*
>
> *(Hartwell and Weinert, 1989)*

To avoid errors, mitotic events must be tightly regulated in time and space. The correct order of succession of events is ensured by mitotic checkpoints, which allow progression to the next cell cycle phase only upon completion of the previous one (**Figure 1.3**). If certain requirements are not satisfied, checkpoints halt the cell cycle to provide additional time to complete the unfinished tasks. To enable the coordination of mitotic processes with the detection and resolution of the problems, a rapid response is essential. Therefore, cells rely on post-translational modifications (PTMs) to control the activity of key proteins in a fast, precise, and reversible manner. Indeed, transcription is largely inhibited during mitosis (Palozola et al., 2017).

PTMs include phosphorylation, ubiquitination, and the more recently described conjugation with small ubiquitin-like modifier (SUMO). Chemical modifications, such as phosphorylation, occur in a single step, while conjugation with small proteins, including ubiquitination and SUMOylation, requires an enzymatic cascade composed of an activating enzyme, a conjugating enzyme, and a ligase, referred to as E1, E2, and E3, respectively. Importantly, ubiquitin-like modifications can target themselves, thus forming a chain of ubiquitin-like proteins. During mitosis, PTMs act together and influence each other by crosstalk mechanisms, thus adding to the complexity of the system (Cuijpers and Vertegaal, 2018).

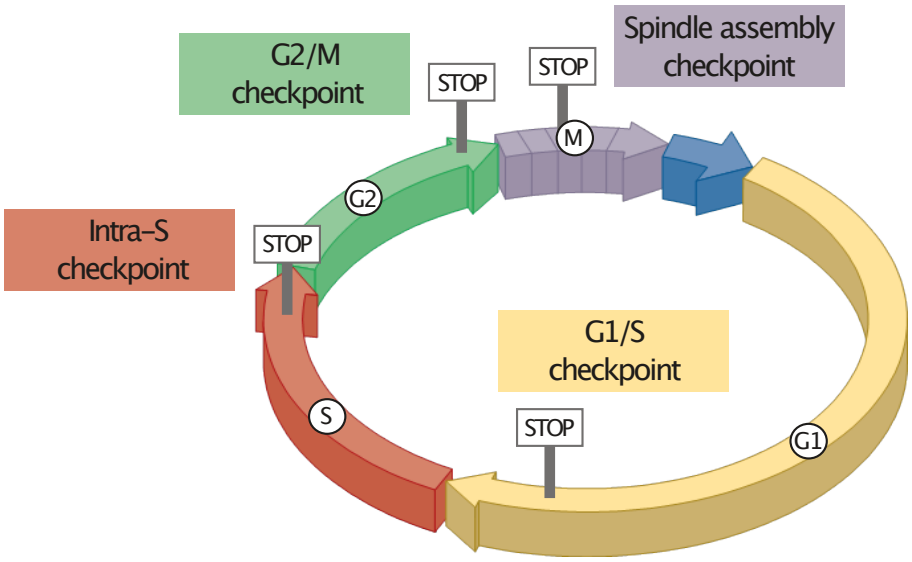

Figure 1.3. Cell cycle checkpoints
Checkpoints halt the cell cycle at specific stages and provide additional time for the completion of unfinished tasks, thus ensuring the correct progression of events.

1.2.1. Ubiquitination by the APC/C

One of the main actors in control of mitotic progression is the Anaphase Promoting Complex or Cyclosome (APC/C), a large ubiquitin-ligase that controls the metaphase-to-anaphase transition, mitotic exit, and the subsequent G1 (Peters, 2006; Pines, 2011; Sudakin et al., 1995). The APC/C performs its numerous functions by catalyzing the formation of polyubiquitin chains on its targets. In turn, polyubiquitination is a signal for the degradation of these targets by the 26S proteasome.

The substrate specificity of the APC/C is regulated through its association with the regulatory subunits Cdc20 or Cdh1, which depends on the cell-cycle stage and is controlled through multiple mechanisms (**Figure 1.4**) (Sivakumar and Gorbsky, 2015). At the metaphase-to-anaphase transition, Cdc20 binds the complex and directs the ubiquitination and degradation of the securin Pds1, an inhibitor of cohesin cleavage (Shirayama et al., 1998; Visintin et al., 1997). In addition, the APC/C^{Cdc20} degrades the S-phase cyclins and begins the degradation of the mitotic cyclins. Therefore, APC/C^{Cdc20} coordinates chromosome separation with the inactivation of S-phase and mitotic cyclin-dependent kinases (Cdks), collectively called Clb-Cdks. In late anaphase, Cdh1 takes the place of Cdc20 as an APC/C activator and drives the complete degradation of the mitotic cyclins, thus keeping Clb-Cdks inactive until the next S phase (Kapanidou et al., 2017; Sullivan and

Morgan, 2007). The late substrates of APC/C^{Cdh1} also include the polo-like and Aurora kinases (Sivakumar and Gorbsky, 2015).

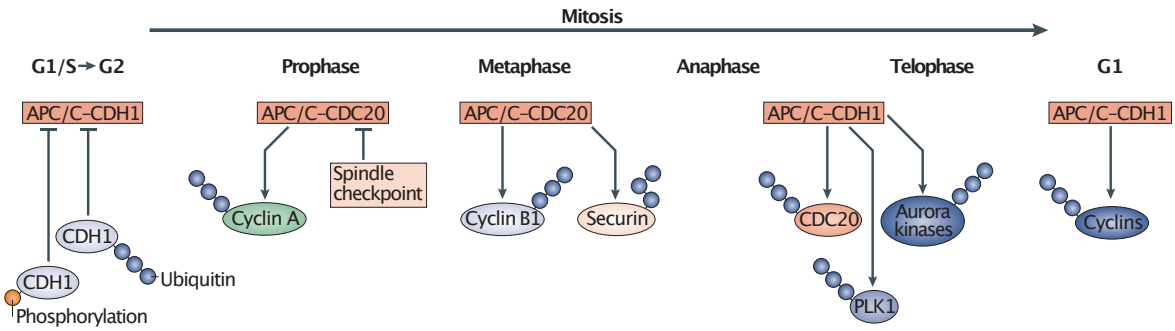

Figure 1.4. Cell cycle-dependent degradation of APC/C targets
APC/C^{Cdh1} is active after anaphase onset, during mitotic exit, and in G1 phase, whereas APC/C^{Cdc20} is active during early and mid-mitosis. Before anaphase onset, the degradation of late APC/C^{Cdc20} substrates is inhibited by the spindle assembly checkpoint. Modified from (Sivakumar and Gorbsky, 2015).

1.2.2. Phosphorylation

Cyclin-dependent kinases

Master regulators of cell cycle progression are the cyclin-dependent kinases, a class of kinases that are activated through the association with subunits named cyclins (**Figure 1.5**). The expression of each type of cyclins (G1, S phase, and mitotic cyclins) at the corresponding cell cycle stage determines the formation of different Cdk-cyclin complexes, each with certain characteristics in terms of substrate specificity (Peeper et al., 1993).

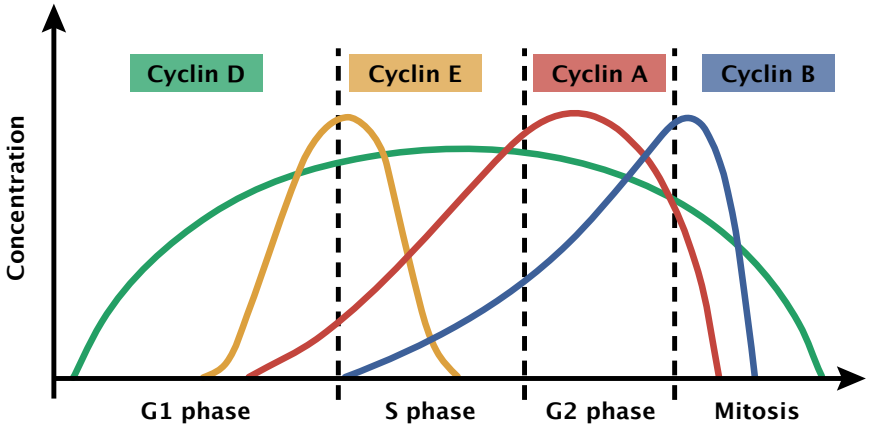

Figure 1.5. Expression of cyclins through the vertebrate cell cycle

While several Cdks are present in higher eukaryotes, budding yeast has only one, Cdc28, meaning that substrate specificity is exclusively determined by the cyclin subunit. By

targeting for phosphorylation different substrates, this system ensures the correct progression of events throughout the cell cycle (Bloom and Cross, 2007).

In *S. cerevisiae*, the mitotic B-type cyclins are Clb1, Clb2, Clb3, and Clb4, among which Clb2 plays the main role. These cyclins promote early mitotic events, such as chromosome condensation and spindle assembly, and control mitotic progression up to metaphase. After anaphase onset, chromosome segregation and mitotic exit are driven by the destruction of mitotic cyclins, which leads to a decrease in Cdk activity (Sullivan and Morgan, 2007). In addition to Cdk inactivation, exit from mitosis also requires the reversion of Cdk-mediated phosphorylations, which, in budding yeast, is carried out by the phosphatase Cdc14 (De Wulf et al., 2009). This way, conditions are reset and the cell is ready to enter a new cell cycle.

The Cdk-counteracting phosphatase Cdc14

Cdc14 plays a pivotal role during anaphase and mitotic exit. In addition to direct dephosphorylation of Cdk substrates, this phosphatase contributes to inactivate mitotic-Cdks by promoting the destruction of mitotic cyclins and accumulation of the mitotic-Cdk inhibitor Sic1 (Jaspersen et al., 1998; Visintin et al., 1998). Indeed, *cdc14* mutant cells arrest in anaphase with high mitotic-Cdk activity (Visintin et al., 1998). Moreover, Cdc14 participates in several early mitotic events, including segregation of certain genomic regions, namely telomeres and the nucleolus, and spindle assembly and stabilization (D'Amours et al., 2004; Khmelinskii et al., 2007; Stegmeier and Amon, 2004; Sullivan et al., 2004; Torres-Rosell et al., 2004).

The activity of Cdc14 is modulated through cell cycle-dependent changes in its localization and association with its inhibitor Cfi1 (also called Net1). Until metaphase, Cfi1, which is located in the nucleolus, binds the phosphatase, inactivates it, and sequesters it to this subnuclear compartment. At anaphase onset, Cfi1 dissociates and the active phosphatase is free to spread into the nucleus and cytoplasm (Shou et al., 1999; Visintin et al., 1999). The interaction between Cdc14 and Cfi1 is controlled through their phosphorylation status. Phosphorylation of both proteins triggers their dissociation, thus activating the phosphatase (Azzam et al., 2004; Manzoni et al., 2010; Visintin et al., 2003).

Cdc14 activation and relocalization occurs gradually and is controlled by two pathways, the Cdc14 Fourteen Early Anaphase Release (FEAR) and the Mitotic Exit Network (MEN) (**Figure 1.6**). Cdc14 is released first within the nucleus, by the FEAR, and subsequently into the whole cytoplasm, by the MEN (Shou et al., 1999; Stegmeier et al., 2002; Visintin et al., 1999). The MEN pathway is essential for mitosis, while the FEAR is dispensable, although FEAR-activated Cdc14 is required for the correct execution of many early anaphase events (D'Amours et al., 2004; Jaspersen et al., 1998; Khmelinskii et al., 2007; Ross and Cohen-Fix, 2004; Sullivan et al., 2004; Torres-Rosell et al., 2004; Wang et al., 2004).

Besides Cdc14, other phosphatases with important roles in mitosis are protein phosphatase type 2A (PP2A) and protein phosphatase type 1 (PP1). Both of these phosphatases counteract the activity of Aurora B at kinetochores once bipolar orientation is achieved (Espert et al., 2014). Moreover, PP2A prevents Cdc14 release before anaphase onset (Queralt et al., 2006).

The FEAR network

The FEAR network (**Figure 1.6**) comprises the separase Esp1, the kinases Cdc5 and Clb2-Cdk1, the phosphatase PP2A and its regulatory subunit Cdc55, the Cdc55 interacting proteins Zds1 and Zds2, the kinetochore protein Slk19 and the nucleolar proteins Spo12/Bns1 and Fob1, which is involved in blocking the replication fork at dedicated ribosomal DNA (rDNA) sites (Stegmeier et al., 2002; Stegmeier and Amon, 2004).

This pathway is activated at anaphase onset, concomitantly with the activation of the separase Esp1. Esp1 associates with the kinetochore protein Slk19 and the complex inhibits the phosphatase PP2A-Cdc55 (Queralt et al., 2006; Wang and Ng, 2006; Yellman and Burke, 2006). This event allows phosphorylation of Cfi1 by Clb2-Cdk, freeing Cdc14 from the binding of its inhibitor (Azzam et al., 2004). Furthermore, Spo12 participates in FEAR activation by counteracting Fob1, which stabilizes the Cdc14-Cfi1 complex (Stegmeier et al., 2002; Tomson et al., 2009). Finally, Cdc5 directly phosphorylates Cdc14, thus promoting its release (Shou et al., 2002; Visintin et al., 2003; Yoshida and Toh-e, 2002).

Evidence indicates that the FEAR network is organized in three parallel branches, represented by Esp1, Spo12, and Cdc5 (Roccuzzo et al., 2015). The details about the organization of this pathway and the role of single components are still largely unknown.

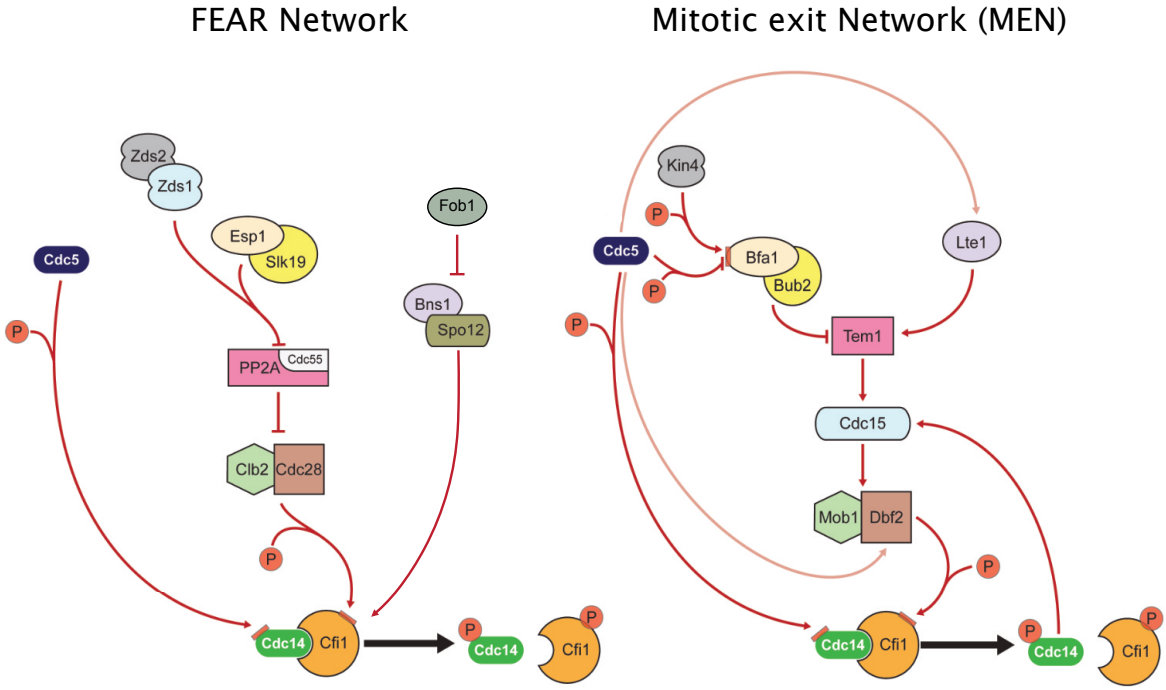

Figure 1.6. FEAR network and MEN
Adapted from (Roccuzzo, 2013).

The MEN

The MEN (**Figure 1.6**) is a Ras-like GTPase signal transduction pathway that promotes exit from mitosis (Jaspersen et al., 1998; Sullivan and Morgan, 2007). It comprises the GTPase Tem1, the GTPase activating protein complex Bub2-Bfa1, the guanine-nucleotide exchanging factor Lte1, the scaffold protein Nud1 and the kinases Cdc5, Cdc15, and Dbf2-Mob1. Tem1 is activated by Lte1 and inhibited by Bub2-Bfa1. At anaphase onset, Cdc5 inhibits Bub2-Bfa1, thus leading to MEN activation (Hu et al., 2001). In addition, FEAR-released Cdc14 contributes to MEN activation by reversing the inhibitory phosphorylation of Cdc15 and Dbf2-Mob1 (Jaspersen and Morgan, 2000; König et al., 2010; Xu et al., 2000). Once MEN signaling is turned on, Tem1 activates Cdc15, which activates Dbf2, which in turn promotes Cdc14 release through phosphorylation of Cfi1 and, likely, of Cdc14 itself (Mah et al., 2001; Manzoni et al., 2010; Mohl et al., 2009).

The action of MEN depends on the localization of its components relative to each other. Bub2-Bfa1 and Tem1 both localize on the SPB destined to the daughter cell, while the MEN activator Lte1 is placed on the bud cortex (Bardin et al., 2000; Fraschini et al., 2006). Therefore, Tem1 can only become active when the daughter SPB enters the bud. Moreover, the kinase Kin4, which activates Bub2-Bfa2, is specifically located on the mother cell cortex. Thus, Kin4 contributes to shutting MEN signaling off when the daughter SPB is in the

mother cell (D'Aquino et al., 2005). These mechanisms allow exit from mitosis only if the correct spindle pole has entered the daughter cell, thus ensuring the right spindle orientation (Piatti et al., 2006).

Polo-like kinase

Besides Cdks, two other classes of kinases regulate mitotic progression, the polo-like kinases and the Aurora kinases, which in *S. cerevisiae* are Cdc5 and Ipl1, respectively (Chan and Botstein, 1993; Francisco et al., 1994; Kitada et al., 1993).

The first polo-like kinase was described in *Drosophila* cells, where it was shown that it is required for the correct positioning of chromosomes along the metaphase plate (Sunkel and Glover, 1988). Since then, the list of mitotic functions attributed to polo-like kinases has kept growing. Cdc5 promotes timely entry into mitosis (Asano et al., 2005; Darieva et al., 2006; Sakchaisri et al., 2004), chromosome condensation (St-Pierre et al., 2009), cohesin cleavage and removal (Gabriela Alexandru et al., 2001; Mishra et al., 2016), spindle elongation (Park et al., 2008; Roccuzzo et al., 2015) and cytokinesis (Song and Lee, 2001; Yoshida et al., 2006). Furthermore, being a shared component of the FEAR and MEN pathways, Cdc5 is required to activate the phosphatase Cdc14 during anaphase (Hu et al., 2001; Pereira et al., 2002; Stegmeier et al., 2002).

The activity and substrate specificity of this kinase is controlled at multiple levels. First of all, the amount of Cdc5 is cell cycle-regulated. The protein starts to accumulate in S phase, it reaches its maximum levels in anaphase and is rapidly degraded upon entry in the next G1 through the APC/C^{Cdh1} (Charles et al., 1998; Cheng et al., 1998; Shirayama et al., 1998). Secondly, substrate specificity is controlled through "priming" phosphorylation of its targets (Elia et al., 2003). Cdc5 recognizes substrates that have undergone previous phosphorylation by other kinases, such as Cdks. Thirdly, Cdc5 is controlled by changes in its localization. In S phase, when this kinase starts to be synthesized, Cdc5 accumulates in the nucleoplasm (Botchkarev et al., 2014; Charles et al., 1998; Cheng et al., 1998; Shirayama et al., 1998; Song et al., 2000). Moreover, Cdc5 associates with the SPB before its duplication, while, after duplication, it localizes at the nuclear surface of both SPBs (Botchkarev et al., 2017, 2014; Lee et al., 2005). In late anaphase, the kinase is released in a Cdc14-dependent fashion into the cytoplasm, where it associates with the outer plaque of the SPB destined

to the daughter cell (Botchkarev et al., 2017, 2014). Finally, Cdc5 localizes at the bud neck in anaphase (Botchkarev et al., 2014; Sakchaisri et al., 2004; Song et al., 2000).

Aurora B kinase

Aurora B is the enzymatic subunit of the Chromosome Passenger Complex (CPC), which also includes INCENP, survivin, and borealin (Sli15, Bir1, and Nbl1 in *S. cerevisiae*, respectively). The CPC changes localization during mitosis, affecting the substrate specificity of Aurora B (van der Horst and Lens, 2014). The complex is recruited at centromeres in early mitosis and moves to the spindle midzone upon anaphase onset. Yeast *IPL1* was the first gene belonging to the family of Aurora kinases to be described. Its name stands for increase in ploidy-1, which is the phenotype associated with its mutation (Chan and Botstein, 1993). Indeed, Aurora B is required to establish the bipolar attachment of chromatids to the metaphase spindle (**Figure 1.2**) and, therefore, prevent chromosome segregation errors (Krenn and Musacchio, 2015). Furthermore, Ipl1 promotes chromosome condensation in anaphase (Lavoie, Hogan and Koshland, 2004) and spindle disassembly at the end of mitosis (Buvelot et al., 2003).

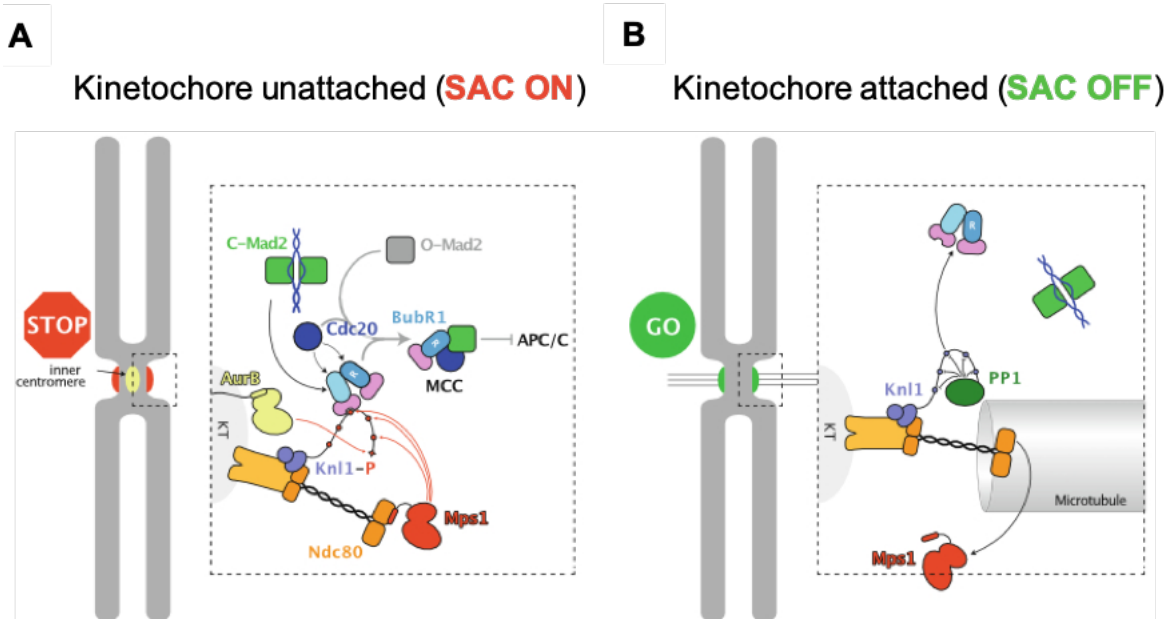

Figure 1.7. The spindle assembly checkpoint
*(**A**) Mps1 is recruited to Ndc80 at unattached kinetochores and phosphorylates Knl1. Aurora B, tethered at the inner centromere, also phosphorylates Knl1 and inhibits PP1 binding. Phosphorylated Knl1 recruits MCC components. O-Mad2 is converted to C-Mad2 and the MCC assembles. The MCC inhibits the APC/C, blocking anaphase onset. (**B**) Upon kinetochore-microtubule attachment, Mps1 is lost, Knl1 phosphorylation is reversed by PP1, and the MCC stops being assembled. Modified from (Corbett, 2017).*

Two mechanisms control the correct chromosome-microtubule attachment during mitosis and Aurora B plays a central role in both of them (Krenn and Musacchio, 2015). These mechanisms are the Spindle Assembly Checkpoint (SAC) and the Error Correction (EC) checkpoint (**Figures 1.7 and 1.8**). The SAC diffuses a cellular "wait anaphase" signal until all chromosomes are attached to the spindle (**Figure 1.7**), while the EC acts locally to stabilize the correct chromosome-microtubule attachments and destabilize the erroneous ones, namely syntelic or merotelic attachments (**Figure 1.8**). Together, these checkpoints halt the cell cycle in metaphase until all the chromosomes are correctly attached to the spindle, that is with bipolar orientation (Corbett, 2017; Krenn and Musacchio, 2015; Musacchio, 2015).

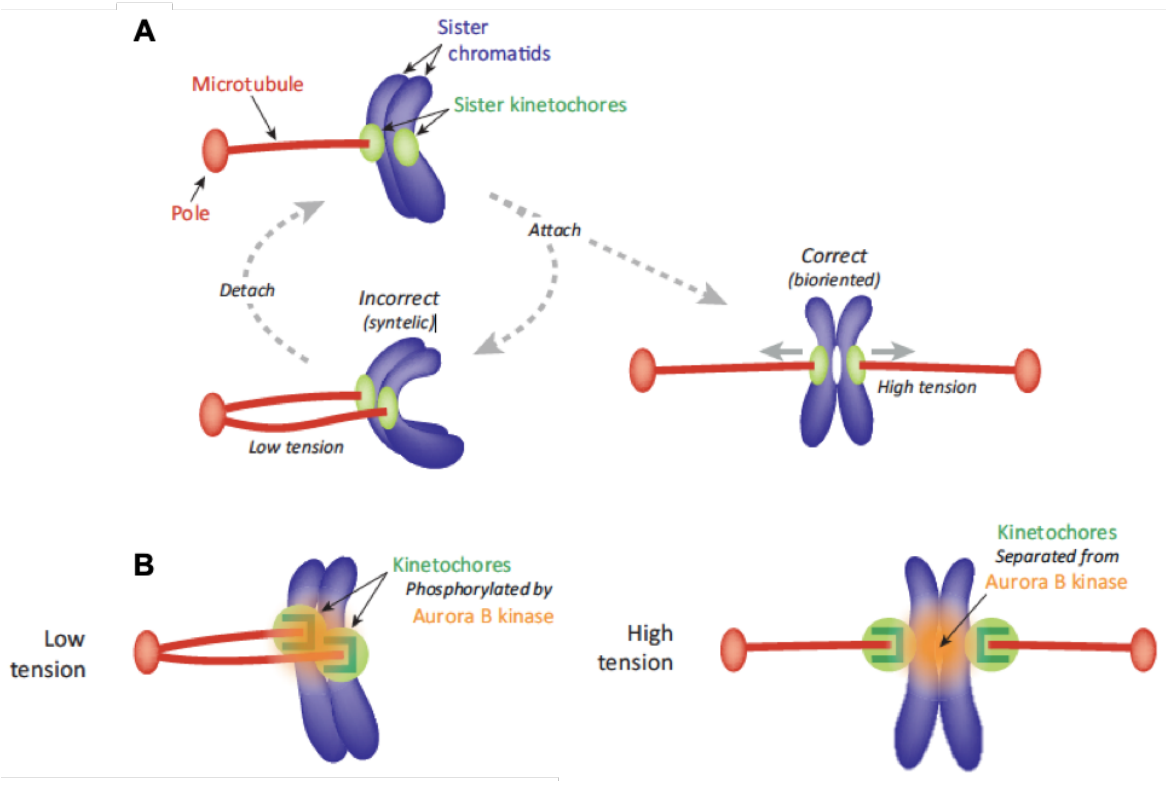

Figure 1.8. Tension-dependent error correction by Aurora B
Modified from (Sarangapani and Asbury, 2014).

Chromosome-microtubule attachments are mediated by large and complex protein assemblies called kinetochores, which assemble around the centromeres. Unattached kinetochores assemble the Mitotic Checkpoint Complex (MCC), which represents the core of SAC signaling and is composed of the proteins Mad2, Cdc20, and BubR1 (**Figure 1.7**). In some organisms, such as humans, BubR1 forms a constitutive dimer with Bub3. Mad2 can be found in an inactive open (O-Mad2) or active closed (C-Mad2) conformation (Luo et al., 2004, 2000). At the kinetochores, O-Mad2 is converted into C-Mad2, which binds and

sequesters Cdc20, thereby inhibiting the APC/C (De Antoni et al., 2005; Hwang et al., 1998; Nezi et al., 2006). BubR1 acts synergistically with Mad2 and stabilizes the Mad2-Cdc20 complex (Sczaniecka et al., 2008; Tang et al., 2001; Tipton et al., 2011). The MCC inhibits APC/C also by directly binding the complex (Alfieri et al., 2016; Izawa and Pines, 2015).

SAC signaling is based on a delicate kinase-phosphatase balance at the kinetochore, with the phosphatases PP1 and PP2A counteracting the kinases Aurora B and Mps1 (Benzi and Piatti, 2020; Krenn and Musacchio, 2015). In the absence of microtubule attachment, Mps1 is recruited to the outer kinetochore and phosphorylates the kinetochore protein Knl1, also known as Spc105 in budding yeast (London et al., 2012; Shepperd et al., 2012; Yamagishi et al., 2012). In turn, phosphorylated Knl1 recruits MCC components and triggers the assembly of the complex (Primorac et al., 2013; Yamagishi et al., 2012). Knl1 is phosphorylated also by Aurora B, which inhibits its interaction with the phosphatase PP1 (Liu et al., 2010). When a kinetochore is attached to the spindle, Mps1 and Aurora B activity is downregulated and the kinase-phosphatase balance is altered (Corbett, 2017; Krenn and Musacchio, 2015). In these conditions, Mps1 and Aurora B phosphorylation are reversed by the phosphatases PP2A and PP1 and the MCC stops being assembled, hence silencing the checkpoint (Espert et al., 2014; Liu et al., 2010; London et al., 2012). According to the current model, the tension generated at the attached kinetochores regulates Aurora B through spatial separation from its substrates (**Figure 1.8**) (Biggins and Murray, 2001; Liu et al., 2009; Tanaka et al., 2002). When a chromosome is bioriented, the kinetochore is under high tension and Aurora B, located at the inner kinetochore, can no longer phosphorylate the substrates placed at the outer kinetochore. Therefore, the chromosome-microtubule attachment is stabilized and the checkpoint is satisfied.

1.2.3. SUMOylation

The SUMO pathway

SUMO is a small protein that, similarly to ubiquitin, can be attached to lysine residues of target substrates. It can be attached to one lysine (monoSUMOylation), multiple lysines (multiSUMOylation), or form a chain (polySUMOylation). Like ubiquitination, the conjugation process consists of three consecutive steps carried out by dedicated E1, E2, and E3 enzymes (**Figure 1.9**). All SUMO conjugation depends on the same E1 and E2 enzymes, while different E3 ligases confer some level of substrate-specificity. On the other

hand, the removal of SUMO from target proteins is catalyzed by SUMO peptidases, which are also involved in SUMO maturation through the proteolytic cleavage of a precursor. SUMOylation may regulate protein activity or association with other proteins, which often occurs through SUMO-interacting motifs (SIMs). SUMO-SIM interaction can drive the formation of large protein assemblies or the recruitment of SUMOylated proteins to certain structures. PolySUMO chains can also interact with the SIMs of SUMO-Targeting Ubiquitin Ligase (STUbLs), thus leading to ubiquitination and proteasomal degradation of the SUMO substrates (**Figure 1.9**).

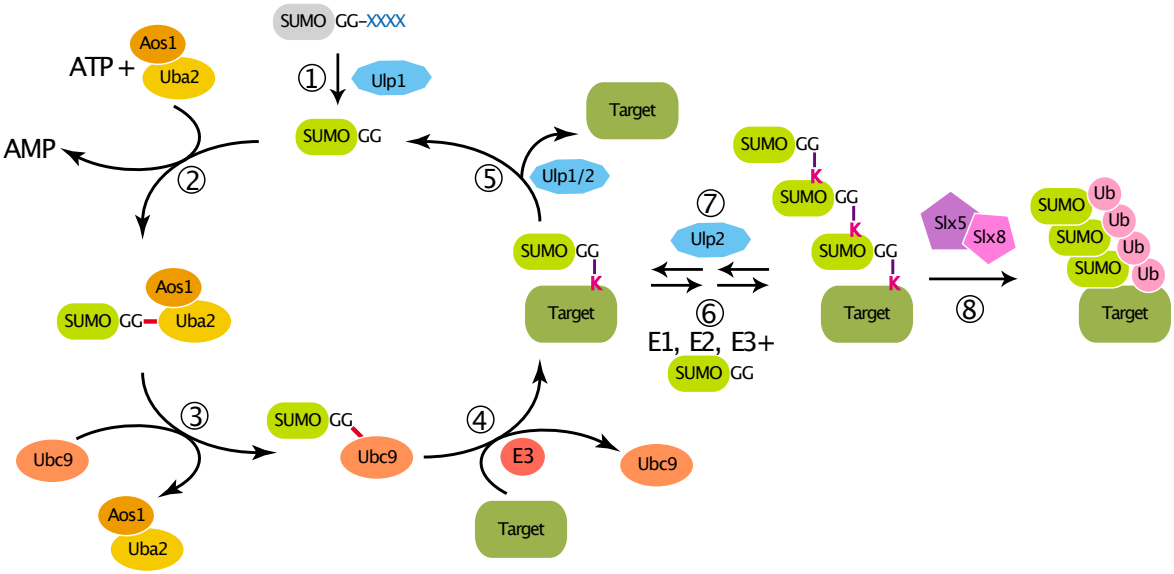

Figure 1.9. The SUMO pathway
Mature SUMO is produced through proteolytic cleavage of a precursor, catalyzed by Ulp1 (Step 1). The E1 enzyme Aos1-Uba2 catalyzes the ATP-dependent activation of SUMO (Step 2). Next, SUMO is transferred to the E2 conjugating enzyme, Ubc9 (Step 3). E3 ligases form a bond between SUMO and a lysine within the target protein (Step 4). SUMO can be removed from the target by SUMO proteases (Step 5). Consecutive steps of conjugation can create SUMO chains on the target protein (Step 6). SUMO proteases, particularly Ulp2, can shorten the chain by removing SUMO moieties (Step 7). PolySUMOylated proteins can be ubiquitinated by the Slx5/8 complex, thus triggering their proteasomal degradation (Step 8). Modified from (Dasso, 2008).

The SUMO pathway is highly conserved, but its complexity and redundancy are lower in *S. cerevisiae* compared to humans. While at least three forms of SUMO are conjugated in humans (SUMO-1, SUMO-2, and SUMO-3), yeast has only one SUMO protein, called Smt3, which is the homolog of SUMO-1. Moreover, this organism has only four SUMO ligases (Siz1, Siz2, Mms21, and Zip3) and two SUMO proteases (Ulp1 and Ulp2). Finally, the best characterized yeast STUbL is the Slx5-Slx8 heterodimer, although Uls1 may also play a role (Chang et al., 2021).

The two paralogues Siz1 and Siz2 are responsible for the bulk of SUMOylation during mitosis (Johnson and Gupta, 2001; Takahashi et al., 2001), while Zip3 and Mms21 play their main functions in meiosis and DNA repair, respectively (Ampatzidou et al., 2006; Andrews et al., 2005; Branzei et al., 2006; Cheng et al., 2006). For what concerns SUMO proteases (**Figure 1.9**), Ulp1 is responsible for SUMO maturation and shows broad substrate specificity *in vitro* (Li and Hochstrasser, 2003, 1999). On the other hand, Ulp2 is particularly efficient in the shortening of polySUMO chains, although it can also cut the bond between SUMO and target substrates (Bylebyl et al., 2003; Li and Hochstrasser, 2000). *In vivo,* the two proteases have different targets, as demonstrated by the fact that mutations of either *ULP1* or *ULP2* are associated with distinct phenotypes and with the accumulation of different sets of SUMO-conjugates (Li and Hochstrasser, 2000).

Roles of SUMO in mitosis

In the past, most studies about PTMs in mitosis focused on ubiquitination and phosphorylation, while the role of SUMO is less clear. Early studies in *S. cerevisiae* pointed to an essential role of this PTM in G2/M, as indicated by the fact that blocking SUMOylation arrests cells in this cell cycle stage (Li and Hochstrasser, 1999; W. Seufert et al., 1995). Since then, SUMO has been implicated in many mitotic processes. Consistently, mutations in the SUMO pathway often result in genomic instability (Li and Hochstrasser, 2000; Takahashi et al., 2006; van de Pasch et al., 2013).

In *S. cerevisiae*, the first targets of SUMOylation to be identified were the septins, cytoskeletal proteins that localize to the bud neck and are involved in cytokinesis. Septins are extensively SUMOylated before anaphase onset (Johnson and Blobel, 1999; Takahashi et al., 1999). The biological significance of this modification remains unclear in yeast, because mutating the SUMO-accepting sites of septins does not greatly impair cell division (Johnson and Blobel, 1999). Conversely, in human cells, expression of non-SUMOylatable septin variants causes defects in cytokinesis (Ribet et al., 2017).

SUMO has also been implicated in sister chromatid cohesion. An early study found that cells lacking the SUMO protease Ulp2 precociously dissociate sister centromeres during a metaphase arrest (Bachant et al., 2002). More recently, it was reported that Ulp2 is essential to establish the correct geometry of pericentromeric chromatin, which in turn is required to resist the pulling force of the spindle and ensure chromosome biorientation

(Stephens et al., 2015). One of the Ulp2 substrates involved in sister chromatid cohesion is the decatenating enzyme, Topoisomerase II. SUMOylation of Top2 is increased in absence of Ulp2 and the cohesion defect and temperature sensitivity of *ulp2* mutants can be partially rescued by overexpression of the topoisomerase or by expression of a non-SUMOylatable Top2 allele (Bachant et al., 2002).

Structural Maintenance of Chromosome (SMC) complexes, namely cohesin, condensin, and the Smc5/6 complex, are all substrates of SUMO (Mukhopadhyay and Dasso, 2017). Cohesin is SUMOylated upon loading onto DNA and this modification is required to correctly establish sister chromatid cohesion (Almedawar et al., 2012; McAleenan et al., 2012). Moreover, polySUMOylation of the kleisin subunit Scc1 leads to its STUbL-mediated degradation, thus inhibiting cohesion. PolySUMOylation of cohesin is reversed by Ulp2, which is recruited by the cohesin subunit Pds5 (D'Ambrosio and Lavoie, 2014; Psakhye and Branzei, 2021). The fact that SUMOylation of SMC complexes can be both a positive and negative regulator of cohesion may be explained by the fact that mono/multiSUMOylation and polySUMOylation can have very different effects. It has been suggested that the formation of SUMO chains, counteracted by Ulp2, may act as a "countdown timer" for degradation through the Slx5/8 pathway (Psakhye et al., 2019; Psakhye and Branzei, 2021).

There is evidence of SUMO controlling sister chromatid segregation by acting specifically at centromeres. SUMO targets a good number of proteins associated with the centromere and the kinetochore, such as the CPC subunit Bir1 and the kinetochore components Ndc10, Ndc80, and Cep3 (Montpetit et al., 2006). SUMOylation of kinetochore components drives the recruitment of the Slx5/8 heterodimer (Schweiggert et al., 2016; van de Pasch et al., 2013). At kinetochores, this complex triggers the degradation of the spindle positioning factor Kar9, independently of its SUMOylation. This mechanism prevents the accumulation of Kar9 at abnormal levels, which in turn can compromise spindle positioning and faithful chromosome segregation (Schweiggert et al., 2016).

Another function of SUMO at centromeres is the silencing of the error correction pathway through SUMOylation of Shugoshin (Sgo1). During metaphase, Shugoshin recruits condensin and PP2A and maintains the CPC at centromeres, thus facilitating chromosome biorientation (Peplowska et al., 2014; Verzijlbergen et al., 2014). SUMOylation of Sgo1 stabilizes bioriented chromosome-microtubule attachments, likely by promoting the release of CPC from the kinetochores. This mechanism ensures timely anaphase onset (Su

et al., 2021). Interestingly, SUMOylation of Ndc10 also triggers its relocalization from the kinetochores to the spindle midzone during anaphase (Montpetit et al., 2006).

Finally, SUMOylation controls the localization of the centromere-specific histone variant Cse4. Degradation of Cse4 through the Slx5/8 pathway prevents its mislocalization to euchromatin, which in turn can compromise chromosome segregation and result in aneuploidy (Au et al., 2008; Ohkuni et al., 2016).

Placing SUMO in the mitotic network of post-translational modifications

The substrate specificity of the SUMO enzymes is greatly determined by their localization (Li and Hochstrasser, 2003). Siz1/2, Ulp1, and Ulp2 localize in the nucleus during most of the cell cycle, with Ulp1 being mainly associated with the nuclear pore complex and Ulp2 being spread throughout the nucleoplasm (Li and Hochstrasser, 2000; Takahashi et al., 2000). During mitosis, both Siz1 and Ulp1 relocalize to the bud neck, where they target the septins (Elmore et al., 2011; Johnson and Gupta, 2001; Takahashi et al., 2000).

Very little is known about the regulation of the SUMO pathway during mitosis. One possible mechanism involves Ulp2. This SUMO protease is phosphorylated during mitosis in a manner that depends on the kinases Cdk1 and Cdc5. Inactivation of Cdc5 decreases SUMOylation of Pds5 and Top2, two known Ulp2 substrates, in metaphase-arrested cells (Baldwin et al., 2009). These findings suggest that the polo-like kinase may downregulate Ulp2 during mitosis, thus leading to an increase in the SUMOylation of its substrates.

In addition to Ulp2, Siz1 is also phosphorylated in a cell cycle-dependent manner, possibly by Cdk1 (Holt et al., 2009; Johnson and Gupta, 2001). Phosphorylation occurs concomitantly with the relocalization of Siz1 in mitosis. However, the significance of this modification remains unclear.

1.3. SMC complexes: masters of chromosome organization and cohesion

"It's all part and parcel, the whole genie gig: phenomenal cosmic powers, itty-bitty living space"

(Aladdin, 1992)

To maximize the ratio between the volume and the surface, the size of cells is generally pretty small across all living organisms. On the other hand, an increase in organism complexity raises the need for more genetic information, which means longer genomes. As a result, centimeter-long DNA molecules must be stored in micrometer-sized cells and, to this aim, they must be purposefully organized in space according to the cell's need at any given time. This is where Structural Maintenance of Chromosomes (SMC) complexes come to play.

SMC complexes are a family of ring-shaped ATPases that comprises cohesin, condensin, and the Smc5/6 complex. They can be found in virtually all organisms, from bacteria to humans. Indeed, the first SMC protein to be discovered was *Escherichia coli* MukB. Their structure is composed of a heterodimer of two SMC proteins, a kleisin subunit, and additional regulatory proteins (**Figure 1.10**). The two SMC proteins, which outline the ring shape, are formed by two large coiled-coil domains parted by a hinge domain, and two globular domains placed at the N- and C-terminus, which are referred to as Walker A and Walker B motifs, respectively. These two Walker motifs interact to form an ATPase domain. The SMC subunits bind stably through the hinge, while their heads interact in an ATP-dependent fashion. Finally, the kleisin subunit binds the heads, stabilizing their interaction and securing the ring (Hassler et al., 2018; Uhlmann, 2016).

SMC complexes are master organizers of genome architecture and function in many cellular processes like chromosome organization, sister-chromatid cohesion, DNA repair, and regulation of gene expression. Accumulating evidence supports the idea that all kinds of SMC complexes can perform complex and diverse tasks thanks to their unique ability to topologically embrace two DNA segments within their ring structure. The topological entrapment of DNA was first demonstrated for yeast cohesin (Gligoris et al., 2014; Haering et al., 2008; Murayama and Uhlmann, 2014), then for condensin (Cuylen et al., 2011) and the Smc5/6 complex (Kanno et al., 2015). By embracing two DNA regions from the same

molecule and extruding chromatin loops, a mechanism termed “loop extrusion”, SMC complexes can shape DNA topology (Davidson et al., 2019; Ganji et al., 2018; Kim et al., 2020, 2019). Cohesin can also entrap DNA segments of sister chromatids, thus promoting cohesion (Haering et al., 2008).

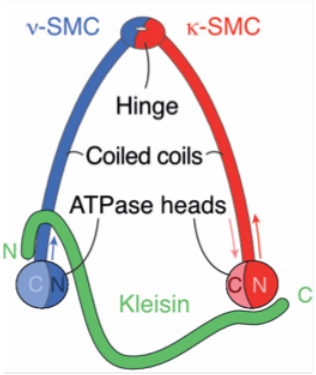

Cohesin	Condensin	Smc5/6 complex
SMC subunits		
Smc1	Smc4	Smc5
Smc3	Smc2	Smc6
Kleisin		
Scc1	Brn1	Nse4
HEAT subunits		
Scc3	Ycs4	Nse5
Pds5	Ycg1	Nse6
Others		
Wpl1		Nse1-Nse3 (ubiquitin ligase)
		Mms21 (SUMO ligase)

Figure 1.10. The structure of SMC complexes
The table lists the subunits of SMC complexes in S. cerevisiae*. Modified from (Hassler et al., 2018).*

1.3.1. Condensin: packing it up

Condensin structure and action

Condensin is highly evolutionarily conserved and condensin-like complexes have been found also in bacteria and archaea. Vertebrates possess two condensin complexes, condensin I and II, which differ in the regulatory subunits, while budding yeast has only one complex, homologous to condensin I. The core complex is constituted by the SMC proteins Smc2 and Smc4 and the kleisin Brn1. In yeast, the additional subunits include the HEAT-repeat containing proteins Ycs4 and Ycg1.

Condensin functions in three-dimensional genome organization throughout the cell cycle and guides chromatid compaction and individualization during mitosis. Initially, condensin was proposed to compact DNA thanks to its ability to induce positive supercoiling *in vitro* (Kimura et al., 1999; Kimura and Hirano, 1997), thus wrapping the chromosomes on

themselves. It was later found that this is not the main mechanism of action (Eeftens et al., 2017; Strick et al., 2004). Currently, the preferred model for chromosome condensation envisions condensin acting through loop-extrusion (Ganji et al., 2018; Gibcus et al., 2018; Kim et al., 2020). According to this model, condensin interacts with a single DNA molecule, embraces it, and then extrudes a loop of increasing size (**Figure 1.11**). In support of this hypothesis, yeast condensin can unidirectionally translocate along DNA in an ATP-dependent manner, providing a mechanism for the extrusion of the loops (Terakawa et al., 2017). Moreover, it was recently shown that condensin complexes can traverse each other and create a more complex loop structure called Z-loop (**Figure 1.11**), which consists of three DNA filaments placed in parallel with one condensin complex at each end (Kim et al., 2020).

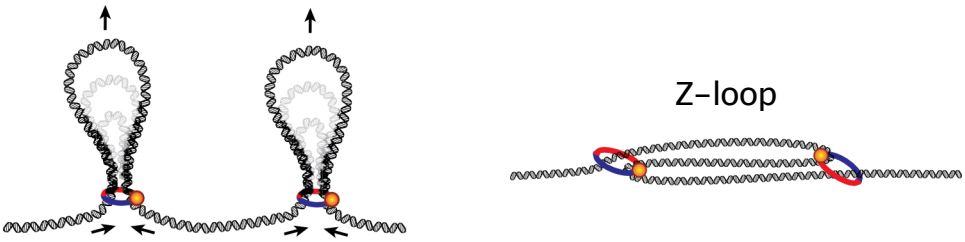

Figure 1.11. Model of loop extrusion by condensin
Modified from (Kim et al., 2020).

Condensin is enriched at the centromeres and at specific regions on the chromosome arms, including rDNA and transfer RNA (tRNA) genes (D'Ambrosio et al., 2008b; Freeman et al., 2000). At the centromeres, condensin and cohesin organize the chromatin according to a precise geometry and control its stiffness (Lawrimore et al., 2018, 2015; Stephens et al., 2011). Centromere architecture is important to confer the spring-like properties that are needed to establish chromosome alignment and biorientation (Lawrimore et al., 2016; Ribeiro et al., 2009).

Condensin regulation in mitosis

In order to achieve chromosome segregation, genome compaction is maximized in mitosis and chromosomes are condensed into discrete entities. *In vitro* studies demonstrated that the essential components required for the formation of mitotic chromosomes are condensin I, core histones, histone chaperones, and the strand passage activity of topoisomerase II, although chromosome-like structures can be observed even in the absence of histones (Shintomi et al., 2017, 2015).

In budding yeast, where mitotic chromosomes are not readily visible, compaction can be monitored by measuring the distance between two fluorescently labeled loci on a chromosome arm (Vas et al., 2007). Alternatively, chromosome condensation was often monitored by looking at the morphology of the nucleolus, the locus of chromosome XII containing the rDNA repeats. These experiments showed that rDNA condensation starts in G2/M, when condensin is activated, occurs stepwise during mitosis, and persists until the next G1 (Guacci et al., 1994; Lavoie et al., 2004). It should be noted that the yeast nucleolus normally condenses and segregates later than the rest of the genome. Indeed, segregation of the rDNA only occurs in late anaphase, both in yeast and human cells (D'Amours et al., 2004; Daniloski et al., 2019; Granot and Snyder, 1991; Sullivan et al., 2004; Torres-Rosell et al., 2004).

More recently, the dramatic changes in chromatin organization between interphase and mitosis have also been observed with high throughput sequencing-based chromosome conformation capture (Hi-C) techniques (Lieberman-Aiden et al., 2009). It was shown that short-range contacts decrease in mitosis compared with interphase, while long-range interactions increase (Kakui and Uhlmann, 2018). This reorganization of the chromatin depends on condensin and, in budding yeast, also cohesin, even though the two complexes play distinct roles. Cohesin drives the general compaction of chromosome arms, whereas condensin is specifically required for the organization of the centromeres and the nucleolus (Guacci et al., 1997; Lavoie et al., 2004; Lazar-Stefanita et al., 2017; Schalbetter et al., 2017).

In budding yeast, condensin is constitutively associated with chromatin, but its localization changes during the cell cycle (Freeman et al., 2000). The mechanisms of condensin regulation are not completely understood. The abundance of all of the complex subunits is cell cycle-regulated and low levels of Ycg1 were shown to limit condensin function in interphase (Doughty et al., 2016; Wei-Shan et al., 2019). In many other cases, the significance of the changes in protein amount remains unclear. Instead, condensin localization and activity seem to be controlled in mitosis through post-translational modifications (PTMs). The cyclin-dependent kinase Cdk1, whose activity increases upon entry into mitosis, phosphorylates Smc3 and initiates chromosome condensation, likely by stabilizing condensin interaction with chromatin (Robellet et al., 2015). Next, the polo-like kinase Cdc5 phosphorylates Brn1, Ycg1, and Ycs4 in anaphase, enhancing condensin supercoiling activity. Mutation of the phosphorylated residues reduced viability and

impaired condensation of the rDNA locus in anaphase (St-Pierre et al., 2009). Moreover, Cdc5 activity is required for the relocalization of condensin from centromeres toward chromosome arms that occurs at anaphase onset (Leonard et al., 2015). In addition to the polo-like kinase, the Aurora kinase Ipl1 contributes to chromosome condensation during anaphase (Lavoie et al., 2004; Neurohr et al., 2011; Vas et al., 2007). Ipl1 was proposed to directly activate condensin through phosphorylation of the Ycg1 subunit (Lavoie et al., 2004). Indeed, inactivation of Ipl1 impairs anaphase condensation of the nucleolus and triggers premature decondensation of the chromosomes (Lavoie et al., 2004; Vas et al., 2007).

Another player in the mitotic regulation of yeast condensin is the Cdk-counteracting phosphatase Cdc14. The FEAR pathway promotes condensin recruitment to the rDNA and telomeres and is required for the proper compaction and segregation of these regions in mid-to-late anaphase (D'Amours et al., 2004; Sullivan et al., 2004). Cdc14 impacts condensin localization indirectly, in two ways. On one hand, it triggers SUMOylation of Ycs4, which was proposed to target condensin to the rDNA (D'Amours et al., 2004; Wang et al., 2004). On the other hand, it promotes transcriptional silencing of the nucleolus and the telomeric regions, which in turn is required for condensin recruitment (Clemente-Blanco et al., 2011, 2009; Tomson et al., 2006). Finally, in late anaphase/telophase, MEN promotes the release of condensin from the nucleolus, thus leading to the decompaction of this locus (Varela et al., 2009). This observation could be explained by the role of Cdc14 in reversing Cdk1 phosphorylation.

Other factors involved in chromosome compaction

To reorganize the chromatin, condensin cooperates with Topoisomerase II (Top2 in *S. cerevisiae*), the only enzyme capable of carrying out the strand-passage reaction on double-stranded DNA (dsDNA). Likely, this reaction is necessary to sustain the movement and reorganization of DNA fibers in space. Accordingly, in yeast, Top2 is required for linear condensation of chromosomes (Vas et al., 2007) and Topoisomerase II is also essential for the reconstitution of mitotic chromosomes *in vitro* (Shintomi et al., 2017, 2015).

In addition to condensin and Topoisomerase II, protein-protein interactions between histones contribute to DNA compaction in mitosis. The finding that chromatin aggregates more efficiently *in vitro* when histones from mitotic cells, rather than interphase cells, are

used, suggested that histone interactions are regulated by the post-translational modifications of the histones, which change drastically during the cell cycle (Zhiteneva et al., 2017). In particular, in yeast, it was found that acetylation of histone H4 on lysine K16 (H4K16) inhibits histone-histone interactions in interphase. In mitosis, this modification is reversed by the deacetylase Hst2, which is recruited via phosphorylation of histone H3 by the kinase Haspin and, subsequently, Aurora B, thus promoting condensation (Neurohr et al., 2011; Shogren-Knaak et al., 2006; Wilkins et al., 2014).

Finally, DNA compaction may be enhanced in mitosis by variations in the solvent composition. It was reported that the concentration of Mg2++ and ATP respectively increase and decrease in mitosis and these changes were proposed to reduce the solubility of chromatin (Maeshima et al., 2018).

1.3.2. Cohesin: pairing the sisters

"A sister can be seen as someone who is both ourselves and very much not ourselves – a special kind of double."

Toni Morrison

Cohesin structure and loading

The ring structure of cohesin is composed of the SMC proteins Smc1 and Smc3 and the kleisin subunit Scc1 (also called Mcd1). The complex also includes two stably-associated HEAT repeat-containing proteins, Scc3 and Pds5, and the additional subunit Wpl1. Unlike condensin, no cohesin homolog was found in prokaryotes. Cohesin collaborates with condensin to genome organization by dynamically engaging with DNA. In higher eukaryotes, cohesin is responsible for the formation of topologically associating domains in interphase (Skibbens, 2019), while in yeast it plays a major role in the mitotic condensation of chromosome arms (Guacci et al., 1997; Lazar-Stefanita et al., 2017; Schalbetter et al., 2017). Moreover, cohesin is the main actor in the establishment and maintenance of cohesion between sister chromatids in all eukaryotes (Guacci et al., 1997; Michaelis et al., 1997). In fact, cohesin likely evolved from condensin to provide this specialized function during cell division.

In vertebrates, cohesin is loaded onto chromatin at the end of the cell cycle, in telophase, whereas in *S. cerevisiae* the loading occurs in late G1, upon the synthesis of Scc1 (Michaelis

et al., 1997). This process is mediated by the loader complex Scc2-Scc4 (Ciosk et al., 2000; Higashi et al., 2020; Murayama and Uhlmann, 2014). Cohesin loading occurs through the opening of the ring and requires ATP-hydrolysis (Arumugam et al., 2003; Higashi et al., 2020; Murayama and Uhlmann, 2015, 2014). In G1, cohesin association with DNA is unstable and the complex tends to detach from the chromosomes, in a process promoted by Pds5 and Wpl1 (Chan et al., 2013; Gandhi et al., 2006; Kueng et al., 2006; Losada et al., 1998; Murayama and Uhlmann, 2015).

Stabilization of cohesin binding to chromosomes occurs in S phase and requires acetylation of Smc3, which is catalyzed by the replication fork-associated acetyltransferase Eco1 (Rolef Ben-Shahar et al., 2008; Unal et al., 2008; Zhang et al., 2008). Eco1 acetylation locks the cohesin ring and provides a way to couple DNA replication with the establishment of sister chromatid cohesion. In addition to Wpl1-mediated cohesin release, Pds5 is also involved in the establishment of cohesion, since it promotes acetylation of Smc3 and protects Scc1 from SUMO-dependent degradation during metaphase (Chan et al., 2013; D'Ambrosio and Lavoie, 2014; Psakhye and Branzei, 2021).

Cohesin loading occurs at dedicated sites, where the loading complex Scc2-Scc4 associates. These sites are located at the centromeres, at the telomeres, and also along chromosome arms, for example at the rDNA and at tRNA genes (Lopez-Serra et al., 2014). DNA sequences are not sufficient to target Scc2-Scc4 to the chromatin, meaning that the loading complex is mainly recruited through protein-protein interaction (Chao et al., 2015). The pathways involved are not entirely understood and may vary depending on the locus (Litwin and Wysocki, 2018). After loading, the complexes are pushed along the DNA by the transcription machinery and they accumulate in regions of convergent transcription (Lengronne et al., 2004; Ocampo-Hafalla et al., 2016). The ability to slide along DNA filaments after being loaded onto chromatin seems to be shared by all SMC complexes.

Cohesin is enriched at the regions flanking the centromeres, called pericentromeres, and at specific locations on the chromosome arms (Blat and Kleckner, 1999; Glynn et al., 2004; Megee et al., 1999; Tanaka et al., 1999). The pericentromeric enrichment is an example of how the final position of cohesin depends on both the loading site and the transcriptional landscape. Cohesin is loaded at the centromeres, then slides towards the pericentromeres, and accumulates at sites marked by convergent genes (Paldi et al., 2020). The distribution of cohesin complexes determines the architecture of the pericentromere and confers the

cohesion needed to resist the pulling force of the mitotic spindle and generate tension during chromosome biorientation (Ng et al., 2009; Paldi et al., 2020; Tanaka et al., 2000).

Cohesin cleavage and its regulation

Removal of sister chromatid cohesion requires the proteolytic cleavage of the cohesin subunit Scc1 by a cysteine-protease named separase or Esp1 in budding yeast (Uhlmann et al., 2000, 1999). Before anaphase, the separase is inhibited by the interaction with the securin, Pds1 in yeast, which is a major target of the APC/C^{Cdc20} (Ciosk et al., 1998; Cohen-Fix et al., 1996). As soon as the APC/C^{Cdc20} gets activated, securin is degraded and cohesin is rapidly cleaved, marking entry into anaphase (**Figure 1.12**). Indeed, cohesin cleavage is sufficient to trigger chromosome segregation in presence of a functional spindle (Uhlmann et al., 2000). To ensure that chromatid separation only begins when all chromosomes are correctly attached to the spindle with bipolar orientation, cohesin cleavage is placed under the control of the spindle assembly checkpoint.

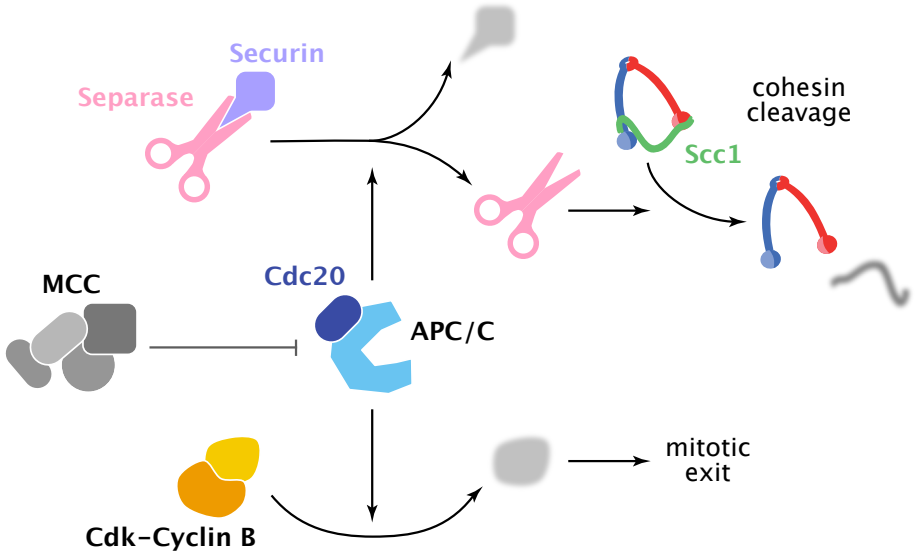

Figure 1.12. Cohesin cleavage
When the spindle assembly checkpoint is satisfied, MCC stops being produced and the APC/C^{Cdc20} becomes active. The APC/C^{Cdc20} triggers the degradation of securin, leading to separase activation. In turn, the separase cleaves the Scc1 subunit of the cohesin complex, allowing sister chromatids to separate. In addition, the APC/C^{Cdc20} degrades the mitotic cyclins and initiates mitotic exit.

Yeast cells lacking Pds1 separate their chromatids with normal kinetics, indicating that, in addition to securin degradation, other factors contribute to sister separation (Alexandru et al., 1999). Cohesin cleavage and removal are enhanced by Pds1 dephosphorylation by Cdc14 (Holt et al., 2008), Scc1 phosphorylation by the polo-like kinase Cdc5 (Gabriela

Alexandru et al., 2001), Smc3 deacetylation by Hos1 (Li et al., 2017) and Esp1 targeting to the nucleus by Pds1 itself (Agarwal and Cohen-Fix, 2002; Hornig et al., 2002).

While, in yeast, cohesin remains bound to the chromatids until anaphase, in vertebrates two pathways for cohesin removal exist (Waizenegger et al., 2000). Through the "prophase pathway", which does not require cohesin cleavage, Wapl (Wpl1 in *S. cerevisiae*) and Pds5 remove most of the complexes in prophase, particularly from the chromosome arms, while centromeric cohesin is protected (Morales and Losada, 2018). As a result, vertebrate chromosomes assume their characteristic X-shape. Centromeric cohesin is cleaved at anaphase entry by the separase, similar to yeast.

In budding yeast, the bulk of cohesin is cleaved upon anaphase entry, but some complexes remain, particularly on chromosome arms. This idea was suggested by the fact that, during chromosome segregation, sister chromatids stretch and recoil and the stretching behavior depends on cohesin. On the other hand, recoiling depends also on condensin. The combined action of condensin and the mitotic spindle was proposed to drive the dissociation of residual cohesin complexes in anaphase (Renshaw et al., 2010).

1.3.3. The Smc5/6 complex: SMC complexes in DNA repair

The Smc5/6 complex plays its main role in DNA repair. It is formed by the SMC proteins Smc5 and Smc6, the kleisin Nse4, the HEAT proteins Nse5 and Nse6, and the additional subunits Nse1-Nse3 and Mms21 (also called Nse2). Like cohesin, this complex can tether two DNA molecules (Kanno et al., 2015). A unique feature of Smc5/6 is that the Mms21/Nse2 subunit possesses SUMO-ligase activity, which is essential for DNA repair (Ampatzidou et al., 2006; Andrews et al., 2005; Branzei et al., 2006).

The Smc5/6 complex promotes repair of DNA double-strand breaks (DSBs) through homologous recombination (HR) between sister chromatids (De Piccoli et al., 2006). Its inactivation leads to the accumulation of toxic recombination intermediates (Ampatzidou et al., 2006; Branzei et al., 2006; Torres-Rosell et al., 2005).

In unchallenged cells, Smc5/6 is essential in the G2/M phase, when it is required to solve the lesions arising during DNA replication (Menolfi et al., 2015). This complex is loaded on chromosomes in a replication-dependent manner during S phase and colocalizes with cohesin in G2/M (Jeppsson et al., 2014; Lindroos et al., 2006). During DNA replication,

Smc5/6 stabilizes stalled forks and facilitates the resolution of the recombination intermediates formed through DNA damage tolerance by template switching (Bermúdez-López et al., 2010; Branzei et al., 2006; Irmisch et al., 2009; Menolfi et al., 2015; Torres-Rosell et al., 2005). Moreover, it aids relaxation of replication-induced topological stress (Kegel et al., 2011). When cells undergo S phase in the absence of Smc5/6, they accumulate recombination intermediates and replication-induced supercoil, which prevent them from completing replication (Menolfi et al., 2015). For these reasons, *smc5* and *smc6* mutants are defective in the replication and segregation of repetitive regions, such as the rDNA locus (Torres-Rosell et al., 2007, 2005).

Finally, cohesin collaborates with Smc5/6 to DNA repair. Both complexes are recruited at DSBs to reinforce cohesion at the site and assist homologous recombination (De Piccoli et al., 2006; Ström et al., 2004; Unal et al., 2004)

1.4. Sister chromatid cohesion: DNA linkages

> *"Since the two chains in our model are intertwined, it is essential for them to untwist if they are to separate. […] Although it is difficult at the moment to see how these processes occur without everything getting tangled, we do not feel that this objection will be insuperable."*
>
> *(Watson and Crick, 1953)*

Before the discovery of SMC complexes, another model was proposed to explain cohesion between sister chromatids. This model attributed cohesion to the intertwining between sister DNA molecules, particularly catenation (Murray and Szostak 1985). Since the DNA double-helix was described, it was clear that such structure would cause topological issues during cellular processes like replication. The simple duplication of a DNA molecule, in which every strand serves as a template for the synthesis of a new complementary strand, will result in two intertwined double-helixes. Furthermore, any process that implies the unwinding of the two strands of a DNA molecule (such as replication, transcription, and recombination) will produce supercoiling. Therefore, the eventuality that the sister DNA molecules would become entangled in the process immediately seemed likely. These DNA linkages are collectively called sister chromatid intertwines (SCIs). The idea that DNA linkages were responsible for cohesion was supported by the early observations that, in *S. cerevisiae* and *S. pombe*, mutation of Topoisomerase II, the decatenating enzyme, is lethal at the time of mitosis and hampers the separation of sister chromatids (DiNardo et al.,

1984; Holm et al., 1985; Uemura et al., 1987; Uemura and Tanagida, 1986; Uemura and Yanagida, 1984). Later, the fact that, in budding yeast, DNA plasmids are kept together in metaphase-arrested cells even in absence of catenation demonstrated that, although DNA intertwines contribute to cohesion during mitosis, they are not the main factor (Guacci et al., 1994).

Three types of SCIs can be distinguished (**Figure 1.13**): patches of unreplicated DNA, also called Late-Replication Intermediates (LRIs), recombination intermediates, also called Joint Molecules (JMs), and double-stranded DNA (dsDNA) catenanes. Certain types of SCIs are more commonly retained at specific loci, but their position in the genome is not sufficient to infer their molecular structure. Intertwining naturally arises during replication and is mostly removed before entry into mitosis. However, some linkages persist and manifest themselves during anaphase as threads of DNA stretching between the two segregating masses, termed anaphase bridges (**Figure 1.13**).

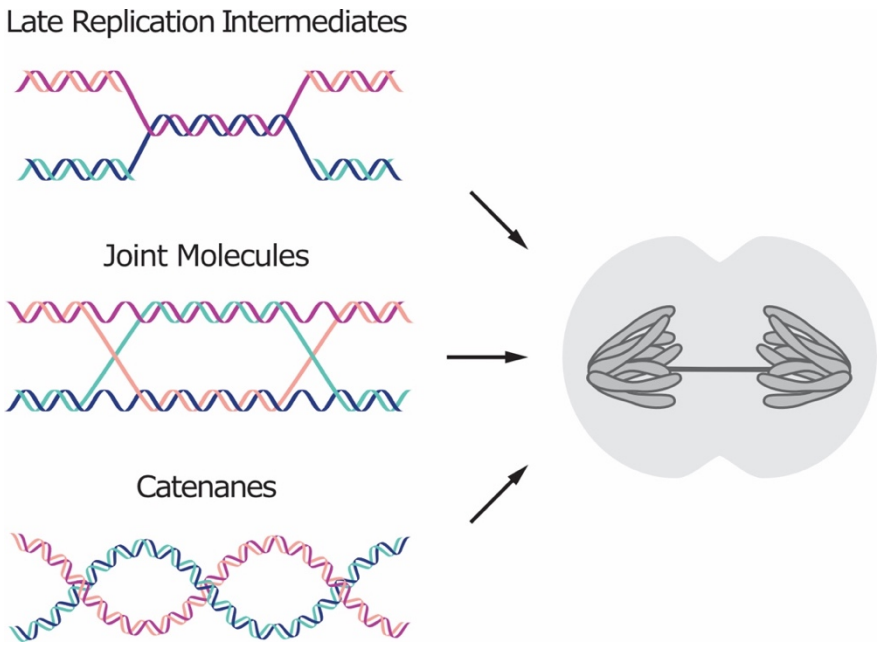

Figure 1.13. Structure of sister chromatid intertwines
Three types of sister chromatid intertwine (SCI) are observed during mitosis. Molecular structures of late replication intermediates, joint molecules (here exemplified by a double Holliday junction), and catenanes are shown. During mitosis, persistent SCIs will form anaphase bridges. Adapted from (Finardi et al., 2020).

1.4.1. Anaphase bridges

Although anaphase bridges increase in the presence of stressors, such as treatment with replication inhibitors or inactivation of the DNA repair machinery, DNA bridges occur even

during normal mitosis, particularly at the centromeres in mammalian cells (Chan et al., 2009, 2007).

Anaphase bridges can be distinguished between chromatin bridges or ultra-fine bridges (UFBs). Chromatin bridges are chromatinized (that is, packaged with histones and other proteins) and can be stained with DNA dyes like DAPI or Hoechst. Conversely, UFBs are not chromatinized and can only be observed through the staining of associated proteins. In yeast, chromatin bridges rarely occur during an unperturbed cell cycle and they have been mostly attributed to unresolved recombination intermediates (Germann et al., 2014). On the other hand, UFBs are often observed in normal anaphase, and they are enriched at the centromere in human cells (Chan et al., 2007; Germann et al., 2014). Currently, little is known about what determines the chromatinized status of the bridges. The fact that the same kind of stressor can induce the formation of both chromatin bridges and UFBs suggests that chromatinization does not depend on the type of DNA intertwining.

1.4.2. Incomplete replication and recombination intermediates

Structure and origin of late-replication intermediates

Incomplete replication is a source of late-replication intermediates (LRIs), DNA linkages consisting of short unreplicated patches of dsDNA, formed by the parental strands of the two sisters. In unperturbed cells, LRIs rarely form anaphase bridges, because most of the genome is replicated before anaphase. However, in *S. cerevisiae*, where there is no clear separation between G2 and metaphase, replication is completed in metaphase for what concerns the highly repetitive rDNA and in late anaphase for what concerns other specific loci (sub-telomeres, fragile sites, and other hard-to-replicate regions) (Ivanova et al., 2020; Torres-Rosell et al., 2007). Indeed, inhibition of DNA synthesis after metaphase enhances the appearance of chromatin bridges, indicating that some LRIs are removed through replication in anaphase (Ivanova et al., 2020).

In higher organisms, LRIs have not been reported to turn into anaphase bridges in unperturbed conditions. However, in human cells, replicative stress delays replication of common fragile sites and increases anaphase bridges at these loci (Chan et al., 2009; Le Beau et al., 1998). In this case, mitotic DNA synthesis takes care of unreplicated regions

and prevents the formation of anaphase bridges (Minocherhomji et al., 2015; Pedersen et al., 2015).

Structure and origins of recombination intermediates

Homologous recombination (HR) is a DNA repair pathway that can correct many types of lesions, including double-strand breaks, in one chromosome, by using the genetic information available on the sister chromatid (or, less frequently, homologous chromosome) (Prado, 2018). DNA repair through recombination mainly takes place in G2 and S phases, when sister chromatids are readily available. Besides repair, HR is essential for template switching, a mechanism used to allow replication in presence of a DNA lesion (Branzei et al., 2008, 2006; Liberi et al., 2005).

Recombination occurs through the formation of an X-shaped structure known as Holliday junction, which covalently links the sister chromatids. Holliday junctions can be either single or double, depending on whether only one or both ends of the DSB are invading the sister chromatid. Collectively, the DNA linkages produced by HR are called recombination intermediates or Joint Molecules (JMs). The simultaneous inactivation of multiple pathways dedicated to JM resolution compromises chromosome segregation and is lethal even in the absence of DNA damaging agents (Blanco et al., 2010; Chan et al., 2018; Mullen et al., 2001; Wechsler et al., 2011). These observations indicate that HR-derived intertwines occur during a normal cell cycle, likely deriving from template switching, which is used to rescue stalled replication forks.

Dissolution by the STR/BTR complex

Both regions of unreplicated DNA and double Holliday junctions contain (or can be converted into) an hemicatenane structure, which is an entanglement between single-stranded DNA filaments. Thus, as the parental strands attempt to separate, these linkages will form bridges that contain ssDNA. Indeed, the ssDNA binding protein Replication Protein A (RPA) localizes on anaphase bridges associated with recombination intermediates (Chan et al., 2009, 2018; Germann et al., 2014; Sarlós et al., 2018).

Thanks to their common feature, LRIs and JMs can be removed by the STR/BTR complex (Barefield and Karlseder, 2012; Chan and West, 2018; Sarlós et al., 2018), which is composed by the RecQ helicase Sgs1 (BLM in metazoans), the Type I topoisomerase Top3

and the ssDNA binding protein Rmi1, in a process called dissolution (**Figure 1.14**) (Manthei and Keck, 2013). First, the helicase opens the heteroduplex. Next, Top3 catalyzes the strand-passage reaction on the exposed ssDNA and removes the entanglement, while Rmi1 promotes supercoil relaxation and topoisomerase activity. The function of STR/BTR-mediated dissolution in the processing of the bridges is supported by the observation that, in human cells, BLM is required for RPA recruitment to UFBs during anaphase (Chan et al., 2018).

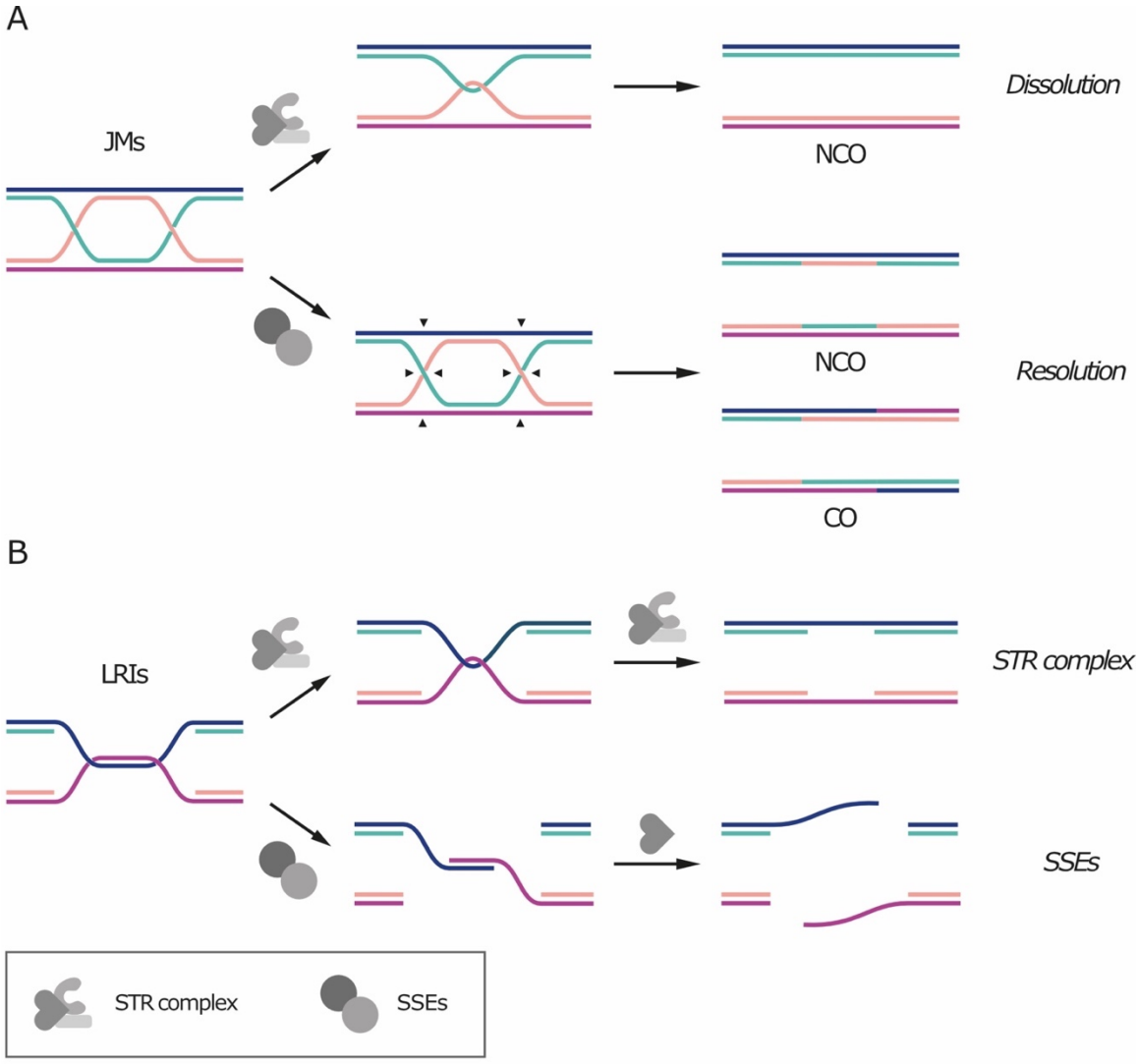

Figure 1.14. Processing of joint molecules and late replication intermediates
*Joint molecules (JMs) and late replication intermediates (LRIs) can be disentangled by the Sgs1-Top3-Rmi1 (STR) complex (BTR in human cells) or cleaved by structure-specific endonucleases (SSEs). (**A**) JMs can undergo STR-mediated dissolution or SSE-mediated resolution. Arrows indicate the possible sites of cleavage by nucleases. Dissolution always results in non-crossover products (NCO), whereas resolution can result in crossover (CO) or non-crossover products. (**B**) LRIs can be processed by the STR/BTR complex or by SSEs, leading to single-stranded DNA gaps or overhangs, respectively. Adapted from (Finardi et al., 2020).*

Dissolution of unreplicated regions by the STR/BTR complex leads to the exposure of ssDNA gaps. If the processing occurs during S phase, the gaps are filled by replication, otherwise, they can be repaired in the next cell cycle. Alternatively, since DNA synthesis can occur as late as anaphase (at least in yeast), replication of LRIs may be completed during mitosis, after STR/BTR-dependent disentanglement. Consistently, in human cells, mitotic DNA synthesis is triggered by the nuclease-mediated processing of fragile sites (Minocherhomji et al., 2015; Pedersen et al., 2015).

For what concerns recombination intermediates, after dissolution, the heteroduplex is disentangled, each filament anneals to its complementary strand and the sister chromatids can be separated. Since dissolution by the STR/BTR complex does not introduce any additional nick or gap, processing of JMs generates non-crossover products (**Figure 1.14A**), meaning that there is no exchange of genetic information between the chromosomes and the DNA molecule is restored as it was before recombination (Branzei et al., 2006; Harmon et al., 1999; Ira et al., 2003).

Finally, the STR/BTR complex was shown to be able to decatenate dsDNA *in vitro*, suggesting that it may be involved in the processing of catenanes (Cejka et al., 2012; Sarlós et al., 2018). This hypothesis is supported by the fact that, in yeast, Top3 and Sgs1 can support replication of the rDNA in the absence of Top2 activity (Mundbjerg et al., 2015). However, the STR/BTR complex cannot fully rescue the defects of Top2 mutants, particularly at later stages of mitosis, namely chromosome segregation errors and accumulation of DNA damage during mitosis. Therefore, while this complex may contribute to removing catenation in specific contexts, Top2 is essential to take care of catenanes that persist in anaphase. Interestingly, BLM/Sgs1 and Top2 physically interact in mitosis, both in yeast and in human cells. This interaction seems to be important for faithful chromosome segregation (Russell et al., 2011; Watt et al., 1995), but the mechanism is still unknown.

The STR/BTR complex is mainly active in S phase, when Cdk1-dependent phosphorylation stimulates Sgs1 activity (Grigaitis et al., 2020). The complex was also proposed to act on DNA linkages in anaphase. This idea was suggested by the fact that, in human cells, BLM and the other components of the complex are recruited to DNA bridges in anaphase and that BLM depletion enhances anaphase bridging (Chan et al., 2007). However, the increase in anaphase bridges may be due to the function of BLM earlier in the cell cycle, particularly in DNA replication and repair.

Resolution by nucleases in mitosis

Even though the preferred pathway for the removal of late replication and recombination intermediates is dissolution by the STR/BTR complex, these structures can also be cleaved by dedicated structure-specific nucleases (SSEs), in a process termed resolution (**Figure 1.14**) (Falquet and Rass, 2019; Wyatt and West, 2014). In yeast, these nucleases are the heterodimer Mus81-Mms4, in which Mus81 has catalytic activity while Mms4 has a regulatory function, and Yen1. Simultaneous inactivation of multiple SSEs is often synthetically lethal, indicating that they represent an essential backup mechanism for the removal of those structures that cannot be processed by the STR/BTR complex, such as single or nicked Holliday junctions (García-Luis and Machín, 2014; Garner et al., 2013; Mazón and Symington, 2013; Sarbajna et al., 2014; Wyatt et al., 2013). Unlike dissolution, nuclease-mediated resolution of double Holliday Junctions can give rise to both crossover and non-crossover products, depending on how DNA filaments are cleaved (**Figure 1.14A**).

The activity of SSEs is mostly limited to mitosis, whereas the STR/BTR complex mainly acts earlier in the cell cycle (Wild and Matos, 2016). In case of premature activation, SSEs may cleave intermediates of DNA replication and repair, with toxic effects like chromosome pulverization (Duda et al., 2016). In human cells, limiting nuclease activity is important also to prevent crossover events, which can cause loss of heterozygosity and, therefore, promote tumor development.

During mitosis, the activity of SSEs is distributed in two consecutive time frames, with Mus81-Mms4 and Yen1 peaking at G2/M and anaphase, respectively (Wild and Matos, 2016). These two waves of activation ensure the presence of one active nuclease throughout mitosis. In addition, they may be justified by differences in substrate specificity between the enzymes (Falquet and Rass, 2019; Wyatt and West, 2014). Yen1, which has the broadest substrate specificity, may represent the last chance to allow segregation, albeit with a higher risk of compromising genome integrity.

SSE activity is coordinated with the cell cycle through regulation by mitotic kinases and phosphatases. In budding yeast, Mus81-Mms4 is inactive during G1 and S phases. Its activity is promoted by Cdk1 and Cdc5, which collaborate to its phosphorylation in G2/M (Gallo-Fernández et al., 2012; Matos et al., 2013, 2011; Szakal and Branzei, 2013). In S phase, DNA damage checkpoint activation inhibits Cdc5 and, as a consequence, also

Mus81-Mms4 (Szakal and Branzei, 2013). Finally, concomitantly with Cdk1 and Cdc5 inactivation at anaphase onset, the activity of Mus81-Mms4 is gradually lost. This mechanism of regulation is conserved in human cells. CDK1 and PLK1 phosphorylate MUS81-EME1 (orthologue of yeast Mms4) and SLX4 in prometaphase, leading to the assembly of the SMX tri-nuclease complex, which can process Holliday junctions much more efficiently (Duda et al., 2016; Wyatt et al., 2017, 2013).

On the other hand, Yen1 is kept inactive during S and G2/M phase through Cdk1-dependent phosphorylation (Matos et al., 2011). This phosphorylation is reversed at anaphase onset by Cdc14, thereby activating the nuclease (Blanco et al., 2014; Eissler et al., 2014). Yen1 phosphorylation not only decreases its enzymatic activity, but also excludes it from the nucleus (Blanco et al., 2014; Kosugi et al., 2009). Once again, this mechanism is conserved for the human orthologue of Yen1, GEN1. In fact, because of its cytoplasmic localization, GEN1 only gains access to the DNA after nuclear envelope breakdown takes place, at the onset of mitosis (Chan and West, 2014; Matos et al., 2011). Moreover, GEN1 is dephosphorylated at the metaphase-to-anaphase transition, like its yeast counterpart, although the significance of this event remains unclear (Chan and West, 2014).

1.4.3. DNA catenanes: twists and twirls

Structure and origin of topological entanglements

Catenanes are dsDNA entanglements between the sister chromatids and, unlike JMs and LRIs, they represent pure topological linkages (**Figure 1.13**). The name “catenane” was first introduced to indicate the catenation of two circular plasmids (Riou and Delain, 1969), but is now used also for linkages between linear DNA.

During replication, helicases, acting ahead of the fork, unwind the DNA duplex and push the turns of the helix forward, causing supercoiling (**Figure 1.15**). The overwinding of the helix ahead of the fork is called positive supercoiling, while the underwinding behind the fork is called negative supercoiling. Supercoiling ahead of the fork must be relaxed, otherwise, tension will accumulate, eventually stalling the fork. In principle, on linear DNA molecules, the supercoiling can diffuse and be released by rotation around the axis. However, most eukaryotic chromosomes are extremely long DNA molecules and many obstacles hinder their axial rotation, such as anchoring to the nuclear membrane and

association with large DNA-protein complexes. Thus, axial rotation is not sufficient to relax all the replication-induced supercoil *in vivo*, although it was observed in shorter chromosomes (Kegel et al., 2011; Spell and Holm, 1994) and is favored by disruption of tethering to the nuclear membrane (Titos et al., 2014). Therefore, cells have evolved a set of essential enzymes dedicated to the resolution of topological issues, called topoisomerases.

Formation of catenanes through fork rotation

The activity of topoisomerases is sufficient to relax the majority of the supercoils accumulated during DNA replication and to allow fork progression. Alternatively, the tension generated by supercoils can be relieved through the rotation of the replication fork around its axis (**Figure 1.15**). This mechanism transfers the positive supercoiling from the unreplicated dsDNA ahead of the fork to the replicated filaments behind the fork and, therefore, generates entanglements of the sister chromatids. Such entanglements are called precatenanes and they eventually evolve into catenanes once replication is complete. Therefore, fork rotation leads to sister chromatid catenation (Cebrián et al., 2015).

If all supercoiling stress was relieved by fork rotation, one catenane would form for each turn of the parental double-helix. This is not the case, as indicated by the rare occurrence of catenanes, compared with the number of turns of the helix (Sundin and Varshavsky, 1980). Indeed, several factors inhibit fork rotation. First of all, the bulky replisome itself may represent a steric obstacle against its rotation. Secondly, fork rotation is actively counteracted by the replication pausing complex, Timeless/Tipin (Tof1/Csm3 in yeast, (Schalbetter et al., 2015; Shyian et al., 2019)). Thirdly, a recent *in vitro* study showed that the physical properties of chromatin favor the transfer of supercoiling ahead of the fork rather than behind it, because the braided chromatin fiber is much stiffer and resistant to rotation than the unreplicated single chromatin fiber. Moreover, Top2 was found to act more efficiently on single-fiber DNA supercoils than on precatenanes (Le et al., 2019). In conclusion, during replication, supercoiling is directed ahead of the fork, where topoisomerases can relax it with higher efficiency.

The Smc5/6 complex was proposed to act at the replication fork and favor relaxation of supercoil by fork rotation, possibly by sequestering precatenanes forming behind the fork (Kanno et al., 2015; Kegel et al., 2011).

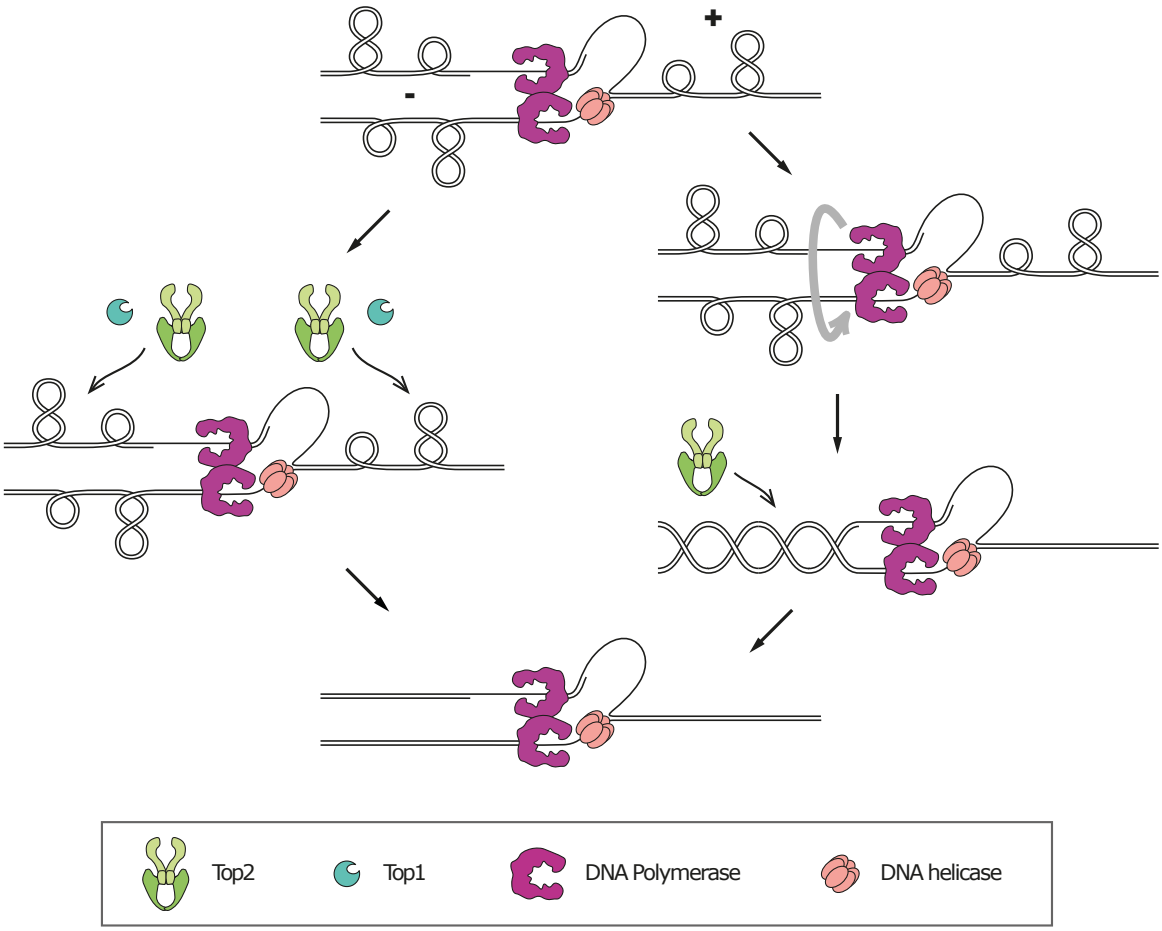

Figure 1.15. Relaxation of replication-induced supercoils through topoisomerase action or fork rotation
During replication elongation, supercoiling accumulates ahead and behind the replication fork. Replication-induced supercoil can be relaxed by Top1 or Top2 (left). Alternatively, fork rotation transfers the supercoiling ahead of the fork to the region behind the fork, thus creating precatenanes between the duplicated DNA molecules, which can only be removed by Top2 (right). Adapted from (Finardi et al., 2020).

Early studies of replication in simian virus SV40 indicated that, while catenation is rarely produced during elongation, it occurs during termination (Sundin and Varshavsky, 1981, 1980). It was proposed that, when the two replisomes converge, topoisomerases cannot access the DNA located between them and, therefore, supercoiling must be relieved through fork rotation. The formation of catenanes at the termination site is supported by the fact that Top2 is essential at replication termination in all organisms (Baxter and Diffley,

2008; DiNardo et al., 1984; Fachinetti et al., 2010; Holm et al., 1985; Zechiedrich and Cozzarelli, 1995).

A study in yeast showed that in cells lacking Top2, in which a catenane is formed at every rotation of the replisome, the amount of catenation of DNA plasmids is not greatly affected by the length of the replicated region. Instead, catenation is increased in the presence of sequences that are prone to pause replication, such as tRNA genes (which are considered fragile sites in yeast), inactive origins, and centromeres (Schalbetter et al., 2015). These observations imply that fork rotation does not occur stochastically during elongation, but rather is restricted to hard-to-replicate sites. This occurrence might be explained by the presence, at these regions, of physical barriers for the action of topoisomerases, such as stable DNA-protein complexes.

Finally, even though catenanes may be formed preferentially at specific regions, an elegant study in yeast demonstrated that they are free to diffuse after replication. This group developed a method based on excision and circularization of chromosomal segments, which allowed to observe catenation between endogenous linear chromatids for the first time. Catenanes were found anywhere along the chromosome with the same frequency, except for the silent mating-type locus, which was devoid of catenation (Mariezcurrena and Uhlmann, 2017). This peculiarity could be due to the fact that this locus is highly compacted, thereby increasing chromatin stiffness and possibly preventing intertwines from diffusing within the region.

Topoisomerases: mechanisms of function

Based on their structure and catalyzed reaction, topoisomerases are classified into two categories (**Figure 1.16**) (Pommier et al., 2016; Vos et al., 2011). Type I topoisomerases are monomeric ATP-independent enzymes, which can be further divided into Type IA (Top3 in yeast) and Type IB (Top1 in yeast). Top3 can only relax negative supercoil, while Top1 can relax both positive and negative supercoil. Top3 acts in the STR/BTR complex, while the main function of Top1 is to relax positive supercoiling ahead of the replication fork, although, in yeast, its absence can be compensated by Top2 (Bermejo et al., 2007).

Type IA (**Figure 1.16A**) enzymes act through a strand-passage mechanism, meaning that they catalyze the cleavage of one DNA strand, navigate the other strand of the same DNA

molecule through the gap and, finally, reseal the break. On the other hand, Type IB topoisomerases (**Figure 1.16B**) act on supercoiled DNA through a rotation mechanism. They catalyze the formation of a single-strand nick and, while remaining bound to one DNA end, they allow the ends to rotate relative to each other around the intact strand, thereby relaxing the supercoil.

Type II topoisomerases (Top2 in yeast, **Figure 1.16C**) are ATP-dependent homodimeric enzymes, organized in three domains: a N-terminal ATP-binding domain, a central catalytic domain, and a regulatory C-terminal domain. Similar to Type IA enzymes, Type II topoisomerases catalyze a strand-passage mechanism. However, they can cleave both strands of a given DNA segment and allow the passage of another double-stranded filament through the break. These characteristics allow Top2 to relax both negative and positive supercoil and make it the only enzyme capable of resolving catenanes (Pommier et al., 2016).

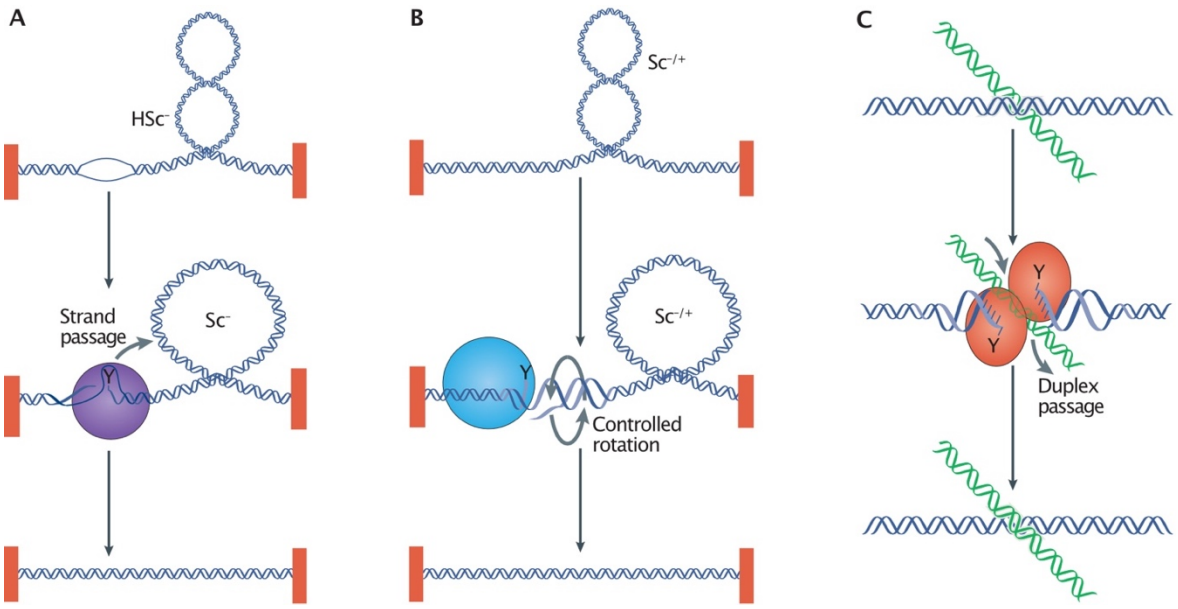

Figure 1.16. Mechanism of action of topoisomerases
*(**A**) Type IA enzymes only relax hypernegative supercoiling (HSc−). They cleave one of the two DNA strands in regions where negative supercoiling promotes the unwinding of the double helix and, then, pass the intact strand through the gap. (**B**) Type IB enzymes relax both negative and positive supercoils (Sc−/+). They form a single-strand nick and allow the broken strand to rotate around the intact strand. (**C**) Type II enzymes function as homodimers and require ATP hydrolysis. They relax both negative and positive supercoils and can resolve DNA catenanes. They cleave both strands of a DNA molecule, allow the intact double-stranded DNA molecule to pass through the gate, and finally re-ligate the cleaved ends. Adapted from (Pommier et al., 2016).*

1.4.4. Catenane resolution in mitosis

Topoisomerase II: roles and regulation in mitosis

While LRIs and JMs are rarely retained in mitosis, catenanes are found in most early anaphase cells and they represent the majority of DNA bridges in physiological conditions (Baumann et al., 2007; Chan et al., 2007; Germann et al., 2014). Normally, complete resolution of sister chromatid catenation occurs concomitantly with chromosome segregation and requires the activity of Top2 (Baxter et al., 2011; Charbin et al., 2014; Farcas et al., 2011; Holm et al., 1985; Uemura et al., 1987; Wang et al., 2008). Cells lacking Top2 activity display conspicuous anaphase bridges and lose viability in the next cell cycle (Clarke et al., 1993; DiNardo et al., 1984; Holm et al., 1985; Lee and Berger, 2019; Uemura et al., 1987).

Upon Top2 inhibition, DNA bridges accumulate at specific genomic regions, suggesting that catenation is preferentially retained at these loci. In mammalian cells, Top2 is enriched at centromeres at metaphase (Lee and Berger, 2019; Rattner et al., 1996; Sumner, 1996) and catenation-derived bridges are by far most commonly formed on centromeric DNA (Baumann et al., 2007; Chan et al., 2007; Wang et al., 2008). The centromeric enrichment of catenanes was not observed in budding yeast. This difference could be explained by the fact that, in higher eukaryotes, the prophase pathway removes cohesin from the chromosome arms, while centromeric cohesin remains bound until anaphase onset and possibly interferes with decatenation of this locus. In both yeast and human cells, Top2 inhibition triggers anaphase bridging particularly at the nucleolus, indicating that this locus remains highly catenated until late mitosis (Daniloski et al., 2019; Sullivan et al., 2004). Consistently, Top2 is required for the correct segregation of this locus, which happens late in anaphase both in yeast and in human cells (D'Ambrosio et al., 2008a; Daniloski et al., 2019). This feature could be due to the fact that transcription, which is active at the rDNA during mitosis, may interfere with the activity of Top2. Indeed, transcriptional silencing of this locus is required for its proper condensation and, therefore, possibly its decatenation (Clemente-Blanco et al., 2009; Tomson et al., 2006).

During mitosis, Top2 is regulated through post-translational modification of its C-terminal regulatory domain, namely ubiquitination, phosphorylation, and SUMOylation (Lee and Berger, 2019), with the latter being the most extensively studied. SUMOylation of Top2

occurs at metaphase (Azuma et al., 2003; Bachant et al., 2002) and controls its recruitment to the centromeres (Antoniou-Kourounioti et al., 2019; Dawlaty et al., 2008; Takahashi et al., 2006) and the nucleolus (Takahashi and Strunnikov, 2008). In human cells, SUMOylation of Top2 at the centromere is involved also in the correct function of Aurora B in the SAC. In particular, SUMOylation promotes Top2 interaction with Claspin and Haspin, both of which participate in the recruitment of Aurora B to the centromeres (Coelho et al., 2008; Edgerton et al., 2016; Ryu et al., 2015; Yoshida et al., 2016)

In *S. cerevisiae*, SUMOylation of Top2 in metaphase is indirectly promoted by Cdc5 through inactivation of the SUMO protease Ulp2 (Baldwin et al., 2009). In addition, human PLK1 directly phosphorylates Topoisomerase II *in vitro* (Li et al., 2008). Together, these findings suggest that the polo-like kinase plays a key role in the mitotic regulation of Top2.

Dpb11/TOPBP1

Dpb11 (TOPBP1 in mammals) is a protein that functions in DNA damage checkpoint, replication, and repair, where it serves as a scaffold for protein recruitment (Liu et al., 2017; Moudry et al., 2016; Navadgi-Patil and Burgers, 2008; Puddu et al., 2008; Tanaka et al., 2007; Zegerman and Diffley, 2007). Several observations pointed to the role of Dpb11/TOPBP1 in the resolution of DNA linkages during mitosis, particularly catenanes. First, this protein localizes to anaphase bridges, especially UFBs (Broderick et al., 2015; Germann et al., 2014; Pedersen et al., 2015). Second, in human cells, TOPBP1 is required for the recruitment of Topoisomerase II to the anaphase bridges. Localization to the bridges and interaction with the topoisomerase both require the BRCA1 C Terminus (BRCT) domains of TOPBP1 (Broderick et al., 2015). As these domains usually recognize phosphorylated substrates, the recruitment of Topoisomerase II may depend on its phosphorylation. Moreover, in human cells, depletion of TOPBP1 after S phase enhances the formation of chromatin bridges (Germann et al., 2014) and increases DNA damage in the next cell cycle (Pedersen et al., 2015).

Finally, TOPBP1/Dpb11 was proposed to contribute to the resolution of the other types of sister chromatid intertwines during mitosis. In particular, TOPBP1/Dpb11 promotes mitotic DNA replication of fragile sites in conditions of replicative stress (Pedersen et al., 2015) and resolution of recombination intermediates generated by template switch, through its

conserved interaction with the nucleases Slx1-Slx4 and Mus81-Mms4 (Gritenaite et al., 2014; Pedersen et al., 2015).

1.4.5. Interplay between SCI resolution and mitotic processes

Reversibility of Top2 reaction

Top2 can both introduce and remove catenanes, depending on the direction of the thermodynamic equilibrium. In the pre-mitotic nucleus, where all duplicated chromatids are crowded together instead of being organized into mitotic chromosomes, the possibility of Top2 inserting catenanes is not unlikely. Indeed, during a metaphase arrest, Top2 can introduce *de novo* intertwining if cells are treated with the microtubule-depolymerizing drug nocodazole (Sen et al., 2016) or if chromosome structure is disrupted (Piskadlo et al., 2017). Even though, thanks to the energy provided by ATP hydrolysis and the enzyme's preference for bent DNA substrates, Top2 has the ability to decatenate DNA below the expected thermodynamic equilibrium *in vitro*, the mere action of the enzyme is not sufficient to remove every single SCI (Dong and Berger, 2007; Rybenkov et al., 1997; Stuchinskaya et al., 2009). Thus, in the cell, decatenation must be sustained by chromatid separation and individualization (**Figure 1.17**).

Chromatid individualization is achieved by compacting the chromosomes in a non-overlapping manner and is driven by SMC complexes (Batty and Gerlich, 2019). During condensation, chromatids come to occupy limited space, separated from that of their sisters, and SCIs are exposed. At the interface between the sister chromatids, the local concentration of SCIs increases, thus pushing the equilibrium of the Top2 reaction toward decatenation. Importantly, if, on the one hand, catenane resolution requires chromatid compaction, on the other hand, chromatid compaction requires Top2 activity. Thus, chromosome individualization requires the cooperation of Top2 activity and SMC-dependent compaction. In addition to individualization, complete removal of DNA linkages is assisted by the physical separation of chromatids, which requires cohesin cleavage and is driven by the elongation of the mitotic spindle during anaphase. Consistently, chromatid individualization and separation were shown to drive the removal of other sources of cohesion, namely cohesin complexes (Renshaw et al., 2010).

Cohesion between sisters prevents their decatenation

It is now well established that cohesin favors DNA catenation and inhibits decatenation (**Figure 1.17A**). Early *in vitro* experiments showed that cohesin promotes catenation of DNA plasmids in the presence of Top2 (Losada and Hirano, 2001). Later, it was shown in yeast that cohesin binding prevents DNA decatenation also *in vivo*, for what concerns both DNA plasmids (Charbin et al., 2014; Farcas et al., 2011) and endogenous chromosomes (Mariezcurrena and Uhlmann, 2017). The idea of cohesin directly inhibiting Top2 or preventing its access to DNA seems unlikely. Instead, cohesin likely directs Top2 activity toward the insertion of catenanes by holding the sister chromatids in close proximity. This model is supported by the fact that linking DNA plasmids with means other than cohesin also increases the degree of catenation (Sen et al., 2016).

In *S. cerevisiae*, besides being responsible for sister chromatid cohesion, cohesin plays an important role in mitotic chromosome condensation, raising the possibility that it might also indirectly promote decatenation (Guacci et al., 1997; Lazar-Stefanita et al., 2017; Schalbetter et al., 2017). This hypothesis is currently difficult to test, as there are no experimental settings suited to distinguish between the cohesin complexes that form inter-chromatid interactions (promoting cohesion) and intra-chromatid interaction (promoting condensation).

Condensin and Topoisomerase II: partners in SCI resolution

The first indication of the essential role of condensin in the resolution of DNA linkages was the finding that condensin mutants display anaphase bridges and chromosome segregation defects, similarly to Top2 mutants (Saka et al., 1994; Strunnikov et al., 1995).

The interplay between condensin and Top2 has been extensively studied at the rDNA locus. Top2 and condensin are both required for proper segregation of the nucleolus and mutations in either of the two cause anaphase bridges at this locus (D'Amours et al., 2004; Daniloski et al., 2019; Potapova et al., 2019; Sullivan et al., 2004). These bridges are removed by ectopic expression of a viral topoisomerase II, indicating that they represent DNA catenanes (D'Ambrosio et al., 2008a). The role of condensin in promoting SCI resolution was confirmed by studies on yeast plasmids (Baxter et al., 2011; Charbin et al., 2014; Sen et al., 2016). It was shown that, at anaphase onset, condensin induces extensive

positive supercoiling of the DNA plasmids, in a manner that requires attachment to a bipolar spindle. In turn, this supercoiling was suggested to drive Top2-mediated decatenation of the plasmids (Baxter et al., 2011; Sen et al., 2016).

As for cohesin, the role of condensin in decatenation is mostly topological. By promoting chromosome condensation and individualization, condensin biases Top2 reaction toward decatenation (**Figure 1.17B**). This model is supported by the finding that removing condensin from already separated sister chromatids leads to their decompaction and Top2-mediated re-intertwining (Piskadlo et al., 2017). Whether condensin additionally has a direct effect on Top2 is still debated. In bacteria, the condensin homolog was found to physically interact with topoisomerase II (Li et al., 2010). If this interaction was conserved in eukaryotes, it could suggest that compaction and decatenation are coupled through condensin-dependent recruitment of Top2. Consistently, in *S. cerevisiae*, Top2 was found to "follow" condensin as it relocates from centromeres toward chromosome arms upon anaphase onset (Leonard et al., 2015).

In budding yeast, condensin inactivation does not seem to increase the amount of intertwining in G2/M (Mariezcurrena and Uhlmann, 2017), maybe because condensin is not the only SMC complex involved in chromosome compaction in this organism (Lazar-Stefanita et al., 2017; Schalbetter et al., 2017). Instead, condensin is required for completing resolution of SCIs specifically after anaphase onset, possibly by increasing chromosome condensation and individualization during anaphase (Lavoie et al., 2004; Neurohr et al., 2011; Vas et al., 2007). Similarly, in anaphase, condensin drives the removal of leftover cohesin complexes through chromosome stretching (Charbin et al., 2014; Renshaw et al., 2010).

The spindle puts some distance between the sisters

As spindle elongation and completion of SCI resolution occur in concert during anaphase, it is tempting to speculate that the former drives the latter. Consistently, in yeast cells arrested in metaphase, treatment with nocodazole prevents decatenation both of DNA plasmids and endogenous chromosomes (Baxter et al., 2011; Charbin et al., 2014; Farcas et al., 2011; Mariezcurrena and Uhlmann, 2017; Sen et al., 2016). Moreover, chromosome attachment to the bipolar metaphase spindle is sufficient to trigger the removal of catenanes from the centromeres (Mariezcurrena and Uhlmann, 2017). An intuitive

explanation for this observation is that, upon attachment to the bipolar spindle, physical separation of the sister centromeres drives their decatenation or simply allows the intertwines to diffuse away from the locus (**Figure 1.17C**).

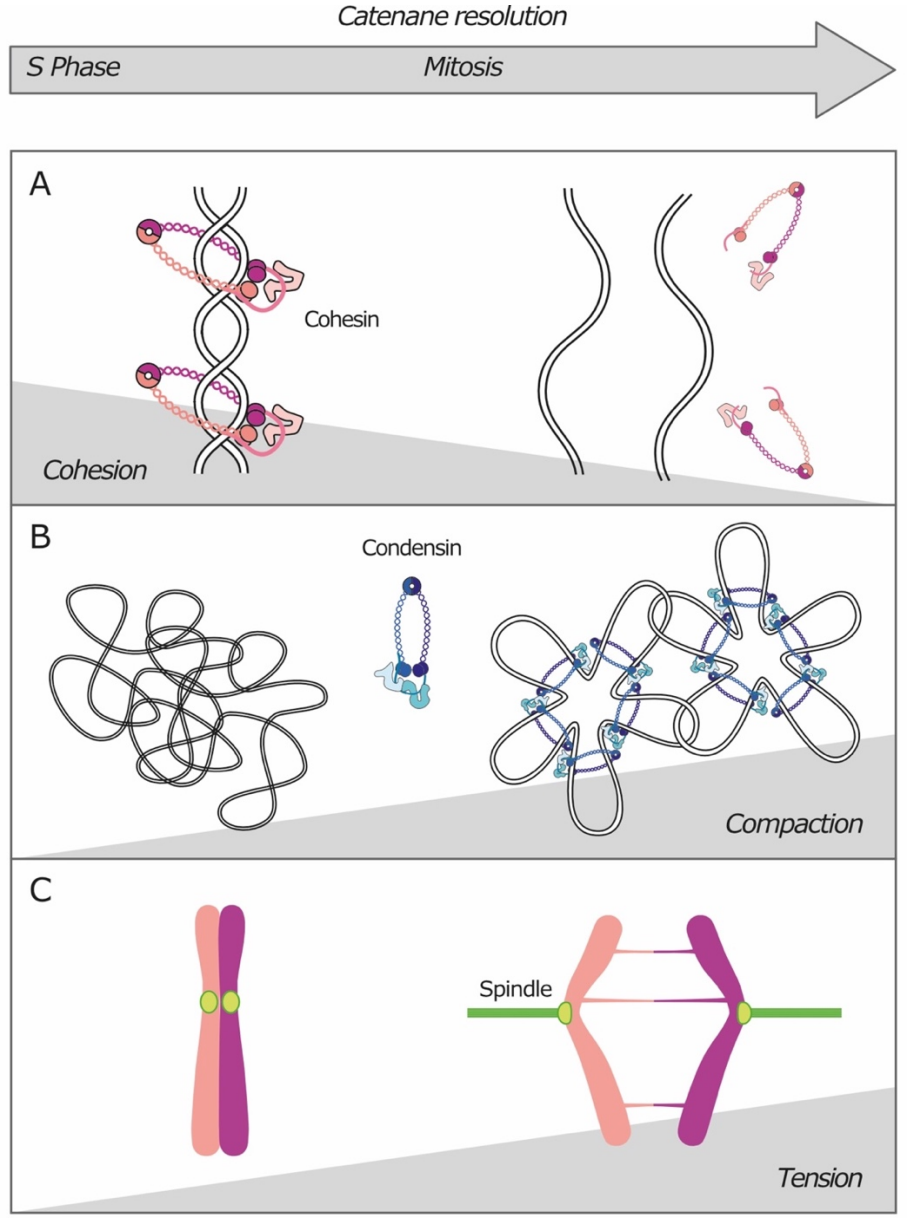

Figure 1.17. Mitotic processes involved in the resolution of DNA linkages
*(**A**) Cohesin cleavage, (**B**) condensin-mediated chromosome compaction, and (**C**) chromatid separation by the mitotic spindle provide directionality to the reaction catalyzed by Top2, favoring the resolution of DNA catenanes. Adapted from (Finardi et al., 2020).*

By extension, spindle elongation during anaphase may assist the complete removal of SCI from the rest of the chromosome. This idea is supported by a study on the segregation of abnormally long chromosomes in yeast cells. Segregation of these longer chromosomes is delayed and heavily depends on Top2 activity in anaphase. The segregation defects of Top2 mutants were ameliorated by removing the attachment of the extra-long chromosome to

the nuclear membrane, indicating unresolved DNA catenanes. Interestingly, inactivation of the microtubule polymerase Stu2 impaired chromosome segregation more intensely in cells with extra-long chromosomes, suggesting that spindle elongation and microtubule dynamics support sister chromatid decatenation also during anaphase (Titos et al., 2014).

In addition to chromatid separation, spindle elongation may help the resolution of anaphase bridges in other ways. The tension imposed by the spindle could alter DNA topology and favor the action of the enzymes devoted to their recognition and resolution. For example, tension may unwind the hemicatenane-like structure of LRIs and JMs, thus facilitating their dissolution by the STR complex.

1.4.6. Consequences of unresolved DNA bridges

Anaphase bridges as a cause of genome instability

If not properly resolved, anaphase bridges will eventually break, causing DNA lesions and genome instability, a hallmark of cancer development. It was recently described how even one single unresolved bridge triggers a cascade of events that progressively lead to dramatic genome rearrangements (Umbreit et al., 2020). Due to the fast proliferation, many cancer cells are subject to high replicative stress (Gaillard et al., 2015). Reasonably, as anaphase bridges are increased by replicative stress (Chan et al., 2009; Germann et al., 2014; Naim and Rosselli, 2009), they may form more frequently in cancer cells. If this was the case, DNA bridges, being both a consequence of replicative stress and a cause of genome instability, might be a driver of tumor progression.

Barbara McClincktock was the first to hypothesize how anaphase bridges could possibly cause genome instability, through the so-called breakage-fusion-bridge (BFB) cycle (McClintock, 1941). According to this model, DNA bridges would be chopped during cytokinesis and then re-sealed in the daughter cells with other chromosome segments, resulting in the reciprocal exchanges of chromosome arms. More recently, Pellman and colleagues extended this model and found that, in addition to the chromosomal aberrations predicted by the BFB model, bridge rupture causes more complex rearrangements. Starting from the second generation after bridge appearance, they observed chromothripsis, which is the shredding of one or a few chromosomes, followed

by the reassembling of the fragments in random order. Chromothripsis was caused by abnormal replication of the DNA within the bridge during mitosis (Umbreit et al., 2020).

For what concerns the causes of rupture, anaphase bridges could snap under the pulling force of the spindle or be severed by the actomyosin ring during cytokinesis. The force generated by the spindle is estimated to be far too weak to break mitotic chromosomes (Houchmandzadeh et al., 1997), but it could be sufficient to break a single DNA fiber (Bustamante et al., 2000), especially if they contain ssDNA. Nevertheless, this mechanism of bridge rupture was not yet confirmed *in vivo*. Instead, in yeast, cytokinesis was demonstrated to severe chromatin bridges and cause DSBs in *top2* and condensin mutants (Baxter and Diffley, 2008; Cuylen et al., 2013).

The NoCut checkpoint

To avoid the rupture of DNA threads during abscission and safeguard genome integrity, cells have evolved a mechanism that delays cytokinesis in the presence of chromatin trapped on the site of cleavage. In yeast cells, this mechanism is termed the NoCut checkpoint, and it requires the activity of Aurora B/Ipl1 at the spindle midzone (Mendoza et al., 2009; Norden et al., 2006). At the cleavage plane, Ipl1 acts as a sensor for chromatin and, in the presence of bridges, delays completion of abscission and inhibits degradation of spindle proteins, thus stabilizing the spindle (Amaral et al., 2016; Mendoza et al., 2009; Norden et al., 2006). The NoCut is activated in conditions of replicative stress and in absence of condensin or Top2 activity, indicating that it can detect various types of SCIs, but does not respond to the bridging of dicentric chromosomes (Amaral et al., 2016). This checkpoint provides additional time for the removal of DNA linkages, but cells eventually divide even if the bridge is not resolved.

An analogous mechanism, called abscission checkpoint, was also described in mammalian cells (Petsalaki and Zachos, 2019). Like the NoCut, this checkpoint relies on Aurora B and delays abscission in the presence of chromatin on the cleavage site.

2. Materials and methods

2.1. Plasmids, primers, and strains

2.1.1. Plasmids

Plasmids used in this study are listed in **Table 2.1**. Plasmids were amplified in TOP10 chemically competent *Escherichia coli* cells.

2.1.2. Primers

Primers used in this study are listed in **Table 2.2**.

2.1.3. Yeast strains

All the *Saccharomyces cerevisiae* strains used in this study are isogenic to the W303 background (*ade2-1, can1-100, trp1-1 leu2-3,112, his3-11,15, ura3*), except for the mating-type tester strains Ry72 and Ry73. Strains were generated either by transformation of circular or linearized plasmids or PCR-generated deletion cassettes, or by dissecting sporulated heterozygous diploid strains obtained by crossing haploid strains of the opposite mating type (see section 2.3.4 and 2.5.1 for procedures). The relevant genotypes of the yeast strains used in this study are listed in **Table 2.3**.

2.2. Growth media and conditions

2.2.1. Media for *Escherichia coli*

Bacterial cells were grown in LB medium.

LB (pH 7.25):

- 1% Bacto Tryptone (DIFCO)
- 0.5% yeast extract (DIFCO)
- 1% NaCl

LB was supplemented with 50 µg/ml ampicillin (LB + amp). For solid media 2% agar (DIFCO) was added to the medium. All strains were grown at 37°C.

2.2.2. Media for *Saccharomyces cerevisiae*

Yeast cells were grown in rich medium (YP) or synthetic minimal medium (SC).

YP (pH 5.4):

- 1% yeast extract
- 2% Bacto Peptone
- 0.015% L-tryptophan

YP was supplemented with 300 µM adenine and either 2% glucose (YPD) or 2% raffinose (YPR) or 2% raffinose and 2% galactose (YPR/G) as carbon sources. For solid media 2% agar (DIFCO) was added.

SC:

- 0.15% yeast nitrogen base (YNB, DIFCO) without aminoacids and ammonium sulfate.
- 0.5% ammonium sulfate
- 200 nM inositol

SC was supplemented with either 2% glucose (SCD), or 2% raffinose (SCR), or 2% raffinose and 2% galactose (SCR/G) as carbon sources and amino acids as required. For solid media 2% agar (DIFCO) was added.

All strains were grown at 23°C unless otherwise stated. Growth conditions for individual experiments are described in the corresponding figure legend.

2.3. DNA-based procedures

2.3.1. *Escherichia coli* transformation

Chemically competent Top10 cells (50 µl) were thawed on ice for approximately 10 minutes (min) prior to the addition of plasmid DNA or ligation mixture. Cells were incubated with DNA on ice for 30 min and then subjected to a heat shock for 30-45 seconds (sec) at 37°C. After the heat shock, cells were placed on ice for 2 min. Finally, 950 µl LB medium was added and the cell suspension was incubated on a shaker at 37°C for 45 min. Cells were plated onto LB + amp plates and incubated overnight (O/N) at 37°C.

2.3.2. Plasmid DNA isolation from *Escherichia coli* (mini prep)

Clones picked from individual colonies were inoculated in 5ml LB + amp and grown O/N at 37°C. Cells were harvested by centrifugation at 3,000 revolutions per minute (rpm) for 10 min and transferred to an eppendorf tube. Then, cells were pelleted for 1 min at 13,000 rpm. Minipreps were performed with QIAprep Spin Miniprep Kit (Qiagen) following the manufacturer's instructions. Plasmids were eluted in 30 µl of sterile double-distilled water (ddH2O).

2.3.3. Plasmid DNA isolation from *Escherichia coli* (maxi prep)

Cells containing the plasmid of interest were inoculated in 100ml LB + amp and grown O/N at 37°C. Cells were harvested by centrifugation at 3,000 rpm for 15 min. Maxipreps were performed with QIAprep Spin Maxiprep Kit (Qiagen) following the manufacturer's instructions. Plasmids were eluted in 500µl of ddH2O.

2.3.4. High-efficiency LiAc-based yeast transformation

Yeast cells were grown O/N in 50 ml YPD, or the appropriate medium. The following morning, the cell culture was diluted to OD_{600} = 0.2 and allowed to grow several cycles until it reached an OD_{600} of 0.4-0.7. Cells were harvested by centrifugation at 3000 rpm for 3 min and washed with 50 ml ddH2O. The pellet was transferred to an eppendorf tube with 1 ml ddH2O and washed with 1 ml 1X TE/LiAc solution. Then, cells were resuspended in 250 µl 1X TE/LiAc solution. A 50 µl aliquot of competent cells was used for each transformation with 300 µl 1X PEG/TE/LiAc solution, 5 µl 10 mg/ml single-stranded salmon sperm denatured DNA and "x" µl (up to 10 µl) DNA. After gentle mixing, the transformation reaction was incubated on a rotating wheel for 30 min at room temperature (RT). Cells were then heat-shocked at 42°C for 15 min, followed by centrifugation for 3 min at 3000 rpm. The pellet was resuspended in 200 µl 1X TE and cells were plated on an appropriate auxotroph selective medium. In case of selection for resistance to the antibiotic geneticin (G418), after resuspension in 1X TE cells were plated on YPD plates to allow the cells to recover after the heat shock before exposure to antibiotics. After two days, the resulting colonies were replica plated on YPD plates containing 220 µm/ml G418.

10X TE:

- mM Tris, brought to pH 8.0 with HCl
- 10 mM EDTA, pH 8

10X LiAc:

- 1 M LiAc, brought to pH 7.0 with acetic acid

1X TE/LiAc:

- 1X TE
- 1x LiAc

1X PEG/TE/LiAc:

- 1X TE
- 1X LiAc
- 40% PEG 4000

2.3.5. Quick yeast genomic DNA preparation (Smash and Grab)

Cells were picked from individual yeast colonies and resuspended in 200 µl Lysis buffer in eppendorf tubes. Next, 200 µl phenol/chloroform/isoamyl alcohol 25:24:1 (SIGMA) and 1 volume of glass beads were added to the tubes and cells were lysed by shaking for 10 min on Vxr Ika-Vibrax shaker at 4°C. Tubes were centrifuged twice for 4 min at 13,000 rpm and the upper aqueous layer was transferred to new tubes. 1 ml ice-cold 100% ethanol (EtOH) was added to precipitate the DNA. After mixing, tubes were centrifuged for 4 min at 13,000 rpm. After removing the supernatant (SN), the pellets were air-dried and the DNA resuspended in 50 µl 1X TE.

Lysis buffer:

- 2% Triton X-100
- 1% sodium dodecyl sulfate (SDS)
- 100 mM NaCl
- 10 mM Tris, brought to pH 8.0 with HCl
- 1 mM EDTA, pH 8.0

2.3.6. Yeast genomic DNA extraction

Yeast cells were grown in 10 ml YPD medium to stationary phase. Cells were harvested by centrifugation and washed with 1 ml of ddH2O. Pellets were resuspended in 200µl of SCE solution with 1.5 mg/ml Zymolyase 100T (AMS Biotechnology) and 8µl β-mercaptoethanol and incubated at 37°C in an eppendorf tube until complete spheroplast formation (30 min-60 min). Digestion was checked under an optical microscope by mixing a drop of reaction with an equal volume of 1% SDS and looking for burst spheroplasts. Next, 200 µl of SDS solution were added and samples were incubated at 65°C for 5 min. After the addition of 200 µl of 5M KAc, samples were mixed and left on ice for 20 min. Samples were centrifuged for 10 min at 13000 rpm and the SN was carefully transferred to new tubes. The DNA was then precipitated with 200 µl of 5M NH_4Ac and 1 ml of isopropanol, collected by centrifuging 15-30 sec at 3000 rpm, and resuspended in 180 µl of 1X TE. Then, the precipitation step was repeated twice, first with 20µl NH4Ac 5M and 400µl isopropanol and next with 10µl NH4Ac 5M and 200µl isopropanol. Finally, the DNA was resuspended in 30µl 1X TE.

SCE Solution (pH 7.0):

- 0.1M sorbitol
- 60mM EDTA
- 0.1M NaCitrate

SDS solution:

- 50mM EDTA pH 8.0
- 0.1M Tris pH 9.0
- 2% SDS

2.3.7. DNA precipitation with NaAcetate and EtOH

Samples were mixed with 1/10 volume of NaAcetate 3M and two volumes of ice-cold EtOH 100% and, then, incubated at -20°C for 1 hour (hr). Next, tubes were centrifuged for 15 min at 13000 rpm at 4°C and SN was removed. The pellet was washed with 1 ml of ice-cold EtOH 70% and centrifuged for 15 min at 13000 rpm at 4°C. After removing the SN, the pellet was air-dried and resuspended in the appropriate volume of TE.

2.3.8. DNA digestion with restriction enzymes

For diagnostic DNA restriction, 0.5-2 µg of plasmid DNA were digested for 1 hr at 37°C with 1-10 units of the appropriate restriction enzyme (New England Biolabs, NEB). The reaction volume (20-50µl, depending on DNA concentration) was adjusted with the appropriate buffer and ddH2O. For preparative DNA restriction 5-10µg of plasmid DNA were incubated for 3 hrs at 37°C with 1-10 units of restriction enzyme. Enzymes were inactivated following manufacturer instructions. In the case of integrative plasmids to be used for yeast transformation, the DNA was then concentrated by precipitation (see section 2.3.7) and resuspended in 10 µl ddH2O.

2.3.9. DNA amplification through polymerase chain reaction (PCR)

PCR was performed using genomic yeast DNA or plasmid DNA as a template, ExTaq (TaKaRa) DNA polymerase, 0.2 mM dNTPs, 0.2 µM forward and reverse primers (listed in Table 2.2), and with Biometra T3000 Thermocycler. For each yeast transformation, 50 ul reaction of amplified DNA was concentrated by precipitation (see section 2.3.7) and resuspended in 10ul ddH2O. Gene tagging with the auxin-inducible degron (AID) tag (Nishimura et al., 2009) was performed as described in (Morawska and Ulrich, 2013). Otherwise, PCR-mediated gene deletion and tagging were performed as described in (Longtine et al., 1998).

2.3.10. Agarose gel electrophoresis

Following the addition of 1/5 volume of bromophenol blue solution 6X, DNA samples were loaded on agarose gels of appropriate concentration, along with DNA markers. Gels were made in 1X Tris-Acetate-EDTA (TAE) buffer containing 1X SybrSafe (Invitrogen) and run at 80-120V until the desired separation was achieved. DNA bands were visualized with the GelDoc EZ Imager (Biorad).

6X bromophenol blue solution:

- 0.2% bromophenol blue
- 50% glycerol

10X TAE buffer:

- 0.4M Tris acetate
- 0.01M EDTA

2.3.11. Purification of DNA from agarose gel

Digested DNA was first loaded into an agarose gel to separate the DNA fragments by electrophoresis. The fragments of interest were then excised from the gel with a sharp scalpel. DNA extraction was performed with QIAquick Gel Extraction Kit (Qiagen) following the manufacturer's instructions. The DNA fragments were eluted in 30-50 µl ddH2O.

2.3.12. DNA ligation

Vector DNA (50ng) was ligated with a 3- and a 6-fold molar excess of insert DNA in the following conditions: 1X Quick DNA ligase buffer, 1µl Quick DNA ligase (New England Biolabs, NEB) and ddH2O up to 10-20µl (depending on DNA concentration). Reactions were incubated for 10 min RT and then transformed into TOP10 *E. coli* competent cells.

2.3.13. *ULP2* constructs

For *ULP2* overexpression, the *ULP2* gene was amplified by PCR from genomic yeast DNA with primers containing XbaI and HindIII restriction (AF1 and AF2, see **Table2.2**) sites and, then, cloned under the control of *PGAL1-10* promoter in the integrative vector YIplac204, to obtain plasmid Rp703. After cloning, *ULP2* was sequenced to check for the absence of mutations. Rp703 was linearized with Bsu36I before being used to transform yeast. To discriminate between single or multiple events of plasmid integration, transformed clones were analyzed by PCR with dedicated primers (AD80, AD81, and AD82, see **Table 2.2**).

For expression of *ULP2* under its own promoter, the 1000 base-pair (bp) region upstream of the *ULP2* gene was amplified by PCR from genomic yeast DNA with primers containing KpnI and XbaI restriction sites and, then, cloned into the centromeric vector YCplac33. Next, the *ULP2* gene was excised from Rp703 and cloned into YCplac33/PULP2 by digestion with XbaI and HindIII, to obtain Rp704.

2.3.14. *TOP2* constructs

Plasmids pCC117 and pML251 were gifts from S. Elledge lab (Bachant et al., 2002). To replace *TOP2* gene with *TOP2-HA3-KanMX* or *top2-snm-HA3-KanMX*, the pCC117 or pML251, respectively, were digested with DraIII. The 5349 bp fragment obtained by digestion was isolated from an agarose gel and used to transform yeast. The *top2-snm-HA3-KanMX* construct contains an XhoI site. To check for the presence of *top2-snm* mutation, transformed clones were analyzed by PCR spanning the locus, followed by XhoI digestion and visualization of the obtained fragments by agarose gel electrophoresis.

2.4. Protein-based procedures

2.4.1. Yeast protein extraction (Tris-HCl extracts)

Samples of 10ml cell culture at OD_{600} = 0.2-1 were pelleted by centrifugation for 3 min at 4000 rpm. The pellets were washed with 1ml of cold 10mM Tris-HCl pH 7.5 and transferred to 2ml Sarstedt tubes. Tubes were centrifuged for 1 min at 13,000 rpm and the SN was removed. The pellets were frozen in liquid nitrogen and stored at -80°C. Pellets were then resuspended in 100µl lysis buffer with complete protease inhibitor cocktail (Roche), phosphatase inhibitor cocktail 2 (Sigma), and N-Ethylmaleimide (NEM). An equal volume of acid-washed glass beads (Sigma) was added and the cells were lysed in 4-7 rounds of Fast Prep (speed 6.5 for 45 sec) at 4°C. Cell breakage was checked under the optical microscope. Lysates were transferred to new Eppendorf tubes. In order to quantify the protein concentration, 10µl of each lysate were diluted 1:3 in cold 50mM Tris-HCl pH 7.5 / 0.3M NaCl and 3µl of the mixture were used for the Biorad protein quantification assay. The absorbance was read at λ = 595 nm. Lysates were added with 50µl of 3X SDS blue loading buffer, boiled at 95°C for 5 min, and then centrifuged at 13000 rpm for 3 min. The SN was moved to a new tube. Extracts were stored at -20°C.

Lysis buffer:

- 50mM Tris-HCl pH 7.5
- 1mM EDTA pH 8
- 50mM DTT

3X SDS blue loading buffer:

- 9% SDS 30% glycerol
- 0.05% Bromophenol blue
- 6% β-mercaptoethanol
- 0.1875M Tris-HCl pH 6.8

2.4.2. Yeast protein extraction with TCA (TCA extracts)

Samples of 10 ml cell culture at OD_{600} = 0.2-1 were pelleted by centrifugation for 5 min at 4000 rpm. The pellets were resuspended in an equal volume of ice-cold 5% trichloroacetic acid (TCA) and incubated for 10 min on ice. After centrifugation for 5 min at 4000 rpm at 4°C, pellets were transferred to a 2 ml Sarstedt tube. Tubes were centrifuged for 1 min at 13,000 rpm at 4°C and SN discarded. Pellets were frozen in liquid nitrogen and stored at -80°C. Then, pellets were washed with 1 ml absolute acetone and air-dried. Pellets were then resuspended in 100 µl lysis buffer with complete protease inhibitor cocktail (Roche), phosphatase inhibitor cocktail 2 (Sigma), and NEM. An equal volume of acid-washed glass beads (Sigma) was added and cells were lysed in 4-7 rounds of Fast Prep (speed 6.5 for 45 sec) at 4°C. Cell breakage was verified using an optical microscope. Lysates were added with 50µl of 3X SDS blue loading buffer, boiled at 95°C for 5 min, and then centrifuged at 13000 rpm for 3 min. The SN was moved to a new tube. Extracts were stored at -20°C.

2.4.3. SDS polyacrylamide gel electrophoresis

Appropriate amounts of total protein extracts (50-100 µg) were separated based on their molecular weight on polyacrylamide gels of the appropriate concentration. For gradient gels, 4-15% polyacrylamide precast gels (BioRad) were used. The gels were prepared from a 30% 30:0.8 acrylamide:bisacrylamide mixture (Sigma), 4X Separating buffer, 2X Stacking buffer, and an appropriate amount of ddH2O. As polymerization catalysts, ammonium persulfate (APS) and TEMED (BDH) were used. 1.5 mm thick polyacrylamide gels were run in 1X running buffer at 60-120 V for the appropriate time. Phos-tag gels were performed according to (Kinoshita et al., 2009).

4X Resolving buffer:

- 1.5 M Tris base, brought to pH 8.8 with glacial acetic acid
- 0.4% SDS

2X Stacking buffer:

- 0.25 M Tris base, brought to pH 6.8 with glacial acetic acid
- 0.2% SDS

10X Running buffer (pH 8.3):

- 2 M glycine
- 0.25 M Tris-HCl
- 0.02 M SDS

2.4.4. Western blot hybridization

Proteins were transferred in western transfer tanks to nitrocellulose (Protran, Whatman) in 1X transfer buffer at 30 V O/N. Ponceau S staining was used to roughly reveal the amount of proteins transferred onto the filters. Membranes were blocked with 1X phosphate-buffered saline (PBS) with 1% Tween (PBS-T) and 3% milk for 1 hr at RT. After blocking, the membranes were incubated with the primary antibody, then washed 3 times for 10 min in 1X PBS-T. Afterward, the membranes were incubated with the horseradish-peroxidase (HRP)-conjugated secondary antibody in 1% milk / 1% BSA / 1X PBS-T for 1 hr. After incubation with the secondary antibody, the membranes were washed 3 times for 10 min in 1X PBS-T and the bound secondary antibody was revealed using ECL (Enhanced Chemiluminescence, Amersham) and imaged with ChemiDoc System (BioRad).

The primary antibodies used were SV5-Pk1 monoclonal anti-PK (AbD Serotec, used at 1:5000 dilution) to detect Top2-9PK; HA.11 monoclonal anti-HA (CVMMS-101R-1000, Covance, used at 1:1,000 dilution) to detect and Ulp2-3HA; 9E10 monoclonal anti-myc (CVMMS-150R-1000, Covance, used at 1:1,000 dilution) to detect Cdc5-13myc; anti-Clb2 (Y-180; SC-9071, Santa Cruz Biotechnology, used at 1:1,000 dilution); goat anti-Cdc5 (Santa Cruz, used at 1:1000 dilution); rabbit anti-SMT3 (gifted by I. Psakhye, used at 1:2000 dilution); monoclonal anti-Pgk1 (A-6457, Molecular Probes, used at 1:5,000 dilution); rabbit anti-Kar2 (gifted by Dr. Kilmartin, used at 1:2000.000 dilution); monoclonal anti-AID (Invitrogen). Secondary antibodies used were goat anti-rabbit IgG (H + L)-HRP conjugate (170-6515, Bio-Rad, used at 1:10,000 dilution), goat anti-mouse IgG (H + L)-HRP conjugate (170-6516, Bio-Rad, used at 1:10,000 dilution) and anti-goat IgG (H + L)-HRP conjugate (used at 1:5000 dilution).

1X Transfer buffer:

- 0.2 M glycine
- 0.025 M Tris base
- 20% methanol

10X PBS buffer:

- 1.37 M NaCl
- 27 mM KCl
- 14.7 mM KH2PO4
- 80 mM Na2HPO4

1X PBS-T buffer:

- 0.1% Tween
- 1X PBS

2.4.5. Immunoprecipitation of Top2 and Ulp2 and phosphatase treatment

Protein extraction was performed as in (Baldwin and Bachant, 2009). Samples of 50 ml cell culture at OD_{600} = 0.2-1 were pelleted by centrifugation for 10 min at 3000 rpm. The pellets were resuspended in 20 ml of ice-cold 5% TCA and incubated for 10 min on ice. After centrifugation for 5 min at 4000 rpm at 4°C, pellets were transferred to a 2 ml Sarstedt tube. Tubes were centrifuged for 1 min at 13,000 rpm at 4°C and SN discarded. Pellets were frozen in liquid nitrogen and stored at -80°C. Then, pellets were resuspended in 300 µl of ice-cold 20% TCA with protease inhibitor cocktail (Roche), phosphatase inhibitor cocktail 2 (Sigma), and NEM. An equal volume of acid-washed glass beads (Sigma) was added and cells were lysed in 4-7 rounds of Fast Prep (speed 6.5 for 45 sec) at 4°C. The lysate was separated from the beads and centrifuged 5min at 13000 rpm at 4°C. The protein precipitate was resuspended in 200 µl of 1:1 mix of 1M Tris base and HEPES solution, supplemented with inhibitors. To solubilize the proteins, SDS was added to the final concentration of 2% and samples were boiled for 5min at 95°C. Then, samples were centrifuged for 5min at 13000 rpm and the SN was transferred to a new 2 ml tube. The lysate was diluted with 9 volumes of NP40 buffer with inhibitors and used for immunoprecipitation (IP). An aliquot of 10 µl of input was taken, mixed with 3x SDS buffer,

and stored for quality control. To perform IP, SV5-Pk1 monoclonal anti-PK (AbD Serotec, used at 1:5000 dilution) and monoclonal 12CA5 anti-HA were used at 1:100 dilution for Top2-9PK and Ulp2-3HA, respectively. Samples were incubated on a rotating wheel at 4°C O/N. The next morning, each sample was added with 50 µl of Dynabeads Protein G (Invitrogen) and incubated on a rotating for 1 hr at 4°C. An aliquot of 50 µl of flow-through was taken, mixed with 3x SDS buffer, and stored for quality control. The beads were washed four times with NP40 buffer, once with 10 mM Tris-HCl, pH 7.5, and, for phosphatase treatment, once with phosphatase buffer. During each wash, samples were centrifuged at 2500 rpm and incubated on a rotating wheel for 5min at 4°C with 1 ml of wash solution. For phosphatase treatment, beads were resuspended in phosphatase buffer and split equally into two tubes ("phosphatase" and "no phosphatase"). After removing the SN, each sample was resuspended in 50 µl of phosphatase buffer/1 mM $MgCl_2$ solution, 1 µl of lambda protein phosphatase (NEB) was added where needed, and tubes were incubated for 30 min at 30°C. Finally, SN was removed and proteins were eluted in 30 µl of 3x SDS buffer.

HEPES solution:

- 25 mM HEPES pH7.5
- 100 mM KCl
- 2 mM EDTA
- 10% glycerol

Lambda-phosphatase buffer:

- 50 mM HEPES
- 100 mM NaCl
- 1 mM MgCl2

2.4.6. Purification of His8-SUMO conjugates

The following protocol is derived from (Thu et al., 2016) and applies to scaled-up experiments. For scaled-down tests, the purification was performed with 10-fold decreased quantities.

Samples of 500 ml cell culture at OD_{600} = 0.6-0.8 were centrifuged for 10 min at 3000 rpm. Cells were washed with ice-cold ddH2O, centrifuged again, and SN was removed. Pellets

were frozen in liquid nitrogen and stored at -80°C. Then, each pellet, corresponding to 500ml cell culture, was resuspended in 40 ml ice-cold ddH2O and split into two tubes. To lyse the cells, 3.2 ml of NaOH/β-mercaptoethanol was added to each tube and samples were left for 20 min on ice. Next, samples were centrifuged for 20 min at 3500 rpm at 4°C and SN was discarded. To solubilize the proteins, 3 ml of urea buffer/15 mM imidazole were added to each tube, samples were incubated on a shaker for 1 hr at RT, and the resuspension was transferred to a new tube. These steps were repeated until the pellet was completely dissolved. Then, tubes were centrifuged for 1 min at 13000 rpm and the SN was moved to a new tube, pooling identical samples. An aliquot of 50 µl of input was taken, mixed with 3x SDS buffer, and stored for quality control. For each purification, 5 ml of 50% slurry of Talon Metal Affinity Resin (Clontech) were used. The resin was washed with 10 volumes of ddH2O, then with five volumes of urea buffer, and then resuspended in one volume of urea buffer. After washing, the resin was used to prepare an adequate amount of gravity flow columns. To bind the proteins, the lysate was added to the column and incubated for 2h at RT rotating. Then, the column was allowed to drain and an aliquot of 50 µl of flow-through was taken, mixed with 3x SDS buffer, and stored for quality control. The columns were washed three times with 10 volumes of urea buffer/25 mM imidazole and three times with 10 volumes of urea buffer/30 mM imidazole. During each wash, the column was allowed to drain and then incubate with the wash solution for 5 min at RT rotating. Proteins were eluted three times in one volume of elution buffer/200 mM imidazole. During each elution, columns were incubated on a shaker for 5 min at RT. The eluate was collected in new tubes. In scale-up experiments, the eluted proteins were precipitated with 6 volumes of ice-cold 50% ethanol/25% methanol/25% acetone solution and incubated at -20°C O/N. The next morning, samples were centrifuged for 20 min at 13000 rpm at 4°C, the SN was removed and the pellet was air-dried. Finally, 30 µl of elution buffer were added and the pellet was dissolved by shaking at RT for 30 min.

NaOH/β-mercaptoethanol:

- 1.85 M NaOH
- 7.5% β-mercaptoethanol

Urea buffer (pH 8.0):

- 8 M urea
- 300 mM NaCl
- 0.5% NP-40
- 50 mM Na2HPO4
- 50 mM Tris-HCl pH 8.0
- 0.05% Tween

Elution buffer (pH 7.0):

- 8 M urea
- 200 mM NaCl
- 2% SDS
- 50 mM Na2HPO4
- 50 mM Tris-HCl pH 7.0

2.4.7. Chromatin Immunopurification and sequencing (ChIP-seq) of Top2

Samples of 50 ml cell culture at OD_{600} = 0.6 were crosslinked with formaldehyde 1% final concentration for 40 min at RT shaking. Crosslinking was stopped by adding glycine to 125 mM final concentration and incubating for 5 min at RT shaking. Cells were pelleted by centrifugation for 5min at 3000 rpm at 4°C. The pellet was washed twice with 20 ml of ice-cold TBS and then moved to a tube. Tubes were centrifuged for 1 min at 13000 rpm at 4°C, the SN was removed and pellets were frozen in liquid nitrogen and stored at -80°C. Then, cells were resuspended in 500 ul of ChIP lysis buffer supplemented with protease inhibitor cocktail (Roche) and 1 mM PMSF. An equal volume of acid-washed glass beads (Sigma) was added and cells were lysed in 4-7 rounds of Fast Prep (speed 6.5 for 45 sec) at 4°C. Next, the lysate was separated from the beads. The chromatin was shared by sonicating 20 times for 30 sec with 1 min interval using Bioruptor UCD-300 (Diagenode) water-bath sonicator at 4°C set on “high”. Then, samples were centrifuged for 5 min at 13000 rpm at 4°C and SN was moved to a new tube. An aliquot of 5 µl was taken as input and stored O/N at 4°C. For IP, 3 µl of SV5-Pk1 monoclonal anti-PK (AbD Serotec) were added to the lysate, the final volume was adjusted to 500 µl with ChIP lysis buffer with inhibitors, and samples were incubated on a rotating wheel O/N at 4°C. The next morning, 30 µl of Dynabeads Protein G

(Invitrogen) for each sample were equilibrated by washing twice in ChIP lysis buffer and then resuspended in the same volume of ChIP lysis buffer supplemented with inhibitors. Then, the beads were added to the IP and samples were incubated on a rotating wheel for 2 hrs at 4°C. The beads were washed twice with 1 ml ChIP lysis buffer, twice with 1 ml ChIP lysis buffer/360 mM NaCl, twice 1 ml with ChIP wash buffer, and once with 1 ml TE. After the last wash, the SN was removed and beads were resuspended in 30 µl ChIP elution buffer and incubated at 65°C for 1 min. The IP was separated from the beads and moved to a new tube. From now on, IP and input samples were processed together. To revert crosslink, TE/1% SDS was added up to 100 µl and 150 µl for input samples and IPs, respectively, and tubes were incubated at 65°C O/N. The next morning, Proteinase K was added to 1 mg/ml final concentration and samples were incubated at 37°C for 2 hrs to reverse crosslink. Then, samples were moved to phase lock gel tubes and an equal volume of phenol/chlorophorm/isoamylalchol (25:24:1, pH 8.0) was added. Tubes were centrifuged for 5 min at 13000 rpm and the upper phase was transferred to a new tube. Then, DNA was precipitated with NaCl 100 mM final concentration and one volume of ice-cold EtOH 100%, followed by incubation at -20°C O/N. The next morning, tubes were centrifuged for 15 min at 13000 rpm at 4°C, SN was removed, and pellets were air-dried. Pellet was resuspended in 70 µl of TE, 1 µl of 10 mg/ml RNase A was added, and samples were incubated for 1h at 37°C. Finally, DNA was purified with QIAquick PCR purification kit (QIAGEN), following manufacturer instructions. DNA library preparation was performed by the Genomic Unit of the IFOM/IEO/IIT campus according to established protocol (Blecher-Gonen et al., 2013) and sequenced with the Illumina Novaseq 6000 instrument at 50bp paired-end read length and coverage of 30 million reads per sample. The data were analyzed in collaboration with D. Fernandez-Perez as follows. Raw reads were aligned to sacCer3 genome downloaded from UCSC (https://genome.ucsc.edu/). The alignment was performed using Bowtie2 (PMID: 22388286) with *parameters --local --very-sensitive-local --no-unal --no-mixed --no-discordant --phred33 -I 10 -X 700*. PCR duplicates were removed using samblaster (PMID: 24812344) with the flag -r. To call peaks, PCR duplicate-free bam files were used as input to MACS2 (PMID: 18798982), which was executed with the following parameters: *-f BAMPE -g 1.21e07 -p 1e-5*. Bigwig files were generated using deeptools (PMID: 27079975) with the function bamCoverage with parameters *--normalizeUsing CPM --extendReads -bs 5*. Annotation files of genomic features were downloaded from the SGB database (https://www.yeastgenome.org/), in particular the file saccharomyces_cerevisiae.gff, which was downloaded to perform ChIP-seq signal quantification across ARS, Centromeres,

LTRs and Telomeres. Quantification of ChIP-seq signal across different genomic features was performed with the R packages GenomicFeatures (PMID: 23950696) and Plyranges (PMID: 30609939), meanwhile heatmaps were produced using deeptools (PMID: 27079975), with the functions computeMatrix and plotHeatmap.

TBS 10x:

- 250 mM Tris
- 1.5 M NaCl
- 25 mM KCl

ChIP lysis buffer:

- 50 mM HEPES-KOH pH 7.5
- 140 mM NaCl
- 1 mM EDTA
- 1% Triton-x100
- 0.1% NaDeoxycholate

ChIP wash buffer:

- 10 mM Tris-HCl pH 8.0
- 250 mM LiCl
- 0.5% NP-40
- 0.5% NaDeoxycholate
- 1 mM EDTA

ChIP elution buffer:

- 50 mM Tris-HCl pH 8.0
- 10 mM EDTA
- 1% SDS

2.5. Cell biology procedures

2.5.1. Tetrad dissection and analysis

MATa and *MATalpha* strains were mixed on solid medium appropriate for the growth of both the haploids and incubated O/N at permissive conditions. Cells were then streaked to single colonies in medium and temperature conditions selective for diploid cells. Single

colonies of diploids were next amplified on rich medium for 1 day and next patched onto sporulation plates to induce sporulation by starvation. Sporulation was checked after 3-5 days under the microscope. To allow dissection of the individual spores, the ascus wall was digested with 200 µl of 0.1mg/ml Zymolyase 100T in ddH2O at 37°C for 3 min. Approximately 20 µl were then dripped in a line onto the appropriate agar plate. Individual tetrads were dissected using the Nikon dissection microscope. Spores were left to grow at 23°C for 3-5 days. Colonies were replica plated onto selective media to determine their genotype.

Sporulation plates:

- 30g K-Acetate
- 60g Agar (DIFCO)
- all amino acids at 1/4 of the normal concentration
- Adjust to 3L volume with ddH2O

2.5.2. Conditional mutants

Regulation of gene expression

To regulate the expression of specific proteins, yeast strains in which the encoding genes were placed under the control of inducible promoters were used. The *PGAL1/10* promoter (West et al., 1984) induces expression at high levels after the addition of galactose, while it shuts it off after the addition of glucose. To induce the overexpression of a gene of interest, 2% galactose was added to cells growing in a media containing raffinose, a poor carbon source. The *PMET3* promoter (Care et al., 1999) is a repressible promoter that switches off gene expression upon the addition of methionine. For gene repression, fresh methionine was added at 8 mM final concentration to cells growing in methionine-free medium. Methionine was added every hour at 4 mM final concentration to maintain repression.

Protein degradation

In this thesis, the AID degron system was used to induce the degradation of specific proteins (Nishimura et al., 2009). To deplete proteins through the AID system, 0.5mM of

indole-3-acetic acid (IAA, a natural auxin; Sigma) were added to the medium at the desired time.

Inactivation of temperature-sensitive alleles

Temperature-sensitive alleles were inactivated by shifting cells from permissive (23°C) to restrictive temperature (usually 37°C).

Inactivation of kinases with ATP-analogues

The *cdc5-as1* ATP-analogue sensitive allele (Snead et al., 2007) was inactivated by addition to the media of 5μM CMK inhibitor (Accenda Tech; dissolved in DMSO). The *cdc15-as1* and *cdc28-as1* ATP-analogue sensitive alleles were inactivated by adding 5μM 1NM-PP1 (Bishop et al., 2000).

2.5.3. Serial dilution spot assays

Cells were grown O/N in 5 mL in the appropriate medium at 23°C. Next morning, cells were diluted to OD_{600} = 0.2 in fresh medium and left to grow until they reached OD_{600} = 0.8-1.0. Then, serial dilutions (1:5) of yeast cell suspensions starting from OD_{600} = 1 were spotted onto plates of the appropriate medium and incubated at the desired temperature. Plates were imaged after 24 and 48 hrs.

2.5.4. Synchronization experiments

All synchronization procedures are derived from (Amon, 2002).

G1 phase arrest and release

Cells were grown O/N in the appropriate medium at 23°C. The next morning, cells were diluted to OD_{600} = 0.2 in fresh medium and left to grow for 1-2 hrs. Then, cells were diluted again to OD_{600} = 0.2 and 5 μg/ml α-mating factor synthetic peptide (Primm) dissolved in ddH2O were added. After 90 min, 2.5μg/ml α-factor was re-added to the culture. The G1 arrest was considered complete when more than 90% of the cells had the shmoo (after 2.30-3.30 hrs). At the arrest, cells were released from the G1 block by filtrating them and washing out α-factor with 10 volumes of medium without the pheromone. Cells were next released into the appropriate medium in the absence of α-factor.

S phase arrest

Cells were grown O/N in the appropriate medium at 23°C. The next morning, cells were diluted to OD_{600} = 0.2 in fresh medium and left to grow for 1-2 hrs. Then, cells were diluted again to OD_{600} = 0.2 and hydroxyurea powder (HU, Sigma) was added directly to the medium, to the final concentration of 10mg/ml. S phase arrest was considered complete after 3 hrs in HU.

Nocodazole-mediated metaphase arrest

Cells were grown O/N in the appropriate medium at 23°C. The next morning, cells were diluted to OD_{600} = 0.2 in fresh medium and left to grow for 1-2 hrs. The cells were then pre-synchronized in G1 by the addition of α-factor and then released in a medium containing 15 µg/ml nocodazole (NOC, Sigma) dissolved in DMSO. After 90 min from release, 7.5 µg/ml nocodazole was re-added to the culture.

Cdc20 depletion-mediated metaphase arrest

Cdc20 depletion arrests cells in metaphase. In this thesis, it was achieved by inducing Cdc20 degradation with the AID degron. Cells were first arrested in G1 as previously described, and next released in a medium containing 0.5mM IAA (Sigma).

2.5.5. Indirect immunofluorescence (IF)

The following protocol is adapted from (Kilmartin and Adams, 1984)

Samples of 1ml of cell culture at OD_{600} = 0.2-0.4 were collected by centrifugation for 1 min at 13000 rpm at RT and incubated O/N at 4°C in 1ml of fixative solution. Cells were then pelleted and washed 3 times with 1ml of 0.1M KPi pH 6.4 and once with 1ml of sorbitol-citrate solution. Cells were then resuspended in 200µl of digestion solution and incubated at 35°C for 20-30 min to enzymatically digest the cell wall, creating spheroplasts. Digestion was checked at the microscope. Spheroplasts were pelleted at 2000 rpm for 2 min and washed with 1ml of sorbitol-citrate solution. Pellets were then resuspended in the appropriate volume of sorbitol-citrate solution (20-200µl, depending on pellet size). 5µl of the resuspended spheroplasts were then loaded on a 30-well slide (ThermoScientific) previously treated for 10 min with 0.1% polylysine (Sigma). To fix cells, the slide was

incubated in ice-cold methanol for 3 min and then in ice-cold acetone for 10 sec. Cells were incubated for 60-90 min in a humid dark incubation chamber with a primary antibody diluted in PBS-BSA. Primary antibodies used were rat anti-tubulin (MCA78G, AbD Serotec, 1:100 dilution) and mouse anti-Nop1 (MCA-28F2, EnCore Biotechnology, 1:500 dilution). Then, cells were washed 5 times with PBS-BSA and incubated with the secondary antibody diluted in PBS-BSA for 60-90 min. Secondary antibodies used were FITC-conjugated anti-rat (1:100 dilution) and CY3-conjugated anti-mouse (1:500 dilution). Then, cells were washed 5 times with PBS-BSA and covered with a DAPI mount solution. Finally, the slide was covered with a coverslip and sealed with nail polish.

0.1M KPi buffer pH 6.4:

- 27.8ml 1 M K2HPO4
- 72.2ml 1 M KH2PO4
- 900ml ddH2O

Fixative solution:

- 3.7% formaldehyde
- 0.1M KPi pH 6.4

1.2 M Sorbitol-citrate:

- 17.4g Anhydrous KH2PO4
- 7g Citric acid
- 218.64g Sorbitol
- up to 1L with ddH2O

Digestion solution:

- 1.2M sorbitol-citrate
- 10% glusulase (Perkin-Elmer)
- 0.1mg/ml Zymolyase 100T

PBS-BSA:

- 1% crude BSA (Sigma)
- 0.04M K2HPO4
- 0.01M KH2PO4
- 0.15M NaCl
- 0.1% NaN3

DAPI mount solution:

- 0.04M K2HPO4
- 0.01M KH2PO4
- 0.15M NaCl
- 0.1% NaN3
- 0.05 µg/ml DAPI
- 0.1% p-phenylenediamine
- 90% glycerol

2.5.6. Analysis of immunofluorescence samples

Cell cycle progression

IF slides were visualized with a Leica DMR HC BIOMED fluorescence microscope using a 100X oil immersion objective. Cell cycle progression was scored by subdividing cells into three categories based on nuclear and spindle morphologies, namely interphase (G1/S), G2/metaphase, and anaphase/telophase cells (**Figure 2.1**). 100 cells were analyzed for each sample.

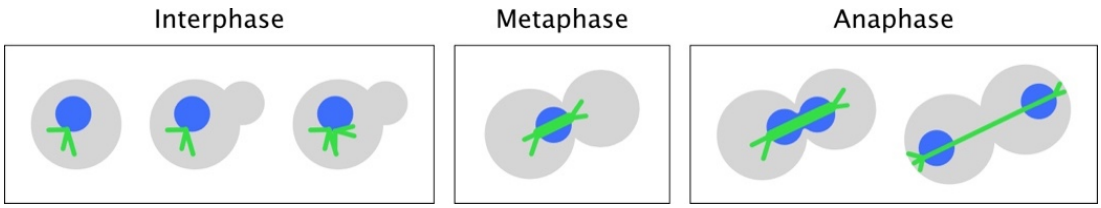

Figure 2.1. Yeast cells morphology in interphase, metaphase, and anaphase
In blue, the nucleus; in green, the spindle.

Analysis of anaphase bridges and spindle length measurements

For nuclear, nucleolar, and spindle morphology analysis, images were acquired with a DeltaVision Elite deconvolution microscope (Applied Precision) equipped with an Olympus IX71 inverted microscope and a CoolSnap HQ2 (Photometrics) CCD camera and driven by SoftWoRx software. Images were acquired with a UPlanSApo 100X oil immersion objective (NA 1.4) as 12 z-stacks (0.5µm step) with FITC, TRITC, and DAPI filters. Stacks were deconvoluted by the Delta Vision SoftWoRx program (Applied Precision) and converted into a projection of sum of intensity using Fiji software. At least 100 cells were analyzed for each condition.

Flow cytometry

Samples of 1ml of cell culture at OD_{600} = 0.2-0.4 were collected by centrifugation for 1 min at 13000 rpm at RT and incubated O/N at 4°C in 70% EtOH. Cells were then washed with 1ml of 50mM Tris-HCl pH 7.4 and incubated O/N at 37°C in 0.5ml of the same buffer containing 1 mg/ml RNase A. Next, cells were collected by centrifugation, resuspended in 55mM HCl containing 5mg/ml of pepsin (Sigma), and incubated at 37°C for 30 min. Next, cells were collected, resuspended in 50mM Tris-HCl pH 7.4, and sonicated 10 sec for three times with 30 sec intervals using Bioruptor UCD-300 (Diagenode) water-bath sonicator set on "low". Just before FACS reading, 100µl of cell suspension were added to 1ml of Sytox Green staining solution. Samples were acquired with the FACSCalibur system (Becton Dickinson) operated via the CellQuest software. Data were analyzed with FlowJo Analysis software.

<u>Sytox green stock solution:</u>

- 1mM Sytox green (Invitrogen)
- DMSO

<u>Sytox green staining solution:</u>

- 1µl/ml 5 mM Sytox green
- 50mM Tris-HCl pH 7.4

2.6. Tables of plasmids, primers, and strains

Table 2.1. Plasmids used in this study

NAME	DESCRIPTION	REMARKS	ORIGIN
Rc74	YIplac211/PGAL-cvTopoII	Used to integrate *GAL-NLS-NLS-cvTopoII-PK3* in *URA3* locus	D'Ambrosio et al., 2008a
Rp94	pFA6a-kanMX6		Longtine et al., 1998
Rp102	pFA6a-3HA-kanMX6		Longtine et al., 1998
Rp701	pCC117	Used to replace *TOP2* with *TOP2-HA3 - KanMX - 3'UTR Top2*	Bachant et al., 2002
Rp702	pML251	Used to replace *TOP2* with *top2-snm-HA3 - KanMX - 3'UTR Top2*	Bachant et al., 2002
Rp703	YIplac204/PGAL-ULP2	Used to integrate *GAL-ULP2* in *TRP1* locus	This thesis
Rp704	YCplac33/PULP-ULP2	Centromeric plasmid with *URA3* marker, used to express *ULP2* under its own promoter	This thesis
Rp718	YIplac128/PGAL-YEN1	Used to integrate *GAL-3HA-YEN1* in *LEU2* locus	Visintin lab

Table 2.2. Primers used in this study

NAME	GENE		SEQUENCE 5'-3'	PURPOSE
AF1	ULP2	FW	CGCGTCTAGAATGTCTGCCAGAAAACGCAAG	Cloning ULP2 gene. Contains XbaI site
AF2	ULP2	RV	CGCGAAGCTTTCAAGGGTCTTCATCTTCC	Cloning ULP2 gene. Contains HindIII site
AF3	ULP2	FW	GCCCAAAAGATATAACACTTTTCG	ULP2 sequencing
AF4	ULP2	RV	GGAACAAAAGACCATTGGAAGTGC	ULP2 sequencing
AF5	ULP2	FW	CATTGTATTTTCAACAATCGG	ULP2 sequencing
AF6	ULP2	RV	GCTCTTTATGATCTAAAATTTCG	ULP2 sequencing

AF7	ULP2	FW	GCCAGCCTTGGGAAAAAAGAGC	ULP2 sequencing
AF8	ULP2	RV	CCAAAATGCTATCATTAACCC	ULP2 sequencing
AF9	ULP2	FW	CTAATGTAAAAAAGTGGG	ULP2 sequencing
AF10	ULP2	RV	CTTTGTTTTGATGAAAATCC	ULP2 sequencing
AF11	ULP2	FW	CCTAATATGAGCGATTGTGG	ULP2 sequencing
AF12	ULP2	RV	GCTTACTTTTAATCTTAGAATTC	ULP2 sequencing
AF13	ULP2	FW	CGCGCAGTTAACCTCGGAACC	ULP2 sequencing
AF14	ULP2	RV	GCTGTTTCTGGAGAAGCAGCGCG	ULP2 sequencing
AF15	ULP2	FW	GCCGTCGCCTAAACCTAAAAGG	ULP2 sequencing
AF16	ULP2	RV	CCAATTAAATTGACGTCCG	ULP2 sequencing
AF17	ULP2	FW	GGGCAGAGATAATCCTATAC	ULP2 sequencing
AF18	ULP2	FW	GTTTGGGATGAGGGCAGAGATAATCCTATACTCTTGGAAGATGAAGACCCTCGTACGCTGCAGgtcgac	Tagging ULP2 with AID
AF19	ULP2	RV	AAAATAAAGAGGAAAAGAATAAAAAATATAAAACTATGCGTGCGAGTGCTTATCGATGAATTCGAGCTCg	Tagging ULP2 with AID
AF20	ULP2	FW	GGTGCAATAATACACGTATATCTATGTTTATTGCACATCAAACCCCACATATcggatccccgggttaattaa	ULP2 deletion
AF21	ULP2	RV	AAATAAAGAGGAAAAGAATAAAAAATATAAAACTATGCGTGCGAGTGCTTgaattcgagctcgtttaaac	ULP2 deletion and tagging
AF22	ULP2	FW	GTTTGGGATGAGGGCAGAGATAATCCTATACTCTTGGAAGATGAAGACCCTcggatccccgggttaatt	ULP2 tagging
AF26	ULP2	FW	GAGAGAGAAATAAAGAGCGGG	Checking ULP2 deletion
AF27	ULP2	FW	GCGCGGTACCGGGCAAAGAAGATACCATCG	Cloning ULP2 promoter. Contains KpnI site
AF28	ULP2	RV	GCGCTCTAGAATATGTGGGGTTTGATGTGC	Cloning ULP2 promoter. Contains XbaI site
AF36	ULP2	RV	TCCAAGCAACTGTGCTGTTC	Checking ULP2 deletion and tagging

AF42	AID	FW	ATGCCATTGGTCTCGCTCCGAGGGCGATGGAGAAGTGCAAGAGCAGAGCTCGGATCCCCGGGTTAATT	Checking ULP2 tagging with AID
AF43	TOP2	RV	CTGGTCCGTTCGAGTTTTCG	Checking TOP2 gene replacement
AF44	KANMX	FW	AAGTTAAGTGCGCAGAAAGT	Checking TOP2 gene replacement
AD80	TRP1	FW	ATGACGCCAGATGGCAGTAG	Checking integration of Rp703 in TRP1 and copy number
AD81	TRP1	FW	GCATCCGCTTACAGACAAGC	Checking integration of Rp703 in TRP1 and copy number
AD82	TRP1	RV	ACATTTCCCCGAAAAGTGCC	Checking integration of Rp703 in TRP1 and copy number
RV134	KANMX	RV	CACCTGATTGCCCGACAT	Checking TOP2 gene replacement
RV164	TOP2	FW	GCAACTGACAACAAGAGTC	Checking TOP2 gene replacement
RV171	TOP2	RV	CAGCTGTTTTTTTAGCGG	Checking top2-snm mutation
RV212	TOP2	FW	CAACGAGATGCAGAAGCTCG	Checking top2-snm mutation

Table 2.3. Strains used in this study

NAME	RELEVANT GENOTYPE	ORIGIN
Ry1	*MATa, ade2-1, leu2-3, ura3, trp1-1, his3-11,15, can1-100, GAL, psi+*	Visintin lab
Ry2	*MATalpha, ade2-1, leu2-3, ura3, trp1-1, his3-11,15, can1-100, GAL, psi+*	Visintin lab
Ry72	*MATa (mating type tester)*	Fink lab
Ry73	*MATalpha (mating type tester)*	Fink lab
Ry1112	*MATa, cdc15::cdc15-as1(L99G)::URA3*	Visintin lab

Ry1573	*MATa, cdc14-1*	Visintin lab
Ry1602	*MATa, cdc14-1, cdc5L158G*	Visintin lab
Ry2249	*MATa, RAD5+, ulp2::LoxP-:kanMX-LoxP*	Branzei lab
Ry2446	*MATa, cdc5L158G*	Visintin lab
Ry4934	*MATa, cdc14-1, ura3::PADH1-OsTIR1-9MYC::URA3, cdc20-aid::KanMX*	Visintin lab
Ry4936	*MATa, cdc5L158G, ura3::PADH1-OsTIR1-9MYC::URA3, cdc20-aid::KanMX*	Visintin lab
Ry5156	*MATa, cdc14-1, ura3::PGAL-NLS-NLS-ChVTOP2-PK3::URA3, cdc5L158G*	Visintin lab
Ry5158	*MATa, cdc14-1, ura3::PGAL-NLS-NLS-ChVTOP2-PK3::URA3*	Visintin lab
Ry5160	*MATa, ura3::PGAL-NLS-NLS-ChVTOP2-PK3::URA3, cdc5L158G*	Visintin lab
Ry7566	*MATa, ura3::PADH1-OsTIR1-9MYC::URA3, cdc20-aid::KanMX, cdc15::cdc15-as1(L99G)::URA3*	Visintin lab
Ry7860	*MATa, ulp2::KanMX*	This thesis
Ry7861	*MATa, ulp2::KanMX*	This thesis
Ry7865	*MATa, ULP2-HA3::KanMX*	This thesis
Ry7893	*MATalpha, ura3::PADH1-OsTIR1-9MYC::URA3, ulp2-AID::KanMX*	This thesis
Ry7895	*MATa, leu2::PTEF1-osTIR1::LEU2, ulp2-AID::KanMX*	This thesis
Ry7920	*MATa, TOP2-HA6::HIS3*	Visintin lab
Ry7921	*MATa, TOP2-PK9::HIS3*	Visintin lab
Ry7948	*MATa, smt3::SMT3+3'UTR::TRP1*	Bielinsky lab
Ry7949	*MATa, smt3::8HisSmt3+3'UTR::TRP1*	Bielinsky lab
Ry7970	*MATa, cdc5L158G, leu2::PTEF1-osTIR1::LEU2, ulp2-AID::KanMX*	This thesis
Ry7973	*MATa, cdc14-1, leu2::PTEF1-osTIR1::LEU2, ulp2-AID::KanMX*	This thesis
Ry7998	*MATa, cdc14-1, TOP2-PK9::HIS3, cdc5L158G*	Visintin lab
Ry8001	*MATa, cdc14-1, TOP2-PK9::HIS3*	Visintin lab
Ry8004	*MATa, TOP2-PK9::HIS3, cdc5L158G*	Visintin lab
Ry8126	*MATa, ura3::PADH1-OsTIR1-9MYC::URA3, cdc20-aid::KanMX, ULP2-HA3::KanMX*	This thesis

Ry8129	*MATa, trp::PGAL-ULP2::TRP (multiple integrants)*	This thesis
Ry8130	*MATa, trp::PGAL-ULP2::TRP (single integrant)*	This thesis
Ry8183	*MATa, cdc5L158G, ura3::PADH1-OsTIR1-9MYC::URA3, cdc20-aid::KanMX, ULP2-HA3::KanMX*	This thesis
Ry8184	*MATa, cdc5L158G, ura3::PADH1-OsTIR1-9MYC::URA3, cdc20-aid::KanMX, ULP2-HA3::KanMX*	This thesis
Ry8229	*MATalpha, ulp2::KanMX, pPULP-ULP2 (CEN, URA3)*	This thesis
Ry8315	*MATa, TOP2-PK9::HIS3, ura3::PADH1-OsTIR1-9MYC::URA3, cdc20-aid::KanMX*	Visintin lab
Ry8782	*MATa, cdc14-1, TOP2-PK9::HIS3, ura3::PADH1-OsTIR1-9MYC::URA3, cdc20-aid::KanMX*	Visintin lab
Ry8785	*MATa, TOP2-PK9::HIS3, cdc5L158G, ura3::PADH1-OsTIR1-9MYC::URA3, cdc20-aid::KanMX*	Visintin lab
Ry8943	*MATa, leu2::PTEF1-osTIR1::LEU2, cdc20-aid::KanMX, ULP2-HA3::KanMX6*	This thesis
Ry8946	*MATa, leu2::PTEF1-osTIR1::LEU2, cdc20-aid::KanMX, cdc28-as1, ULP2-HA3::KanMX*	This thesis
Ry8980	*MATa, leu2::PTEF1-osTIR1::LEU2, cdc20-aid::KanMX, ULP2-HA3::KanMX, cdc5L158G*	This thesis
Ry8993	*MATa, cdc5::KanMX, ura3::CDC5dB::URA3 (2x integrants), leu2::PTEF1-osTIR1::LEU2, cdc20-aid::KanMX, ULP2-HA3::KanMX, cdc28-as1*	This thesis
Ry9325	*MATa, ura::PGAL-3Myc-CDC5::URA3, TOP2-PK9::HIS3*	This thesis
Ry9947	*MATa, cdc14-1, TOP2-PK9::HIS3, ULP2-HA3::KanMX*	This thesis
Ry9948	*MATa, TOP2-PK9::HIS3, ULP2-HA3::KanMX, cdc5L158G*	This thesis
Ry9951	*MATa, cdc14-1, TOP2-PK9::HIS3, ULP2-HA3::KanMX, cdc5L158G*	This thesis
Ry10137	*MATa, leu2::PTEF1-osTIR1::LEU2, cdc20-aid::KanMX, TOP2-PK9::HIS3*	This thesis
Ry10139	*MATa, leu2::PTEF1-osTIR1::LEU2, cdc20-aid::KanMX, ura::PGAL-3Myc-CDC5::URA3, TOP2-PK9::HIS3*	This thesis
Ry10143	*MATa, leu2::PTEF1-osTIR1::LEU2, cdc20-aid::KanMX, TOP2-PK9::HIS3, trp::PGAL-ULP2::TRP (single integrant)*	This thesis

Ry10151	*MATa, leu2::PTEF1-osTIR1::LEU2, cdc20-aid::KanMX, TOP2-PK9::HIS3, trp::PGAL-ULP2::TRP (multiple integrants)*	This thesis
Ry10270	*MATa, cdc14-1, leu2::PGAL-3HA-YEN1::LEU2, cdc5L158G*	This thesis
Ry10272	*MATa, cdc14-1, leu2::PGAL-3HA-YEN1::LEU2*	This thesis
Ry10275	*MATa, leu2::PGAL-3HA-YEN1::LEU2, cdc5L158G*	This thesis
Ry10464	*MATa, top2::TOP2-HA3-KanMX:pCC117*	This thesis
Ry10466	*MATa, top2::top2-SNM-HA3-KanMX:pML251*	This thesis
Ry10473	*MATa, cdc14-1, top2::TOP2-HA3-KanMX:pCC117*	This thesis
Ry10476	*MATa, cdc5L158G, top2::TOP2-HA3-KanMX:pCC117*	This thesis
Ry10482	*MATa, cdc5L158G, top2::top2-SNM-HA3-KanMX:pML251*	This thesis
Ry10485	*MATa, cdc14-1, top2::top2-SNM-HA3-KanMX:pML251*	This thesis
Ry10529	*MATa, cdc15::CDC15-as1(L99G)::URA3, leu2::PTEF1-osTIR1::LEU2, ulp2-AID:KanMX*	This thesis
Ry10539	*MATa, cdc15::CDC15-as1(L99G)::URA3, top2::TOP2-HA3-KanMX:pCC117*	This thesis
Ry10542	*MATa, cdc15::CDC15-as1(L99G)::URA3, top2::top2-SNM-HA3-KanMX:pML251*	This thesis
Ry10659	*MATa, TOP2-PK9::HIS3, PGAL-CDC5(dN70aa)-HA::URA3 (single integrant)*	This thesis
Ry10766	*MATa, cdc14-1, ura3::PADH1-OsTIR1-9MYC::URA3, cdc20-aid::KanMX, trp::PGAL-ULP2::TRP (single integrant)*	This thesis
Ry10769	*MATa, cdc5L158G, ura3::PADH1-OsTIR1-9MYC::URA3, cdc20-aid::KanMX, trp::PGAL-ULP2::TRP (single integrant)*	This thesis
Ry10772	*MATa, cdc15::CDC15-as1(L99G)::URA3, ura3::PADH1-OsTIR1-9MYC::URA3, cdc20-aid::KanMX, trp::PGAL-ULP2:TRP (single integrant)*	This thesis

3. Results

3.1. Aim of the study

In budding yeast, spindle elongation relies on Cdc5, the Polo-like kinase, and Cdc14, the Cdk-counteracting phosphatase. Cells lacking the activity of both proteins arrest after cohesin cleavage, with short metaphase-like spindles and undivided nuclei, in a cell cycle stage termed mini-anaphase. The mini-anaphase arrest is mainly caused by a defect in spindle elongation, but evidence suggests that these cells have also a secondary defect in sister chromatid separation. In particular, uncoupling spindle elongation from sister chromatid separation in *cdc5 cdc14* cells, either by generating sister-less chromatids or by preventing chromosome attachment to the mitotic spindle, resulted in slightly longer, albeit more fragile, spindles (Roccuzzo et al., 2015). This observation indicates that these cells retain some sort of cohesin-independent cohesion, which prevents proper separation of the sister chromatids. Intrigued by this observation, we moved to characterize the sister chromatid separation defect of *cdc5 cdc14* cells. Knowing that these cells are defective both in spindle elongation and in the resolution of sister chromatid intertwines, we hypothesize that Cdc5 and Cdc14 coordinate the two events in mitosis.

This work is complementary to the unpublished doctoral research of L. Massari (Massari, 2018). The common aim of the two projects is to identify the nature of the cohesion between sister chromatids and to understand the mechanisms underlying the sister chromatid separation defect in *cdc5 cdc14* cells, with the ultimate purpose of expanding our knowledge about the resolution of DNA linkages in mitosis. In her work, L. Massari demonstrated that *cdc5 cdc14* cells retain DNA linkages, mainly DNA catenanes, which counteract spindle elongation (Massari, 2018). Here, we provide evidence that Cdc14 and Cdc5 play distinct functions in the removal of sister chromatid intertwines. Cdc14 mainly promotes nucleolar segregation and processing of recombination intermediates through its known substrate, the nuclease Yen1. On the other hand, Cdc5 seems to help the disentangling of DNA catenanes throughout the genome, by acting on the decatenating enzyme Top2. In addition, we found that the polo-like kinase controls post-translational modification of Top2, particularly phosphorylation and conjugation with small ubiquitin-like modifier (SUMO).

3.2. Investigating the nature of the cohesion retained between sister chromatids in *cdc5 cdc14* cells

3.2.1. Cdc5 and Cdc14 both contribute to the resolution of anaphase bridges, with different effects

We previously found that in *cdc5 cdc14* cells, arrested in mini-anaphase, forcing spindle elongation by overexpression of the motor protein Cin8 originates anaphase bridges (Massari, 2018). On the other hand, ectopic cleavage of cohesin in cells arrested in metaphase through depletion of Cdc20, the activator of the anaphase-promoting complex (APC/C), is sufficient to induce spindle elongation and chromosome segregation, without forming anaphase bridges. Altogether, these results suggest that i) *cdc5 cdc14* cells retain unresolved DNA intertwines, ii) by metaphase the conditions are set for the resolution of SCIs, and iii) Cdc5 and/or Cdc14 are required for this process.

First of all, we wished to evaluate the individual contribution of Cdc5 and Cdc14 in the resolution of SCIs. To this aim, we decided to image *cdc14* and *cdc5* single mutant cells and score for the presence of anaphase bridges, which indicate the presence of unresolved SCIs. Since *cdc5* and *cdc14* single mutant cells arrest in anaphase, to appreciate the contribution of the cell cycle phase to the phenotype observed we compared these mutants not only to normally dividing wild-type cells, but also to *cdc15* cells, which arrest in anaphase because they are defective in the mitotic exit network (Jaspersen et al., 1998; Mah et al., 2001). Cdc5 and Cdc14 are required for the correct segregation of the nucleolus, the genomic region containing the ribosomal DNA (rDNA) repeats, as both proteins are involved in its condensation which, in turn, promotes resolution of DNA intertwines (D'Amours et al., 2004; St-Pierre et al., 2009; Sullivan et al., 2004). Therefore, to assess for a more general contribution in mitotic SCI resolution, we set to distinguish between the DNA bridges occurring at the nucleolus from the ones occurring elsewhere in the genome. To this aim, DNA was stained with DAPI, while immunostaining of the nuclear protein Nop1 was used to visualize the nucleolus (Schimmang et al., 1989), which is refractory to DAPI staining.

To inactivate Cdc14 we used the thermosensitive allele *cdc14-1*, while to inhibit Cdc5 and Cdc15 we used the ATP-analog sensitive alleles *cdc5-as1* and *cdc15-as1*, respectively (Bishop et al., 2000; Snead et al., 2007). Wild-type, *cdc5-as1*, *cdc14-1,* and *cdc15-as1* cells

were arrested in G1 using the α-factor pheromone and released into the cell cycle in restrictive conditions for all mutations. To monitor cell cycle progression, we performed immunofluorescence of the alpha-tubulin Tub1 and analyzed the morphology of the mitotic spindle, which allows us to distinguish between interphase (G1/S phase), G2/metaphase, and anaphase (see **Figure 2.1** of Materials and Methods). We imaged *cdc5*, *cdc14,* and *cdc15* cells at their terminal anaphase arrest (after 3 hours), in addition to wild-type cells undergoing a synchronized cell cycle, and analyzed nuclear and nucleolar morphology relative to time and spindle length. Cells were divided according to their nuclear and nucleolar morphology in the following categories:

1. Cells displaying a single nucleus, in a metaphase-like fashion ("undivided nuclei")
2. Cells with a single nucleolus, but in which the nucleus formed a bridge between the daughters ("DAPI bridge, 1 nucleolus")
3. Cells displaying both DAPI-positive and Nop1-positive anaphase bridges ("DAPI bridge, Nop1 bridge")
4. Cells displaying DAPI-positive anaphase bridges, in which the nucleolus appeared to be fully segregated ("DAPI bridge, 2 nucleoli")
5. Cells displaying Nop1-positive anaphase bridges, in which the nuclei appeared fully segregated ("Nop1 bridge")
6. Cells in which the nuclei appeared fully segregated without any bridge ("No bridge")

Whilst about 90% of *cdc15* cells completed the segregation of the nucleus and the nucleolus, Cdc5 or Cdc14 inactivation alone is sufficient to increase the presence of anaphase bridges. The percentage of anaphase cells which fully segregated their genome at the end of the experiment (3 hours after release) was down to 42% and 28% in *cdc5* and *cdc14* cells, respectively (**Figure 3.1**). This finding indicates that Cdc5 and Cdc14 are both involved in the resolution of mitotic DNA intertwines.

Moreover, we found that, in wild-type and *cdc15* cells, anaphase bridges decreased with time and, importantly, with spindle elongation. This observation suggests that, during a normal cell cycle, spindle elongation drives the resolution of leftover DNA linkages. Therefore, we considered the hypothesis that the accumulation of anaphase bridges in *cdc5* and *cdc14* cells depends on their role in promoting spindle elongation. However, when we compared cells having spindles of similar length (between 6 μm and 8 μm), we found

that *cdc5* and *cdc14* cells retain more anaphase bridges than *cdc15* cells. Moreover, despite the fact that, in many *cdc14* cells, the spindle reaches 8 μm of length, this is not sufficient to drive SCI resolution. These results indicate that these two proteins have a function in the resolution of DNA intertwines which is distinct from their role in spindle elongation.

We also noted that anaphase bridges decreased with time in a protracted anaphase arrest in *cdc5* cells, but not in *cdc14* cells.

Interestingly, at the end of the experiment, the percentage of anaphase cells with fully divided nuclei in which the nucleolus did not correctly segregate was 8% and 25% in *cdc5* and *cdc14* cells, respectively, while the percentage of cells with segregated nucleoli but showing DAPI-positive bridges was 18% and 7% in *cdc5* and *cdc14* cells, respectively. The percentage of cells displaying both DAPI-positive and Nop1-positive bridges was 12% and 23% in *cdc5* and *cdc14* cells, respectively. The differences between *cdc5* and *cdc14* cells, albeit small, suggest that the two proteins may be involved in different aspects of SCI resolution, with Cdc14 having a specific effect on the segregation of the rDNA and Cdc5 having a more general function.

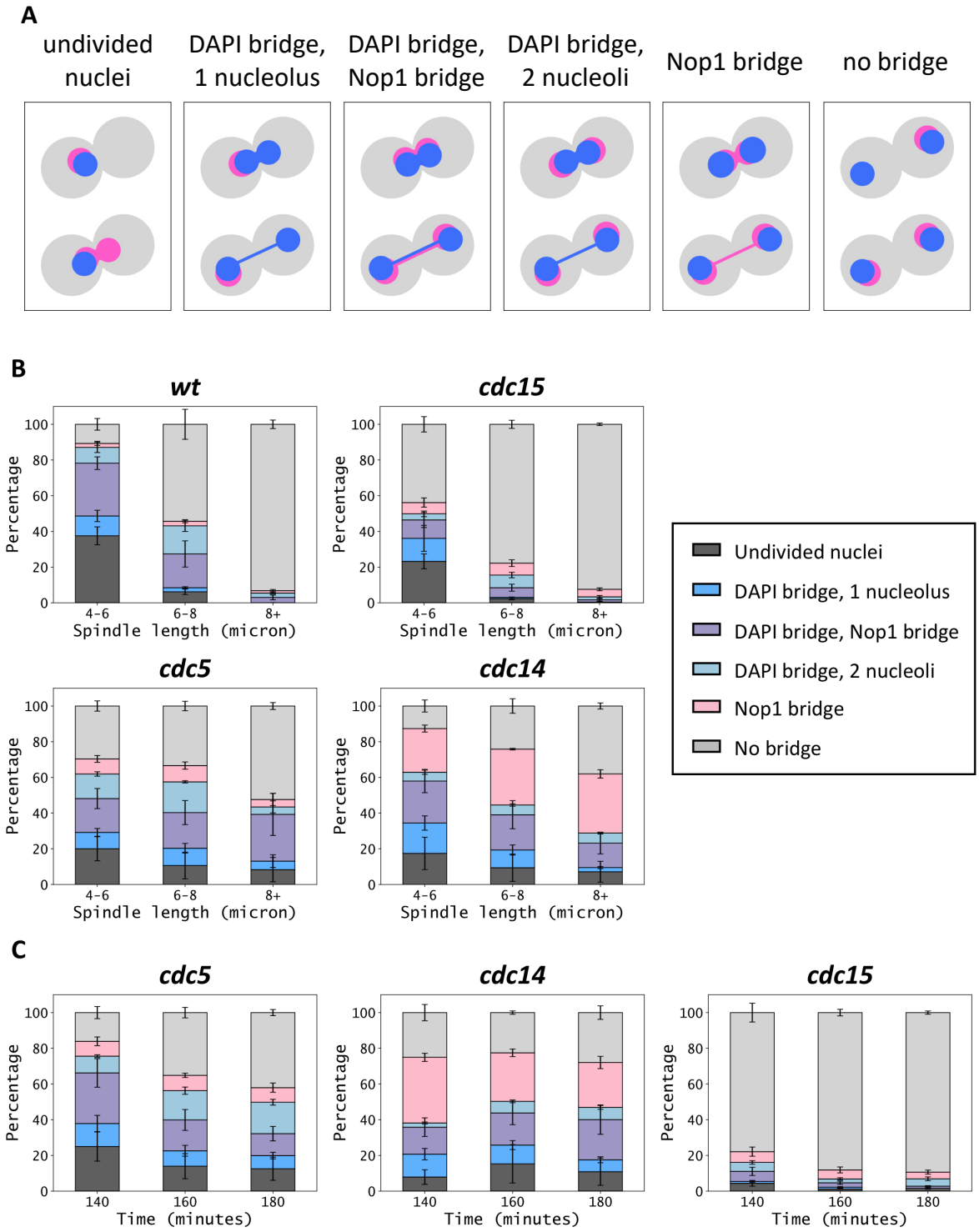
A
undivided nuclei
DAPI bridge, 1 nucleolus
DAPI bridge, Nop1 bridge
DAPI bridge, 2 nucleoli
Nop1 bridge
no bridge
B
wt
cdc15
cdc5
cdc14
Percentage
Spindle length (micron)
4-6
6-8
8+
Undivided nuclei
DAPI bridge, 1 nucleolus
DAPI bridge, Nop1 bridge
DAPI bridge, 2 nucleoli
Nop1 bridge
No bridge
C
cdc5
cdc14
cdc15
Time (minutes)
140
160
180

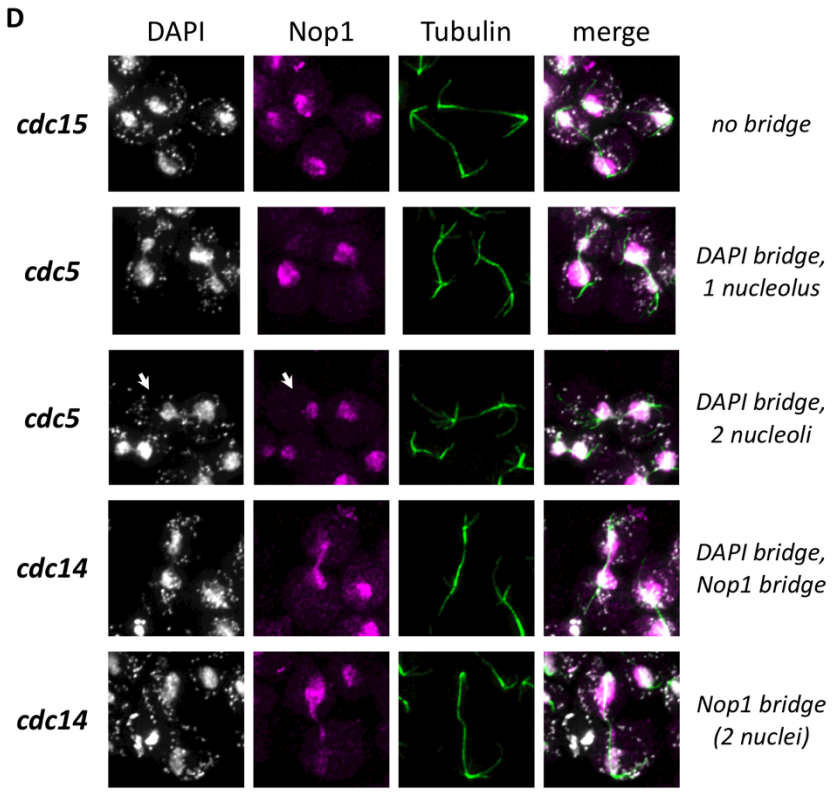

Figure 3.1. Inactivating Cdc5 or Cdc14 enhances anaphase bridges
*Wild-type (Ry1), cdc5-as1 (Ry2446), cdc14-1 (Ry1573), and cdc15-as1 (Ry1112) cells were arrested in G1 by addition of α-factor in YPD at 23°C and synchronously released into the next cell cycle in fresh media supplemented with the CMK and NMPPi inhibitors to inactivate cdc5-as1 and cdc15-as1, respectively, at the non-permissive temperature for cdc14-1 (37°C). Cell cycle progression was monitored through IF (anti-Tub1, DAPI; not shown). Samples with anaphase cells were analyzed through IF (anti-Tub1, anti-Nop1, DAPI) to score for the presence of anaphase bridges. For wild-type cells we chose samples from 80 min to 120 min after release, while for cdc5, cdc14, and cdc15 cells we analyzed samples 140 min, 160 min, and 180 min after release. At least 100 cells were analyzed for each time point. Spindles were measured and cells were assigned to the indicated categories (**A**) according to nuclear and nucleolar morphology. (**B**, **C**) Plots show the distribution of anaphase cells between categories according to (**B**) spindle length and (**C**) time after release. Three independent experiments were performed. Error bars indicate S.E.M. (**D**) Representative images are shown.*

3.3. Investigating the nature of SCIs retained in *cdc5 cdc14* cells

3.3.1. The presence of recombination intermediates is not responsible for the sister chromatid separation defect of *cdc5 cdc14* cells

Having established that Cdc5 and Cdc14 inactivation leads to the accumulation of unresolved SCIs, we sought to determine the nature of these intertwines. In mitosis, DNA intertwining can arise from three different structures: recombination intermediates, regions of unreplicated DNA, and catenanes. Recombination and late replication intermediates that persist in mitosis are targeted by structure-specific endonucleases (SSEs), namely Mus81-Mms4 and Yen1, the activity of which is distributed in two waves. The sequential activation of SSEs involves both Cdc5 and Cdc14. Mus81-Mms4 is activated in G2/M by Cdc5 phosphorylation (Gallo-Fernández et al., 2012; Matos et al., 2013, 2011; Schwartz et al., 2012; Szakal and Branzei, 2013), while Yen1, which represents the last chance of DNA intertwine resolution, is activated by Cdc14 dephosphorylation in early anaphase (Blanco et al., 2014, p. 201; Eissler et al., 2014; García-Luis and Machín, 2014). In addition, although a substantial fraction of wild-type yeast cells does not complete DNA replication until anaphase (Ivanova et al., 2020), the extent of non-replicated regions is even greater in *cdc14* cells (Dulev et al., 2009). In light of these observations, the presence of recombination and late replication intermediates seemed likely in *cdc5 cdc14* cells.

To address the contribution of recombination and late-replication intermediates to the *cdc5 cdc14* phenotype, we asked whether the nuclease Yen1, which is capable of removing both types of DNA linkages, can rescue the sister chromatid separation defect of these cells. To overexpress Yen1, we placed it under the galactose inducible promoter *GAL1/10*. *GAL-YEN1 cdc5-as1*, *cdc5-as1*, *GAL-YEN1 cdc14-1*, *cdc14-1*, *GAL-YEN1 cdc5-as1 cdc14-1,* and *cdc5-as1 cdc14-1* cells were grown in raffinose-containing media, arrested in G1, and released in fresh media in restrictive conditions for all mutations. When cells reached their terminal arrest (3h30 after release), galactose was added to the medium to induce *YEN1* expression. We imaged cells after induction to analyze nuclear and nucleolar morphology, in addition to the mitotic spindle, and scored for the presence of anaphase bridges.

We found that Yen1 rescued chromatid separation in *cdc14* cells, in agreement with the role of the phosphatase in the activation of this nuclease. The percentage of cells which fully segregated their genome at the end of the experiment (1h30 after induction) increased from 24% in *cdc14* cells to 74% in *GAL-YEN1 cdc14* cells (**Figure 3.2**). Interestingly, Yen1 overexpression seemed to reduce the number of cells presenting Nop1-positive bridges, while the percentage of cells displaying only a DAPI-positive bridge remained unchanged.

Strikingly, we also observed that, after *YEN1* induction, spindles became shorter in *cdc14* cells. The possibility that the nuclease is acting directly on the mitotic spindle seems unlikely. Instead, we think that this phenomenon occurs because spindle elongation and chromatid separation are coordinated. For example, spindle elongation continues in presence of DNA on the cleavage plane, as cells divide with longer spindles if DNA condensation is compromised or if the length of chromosome arms is increased (D'Ambrosio et al., 2008a; Oliveira et al., 2014). Therefore, we hypothesize that, in *cdc14* cells, Yen1 promotes the overall resolution of anaphase bridges, thus removing DNA from the cleavage plane and stopping spindle elongation. Consistently, we found that anaphase bridges were most common in *cdc14 GAL-YEN1* cells when the spindle was more than 8 μm long (not shown).

On the other hand, Yen1 overexpression seemed to have little or no effect on the terminal phenotype of *cdc5* and *cdc5 cdc14* cells. This result, in addition to the previous observation that expression of a constitutively active form of Yen1, termed YEN^{ON} (Blanco et al., 2014), also fails to rescue the *cdc5 cdc14* arrest (Massari, 2018), indicates that recombination and late replication intermediates are not the main source of SCIs retained in *cdc5 cdc14* cells.

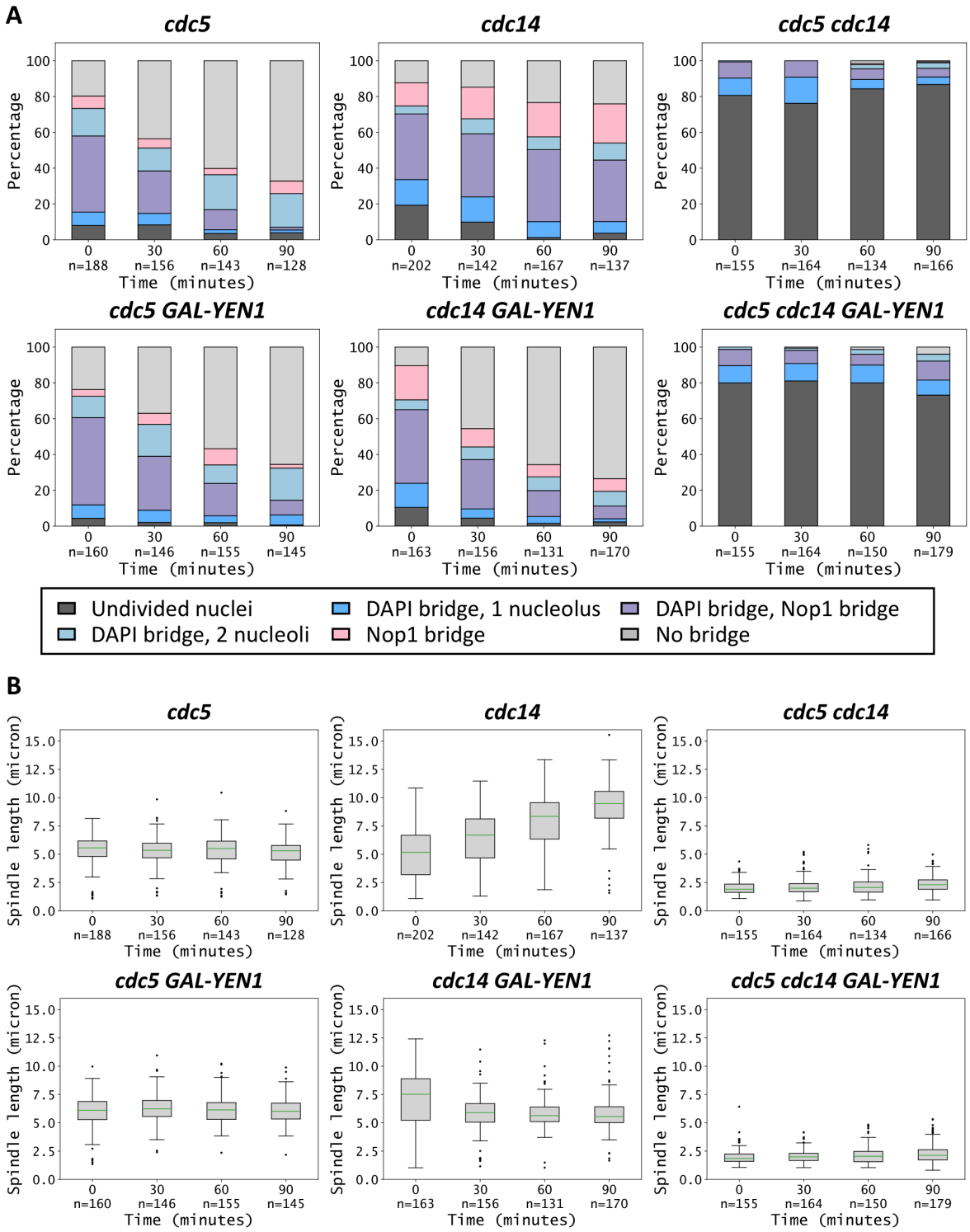

Figure 3.2. Yen1 overexpression rescues nuclei separation in cdc14 cells, but not in cdc5, and cdc5 cdc14 cells

*cdc5-as1 GAL-YEN1 (Ry10275), cdc5-as1 (Ry2446), cdc14-1 GAL-YEN1 (Ry10272), cdc14-1 (Ry1573), cdc5-as1 cdc14-1 GAL-YEN1 (Ry10270), and cdc5-as1 cdc14-1 (Ry1602) cells were arrested in G1 in YPR at 23°C and released into the next cell cycle in YPR media with the CMK inhibitor at 37°C to inactivate cdc5-as1 and cdc14-1. At the arrest (3h30 after release), galactose was added (2% final concentration) to induce Yen1 expression. Samples were collected every 30 min after induction and analyzed through IF (anti-Tub1, anti-Nop1, DAPI). At least 100 cells were analyzed for each time point. (**A**) Spindles were measured (box plot) and (**B**) cells were assigned to the indicated categories.*

3.3.2. *cdc5* and *cdc5 cdc14* cells are defective in the resolution of DNA catenanes

Having assessed that unreplicated DNA regions and recombination intermediates are not the main cause of the sister chromatid separation defect of *cdc5* and *cdc5 cdc14* cells, we wondered whether this was the case for DNA catenanes. Catenanes are double-stranded SCIs that arise as a natural consequence of the DNA double-helix structure during replication and they can only be resolved by type II Topoisomerases (Top2 in *S. cerevisiae*). The majority of catenanes are removed during S phase, but some of them normally persist in mitosis and are resolved concomitantly with chromosome segregation.

Previously, to test for the presence of residual catenanes, we asked whether the expression of type II topoisomerase could rescue the phenotype of *cdc5 cdc14* cells. We found that overexpression of the yeast endogenous Top2 did not affect nuclei separation in *cdc5 cdc14* cells, although it led to a minor increase in spindle elongation (Massari, 2018). On the other hand, overexpression of type II topoisomerase from *Paramecium bulsaria* chlorella virus 1 (PBCV-1), hereafter named cv-TopoII, had a striking effect, rescuing both spindle elongation and nuclei division (Massari, 2018). This result indicates that the sister chromatid separation defect of *cdc5 cdc14* cells is mainly due to the presence of unresolved catenanes. Several hypotheses can explain the discrepancy between the effects of the two topoisomerases (see Results 3.3.1 and Discussion).

Given that overexpression of cv-TopoII rescues the *cdc5 cdc14* arrest, Top2 could act downstream of Cdc5, Cdc14, or both. To distinguish between these possibilities, we tested whether overexpression of cv-TopoII rescues the phenotype of *cdc5* and *cdc14* single mutant cells. *cdc5-as1*, *cdc14-1,* and *cdc5-as1 cdc14-1* cells were grown in raffinose-containing media and released from G1 block in restrictive conditions for all mutations. When cells reached their terminal arrest (3h30 after release), galactose was added to the medium to induce cv-TopoII expression. We imaged cells after induction to analyze nuclear and nucleolar morphology, in addition to the mitotic spindle.

For this experiment, cells were grouped according to their nuclear and nuclear morphology in three categories:

1. Cells displaying a single nucleus, in a metaphase-like fashion ("undivided nuclei")
2. Cells displaying any Nop1-positive or DAPI-positive anaphase bridge ("bridge")
3. Cells in which the nuclei appeared fully segregated ("no bridge")

The portion of cells displaying a single nucleus at the end of the experiment (1h30 after induction) decreased from 77% in *cdc5 cdc14* cells to 39% in *GAL-TopoII cdc5 cdc14*, while the percentage of cells which fully segregated their genome went from 2% to 13% (**Figure 3.3**). Moreover, the average spindle length of *cdc5 cdc14* cells slightly increased after cv-TopoII overexpression. These results confirm that cv-TopoII ameliorates nuclei division and spindle elongation in *cdc5 cdc14* cells, in agreement with previous work from our lab (Massari, 2018). In addition, we found that, while Topoisomerase II overexpression did not affect *cdc14* cells, it increased the percentage of *cdc5* cells which displayed no DNA bridges at the terminal arrest from 54% to 71%. Altogether, these observations strongly suggest that Top2 acts downstream of Cdc5.

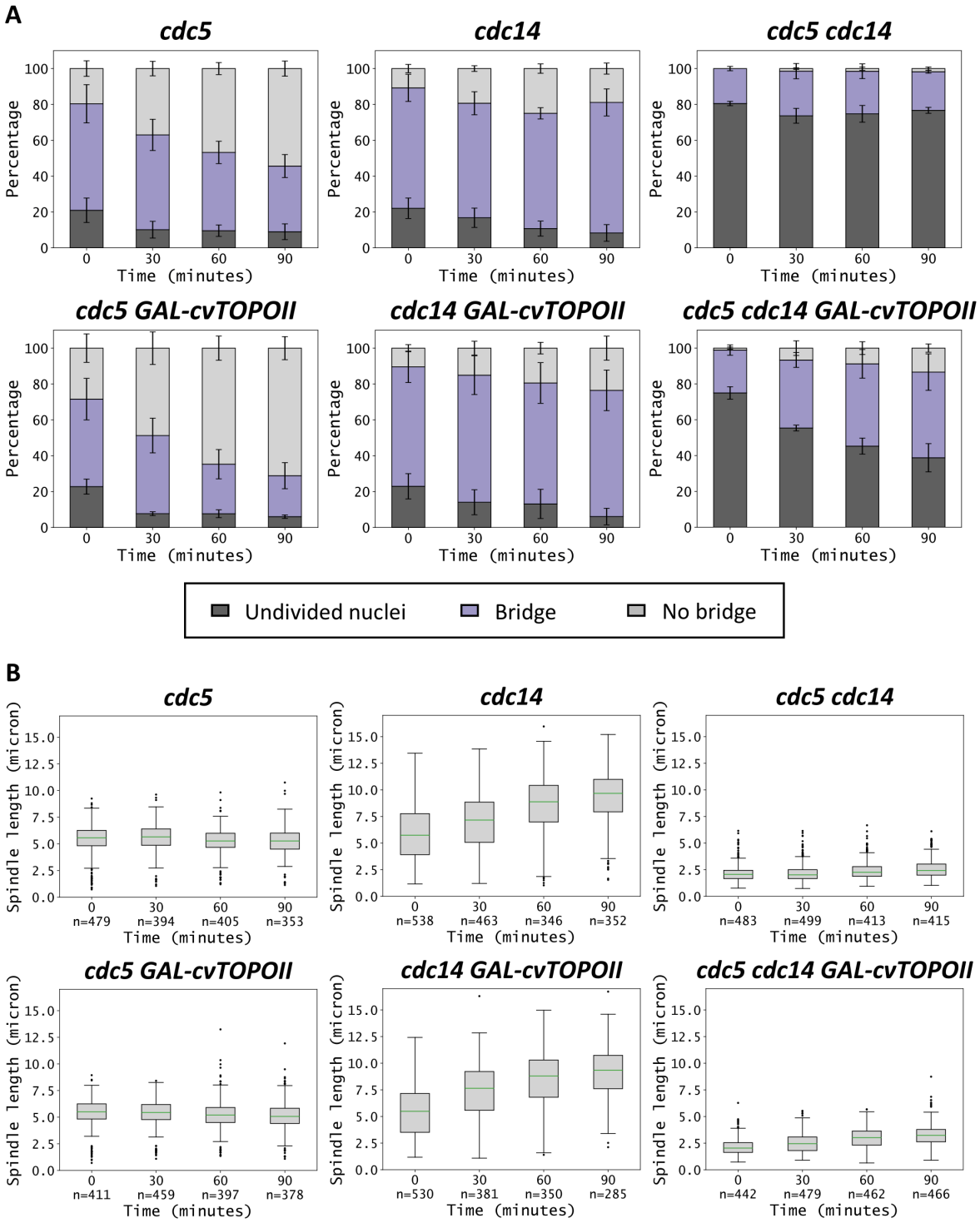

Figure 3.3. cv-TopoII overexpression rescues nuclei separation in cdc5 and cdc5 cdc14 cells, but not in cdc14 cells

*cdc5-as1 GAL-cvTOPOII (Ry5160), cdc5-as1 (Ry2446), cdc14-1 GAL-cvTOPOII (Ry5158), cdc14-1 (Ry1573), cdc5-as1 cdc14-1 GAL-cvTOPOII (Ry5156), and cdc5-as1 cdc14-1 (Ry1602) cells were arrested in G1 in YPR at 23°C and released in YPR media with the CMK inhibitor at 37°C to inactivate cdc5-as1 and cdc14-1, respectively. At the terminal arrest (3h30 after release), 2% galactose was added to induce cv-TopoII expression. Samples were collected every 30 min for 90 min after induction and analyzed through IF (anti-Tub1, anti-Nop1, DAPI). At least 100 cells were analyzed for each time point. (**A**) Spindles were measured and (**B**) cells were assigned to the indicated categories. Three independent experiments were performed. Error bars indicate S.E.M.*

3.4. Mechanisms of Top2 regulation by Cdc5 and Cdc14

After establishing that Cdc5 controls resolution of DNA intertwines genome-wide and is required for the proper resolution of DNA catenanes by Top2, we moved to investigate the mechanisms of regulation of the decatenating enzyme by the polo-like kinase.

Cdc5 may directly target Top2 or impact other players involved in SCI resolution. Besides Top2 activity, the removal of DNA catenanes in mitosis requires cohesin cleavage, bipolar attachment to the mitotic spindle, and condensin-mediated chromosome compaction. As highlighted by the *cdc5 cdc14* arrest (Roccuzzo et al., 2015), Cdc5 and Cdc14 both contribute to spindle elongation in anaphase and thus, indirectly, to the resolution of DNA linkages. Nevertheless, in *cdc5 cdc14* cells, the mitotic spindle is still bipolar and forcing its elongation is not sufficient to rescue catenane resolution, indicating that the spindle defect is not the main reason why these cells fail to resolve DNA catenanes. On the other hand, the fact that Cdc5 promotes condensin activity in mitosis (Leonard et al., 2015; St-Pierre et al., 2009) raised the possibility of condensin being defective in these cells. However, ectopic expression of Top2 overexpression failed to overcome the *cdc5 cdc14* arrest if condensin was inactivated (Massari, 2018), suggesting that condensin is at least partially active in these conditions. Finally, cohesin has already been cleaved in the mini-anaphase arrest (Massari, 2018; Roccuzzo et al., 2015). By exclusion, the main reason for the decatenation defect of *cdc5* and *cdc5 cdc14* cells likely lies in Top2 function, although the other factors may contribute.

3.4.1. Top2 is modified in a cell-cycle dependent manner

The fact that ectopic cv-TopoII overexpression overcomes the *cdc5 cdc14* arrest while overexpressing endogenous yeast Top2 has only a mild effect on nuclei division and spindle elongation (Massari, 2018), suggests that the decatenation defect of *cdc5 cdc14* cells is not simply due to scarcity of Top2 protein. Instead, this discrepancy points to the existence of an activation step of this enzyme in early mitosis. Thus, we wished to investigate the molecular mechanisms of mitotic regulation of Top2.

The activity of Top2 during the cell cycle is controlled through post-translational modifications (PTMs) (Lee and Berger, 2019). The human orthologue of Cdc5, Plk1, directly phosphorylates Topoisomerase II in human cells (Li et al., 2008). In addition, Cdc5 is also

indirectly involved in the SUMOylation of Top2 in metaphase (Bachant et al., 2002; Baldwin et al., 2009). Building from this information, we hypothesized that the dysregulation in Top2 SUMOylation and/or phosphorylation might be at the origin of the sister chromatid separation defect of *cdc5 cdc14* cells.

First of all, we wanted to characterize Top2 PTMs during mitosis. To do so, we used a tagged version of the protein, Top2-9PK, and visualize it by western blot with antibodies against the tag. PTMs can be detected as changes in the protein electrophoretic mobility. We synchronously released *TOP2-9PK* cells from G1 and monitored cell cycle progression through indirect immunofluorescence of the mitotic spindle. We analyzed Top2 by western blot as cells were synchronously dividing and we could see the appearance of slower migrating forms of the protein, indicating post-translational modification (**Figure 3.4**). The modified forms of Top2 started to appear at 90' after release from G1, at the time when cells were going from metaphase to anaphase, as indicated by the spindle morphology, and peaked at 105' after release, when most cells were in anaphase. Modified Top2 fully disappears at 150' after release, when most cells completed cell division and reached the next G1 phase.

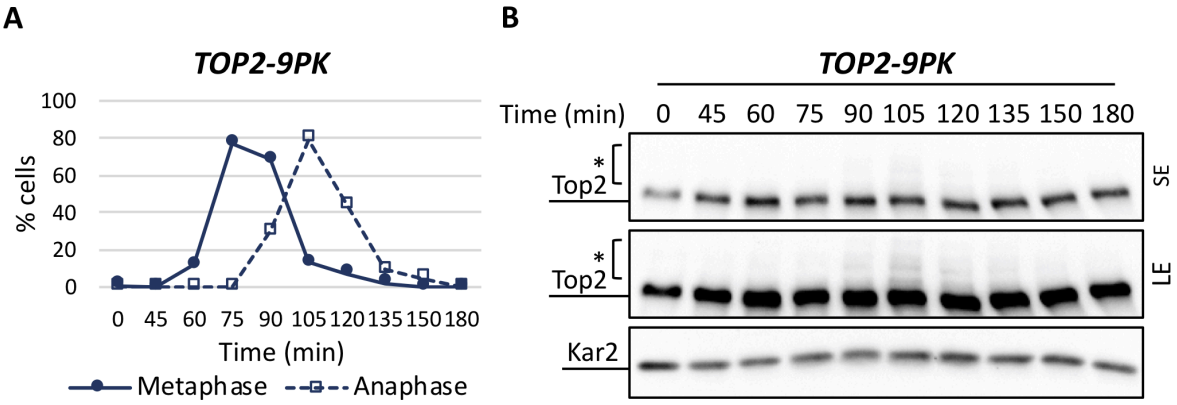

Figure 3.4. Top2 is modified in a cell cycle-dependent manner
*TOP2-9PK (Ry7921) cells were arrested in G1 with α-factor in YPD and synchronously released into the next cell cycle in YPD media. At 75 min after release, α-factor was added to the medium to re-block the cells in G1 at the end of the cell cycle. Samples were collected at the indicated times after release to monitor (**A**) cell cycle progression through IF (anti-Tub1, DAPI) and (**B**) Top2 status by western blot. The signal for Top2-PK is shown at two levels of exposure, short (SE) and long (LE). Asterisks (*) indicate modified forms of Top2. Kar2 was used as a loading control.*

To pinpoint the timing of Top2 modification, we analyzed the protein in cells arrested in metaphase through Cdc20 depletion. To achieve conditional depletion of Cdc20 we took

advantage of the auxin-inducible degron (AID) system (Nishimura et al., 2009). We synchronously released *TOP2-9PK* and *TOP2-9PK cdc20-aid* cells from G1 into a metaphase block and monitored Top2 modification by western blot. Once again, we found that, as wild-type cells were undergoing a synchronous cell cycle, the slower migrating forms of the protein accumulated and then disappeared, as cells were going from metaphase to anaphase (**Figure 3.5**). On the other hand, in *cdc20* cells, the bands corresponding to modified Top2 appeared with similar kinetics, but then remained stable. This result confirms that Top2 is modified in metaphase.

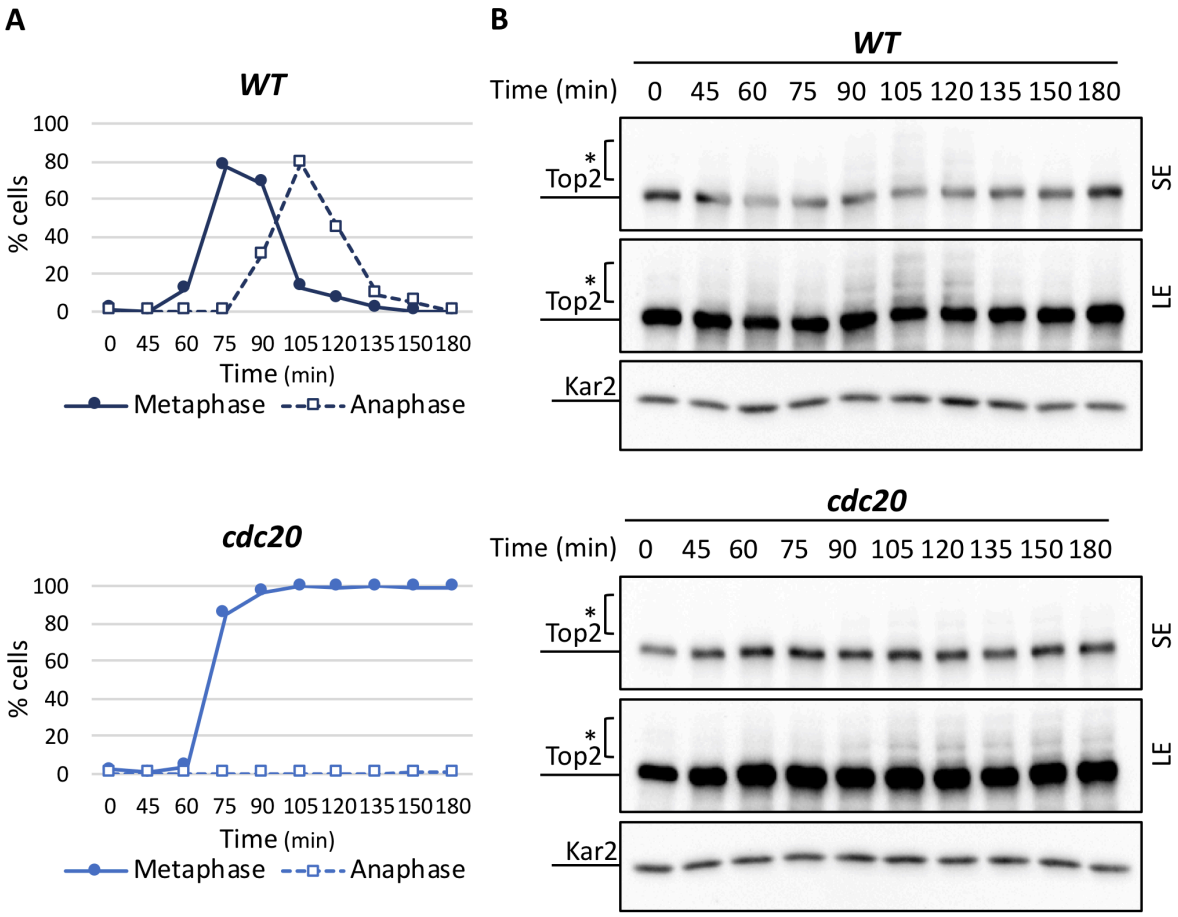

Figure 3.5. Top2 is modified in metaphase
*TOP2-9PK (Ry7921) and TOP2-9PK cdc20-aid (Ry8315) cells were arrested in G1 with α-factor in YPD and synchronously released in media with auxin, to deplete Cdc20-aid. At 75 min after release, α-factor was added to the medium to re-block the cells in G1 at the end of the cell cycle. Samples were collected at the indicated times after release to monitor (**A**) cell cycle progression through IF (anti-Tub1, DAPI) and (**B**) Top2 status by western blot. The signal for Top2-PK is shown at two levels of exposure, short (SE) and long (LE). Asterisks (*) indicate modified forms of Top2. Kar2 was used as a loading control.*

3.4.2. Cdc5, but not Cdc14, is required for the modification of Top2

Having established the timing of Top2 modification, we addressed the contributions of Cdc5 and Cdc14. To this aim, we asked how the inactivation of these two proteins altered the appearance of modified forms of Top2 in metaphase arrested cells, since we previously found that Top2 modification is occurring in this cell cycle stage.

We synchronously released *TOP2-9PK cdc20-aid cdc5-as1*, *TOP2-9PK cdc20-aid cdc14-1,* and *TOP2-9PK cdc20-aid* cells from G1 into a metaphase block, in restrictive conditions for all mutations. We analyzed Top2 by western blot and we found that, as cells were arresting in metaphase, the modified forms of the protein accumulated in *cdc20* and in *cdc20 cdc14* cells, but not in *cdc20 cdc5* cells. In a similar experiment, we synchronously released *cdc14-1*, *cdc5-as1,* and *cdc5-as1 cdc14-1* cells from G1 in restrictive conditions for all mutations, leading to their respective arrests. We detected Top2 by western blot and, once again, we found that the slower-migrating forms of the protein failed to accumulate in strains bearing *cdc5* mutation (**Figure 3.6**). In conclusion, the bulk of Top2 modification depends on Cdc5, but not Cdc14. This is consistent with the polo-like kinase becoming active in metaphase, which is the cell cycle stage at which we normally start to observe Top2 modification.

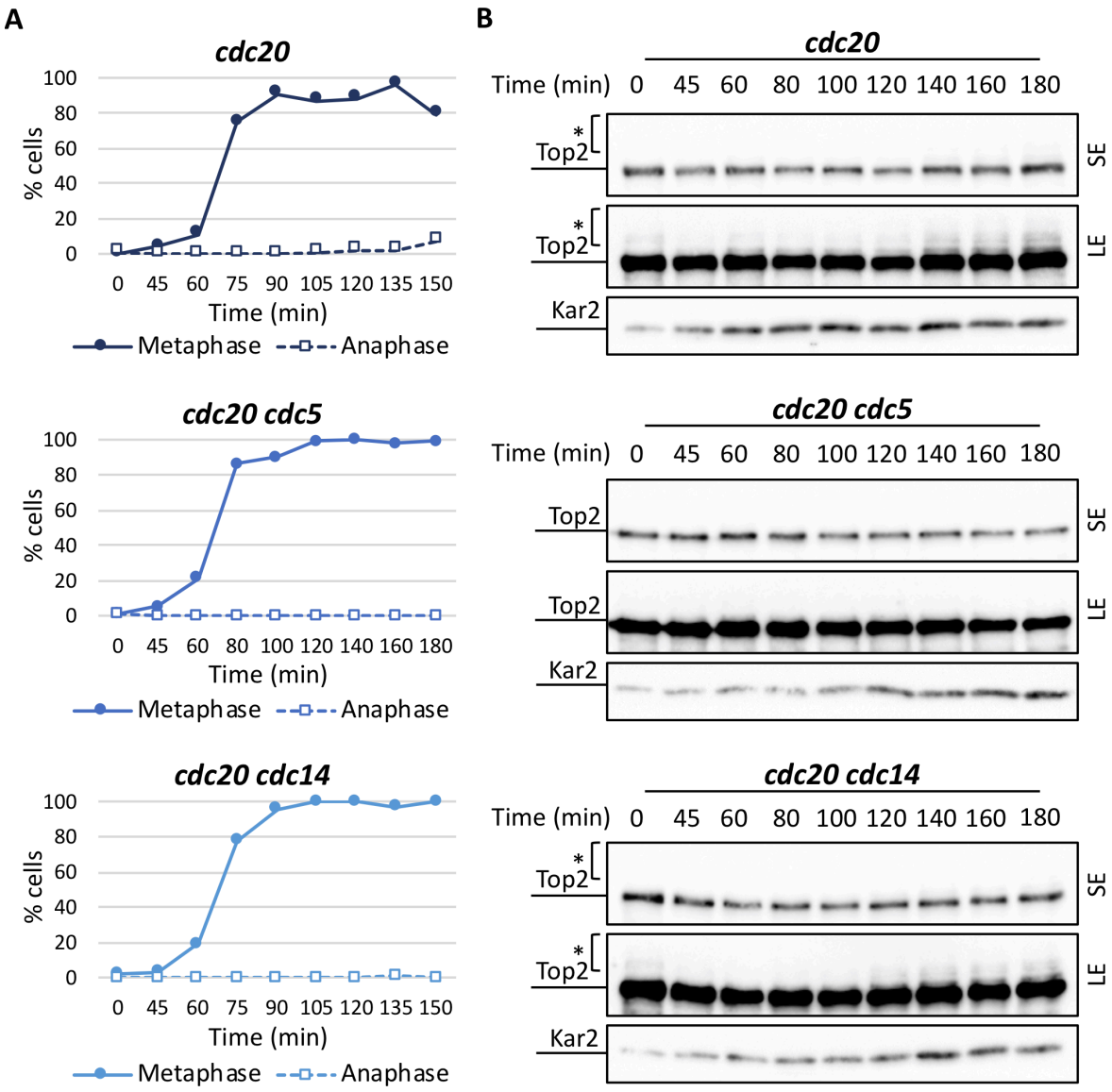
A
cdc20
% cells
Time (min)
Metaphase
Anaphase
cdc20 cdc5
cdc20 cdc14
B
cdc20
Time (min) 0 45 60 80 100 120 140 160 180
Top2
Kar2
SE
LE
cdc20 cdc5
cdc20 cdc14

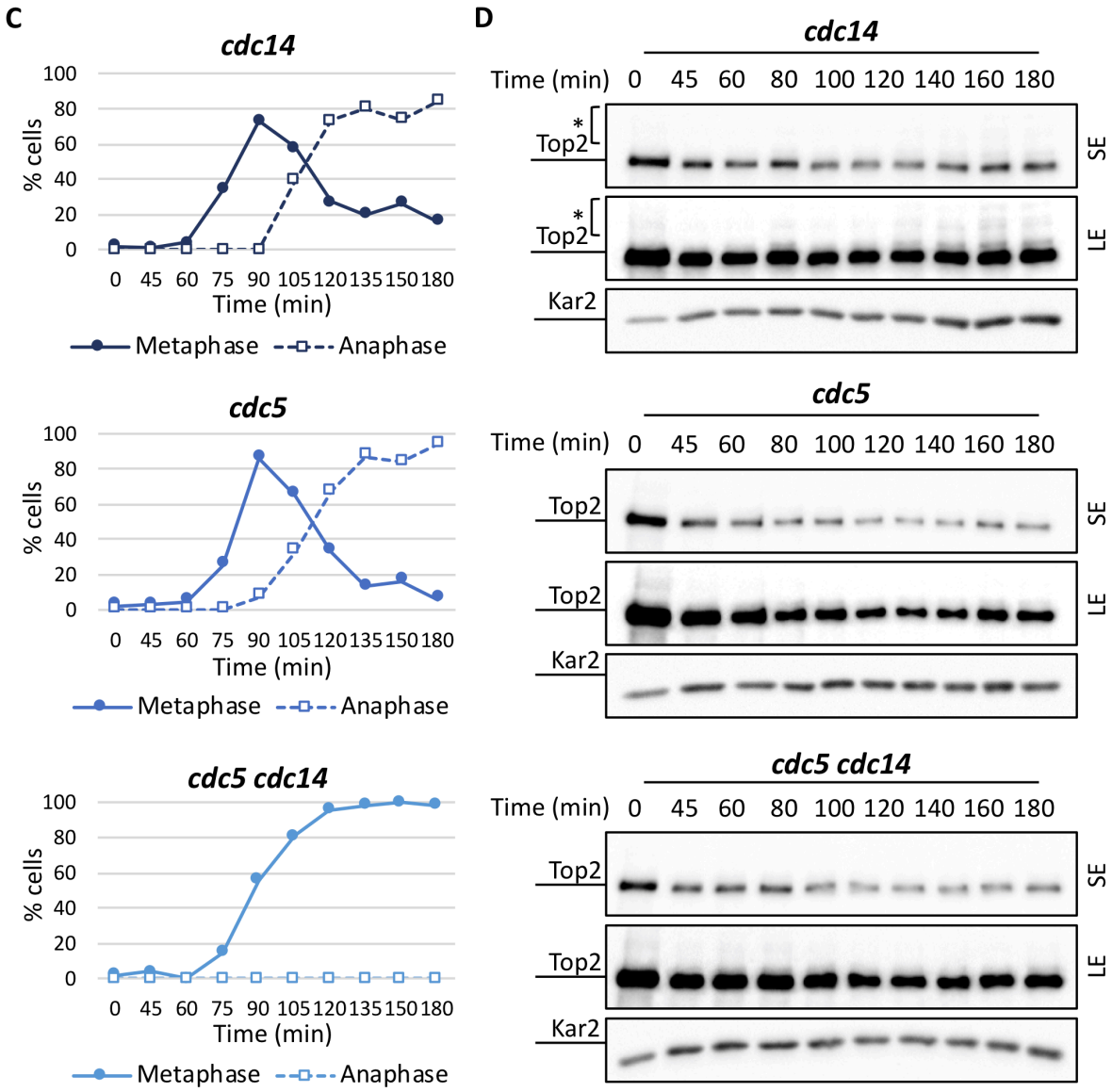

Figure 3.6. Top2 modification depends on Cdc5 but not on Cdc14

*(**A**, **B**) TOP2-9PK cdc20-aid (Ry8315), TOP2-9PK cdc20-aid cdc5-as1 (Ry8785), and TOP2-9PK cdc20-aid cdc14-1 (Ry8782) cells were arrested in G1 with α-factor in YPD at 23°C and synchronously released in media with the CMK inhibitor and auxin at 37°C, to inactivate cdc5-as1, cdc20-aid, and cdc14-1. (**A**) Cell cycle progression was monitored through IF (anti-Tub1, DAPI) and (**B**) samples were collected at the indicated times after release for western blot analysis. (**C**, **D**) The same experiment was performed with TOP2-9PK cdc14-1 (Ry8001), TOP2-9PK cdc5-as1 (Ry8004), and TOP2-9PK cdc5-as1 cdc14-1 (Ry7998) cells. The signal for Top2-PK is shown at two levels of exposure, short (SE) and long (LE). Asterisks (*) indicate modified forms of Top2. Kar2 was used as a loading control.*

3.4.3. Cdc5 is required for the SUMOylation of Top2 in metaphase

We showed that Cdc5 is required for the modification of Top2, but we did not yet determine the nature of such modification. Given its kinase activity, Cdc5 could directly phosphorylate Top2. Alternatively, Cdc5 could indirectly induce SUMOylation of Top2, for example via inactivation of the de-SUMOylating enzyme Ulp2 (Baldwin et al., 2009). To pinpoint the nature of the observed modification, we immunoprecipitated Top2 in *cdc20* metaphase arrested cells, with and without inhibition of Cdc5. *TOP2-9PK cdc20-aid* and *TOP2-9PK cdc20-aid cdc5-as1* cells were released from G1 in restrictive conditions for all mutations. At the metaphase arrest (3 hours after release), samples were collected for Top2 immunoprecipitation. Western blot of the immunoprecipitate revealed that the slower migrating forms of Top2 were stained by anti-SUMO antibodies, meaning that the observed modification is (at least partially) SUMOylation (**Figure 3.7**). The signal of anti-SUMO antibodies was almost completely abolished in *cdc20 cdc5* cells. This result indicates that Cdc5 activity is required for the SUMOylation of Top2 that is occurring in metaphase, consistently with what was reported in the literature (Bachant et al., 2002; Baldwin et al., 2009).

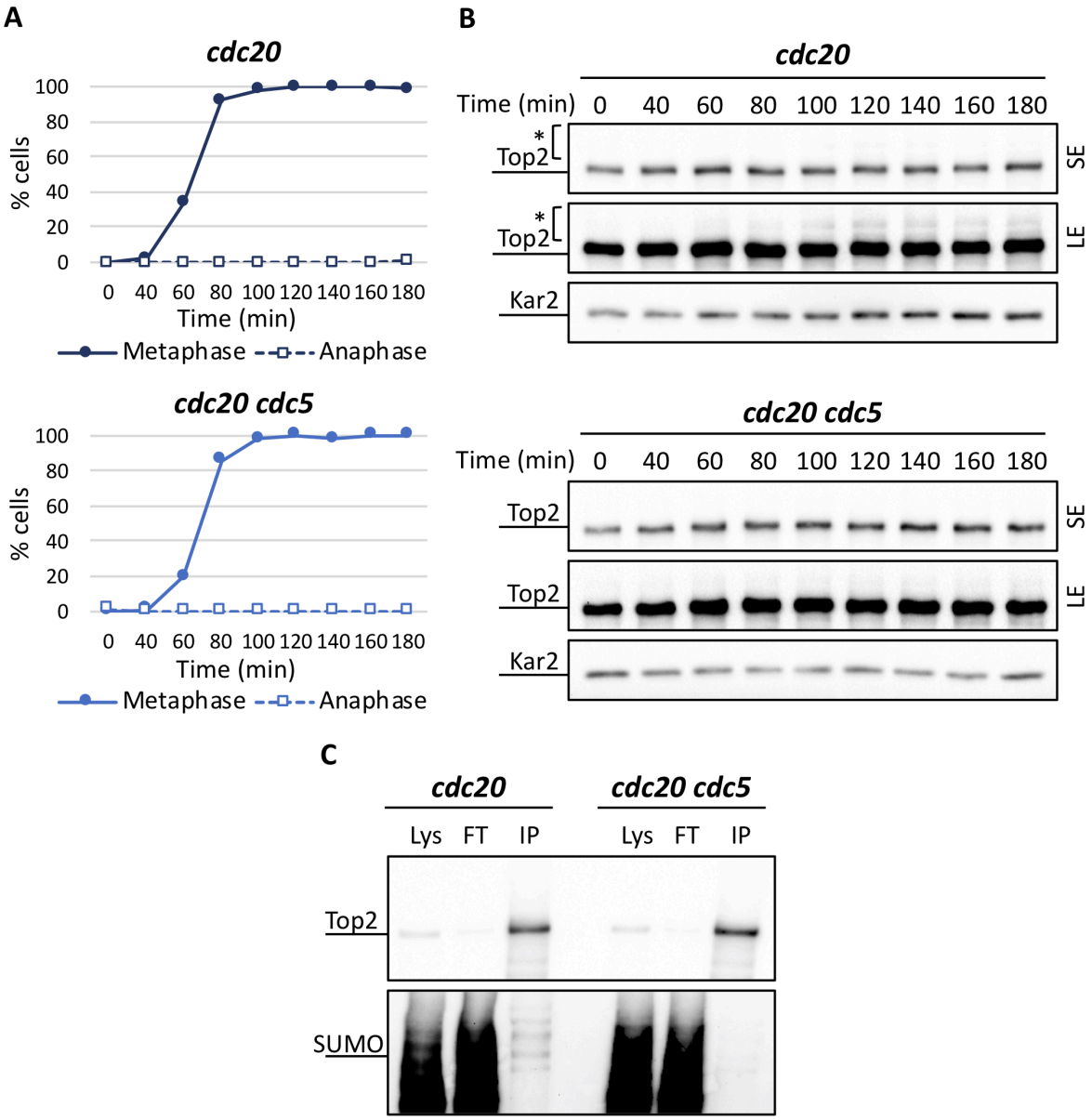

Figure 3.7. Cdc5 is required for Top2 SUMOylation in metaphase

*TOP2-9PK cdc20-aid (Ry8315) and TOP2-9PK cdc20-aid cdc5-as1 (Ry8785) cells were arrested in G1 with α-factor in YPD and synchronously released in media with the CMK inhibitor and auxin, to inactivate cdc5-as1 and cdc20-aid. Cell cycle progression was monitored through IF (anti-Tub1, DAPI; not shown). **A**) Cell cycle progression was monitored through IF (anti-Tub1, DAPI) and (**B**) samples were collected at the indicated times after release for western blot. Top2 signal is shown at two levels of exposure, short (SE) and long (LE). Kar2 was used as a loading control. (**C**) At the terminal arrest (3 hours after release), samples were collected for Top2 immunoprecipitation. SUMO conjugates were detected with an anti-Smt3 antibody. Lys, lysate; FT, flow-through; IP, immunoprecipitate.*

3.4.4. Endogenous phosphorylation of Top2 and requirement of Cdc5

In addition to SUMOylation, Top2 is also targeted by phosphorylation, although less is known about its significance in mitosis. Moreover, the human orthologue of Cdc5, Plk1, phosphorylates Topoisomerase II in human cells (Li et al., 2008). Therefore, we wondered whether Cdc5 could control Top2 through direct phosphorylation.

First of all, we tried to establish a method to monitor endogenous phosphorylation of Top2. Detection of Top2 phosphorylation by regular western blot proved to be challenging, because any potential phosphorylation was masked by the more prominent SUMOylation. For this reason, we used Phos-tag (Kinoshita et al., 2009), which increase the electrophoretic shift of phosphorylated proteins. We released *TOP2-9PK* cells from G1 and, as cells were undergoing a synchronous cell cycle, we collected time points to be analyzed by electrophoresis with Phos-tag gels, followed by western blot against Top2. However, we were not able to detect Top2 phosphorylation as cells were undergoing mitosis (not shown).

We then tried a different strategy and attempted to detect Top2 phosphorylation through immunoprecipitation followed by phosphatase treatment. Given that, in our experiments, we saw Top2 modification occurring in metaphase, we decided to look at the protein at this cell cycle stage and to test whether Cdc5 activity is required for its phosphorylation. We released *TOP2-9PK cdc20-aid* and *TOP2-9PK cdc20-aid cdc5-as1* cells from G1 arrest into a metaphase block, in restrictive conditions for *cdc5* mutation. At the metaphase arrest (3 hours after release), we collected samples for total protein extraction, which we analyzed by western blot with Phos-tag gels, but the results were again inconclusive (not shown). In addition, we collected cells to perform Top2 immunoprecipitation. The immunoprecipitated protein was split in two aliquots, one of which was treated with a viral phosphatase to remove any phosphorylation. If the observed modification is – at least partially – due to phosphorylation, phosphatase treatment should change the electrophoretic mobility of the protein. Western blot with an anti-SUMO antibody revealed that the ladder corresponding to Top2 SUMO-conjugates was present in *cdc20* cells, but not in *cdc20 cdc5* cells, thus confirming the requirement of Cdc5 for this modification. In addition, treatment with phosphatase seemed to slightly increase the electrophoretic mobility of the protein, although no difference was seen between *cdc20* and *cdc20 cdc5* cells in the untreated samples (**Figure 3.8**). Notably, treatment with phosphatase did not

reduce the signal of SUMO-conjugates. These results indicate that Top2 is likely phosphorylated in metaphase cells and seem to suggest that a kinase other than Cdc5 is responsible for this modification. Yet, the observed Cdc5-independent phosphorylation may be constitutive and we cannot exclude that this experimental setup was not sensitive enough to detect Cdc5-dependent phosphorylation of Top2 in mitosis.

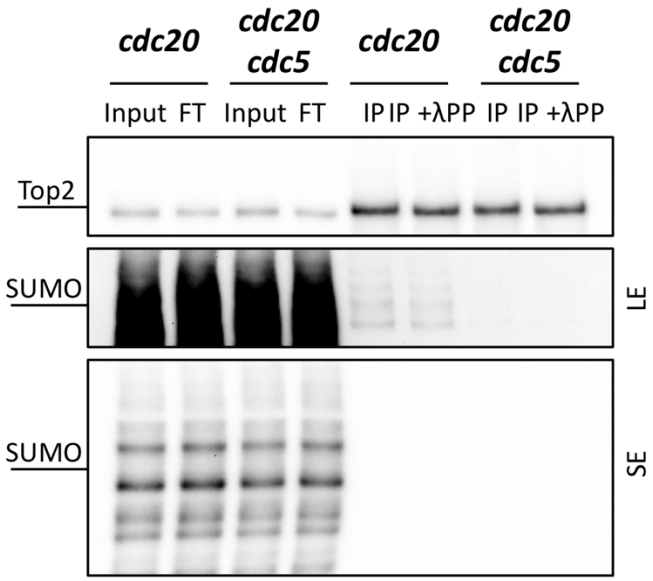

Figure 3.8. Phosphorylation of Top2 in metaphase
TOP2-9PK cdc20-aid (Ry8315) and TOP2-9PK cdc20-aid cdc5-as1 (Ry8785) cells were arrested in G1 with α-factor in YPD and synchronously released in media with the CMK inhibitor and auxin, to inactivate cdc5-as1 and cdc20-aid. Cell cycle progression was monitored through IF (anti-Tub1, DAPI; not shown). At the final metaphase arrest (3 hours after release), samples were collected for Top2 immunoprecipitation. The immunoprecipitate was split into two aliquots, one of which was treated with λ-phosphatase. SUMO conjugates were detected by western blot with an anti-Smt3 antibody, shown at two levels of exposure, short (SE) and long (LE). Lys, lysate; FT, flow-through; IP, immunoprecipitate; λ-PP, λ-phosphatase.

3.4.5. Cdc5 overexpression enhances SUMOylation and phosphorylation of Top2

To further investigate the impact of Cdc5 on Top2 PTMs, we overexpressed the kinase using the galactose-inducible promoter. We decided to perform the experiment with cells arrested in S phase by nucleotide depletion using hydroxyurea (HU), a ribonuclease reductase inhibitor because i) the activity of the polo-like kinase is low in this cell cycle stage (Charles et al., 1998; Cheng et al., 1998) and ii) treatment with HU activates the DNA damage response, which in turn leads to Cdc5 inhibition (Sanchez et al., 1999, 1996; Sun et al., 1996).

TOP2-9PK and *TOP2-9PK GAL-13MYC-CDC5* cells were grown in raffinose-containing media and arrested in S phase. At the arrest (3 hours after HU addition), galactose was added to the medium to induce *CDC5* expression. We monitored Top2 by western blot for 2 hours after induction and we found that slower migrating forms of the protein accumulated in *GAL-CDC5* cells, but not in wild-type cells, meaning that Cdc5 overexpression enhances Top2 modification (**Figure 3.9**). The experiment was also performed in cells arrested in metaphase with the *cdc20-aid* allele or by treatment with the microtubule depolymerizing drug nocodazole, giving identical results. In conditions of Cdc5 overexpression, we noticed the appearance of a ladder of slower migrating forms of Top2, possibly representing SUMO-conjugates. Moreover, in many experiments it was apparent that, upon Cdc5 overexpression, the protein appeared as a doublet, reminiscing phosphorylation.

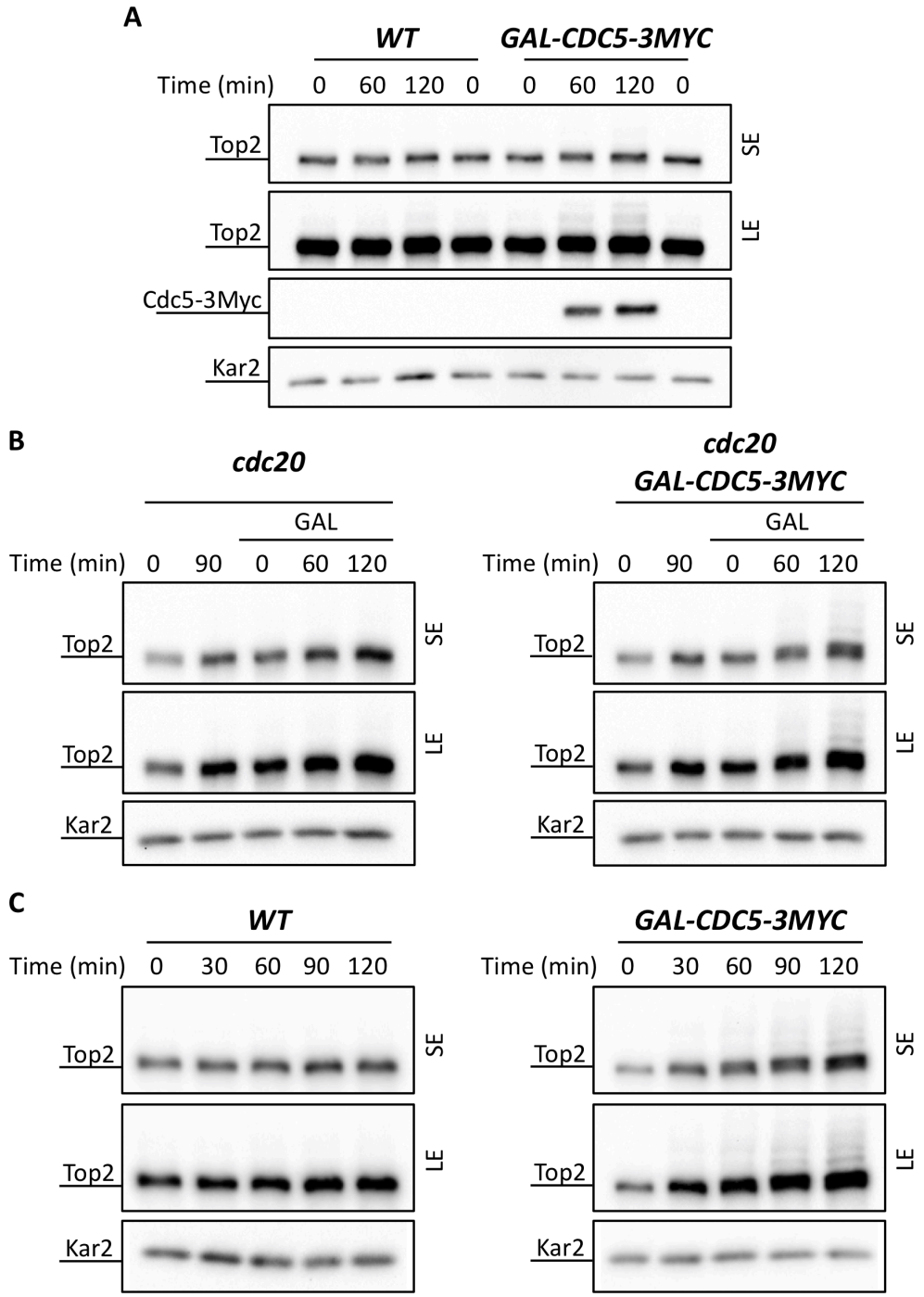

Figure 3.9. Overexpression of Cdc5 enhances Top2 modification

*(**A**) TOP2-9PK (Ry7921) and TOP2-9PK GAL-CDC5-3MYC (Ry9325) cells were grown in YPR and arrested in S phase by addition of hydroxyurea (HU) for 3 hours. At the arrest, 2% galactose was added. (**B**) TOP2-9PK cdc20-aid (Ry10137) and TOP2-9PK cdc20-aid GAL-CDC5-3MYC (Ry10139) cells were arrested in G1 in YPR and released in YPR media with auxin to inactivate cdc20-aid. At the metaphase arrest (120 min after release), 2% galactose was added. (**C**) TOP2-9PK (Ry7921) and TOP2-9PK GAL-CDC5-3MYC (Ry9325) cells were arrested in G1 in YPR and released in YPR media with nocodazole. At the nocodazole arrest (150 min after release), 2% galactose was added. (**A**, **B**, **C**) Cell cycle progression was monitored through IF (anti-Tub1, DAPI; not shown). Samples were collected every 30 min after galactose addition and analyzed through western blot. Top2 signal is shown at two levels of exposure, short (SE) and long (LE). Kar2 was used as a loading control.*

We now wanted to assess the nature of the modification induced by Cdc5 overexpression. To this aim, we collected samples for immunoprecipitation of Top2-PK followed by phosphatase treatment. *TOP2-9PK* and *TOP2-9PK GAL-13MYC-CDC5* cells were grown in raffinose-containing media and arrested in S phase with HU for 3 hours. At the arrest, galactose was added to the medium and, 2 hours after induction, samples were collected for immunoprecipitation of Top2 followed by western blot with an anti-SUMO antibody. In *GAL-CDC5*, but not in wild-type cells, we saw the appearance of a strong signal of Top2 SUMO-conjugates in the IP, meaning that Cdc5 induces SUMOylation of the protein (**Figure 3.10**). Interestingly, Cdc5 overexpression also increased the level of total SUMO conjugates, as indicated by the fact that the signal of anti-SUMO is higher in the lysate of *GAL-CDC5* cells than wild-type cells. These observations are consistent with the notion that Cdc5, by inhibiting the SUMO protease Ulp2, stimulates SUMOylation of its substrates (Baldwin et al., 2009).

We then wondered whether Cdc5 could also impact Top2 by direct phosphorylation, as suggested for Plk1 in human cells. Therefore, we assessed whether overexpression of Cdc5 increases Top2 phosphorylation *in vivo*. To this aim, *TOP2-9PK* and *TOP2-9PK GAL-13MYC-CDC5* cells were grown in raffinose-containing media and arrested in S phase. At the arrest, galactose was added to the medium and 2 hours after induction samples were collected for immunoprecipitation of Top2 followed by phosphatase treatment.

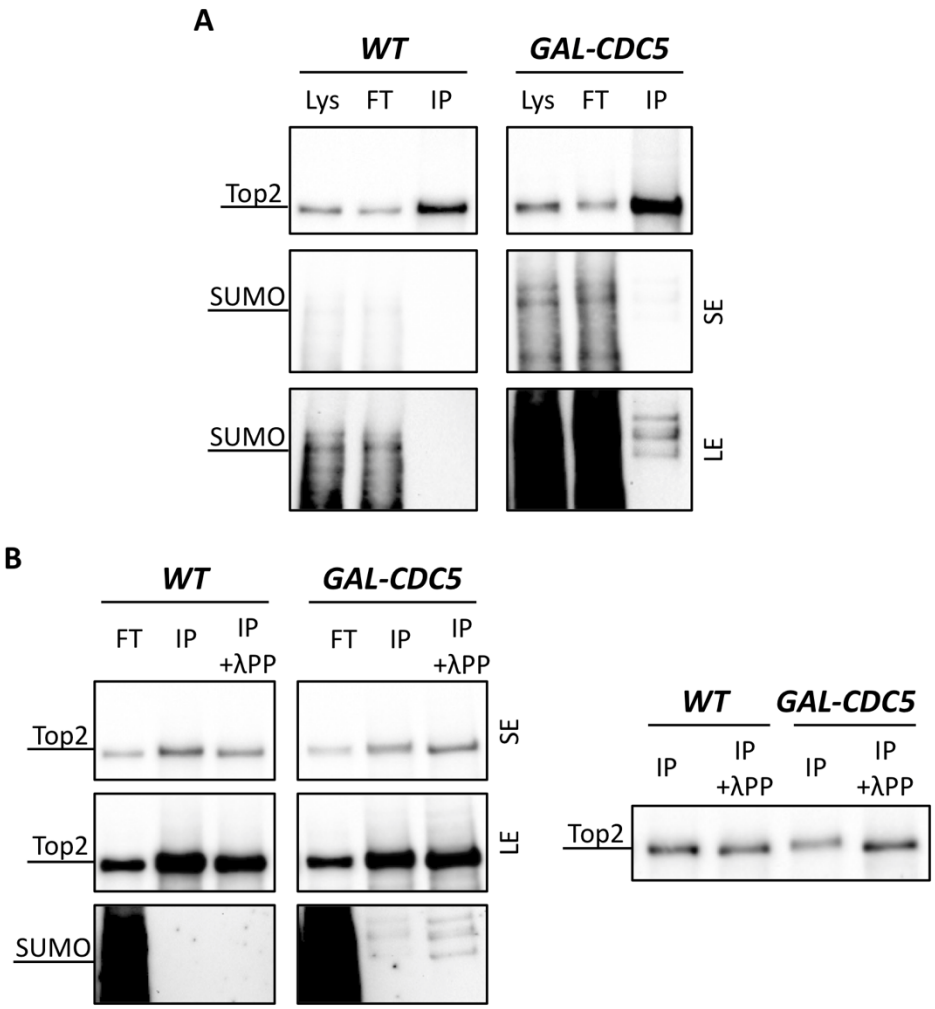

Figure 3.10. Cdc5 overexpression induces Top2 SUMOylation and phosphorylation

*TOP2-9PK (Ry7921) and TOP2-9PK GAL-CDC5-3MYC (Ry9325) cells were grown in YPR and arrested in S phase with hydroxyurea. At the arrest (3 hours after hydroxyurea addition), galactose was added to the medium. 2 hours after galactose addition, samples were collected for Top2 immunoprecipitation. (**A**) SUMO conjugates were detected by western blot with an anti-Smt3 antibody. (**B**) IP was treated with phosphatase and SUMO conjugates were detected with an anti-Smt3 antibody. The left panel shows samples loaded side-by-side for better comparison. SE, short exposure; LE, long exposure; Lys, lysate; FT, flow-through; IP, immunoprecipitate; λ-PP, λ-phosphatase.*

Western blot showed that the Top2 doublet that appeared after Cdc5 overexpression was flattened by treating with phosphatase, indicating that Cdc5 stimulates not only SUMOylation but also phosphorylation of Top2 *in vivo*. Interestingly, phosphatase treatment induced a change in the electrophoretic mobility of Top2 also in wild-type cells, indicating that, in S phase, some level of Top2 phosphorylation persists in conditions of low Cdc5 activity, consistently with what we observed in *cdc20 cdc5* cells.

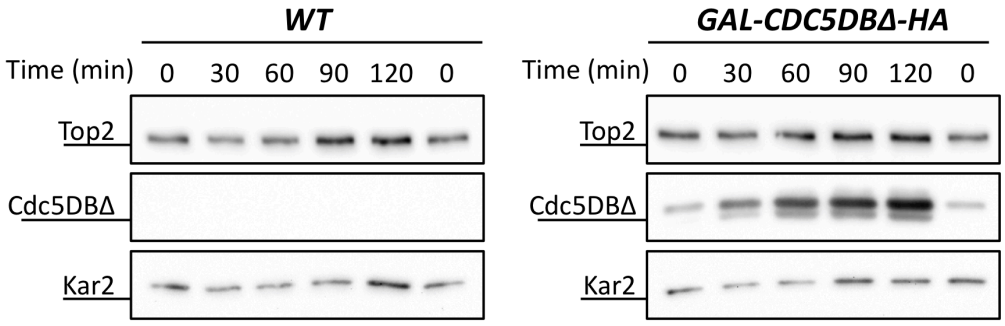

Figure 3.11. Cdc5 overexpression has no effect on Top2 in G1 cells
TOP2-9PK (Ry7921) and TOP2-9PK GAL-CDC5DBΔ-HA (Ry10659) cells were grown in YPR and arrested in G1 phase with α-factor for 150 min. At the arrest, 2% galactose was added to the medium. Samples were collected every 30 min after galactose addition for western blot analysis. Kar2 was used as a loading control.

The Cdc5-independent phosphorylation could be due to residual Cdc5 activity or to other kinases, such as cyclin-dependent kinases. For this reason, we wanted to perform the experiment in a cell cycle stage in which Top2 could be fully dephosphorylated, in the attempt to accentuate the effects of Cdc5 overexpression. Therefore, we arrested cells in G1 with α-factor pheromone for 2h30 and then added galactose to the medium to induce Cdc5 expression. Since, in G1, the polo-like kinase is rapidly degraded by the APC/C^{Cdh1}-dependent proteolysis (Charles et al., 1998; Shirayama et al., 1998), we used the Cdc5DBΔ protein, which lacks the destruction box required for APC-mediated degradation. Samples were taken for 2 hours after induction to analyze Top2 by western blot. We found that Cdc5 expression did not alter Top2 electrophoretic mobility in these conditions, suggesting that Cdc5 alone is not able to induce its phosphorylation nor SUMOylation in G1 cells (**Figure 3.11**). This result may be due to the reduced kinase activity of Cdc5DBΔ. Alternatively, phosphorylation by another kinase could be required to allow Cdc5 to target Top2. Indeed, Cdc5 phosphorylation in mitosis is often directed to substrates that have previously undergone phosphorylation by Cdk1, called Cdk priming (Elia et al., 2003).

In conclusion, we showed that, in addition to being necessary for SUMOylation of Top2, Cdc5 can lead to phosphorylation of the enzyme *in vivo* in S phase and metaphase. Therefore, Top2 is likely a substrate of Cdc5, although a caveat of our experiments is that the expression of the kinase at exceptionally high levels can override the system and bypass other steps of regulation.

3.4.6. Cdc5 and Cdc14 control Top2 recruitment on chromatin in metaphase

After finding that the polo-like kinase stimulates SUMOylation and phosphorylation of Top2, we asked if a dysregulation in Top2 PTMs could explain the decatenation defect observed in the absence of Cdc5 and Cdc14 activities and, if so, what could be the mechanism. SUMOylation is known to regulate the changes in Top2 localization during the cell cycle, particularly by inducing its recruitment to the centromeres and the rDNA after mitotic entry (Lee and Berger, 2019). Therefore, we decided to investigate the impact of Cdc5 and Cdc14 inactivation on the localization of Top2.

In a first attempt to monitor Top2 localization, we opted for immunofluorescence. *TOP2-6HA* cells, expressing a tagged version of the protein, were grown in exponential phase and samples were taken for immunofluorescence using anti-HA antibodies. We imaged cells to analyze Top2 localization, in addition to nuclear morphology, which we used to distinguish between the different cell cycle stages. The signal of Top2 was spread throughout the nucleoplasm and we could not detect any changes in its localization according to different cell cycle stages (**Figure 3.12**).

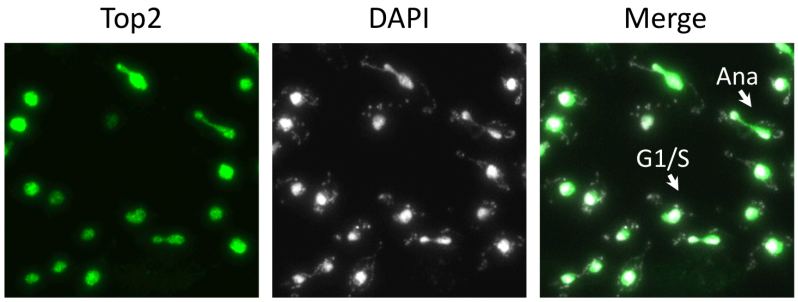

Figure 3.12. Immunofluorescence of Top2
TOP2-6HA (Ry7920) cells exponentially growing in YPD were collected for IF (anti-HA, DAPI). Representative images are shown.

Therefore, we moved to a more sensitive technique, namely chromatin immunoprecipitation followed by DNA sequencing (ChIP-seq). Since ectopic cohesin cleavage in cells arrested in metaphase with *cdc20* mutation leads to spindle elongation without forming anaphase bridges (Massari, 2018) – meaning that in metaphase the conditions are normally already set for the resolution of DNA intertwines – we planned a ChIP-seq experiment to assess the contribution of Cdc5 and Cdc14 to the recruitment of Top2 in metaphase.

We synchronously released *TOP2-9PK cdc20-aid*, *TOP2-9PK cdc5-as1 cdc20-aid*, *TOP2-9PK cdc14-1 cdc20-aid,* and *TOP2-9PK cdc5-as1 cdc14-1* cells from G1 arrest in restrictive conditions for all mutations. We could not test *cdc5-as1 cdc14-1 cdc20-aid* cells, as the combination is lethal. In addition, we also tested *cdc20-aid* cells that were released from G1 in a medium supplemented with the microtubule-depolymerizing drug nocodazole. As DNA intertwines can only be removed in the presence of a functional spindle, nocodazole-treated cells represent a negative control for catenane resolution. When cells reached their final arrest (metaphase or mini-anaphase, 3 hours after release), samples were collected to perform ChIP-seq of Top2-9PK. The experiment was performed by L. Massari and the collected data were analyzed in collaboration with bioinformatician D. Fernandez-Perez.

The results of this preliminary experiment showed that the overall level of chromatin-associated Top2 was the same between the conditions. We then analyzed the ChIP-seq results focusing on genomic regions that behaved differently among the samples (**Figure 3.13**). At the centromere, Top2 binding was highest in nocodazole-treated cells, where catenanes cannot be resolved, while it was abolished in the absence of Cdc5 or Cdc14 activity. At telomeres, Top2 binding was increased in the *cdc5 cdc14* double mutant compared to metaphase-arrested cells. Other regions which displayed reduced Top2 binding in conditions of Cdc5 or Cdc14 inactivation are yeast replication origins (ARS). Finally, Top2 binding at transposable elements was altered in *cdc5* and/or *cdc14* mutants compared to *cdc20* metaphase-arrested cells. More specifically, Top2 binding was lost at the 3' of Long Terminal Repeats (LTRs) retrotransposons in all *cdc5* and *cdc14* mutants, while it increased at the 5' in *cdc5 cdc14* double mutant cells. Interestingly, regions of increased Top2 binding in *cdc5 cdc14* cells, like telomeres and transposons, overlap with loci recently reported to be replicated in late anaphase (Ivanova et al., 2020). Since *cdc5 cdc14* cells arrest after anaphase onset, Top2 recruitment at these loci may reflect their

need to be replicated and decatenated in late mitosis. Collectively, the results of our ChIP-seq experiment suggest that Cdc5 and Cdc14 may influence Top2 recruitment to some genomic regions in metaphase and might indicate a possible reason for the decatenation defect of *cdc5 cdc14* cells.

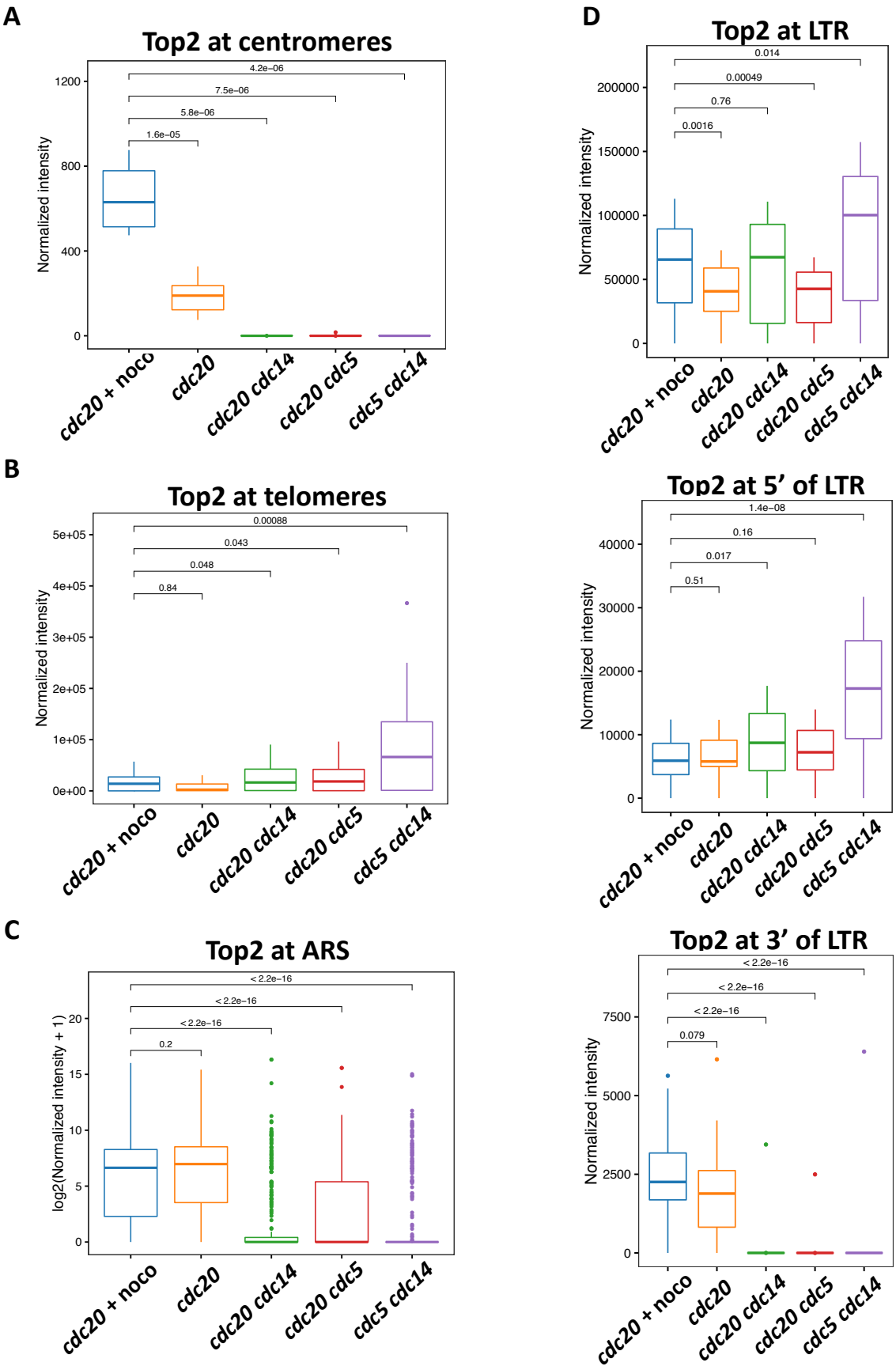
A
Top2 at centromeres
Normalized intensity
4.2e−06
7.5e−06
5.8e−06
1.6e−05
cdc20 + noco
cdc20
cdc20 cdc14
cdc20 cdc5
cdc5 cdc14
B
Top2 at telomeres
Normalized intensity
0.00088
0.043
0.048
0.84
C
Top2 at ARS
log2(Normalized intensity + 1)
< 2.2e−16
< 2.2e−16
< 2.2e−16
0.2
D
Top2 at LTR
Normalized intensity
0.014
0.00049
0.76
0.0016
Top2 at 5’ of LTR
1.4e−08
0.16
0.017
0.51
Top2 at 3’ of LTR
< 2.2e−16
< 2.2e−16
< 2.2e−16
0.079

Figure 3.13. ChIP-seq of Top2 in metaphase arrested cells

*TOP2-9PK cdc20-aid (Ry8315), TOP2-9PK cdc20-aid cdc14-1 (Ry8782), TOP2-9PK cdc20-aid cdc5-as1 (Ry8785), and TOP2-9PK cdc5-as1 cdc14-1 (Ry7998) cells were arrested in G1 with α-factor in YPD at 23°C and synchronously released in media with the CMK inhibitor and auxin at 37°C, to inactivate cdc5-as1, cdc20-aid, and cdc14-1. Nocodazole was added to the release medium where indicated. At the final arrest (3 hours after release), samples were collected for ChIP-seq of Top2. The plots show the level of Top2 binding at genomic regions in which differences between strains emerged, namely (**A**) telomeres, (**B**) centromeres, (**C**) origins of replications (ARS), and (**D**) long terminal repeats (LTR) retrotransposons.*

A caveat of this experiment is that we cannot tell whether the differences (e.g. Top2 enrichment at the telomeres) between *cdc5 cdc14* cells and the other strains are due to the simultaneous inactivation of Cdc5 and Cdc14 or to the difference in the cell cycle stage. For this reason, we wanted to repeat the ChIP-seq using a different strategy for Cdc20 depletion, compatible with *cdc5-as1* and *cdc14-1* mutations, namely the methionine-suppressible construct *MET-CDC20*. *TOP2-9PK MET-CDC20*, *TOP2-9PK MET-CDC20 cdc5-as1*, *TOP2-9PK MET-CDC20 cdc14-1,* and *TOP2-9PK MET-CDC20 cdc5-as1 cdc14-1* cells were grown in the absence of methionine, to allow Cdc20 expression, and released from G1 into the metaphase arrest using methionine-supplemented media, in restrictive conditions for *cdc5* and *cdc14* mutations. Since the *MET-CDC20* allele is less stringent, which makes it more challenging to maintain a prolonged arrest, cells were collected for ChIP-seq 2h30 after release. The ChIP-seq was performed twice, in technical replicates, and the analysis of the collected data was done in collaboration with D. Fernandez Perez.

Unexpectedly, the results of this experiment did not confirm the changes in Top2 binding at centromeres, telomeres, and LTRs that emerged from the previous *cdc20-aid* experiment. These discrepancies could be due to the fact that *cdc20-aid* cells remained arrested in metaphase longer, thus amplifying the differences between the strains. Moreover, we realized that there was little consistency between the *MET-CDC20* replicates. We hypothesized that this could be due to the very scarce amounts of DNA obtained from the ChIP and the variability of fragment length after sonication. Therefore, we decided to move back to the *cdc20-aid* system, and we set to develop a more robust protocol for ChIP-seq of Top2 in our conditions. However, we encountered some experimental problems. We realized that heating the cells at 37°C, the restrictive temperature for *cdc14-1* mutation, greatly reduced the efficiency of crosslinking. Therefore, we performed troubleshooting to find the appropriate conditions to improve the yield of crosslinked chromatin. Unfortunately, changing crosslink conditions affected the subsequent step of chromatin sharing by sonication. We will now focus on the optimization of the sonication condition, to obtain DNA fragments of the optimal length for sequencing in a reproducible fashion.

In conclusion, due to the technical difficulties encountered, we still did not complete the optimization of our protocol for ChIP-seq at the time present and we could not yet replicate the experiment.

3.5. Interplay between Cdc5 and the SUMO pathway

SUMOylation and Cdc5-dependent regulation emerge as common features of Topoisomerase II, condensin, and cohesin, three major players in catenane resolution (Mukhopadhyay and Dasso, 2017). For this reason, we started to investigate the contribution of the SUMO pathway in the resolution of DNA intertwines and its interplay with the Polo-like kinase.

SUMOylation of specific target proteins is cell-cycle regulated and studies from budding yeast pointed to an essential role of this PTM specifically between metaphase and anaphase (Li and Hochstrasser, 1999; Wolfgang Seufert et al., 1995). In *S. cerevisiae*, the SUMO protease Ulp2/Smt4 is phosphorylated in metaphase, in a way that is dependent on Cdc5 and the cyclin-dependent kinase Cdk1 (Baldwin et al., 2009). This phosphorylation inactivates the enzyme and leads to an increase in SUMOylation of key proteins, which in turn controls many mitotic events, including the release of cohesion between sister chromatids (Mukhopadhyay and Dasso, 2017).

Building from these observations, we hypothesized that the sister chromatid separation defect of *cdc5 cdc14* cells could be because, in absence of the polo-like kinase, Ulp2 is hyperactive, which causes a dysregulation in the SUMOylation of substrates involved in the resolution of DNA intertwines, such as Topoisomerase II. To test this hypothesis, we planned to modulate SUMOylation, acting both globally and specifically on Top2, and assess the consequences on the resolution of anaphase bridges.

3.5.1. Timing and requirements of Ulp2 phosphorylation

Ulp2 is phosphorylated in metaphase

Before addressing the role of SUMO in SCI resolution, we wanted to establish the timing and requirements of Ulp2 regulation. We started by analyzing the protein by western blot, as *ULP2-3HA* cells were synchronously released from G1 arrest into the next cell cycle. Cell cycle progression was monitored by looking at spindle morphology and amounts of the mitotic cyclin Clb2. Western blot showed a higher-migrating form of Ulp2, indicating post-translational modification, appearing at 90’ and disappearing at 120’ after release, in correspondence to the metaphase-to-anaphase transition (**Figure 3.14**).

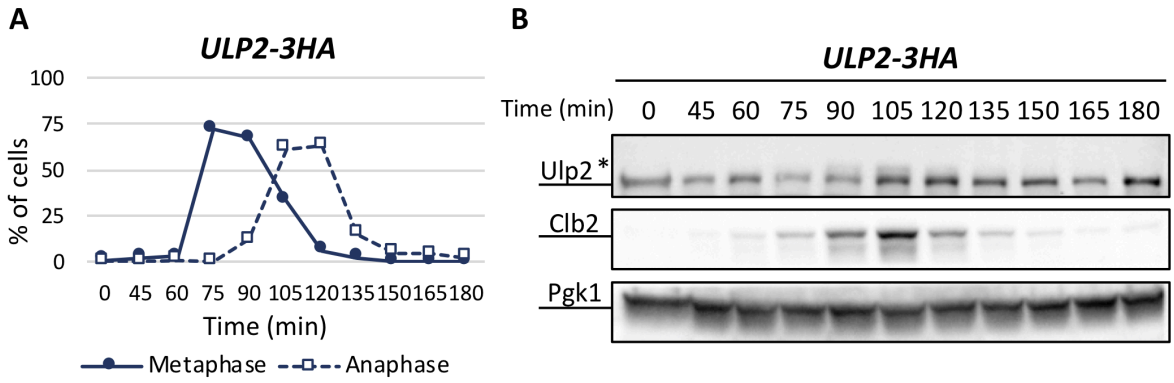

Figure 3.14. Ulp2 is modified in a cell cycle-dependent manner
*ULP2-3HA (Ry7865) cells were arrested in G1 with α-factor in YPD and synchronously released in YPD media. Samples were collected at the indicated times after release to (**A**) monitor cell cycle progression through IF (anti-Tub1, DAPI) and (**B**) perform western blot of Ulp2-3HA and Clb2. Asterisk (*) indicates the modified form of Ulp2. Pgk1 was used as a loading control.*

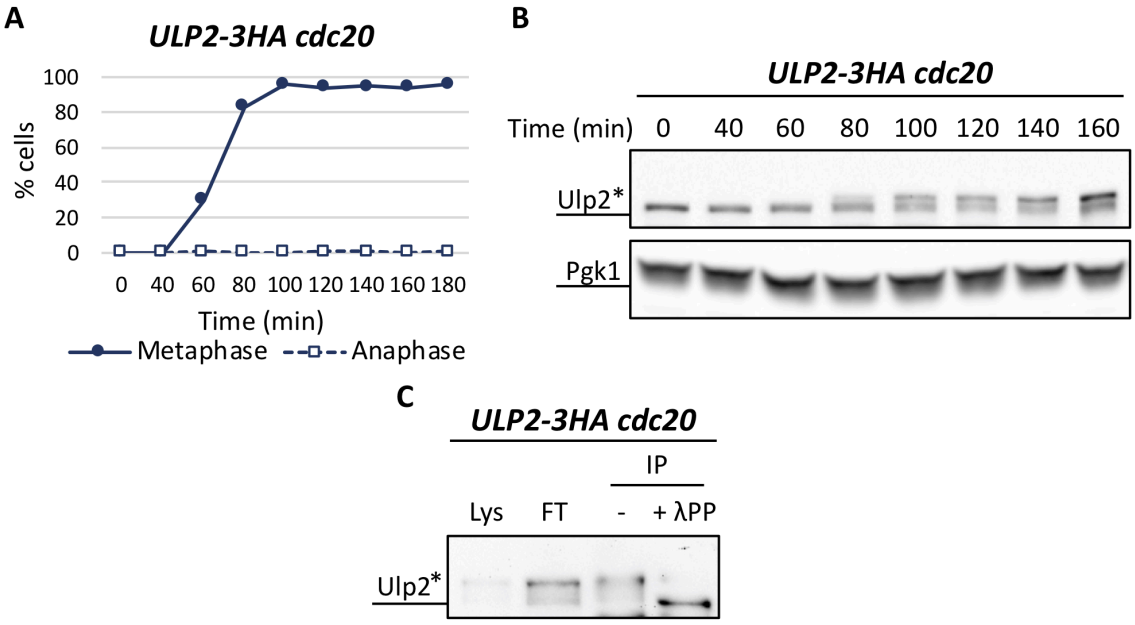

Figure 3.15. Ulp2 is phosphorylated in metaphase
*ULP2-3HA cdc20-aid (Ry8126) cells were arrested in G1 with α-factor in YPD and synchronously released in media with auxin to deplete Cdc20-aid. Samples were collected at the indicated times after release to monitor (**A**) cell cycle progression through IF (anti-Tub1, DAPI) and (**B**) Ulp2 status by western blot. Asterisks (*) indicate the modified form of Ulp2. Pgk1 was used as a loading control. (**C**) At the metaphase arrest (3 hours after release), samples were collected for immunoprecipitation of Ulp2 followed by treatment with phosphatase. Lys, lysate; FT, flow-through; IP, immunoprecipitate; λ-PP, λ-phosphatase.*

To pinpoint the timing of Ulp2 modification, we released *ULP2-3HA cdc20-aid* cells from G1 arrest into the metaphase arrest, we monitored Ulp2 by western blot and we found that the modified form of the enzyme accumulated in these cells (**Figure 3.15**). This result indicates that Ulp2 is modified in metaphase. To confirm that, as reported in the literature (Baldwin et al., 2009), the observed modification is phosphorylation, we collected cells at the metaphase arrest (3 hours after release) to perform immunoprecipitation of Ulp2, followed by treatment with phosphatase. Phosphatase treatment completely abolished the electrophoretic shift of Ulp2. Altogether, these observations confirm that the Ulp2 is phosphorylated in metaphase.

Ulp2 is phosphorylated by Cdc5 upon Cdk priming

After establishing the timing of Ulp2 phosphorylation, we moved to characterize its requirements. To this aim, we analyzed Ulp2 in *cdc20* cells arrested in metaphase with or without Cdc5 inactivation, in addition to wild-type cells undergoing a synchronous cell cycle. We released *ULP2-3HA*, *ULP2-3HA cdc20-aid,* and *ULP2-3HA cdc20-aid cdc5-as1* cells from G1 block in restrictive conditions for all mutations. In *cdc20 cdc5* cells, western blots showed the accumulation of a form of Ulp2 with intermediate electrophoretic mobility (**Figure 3.16**). To better appreciate the changes in electrophoretic mobility, we selected the samples corresponding to the metaphase-to-anaphase transition (as indicated by spindle morphology) and loaded them side by side on a gel. These observations indicate that Cdc5 inactivation partially – but not fully – abolishes Ulp2 phosphorylation.

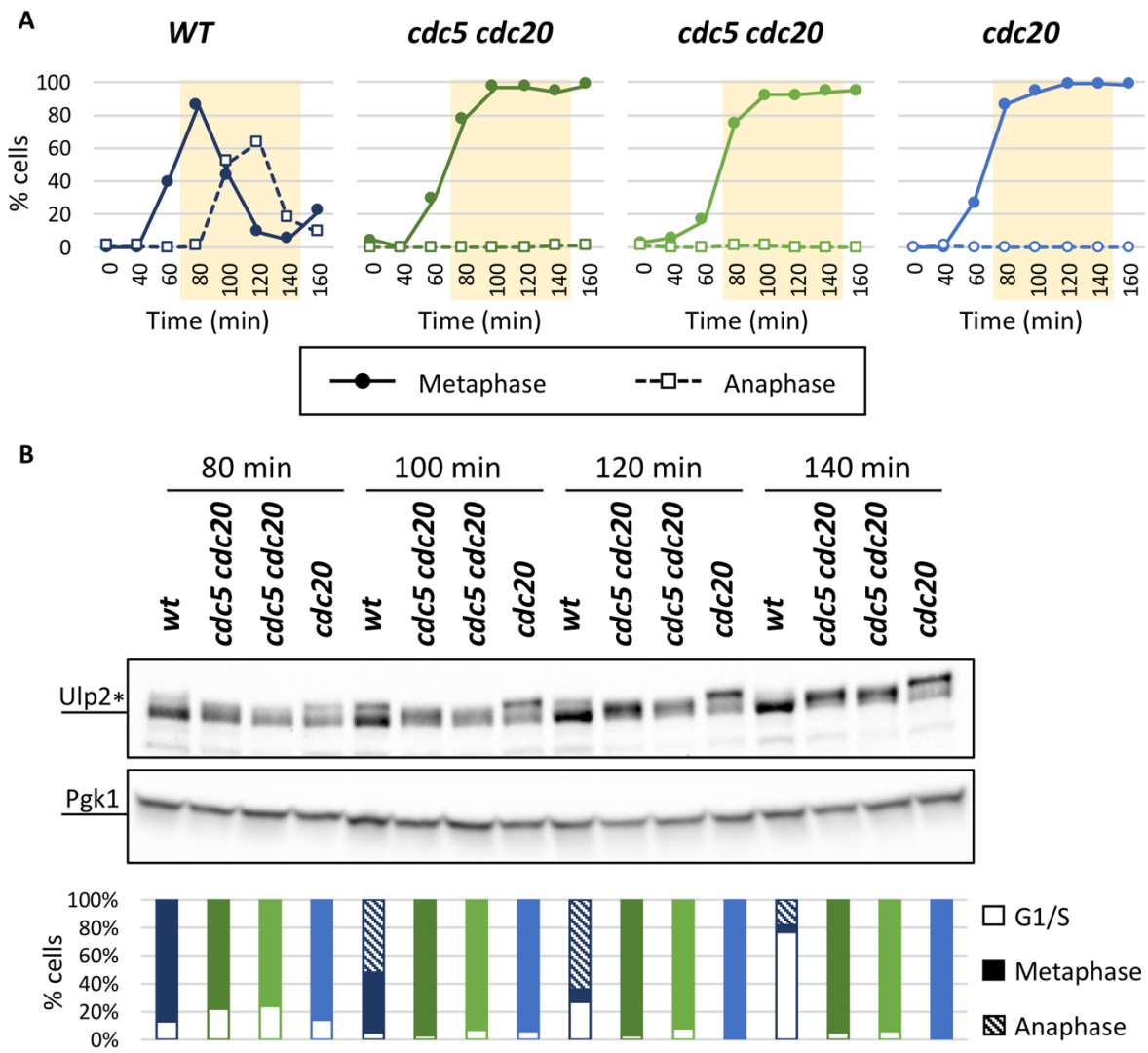

Figure 3.16. Ulp2 phosphorylation partially depends on Cdc5

*ULP2-3HA (Ry7865), ULP2-3HA cdc20-aid cdc5-as1 (Ry8183, Ry8184), and ULP2-3HA cdc20-aid (Ry8126) cells were arrested in G1 in YPD and released in media with the CMK inhibitor and auxin, to inactivate cdc5-as1 and cdc20-aid. Samples were collected at the indicated times after release for western blot. (**A**) Cell cycle progression was monitored through IF (anti-Tub1, DAPI). (**B**) To better appreciate the differences in Ulp2 electrophoretic mobility, samples corresponding to the highlighted time points were loaded side-by-side on the gel. Asterisk (*) indicates modified forms of Ulp2. Pgk1 was used as a loading control.*

As Cdc5 phosphorylation in mitosis often depends on Cdk priming, we wondered whether the residual Ulp2 modification observed in absence of polo-like kinase activity was due to phosphorylation by Cdk1. To address this question, we uncoupled the activities of the two kinases by selective inactivation of Cdc28, the Cdk catalytic subunit, using the analog-sensitive allele *cdc28-as1* (Bishop et al., 2000). We analyzed Ulp2 by western blot in *ULP2-3HA cdc20-aid*, *ULP2-3HA cdc20-aid cdc5-as1*, *ULP2-3HA cdc20-aid cdc28-as1,* and *ULP2-3HA cdc20-aid cdc28-as1 CDC5DBΔ* cells. The *CDC5DBΔ* allele lacks the destruction box, which allows us to avoid the degradation of the kinase that occurs when Cdk1 is inhibited. We released cells from S phase into a metaphase block in restrictive conditions for *cdc5* mutation. Once cells reached metaphase (80 minutes after release), we inactivated Cdc28 and followed cells for an additional 150 minutes.

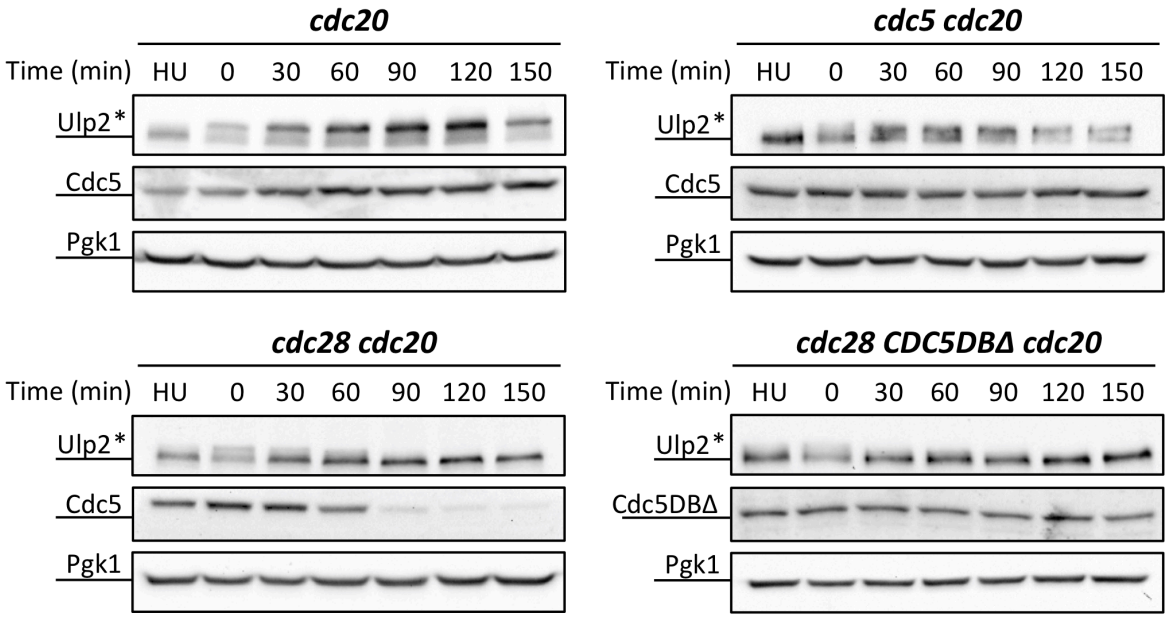

Figure 3.17. Ulp2 phosphorylation requires Cdk1
ULP2-3HA cdc20-aid (Ry8943), ULP2-3HA cdc20-aid cdc5-as1 (Ry8980), ULP2-3HA cdc28-as1 cdc20-aid (Ry8946), and ULP2-3HA cdc28-as1 CDC5DBΔ cdc20-aid (Ry8993) cells were arrested in S phase with hydroxyurea in YPD and synchronously released in media with the CMK inhibitor and auxin, to inactivate cdc5-as1 and cdc20-aid. At the metaphase arrest (80 min after release), NMPPi was added to the medium to inactivate cdc28-as1. Cell cycle progression was monitored through IF (anti-Tub1, DAPI; not shown). Samples were collected at the HU arrest and at the indicated times after Cdc28 inhibition for western blot. Asterisks (*) indicate modified forms of Ulp2. Pgk1 was used as a loading control.

Western blots showed that, as expected, while endogenous Cdc5 was degraded after Cdc28 inhibition in *cdc20 cdc28* cells, Cdc5DBΔ remained stable (**Figure 3.17**). In addition,

we observed that Ulp2 appears as a doublet in all strains during metaphase block. While the slower-migrating band stays stable in *cdc20* and *cdc20 cdc5* cells, it gradually disappears upon Cdc28 inhibition both in *cdc20 cdc28* and *cdc20 cdc28 CDC5DBΔ* cells. This result indicates that Ulp2 phosphorylation is completely abolished in absence of Cdk1 activity, even if Cdc5 is active. Moreover, the fact that Ulp2 phosphorylation is decreasing indicates that a phosphatase is targeting the SUMO protease in these conditions.

In conclusion, we established that Ulp2 is phosphorylated in metaphase cells and we collected evidence of Ulp2 phosphorylation by Cdc5 following Cdk priming, in agreement with the literature (Baldwin et al., 2009). Notably, we also observed that phosphorylation of Ulp2 always correlated with Top2 modification, since the SUMO protease was phosphorylated in *cdc14-1* cells, but not in *cdc5-as1* or *cdc5-as1 cdc14-1* cells (**Figure 3.18**).

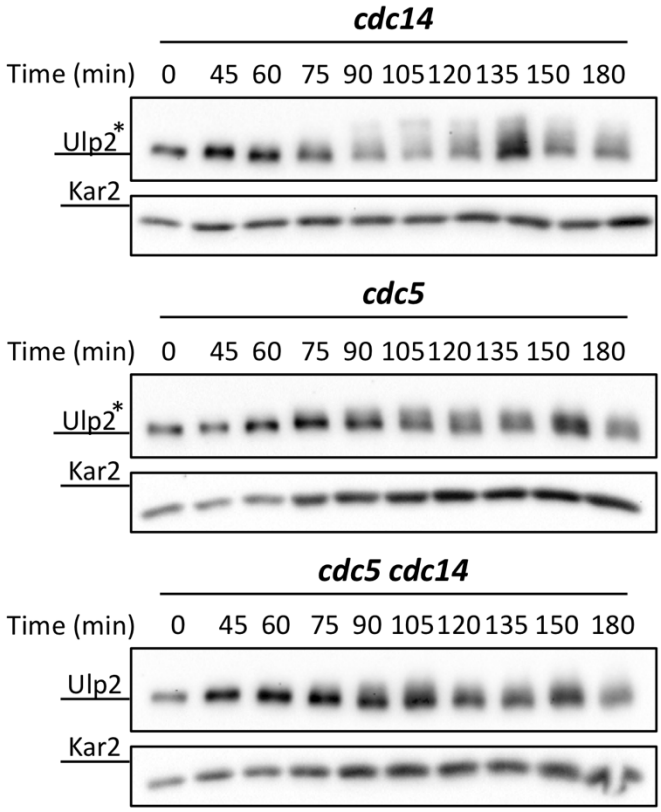

Figure 3.18. Ulp2 modification requires Cdc5 but not Cdc14
ULP2-3HA cdc14-1 (Ry9947), ULP2-3HA cdc5-as1 (Ry9948), and ULP2-3HA cdc5-as1 cdc14-1 (Ry9951) cells were arrested in G1 with α-factor in YPD at 23°C and released in media with CMK inhibitor at 37°C, to inactivate cdc5-as1 and cdc14-1. Samples were collected at the indicated times after release for western blot. Asterisks (*) indicate modified forms of Ulp2. Kar2 was used as a loading control. Cell cycle progression was monitored through IF (anti-Tub1, DAPI; not shown).

3.6. The role of Top2 SUMOylation in the resolution of SCIs

3.6.1. Non-SUMOylatable Top2 does not affect the resolution of anaphase bridges

Based on the observations that i) *cdc5* and *cdc5 cdc14* cells retain unresolved catenanes, ii) Cdc5 is required for Top2 SUMOylation in metaphase, iii) Cdc5 is required for Ulp2 phosphorylation in metaphase, and iv) Top2 is a substrate of Ulp2, we hypothesized that the molecular reason behind the decatenation defect of *cdc5* cells lies in the lack of Ulp2 inactivation by Cdc5 at the metaphase-to-anaphase transition, which in turn hinders SUMOylation of substrates involved in sister chromatid resolution, including Top2.

To test our hypothesis, we asked whether a non-SUMOylatable allele of Top2 (called Top2 SUMO-no-more, *top2-snm*) could recapitulate the sister chromatid separation defects of *cdc5* cells (Bachant et al., 2002). To this aim, we transformed yeast cells to integrate either *top2-snm-3HA* or *TOP2-3HA* at the Top2 locus and we asked whether they retained anaphase bridges. We synchronously released wild-type, *TOP2-3HA*, and *top2-snm-3HA* cells from G1 into the next cell cycle. By looking at spindle morphology, we observed that cells divided with the same kinetics (**Figure 19**). We then looked at nuclear and nucleolar morphology by immunofluorescence and we found that the resolution of anaphase bridges occurred similarly in the three strains.

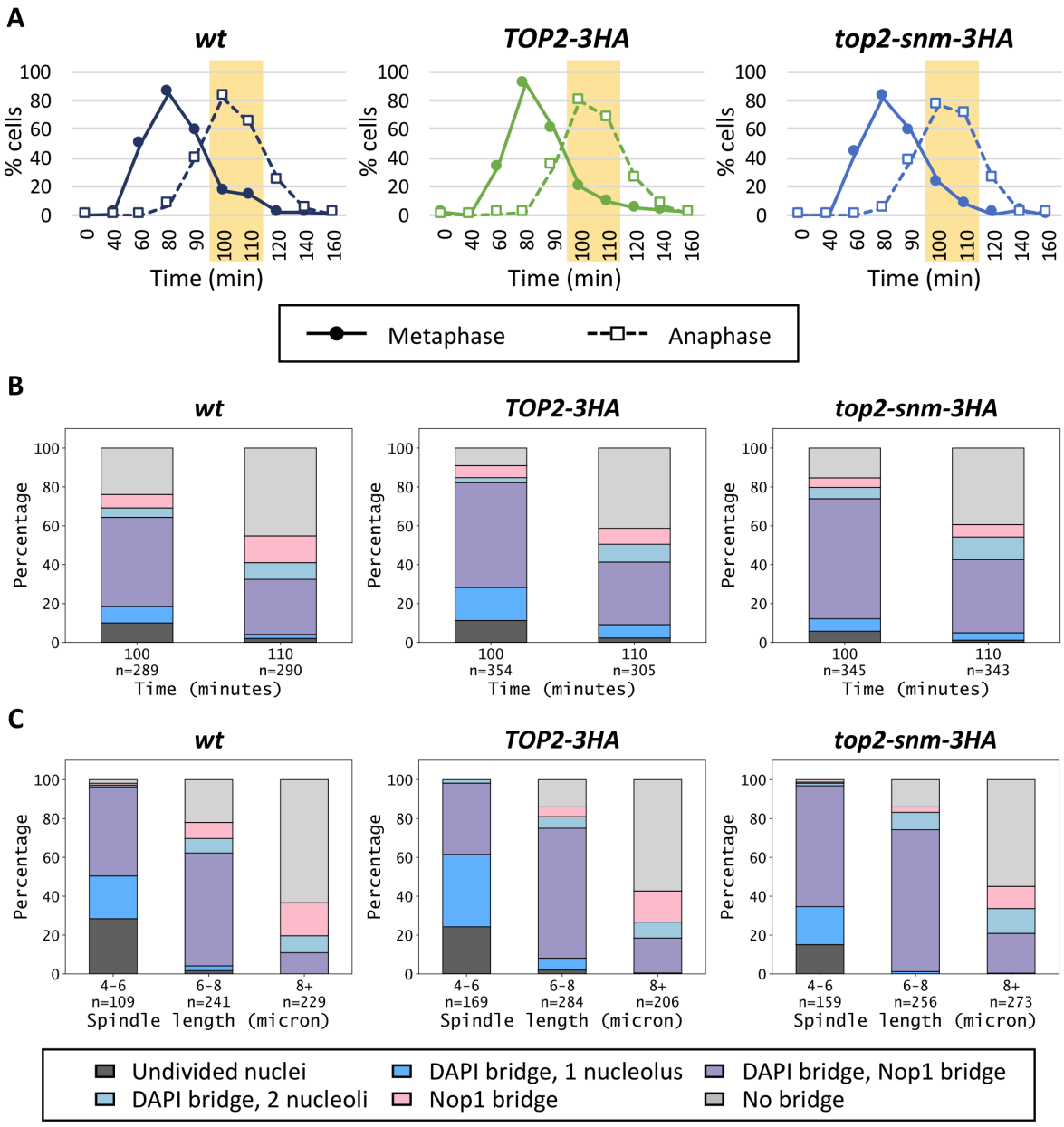

Figure 3.19. The non-SUMOylatable allele of Top2 does not affect anaphase bridge resolution in cycling cells

*Wild-type (Ry1), TOP2-3HA (Ry10464), and top2-snm-3HA (Ry10466) cells were arrested in G1 with α-factor in YPD at 23°C and released in medium. (**A**) Samples were collected at the indicated times after release to monitor cell cycle progression through IF (anti-Tub1, DAPI). (**B**, **C**) Highlighted samples were analyzed through IF (anti-Tub1, anti-Nop1, DAPI) to score for the presence of anaphase bridges. At least 100 cells were analyzed for each time point. Spindles were measured and cells were assigned to the indicated categories according to nuclear and nucleolar morphology. Plots show the distribution of anaphase cells (spindles > 4µm) between categories according to (**B**) time after release and (**C**) spindle length.*

We then tested the *top2-snm* allele in *cdc5*, *cdc14,* and *cdc15* strains, which arrest in anaphase. We synchronously released *cdc5-as1 top2-snm-3HA*, *cdc5-as1 TOP2-3HA*, *cdc14-1 top2-snm-3HA*, *cdc14-1 TOP2-3HA*, *cdc15-as1 top2-snm-3HA,* and *cdc15-as1 TOP2-3HA* cells from G1 in restrictive conditions for *cdc5, cdc14,* and *cdc15* mutations. Even in this case, the non-SUMOylatable allele of Top2 did not alter the number of anaphase bridges (**Figure 3.20**). These results suggest that the lack of Top2 SUMOylation may not be the main reason behind the decatenation defect of *cdc5* and *cdc5 cdc14* cells.

Several explanations for these results are possible. Although western blot confirmed that the bulk of Top2 SUMOylation is abolished in *top2-snm* cells (**Figure 3.20B**), we cannot exclude that some level of modification persists. Alternatively, Cdc5 may drive the resolution of DNA catenanes in other ways. For example, the polo-like kinase may control Top2 through phosphorylation. Finally, the regulation of SCI resolution by Cdc5 and Ulp2 may not be centered solely on Top2, but rather involve several SUMO substrates.

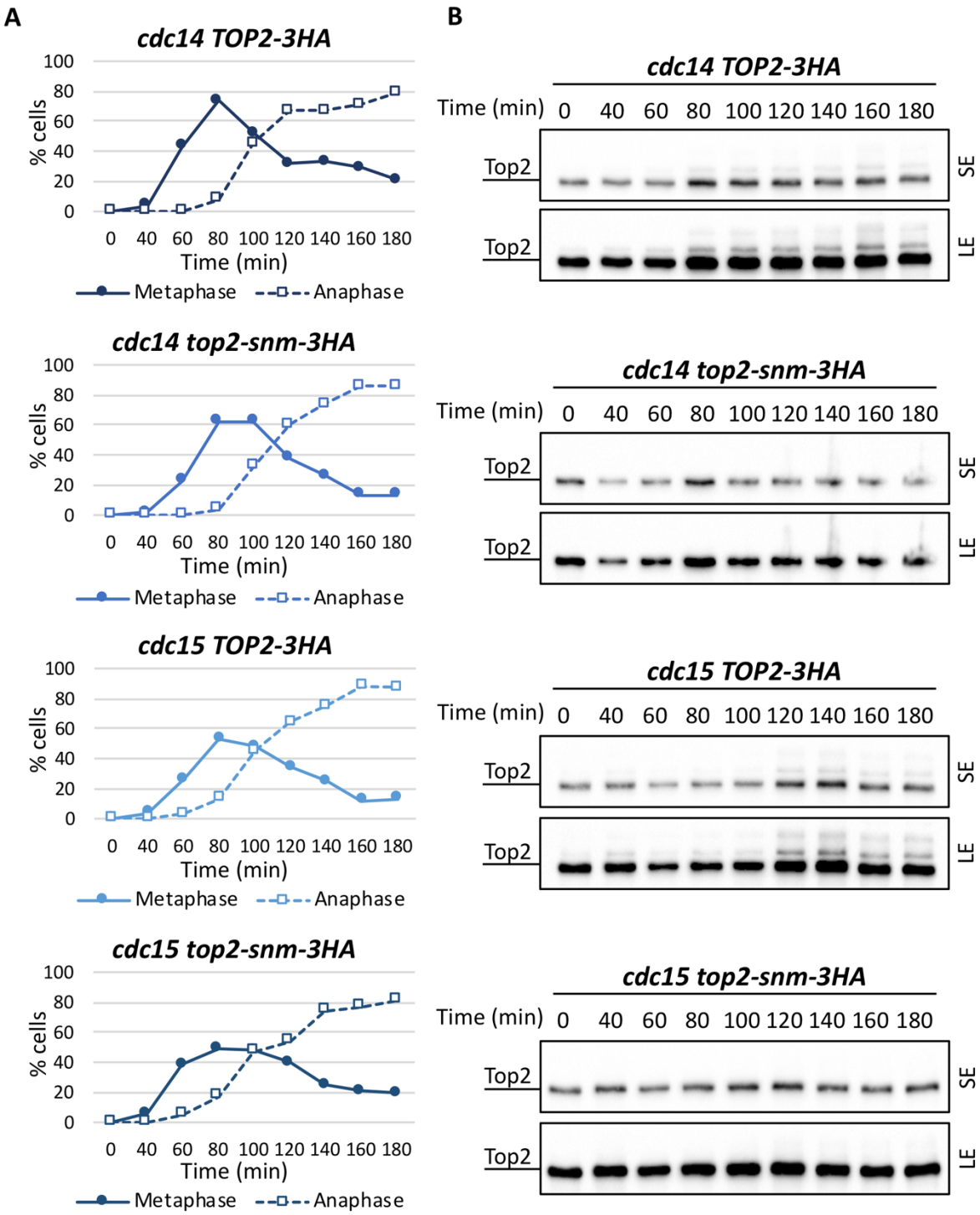

Figure 3.20. The non-SUMOylatable allele of Top2 does not affect anaphase bridges resolution in anaphase-arrested cells

*cdc5-as1 top2-snm-3HA (Ry10482), cdc5-as1 TOP2-3HA (Ry10476), cdc14-1 top2-snm-3HA (Ry10485), cdc14-1 TOP2-3HA (Ry10473), cdc15-as1 top2-snm-3HA (Ry10542), and cdc15-as1 TOP2-3HA (Ry10539) cells were arrested in G1 with α-factor in YPD at 23°C and released in media with the CMK and NMPPi inhibitors at 37°C, to inactivate cdc5-as1, cdc15-as1, and cdc14-1. (**A**) Cell cycle progression was monitored through IF (anti-Tub1, DAPI) and (**B**) Samples were collected at the indicated times after release for western blot of Top2, which is shown at two levels of exposure, short (SE) and long (LE). (**C**, **D**) Samples were*

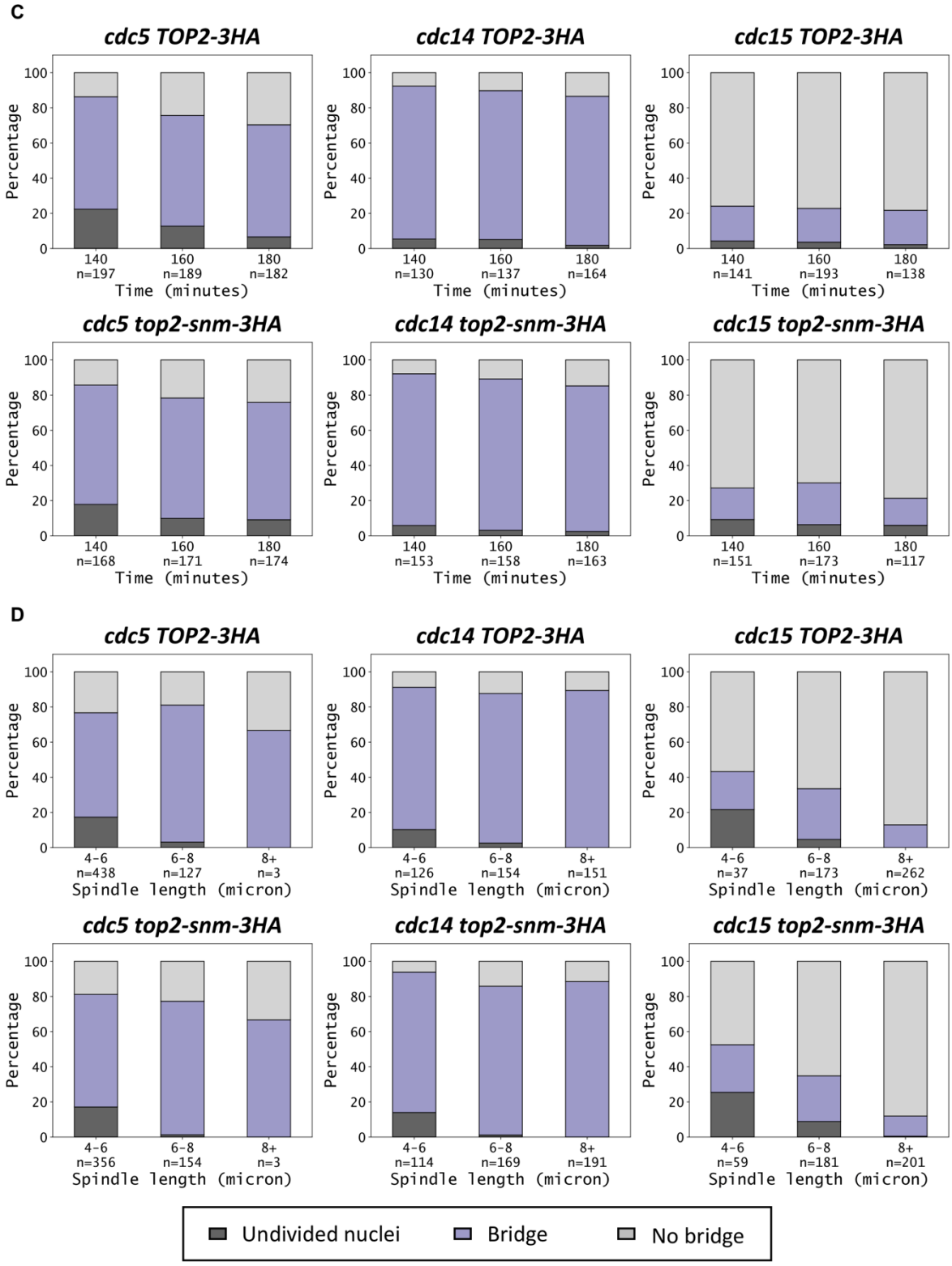

*collected at the indicated times after release and analyzed through IF (anti-Tub1, anti-Nop1, DAPI) to score for the presence of anaphase bridges. At least 100 cells were analyzed for each time point. Spindles were measured and cells were assigned to the indicated categories according to nuclear and nucleolar morphology. Plots show the distribution between categories according to (**C**) time after release and (**D**) spindle length.*

3.7. Effects of Ulp2 dysregulation

The fact that *top2-snm* cells do not accumulate anaphase bridges suggests that lack of Top2 SUMOylation is not the main reason underlying the decatenation defect of *cdc5 cdc14* cells. Besides Top2, other Ulp2 substrates are involved in SCI resolution, such as condensin and the cohesin-associated subunit Pds5 (Baldwin et al., 2009; Stead et al., 2003). Therefore, it is possible that, in *cdc5* cells, the failure to downregulate Ulp2 in metaphase triggers the accumulation of SCI due to the lack of SUMOylation of other players involved in the resolution of anaphase bridges.

To test our hypothesis, we decided to mimic a dysregulation in overall SUMO-conjugation by acting on the amounts of Ulp2 and ask whether and how it affects mitosis in general, and particularly the resolution of anaphase bridges. We reasoned that, if the accumulation of anaphase bridges in *cdc5* and *cdc5 cdc14* cells is due to Ulp2 hyperactivation, depletion of the SUMO protease should ameliorate this phenotype, while its overexpression should worsen it.

3.7.1. Modulation of Ulp2 disrupts normal SUMO-conjugation

We deleted the *ULP2* gene to construct loss-of-function yeast mutants. To construct gain-of-function mutants, we cloned *ULP2* under the galactose-inducible promoter and inserted the *GAL-ULP2* construct in the yeast genome, without altering the endogenous gene. We used PCR to distinguish between the transformants which integrated a single copy or multiple copies of the construct and we selected one clone for each category.

First of all, to investigate how overall SUMOylation is affected by *ULP2* mutation, we probed whole-cell extracts of *ulp2Δ* and *GAL-ULP2* cells with an anti-SUMO antibody. To test the effects of *ULP2* deletion, wild-type and *ulp2Δ* cells were grown in glucose-containing media and collected in the exponential phase. On the other hand, to test *ULP2* overexpression, wild-type cells and *GAL-ULP2* cells bearing either one or multiple copies of the construct were grown in raffinose-containing media, galactose was added to the media in exponential phase and cells were collected at 2 hours and 3 hours after induction. We found that the level of SUMO-conjugates was dramatically affected by changes in the amount of Ulp2 (**Figure 3.21**). In particular, *ulp2Δ* cells showed aberrant accumulation of

high-molecular weight SUMO-conjugates, while induction of *GAL-ULP2* greatly decreased the signal coming from SUMOylated proteins, in a dose-dependent fashion.

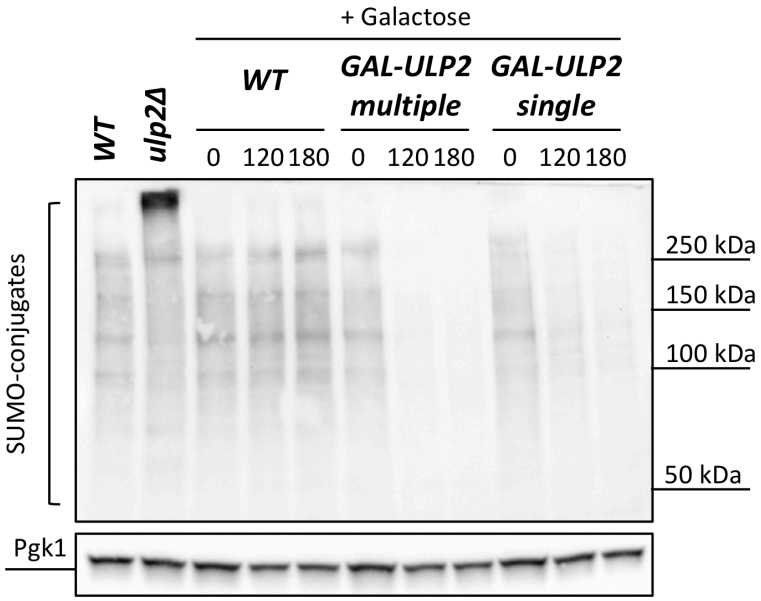

Figure 3.21. Loss of function and gain of function mutations of ULP2 have dramatic effects on the pattern of SUMO-conjugates
Wild-type (Ry1) and ulp2Δ (Ry7921) cells exponentially growing in YPD were collected for western blot analysis. Wild-type cells (Ry1) and GAL-ULP2 cells bearing one (Ry8130) or more (Ry8129) copies of the construct were grown in YPR. When cells reached exponential phase, 2% galactose was added to the media to induce Ulp2 overexpression and samples were collected at the indicated times after induction for western blot analysis. Total protein extracts were probed with an antibody against SUMO.

3.7.2. Ulp2 deletion causes pleiotropic defects

Having established that modulation of Ulp2 is sufficient to alter overall SUMO-conjugation, we moved to characterize cell cycle progression in these mutants. To this aim, we first attempted to analyze the cell cycle of *ulp2Δ* cells synchronously released from G1 arrest. However, *ULP2* deletion causes pleiotropic defects that greatly reduce viability and genome stability (Li and Hochstrasser, 2000; Ryu et al., 2016). For these reasons, we were not able to synchronize *ulp2Δ* cells and perform population analysis.

Because of their growth defects and genomic instability (Li and Hochstrasser, 2000), *ulp2Δ* cells are prone to acquire suppressor mutations. In particular, these cells tend to develop specific aneuploidies, retaining extra copies of chromosomes I and XII (Ryu et al., 2016). The genomic instability of *ulp2Δ* cells became apparent to us when we manipulated them in the lab. A serial dilution assay showed that one of our *ulp2Δ* clones had become capable

of growing at high temperatures (**Figure 3.22**). We then crossed the temperature-proficient *ulp2Δ* clone, in addition to two temperature-sensitive clones, with a wild-type strain, to obtain *ulp2Δ/ULP2* diploid cells. Next, we induced sporulation and dissected the resulting tetrads. We found that tetrads derived from the temperature-proficient *ulp2Δ* clone often formed irregularly shaped colonies and did not segregate the poor-growth phenotype in a 2:2 ratio (**Figure 3.22**). Altogether, these observations suggest that the suppression of the temperature sensitivity is associated with aneuploidy.

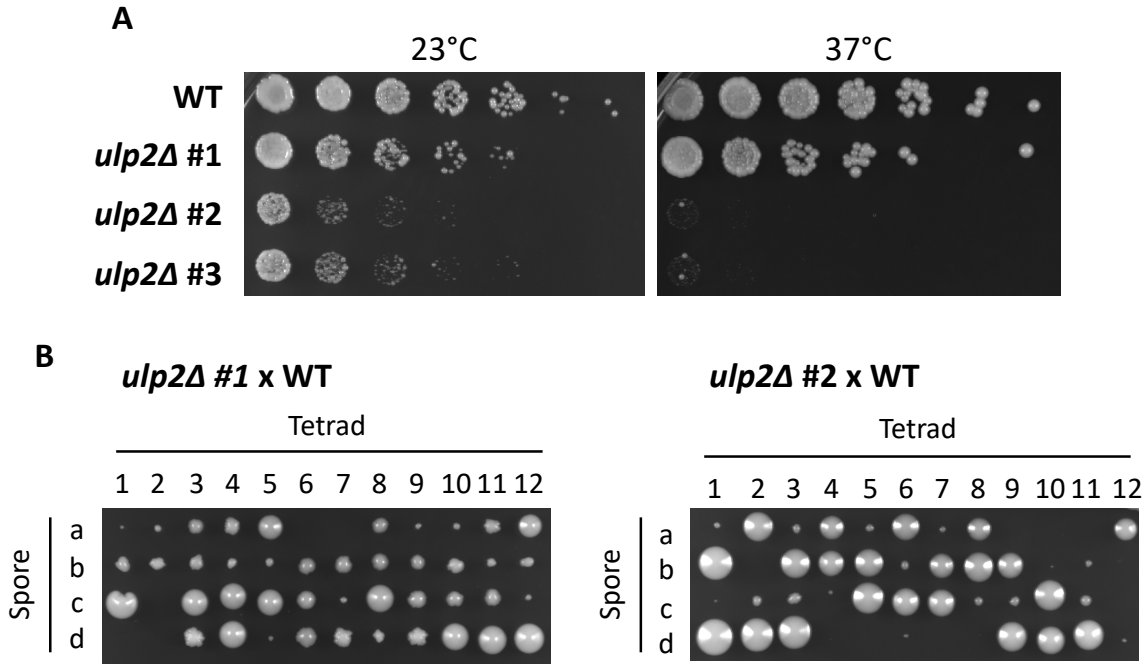

Figure 3.22. Ulp2 deletion causes growth defects and genomic instability
*(**A**) Serial dilutions (1:5, starting from OD600 = 1) of wild-type (Ry1) cells and three clones of ulp2Δ (Ry2246, Ry7860, Ry7861) cells were spotted onto YPD plates and incubated at the indicated temperature for 48 hours. (**B**) Two clones of MATa ulp2Δ (Ry2249, Ry7921) cells were crossed with wild-type MATalpha (Ry2) cells. After inducing sporulation of diploids, tetrads were dissected on YPD plates and grown at 23°C for 5 days to test their survival.*

To overcome the genomic instability of *ulp2Δ* cells, we cloned *ULP2* under its own promoter in a centromeric plasmid, called *pULP2*. As a marker we chose *URA3* because it allows, if needed, to select clones that lost the plasmid by growing cells on plates containing 5-Fluoroorotic acid. Diploid *ulp2Δ/ULP2* cells were transformed with *pULP2* and then placed on sporulation media to obtain haploid *ulp2Δ* cells containing *pULP2*. Serial dilution assays showed that the plasmid bearing the wild-type copy of *ULP2* rescues the temperature sensitivity and growth defects associated with the deletion of the endogenous gene (**Figure 3.23**). The obtained strains are now genetically stable and can be used to study genetic

interaction, for example, to test whether loss of Ulp2 can ameliorate the defects of *cdc5* or *cdc14* cells.

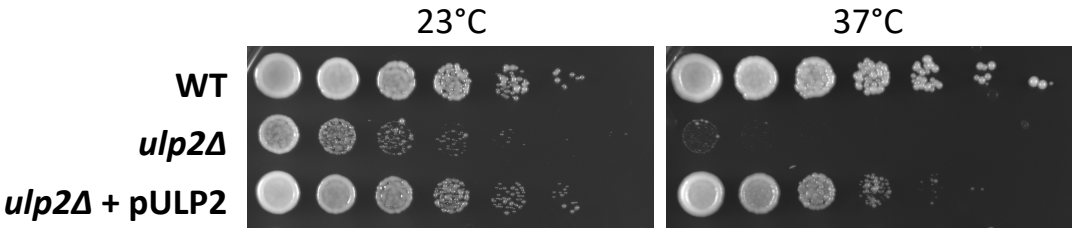

Figure 3.23. The plasmid bearing a wild-type copy of ULP2 rescues the growth defects of ulp2Δ cells
Serial dilutions (1:5, starting from OD600 = 1) of wild-type cells (Ry1), ulp2Δ (Ry7861) cells, and ulp2Δ cells transformed with pULP2 (Ry8229) were spotted onto YPD plates and incubated at the indicated temperature for 48 hours.

3.7.3. Ulp2 depletion has no obvious effect on cell cycle progression or total SUMO-conjugation

To overcome the problems associated with the lack of *ULP2*, we tried a different strategy, namely conditional depletion using the AID system (Nishimura et al., 2009). First of all, with a serial dilution assay, we checked whether Ulp2 depletion with this system could recapitulate the temperature sensitivity of *ulp2Δ* cells, but we found that, in presence of auxin, *ulp2-aid* cells grew normally at high temperatures (**Figure 3.24**).

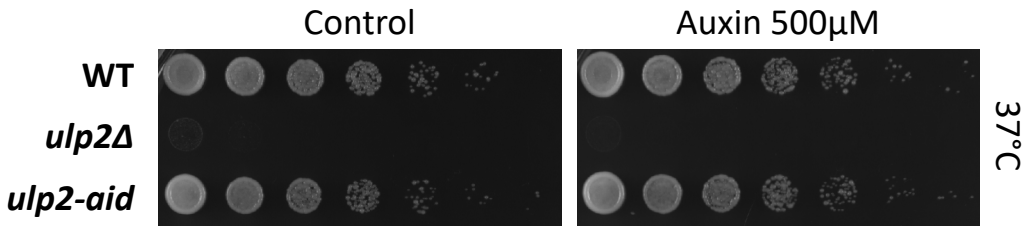

Figure 3.24. Ulp2-aid depletion does not compromise cell growth
Serial dilutions (1:5, starting from OD600 = 1) of wild-type (Ry1), ulp2Δ (Ry7861), and ulp2-aid (Ry7893) cells were spotted onto YPD plates or YPD plates with auxin and incubated at the indicated temperature for 24 hours.

We then tested the effects of Ulp2 depletion on the pattern of SUMO-conjugates. Wild-type and *ulp2-aid* cells were grown to exponential phase and auxin was added to the medium. We also grew *ulp2-aid* cells without auxin as a control. Samples were taken for 3 hours after depletion for western blot analysis with an anti-SUMO antibody. The results showed no difference in the pattern of SUMO-conjugates, even though the bulk of Ulp2-AID protein seemed to be depleted (**Figure 3.25**).

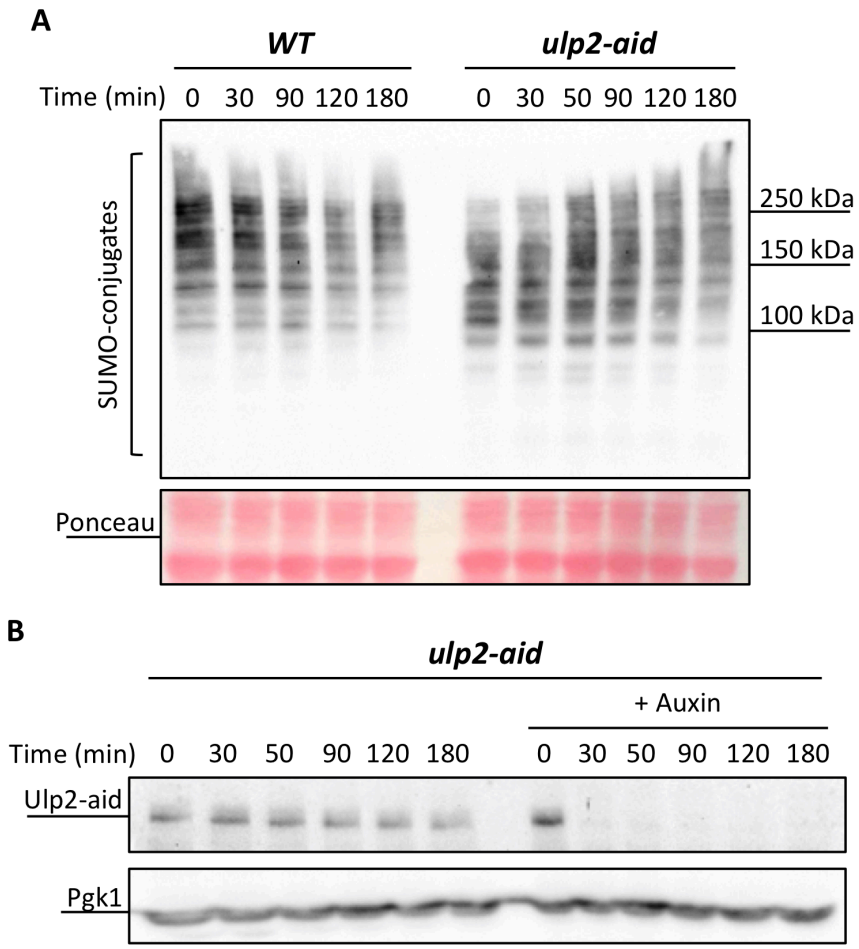

Figure 3.25. Ulp2-aid depletion has no great effect on the pattern of SUMO-conjugates

*Wild-type (Ry1) and ulp2-aid (Ry7895) cells were grown in YPD. When cells reached the exponential phase, auxin was added to the medium to induce Ulp2 depletion. Samples were collected at the indicated times after auxin addition for western blot. (**A**) Total protein extracts were probed with an antibody against SUMO and (**B**) Ulp2-aid was detected with an anti-AID antibody. (**A**) Ponceau staining and (**B**) Pgk1 were used as loading controls.*

We characterized the cell cycle of *ulp2-aid* cells as they were synchronously released from G1. To deplete Ulp2 as strongly as possible, auxin was added to the medium 1 hour before release. We monitored spindle morphology by immunofluorescence and we did not notice any obvious phenotype given by Ulp2 depletion (**Figure 3.26**).

There are several possible explanations for this lack of phenotype. First of all, since Ulp2-aid depletion was monitored by western blot using anti-AID antibodies, it is possible that auxin addition only induced the degradation of the AID tag, leaving the core of the Ulp2 protein intact. Second, even though the bulk of Ulp2-aid was degraded in presence of auxin, a small amount may persist, sufficient to sustain normal cell cycle progression. Third, our analysis may have overlooked minor defects, for example in the maintenance of sister

chromatid cohesion. Finally, it is possible that the cell cycle defects associated with loss-of-function Ulp2 mutation are due to the prolonged accumulation of SUMO-conjugates and, therefore, do not manifest themselves in the first cell division after depletion of the enzyme. However, the fact that *ulp2-aid* cells grew proficiently at high temperatures in presence of auxin argues against this hypothesis.

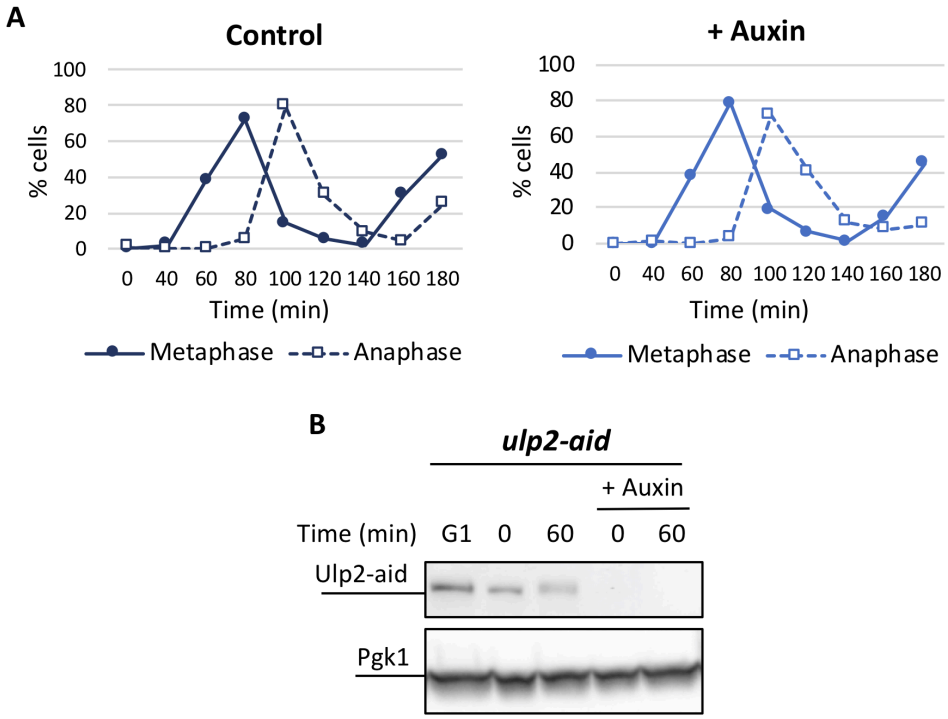

Figure 3.26. Ulp2 depletion has no obvious effect on cell cycle progression
*ulp2-aid (Ry7895) cells were arrested in G1 with α-factor in YPD and released in media at 23°C. Where indicated, auxin was added 1 hour before release and also to the release medium. (**A**) Samples were collected at the indicated times after release to monitor cell cycle progression through IF (anti-Tub1, DAPI). (**B**) Samples were collected at the time of auxin addition, at the time of release (60 min after auxin addition), and 1 hour after release (120 min from auxin addition) for western blot. Pgk1 was used as a loading control.*

3.7.4. Ulp2 depletion does not rescue nuclei division in *cdc5* and *cdc14* cells

The observation that Ulp2 depletion did not obviously affect normal cell cycle progression could be because this enzyme is normally inactivated in metaphase. Thus, we reasoned that depletion of Ulp2 could have a stronger effect on cells in which its normal inactivation is lost, like *cdc5* cells. Therefore, we decided to test if Ulp2 depletion could reduce anaphase bridges in *cdc5* and *cdc14* cells.

To this aim, we arrested *cdc5-as1 ulp2-aid*, *cdc5-as1*, *cdc14-1 ulp2-aid*, *cdc14-1*, *cdc15-as1 ulp2-aid*, and *cdc15-as1* cells in G1 and synchronously released them in restrictive conditions for all mutations. Auxin was added to the medium starting from 1 hour before release to maximize Ulp2 depletion. Cell cycle progression was monitored through spindle morphology. Analysis of nuclear and nucleolar segregation showed that Ulp2 depletion was not sufficient to rescue the accumulation of anaphase bridges in *cdc5* and *cdc14* cells, although it slightly increased the percentage of *cdc5* cells which fully segregated their genome by the end of the experiment, from 33% to 43% (**Figure 3.27**).

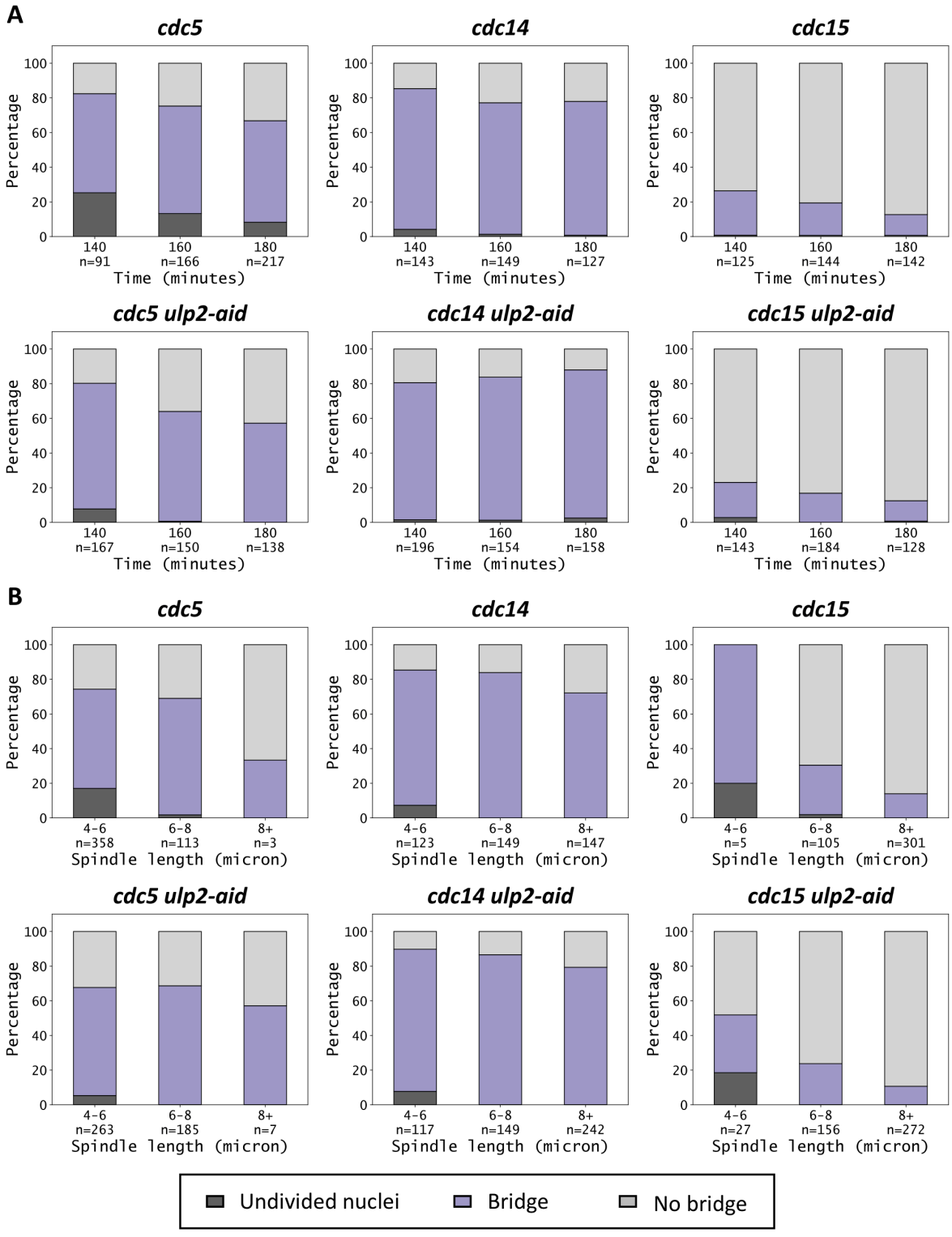
A
cdc5
cdc14
cdc15
cdc5 ulp2-aid
cdc14 ulp2-aid
cdc15 ulp2-aid
Percentage
Time (minutes)
140 n=91
160 n=166
180 n=217
140 n=143
160 n=149
180 n=127
140 n=125
160 n=144
180 n=142
140 n=167
160 n=150
180 n=138
140 n=196
160 n=154
180 n=158
140 n=143
160 n=184
180 n=128
B
Spindle length (micron)
4-6 n=358
6-8 n=113
8+ n=3
4-6 n=123
6-8 n=149
8+ n=147
4-6 n=5
6-8 n=105
8+ n=301
4-6 n=263
6-8 n=185
8+ n=7
4-6 n=117
6-8 n=149
8+ n=242
4-6 n=27
6-8 n=156
8+ n=272
Undivided nuclei
Bridge
No bridge

Figure 3.27. Ulp2 depletion does not rescue nuclei division in cdc5 and cdc14 cells

*cdc5-as1 ulp2-aid (Ry7970), cdc5-as1 (Ry2446), cdc14-1 ulp2-aid (Ry7973), cdc14-1 (Ry1573), cdc15-as1 ulp2-aid (Ry10529), and cdc15-as1 (Ry1112) cells were arrested in G1 in YPD at 23°C and released in presence of CMK and NMPPi inhibitors at 37°C, to inactivate cdc5-as1, cdc15-as1, and cdc14-1. To deplete Ulp2, auxin was added 1 hour before release and to the release medium. Cell cycle progression was monitored through IF (anti-Tub1, DAPI; not shown). Samples were collected at the indicated times after release and analyzed through IF (anti-Tub1, anti-Nop1, DAPI) for the presence of anaphase bridges. At least 100 cells were analyzed for each time point. Plots show the distribution of anaphase cells (spindles > 4µm) between categories according to (**A**) time after release and (**B**) spindle length.*

3.7.5. High amounts of Ulp2 cause several cell cycle defects

Overexpression of Ulp2 compromises cell growth and delays mitosis

In parallel to the analysis of *ULP2* loss-of-function mutations, we tested the effects of its overexpression. Serial dilution assays showed that *GAL-ULP2* cells were not able to grow on galactose plates, indicating that overexpression of the SUMO protease compromises cell growth (**Figure 3.28**). We also noticed that cells bearing one copy of the *GAL-ULP2* construct were prone to develop suppressor mutations, as suggested by the growth of resistant colonies.

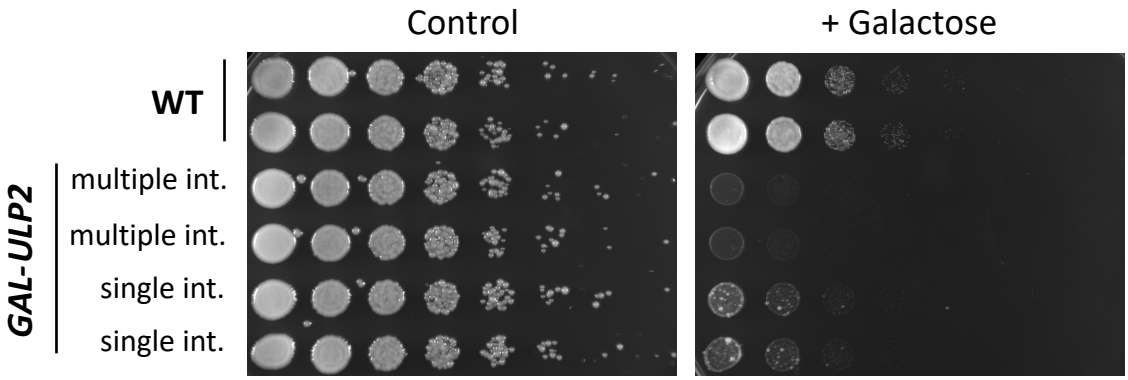

Figure 3.28. Ulp2 overexpression compromises cell growth
Serial dilutions (1:5, starting from OD600 = 1) of wild-type (Ry1) cells and GAL-ULP2 cells bearing either one (Ry8130) or multiple copies (Ry8129) of the construct were spotted onto YPR or YPR + 2% galactose (YPR/G) plates and incubated at 23°C for 48 hours.

To better understand the reasons underlying these growth defects, we characterized the first cell cycle following *ULP2* overexpression. Wild-type and *GAL-ULP2* cells bearing either one or multiple copies of the construct were grown in raffinose-containing media, arrested in G1, and then synchronously released in galactose-containing media. We monitored cell cycle progression through the amounts of the mitotic cyclin Clb2 by western blot, spindle morphology by immunofluorescence, and DNA content by FACS analysis. We also performed western blot with anti-SUMO antibodies to monitor the level of total SUMO-conjugates.

We found that Ulp2 overexpression had dose-dependent effects (**Figure 3.29**). Western blot showed that, in wild-type cells, the level of SUMO-conjugates increased as cells were undergoing mitosis, reaching its peak at 135’ and 150’ after release, when, as indicated by spindle morphology, cells were going from metaphase to anaphase. On the other hand, the

total level of SUMO-conjugates decreased upon *ULP2* overexpression, with this effect being sharper in cells bearing multiple copies of *GAL-ULP2*.

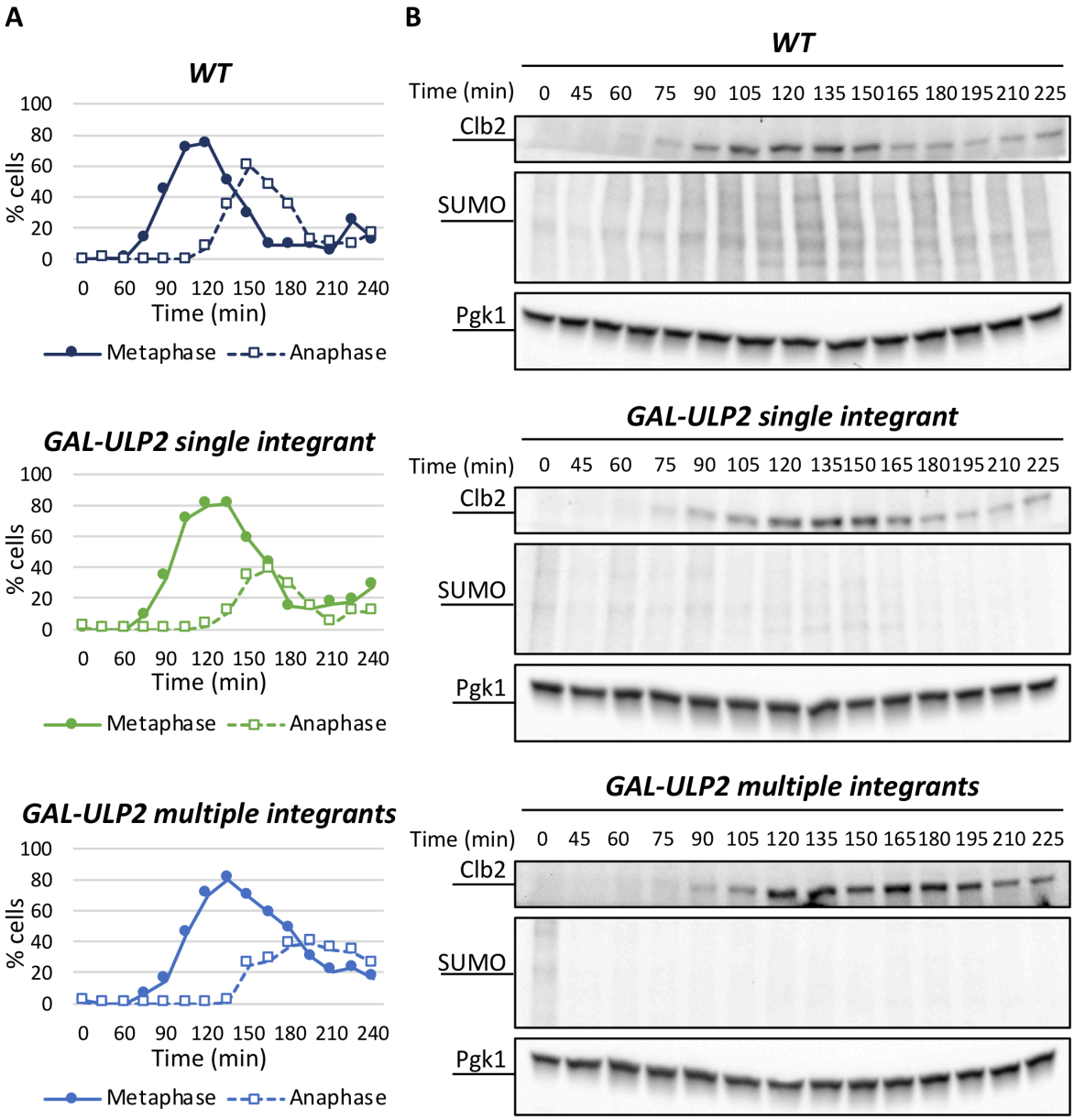
A
WT
100
80
60
40
20
0
% cells
0 60 90 120 150 180 210 240
Time (min)
Metaphase
Anaphase
GAL-ULP2 single integrant
100
80
60
40
20
0
% cells
0 60 90 120 150 180 210 240
Time (min)
Metaphase
Anaphase
GAL-ULP2 multiple integrants
100
80
60
40
20
0
% cells
0 60 90 120 150 180 210 240
Time (min)
Metaphase
Anaphase
B
WT
Time (min) 0 45 60 75 90 105 120 135 150 165 180 195 210 225
Clb2
SUMO
Pgk1
GAL-ULP2 single integrant
Time (min) 0 45 60 75 90 105 120 135 150 165 180 195 210 225
Clb2
SUMO
Pgk1
GAL-ULP2 multiple integrants
Time (min) 0 45 60 75 90 105 120 135 150 165 180 195 210 225
Clb2
SUMO
Pgk1

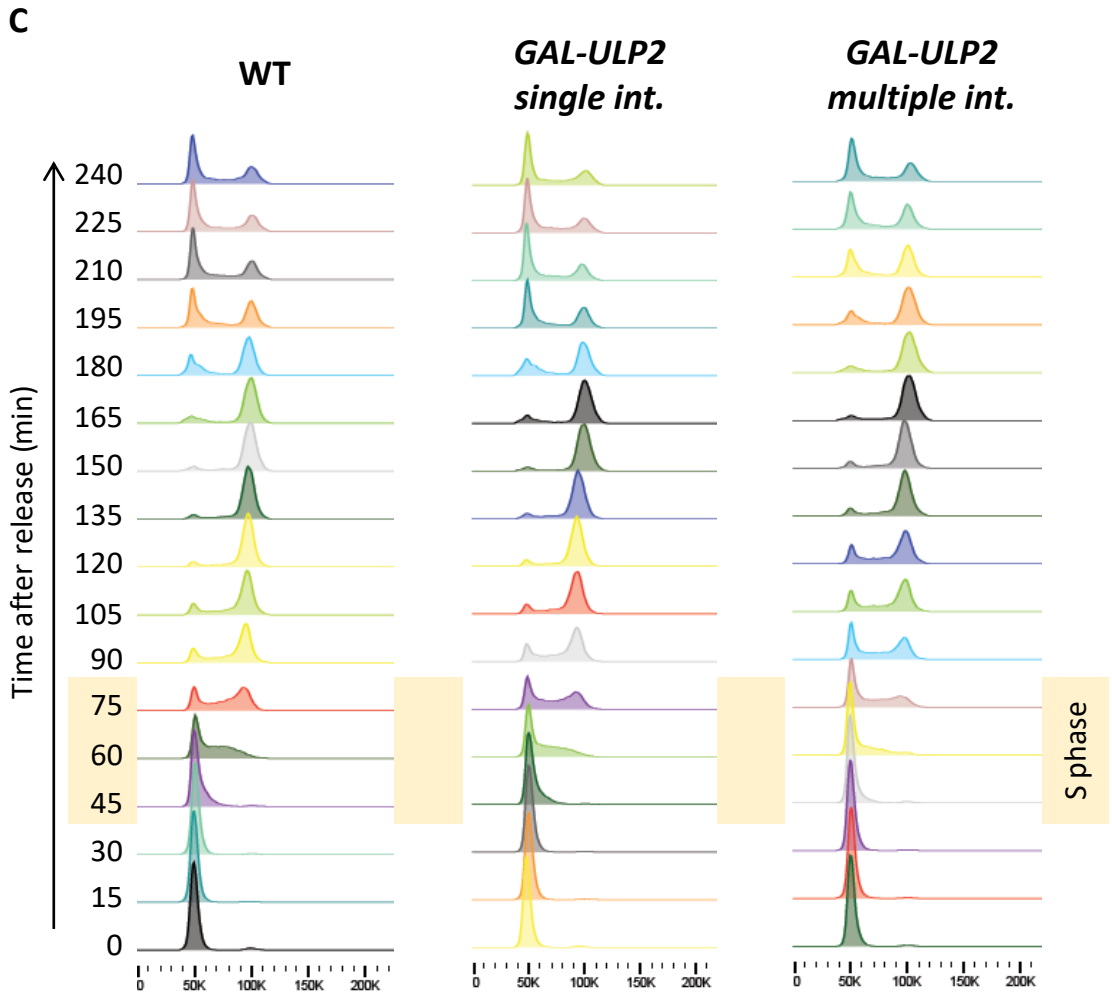

Figure 3.29. Ulp2 overexpression delays cell cycle progression
*Wild-type (Ry1) and GAL-ULP2 cells bearing either one (Ry8130) or multiple copies (Ry8129) of the construct were arrested in G1 with α-factor in YPR and released in YPR media with 2% galactose. Samples were collected at the indicated times after release to monitor cell cycle progression through (**A**) IF (anti-Tub1, DAPI) (**B**) Clb2 amounts (by western blot), and (**C**) DNA content (by FACS). (**B**) The level of SUMO conjugates was also assessed. Pgk1 was used as a loading control.*

Spindle morphology analysis shows that cells bearing a single copy of *GAL-ULP2* enter mitosis and reach metaphase with wild-type kinetics, but they stay in metaphase longer, indicating that *ULP2* overexpression delays mitosis, particularly at the metaphase-to-anaphase transition. This observation is confirmed by the fact that Clb2 accumulation and degradation were delayed by about 15' in single-copy *GAL-ULP2* cells. The mitotic delay is consistent with the fact that overexpression counteracts the normal inactivation of Ulp2 occurring at metaphase (Baldwin et al., 2009).

This behavior is amplified in cells bearing multiple *GAL-ULP2* copies. In addition, these cells display defects even earlier in the cell cycle. FACS analysis showed that replication was delayed, as indicated by the fact that, at 75' after release and onwards, the amount of multiple-copy *GAL-ULP2* cells which had doubled their DNA content was significantly lower than wild-type. Moreover, spindle morphology analysis showed that these cells are delayed also in entry into mitosis, as the majority of them reach metaphase 15'-30' later than wild-type cells. Finally, Clb2 accumulation and degradation occur with a 15' and 45' delay, respectively.

Overexpression of Ulp2 from metaphase does not affect anaphase bridges resolution

We wondered whether the mitotic delay caused by Ulp2 overexpression could be attributed to a failure in SCI resolution. To test this possibility, we decided to monitor the resolution of anaphase bridges in *GAL-ULP2* cells.

To exclude the possibility that the mitotic defects are due to events occurring earlier in the cell cycle, for example during DNA replication, we set up our experiment to induce Ulp2 overexpression starting from metaphase. Before performing the actual experiment, we tested *cdc20-aid* cells and *GAL-ULP2 cdc20-aid* cells bearing either one or multiple copies of the construct. Cells were synchronized in G1 and released in raffinose-containing media into the metaphase arrest. At the arrest (2h30 from release), galactose was added to the medium and, 1h after induction (3h30 from release), cells were released from metaphase in galactose-containing media. Since G1 release, the whole experiment was performed at 37°C, which is the restrictive temperature normally used for *cdc14-1*. We monitored cell cycle progression through spindle morphology and we observed that Ulp2 overexpression delayed mitotic exit, once again in a dose-dependent fashion (**Figure 3.30**). We also looked

at the changes in the pattern of SUMO-conjugates through western blot. Although the signal of SUMO-conjugates decreases after metaphase release even in *cdc20* cells, this reduction appears more marked in single-copy *GAL-ULP2 cdc20* cells. On the other hand, for what concerns multiple-copy *GAL-ULP2 cdc20* cells, SUMO-conjugation seemed to be low throughout the experiment, likely because the galactose-inducible promoter can be leaky at high temperatures. For this reason, in our final experiment, we chose to use yeast strains bearing one copy of *GAL-ULP2*.

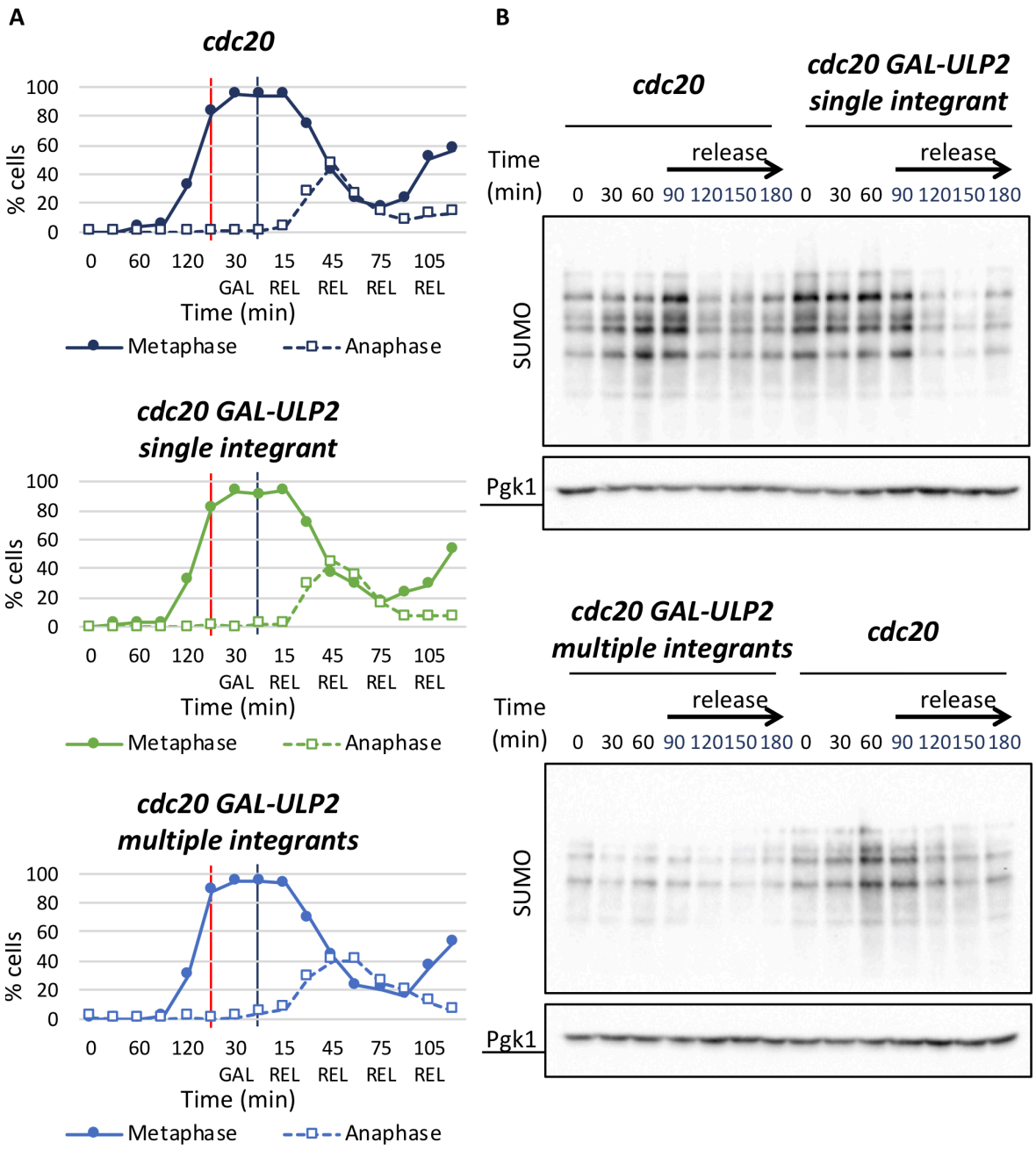

Figure 3.30. Ulp2 overexpression delays mitotic exit

*cdc20-aid (Ry10137) cells and cdc20-aid GAL-ULP2 cells bearing either one (Ry10143) or multiple copies (Ry10151) of the construct were arrested in G1 with α-factor in YPR at 23°C and released in YPR media with auxin at 37°C, to deplete Cdc20-aid. At the metaphase arrest (2h30 from release), 2% galactose was added to the medium (red line) and 1h after induction cells were released in new YPR/G medium without auxin at 37°C (blue line). Samples were collected at the indicated times after release from G1 to monitor (**A**) cell cycle progression through IF (anti-Tub1, DAPI) and (**B**) the level of SUMO conjugates by western blot. Pgk1 was used as a loading control.*

We synchronized *GAL-ULP2 cdc5-as1 cdc20-aid*, *cdc5-as1 cdc20-aid*, *GAL-ULP2 cdc14-1 cdc20-aid*, *cdc14-1 cdc20-aid*, *GAL-ULP2 cdc15-as1 cdc20-aid*, and *cdc15-as1 cdc20-aid* cells in G1 in raffinose-containing medium and released them into the metaphase arrest in restrictive conditions for all mutations. The experiment was performed at 34°C, to inactivate *cdc14-1* and, at the same time, allow precise control of the galactose-inducible promoter. At the *cdc20* arrest (2h30 from release), galactose was added to the medium and, 1h after induction (3h30 from release), cells were released from metaphase in galactose-containing media in restrictive conditions for *cdc5*, *cdc14,* and *cdc15* mutations, to allow them to reach their final anaphase arrest. We monitored cell cycle progression through spindle morphology throughout the experiment. In addition, samples were collected after the release from metaphase to analyze nuclear and nucleolar segregation. We found that Ulp2 overexpression had little to no effect, although it seemed to slightly delay bridge resolution in *cdc15* cells (**Figure 3.31**). These results might suggest that Ulp2 hyperactivation is not the main cause of the SCI resolution defect of *cdc5* cells. However, since we previously found that in normal metaphase the conditions are already set for the resolution of anaphase bridges, cells arrested in metaphase may have already removed most of SCIs. Therefore, Ulp2 overexpression may be insufficient to introduce new entanglements at this cell cycle stage.

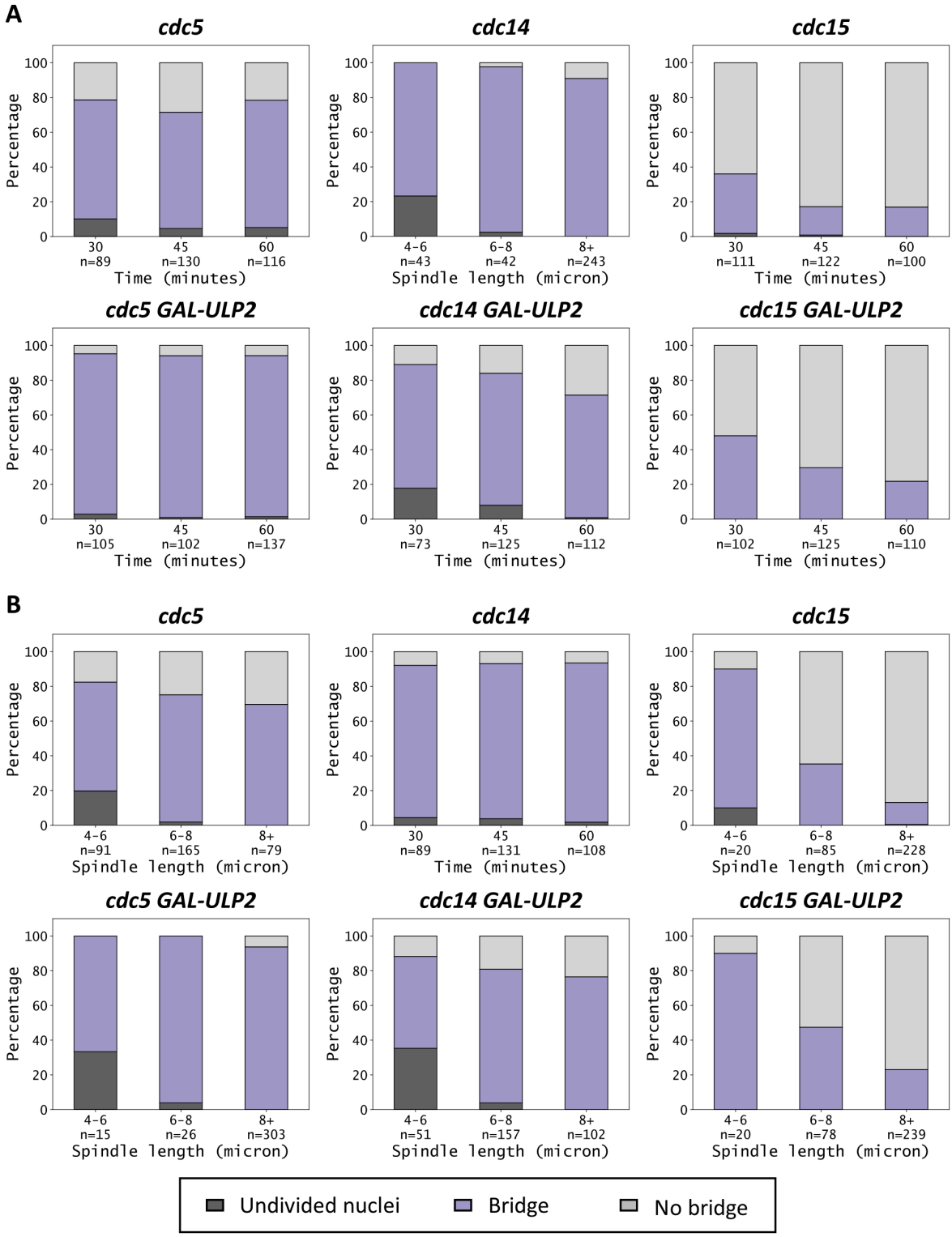
A
cdc5
cdc14
cdc15
cdc5 GAL-ULP2
cdc14 GAL-ULP2
cdc15 GAL-ULP2
Percentage
Time (minutes)
Spindle length (micron)
30 n=89
45 n=130
60 n=116
4-6 n=43
6-8 n=42
8+ n=243
30 n=111
45 n=122
60 n=100
30 n=105
45 n=102
60 n=137
30 n=73
45 n=125
60 n=112
30 n=102
45 n=125
60 n=110
B
4-6 n=91
6-8 n=165
8+ n=79
30 n=89
45 n=131
60 n=108
4-6 n=20
6-8 n=85
8+ n=228
4-6 n=15
6-8 n=26
8+ n=303
4-6 n=51
6-8 n=157
8+ n=102
4-6 n=20
6-8 n=78
8+ n=239
Undivided nuclei
Bridge
No bridge

Figure 3.31. Ulp2 overexpression after metaphase does not increase anaphase bridges

*GAL-ULP2 (x1) cdc5-as1 cdc20-aid (Ry10769), cdc5-as1 cdc20-aid (Ry4936), GAL-ULP2 (x1) cdc14-1 cdc20-aid (Ry10766), cdc14-1 cdc20-aid (Ry4934), GAL-ULP2 (x1) cdc15-as1 cdc20-aid (Ry10772), and cdc15-as1 cdc20-aid (Ry7566) cells were arrested in G1 in YPR at 23°C and released in YPR media with the CMK inhibitor and auxin at 34°C, to inactivate cdc5-as1, cdc14-1, and cdc20-aid. At the metaphase arrest (2h30 from release), 2% galactose was added to the medium and 1h after induction cells were released in new YPR/G medium without auxin at 34°C. Cell cycle progression was monitored through IF (anti-Tub1, DAPI; not shown). Samples were collected at the indicated times after release and analyzed through IF (anti-Tub1, anti-Nop1, DAPI) to detect anaphase bridges. At least 100 cells were analyzed for each time point. Plots show the distribution of anaphase cells (spindles > 4µm) between categories according to (**A**) time after release and (**B**) spindle length.*

3.8. Identification of SUMO substrates in mitosis

We found that, although SUMOylation of Top2 is not the main reason behind the decatenation defect of *cdc5 cdc14* cells, Ulp2 overexpression, which decreases overall SUMOylation, can cause several cell cycle defects, including the accumulation of anaphase bridges. Therefore, it is possible that other targets of Ulp2, besides Top2, may contribute to the sister chromatid separation defect of *cdc5 cdc14* cells.

To test this hypothesis, we wanted to characterize the changes in the SUMO landscape that follow Cdc5 and Cdc14 inactivation, with a proteomic approach. Since SUMO conjugation cannot be directly detected by mass spectrometry, protein identification requires previous enrichment for SUMOylated substrates. In our case, we chose to purify SUMO conjugates using a yeast strain in which endogenous SUMO was substituted with a His-tagged version of the protein, as described in (Thu et al., 2016).

First, we optimized the protocol in a scaled-down experiment. *HIS8-SUMO* cells and control cells expressing untagged SUMO were grown to exponential phase and collected to perform cobalt affinity purification. We tested the efficacy of the purification by western blot and found that we successfully enriched for SUMO-conjugates in *HIS8-SUMO* cells (**Figure 3.32**). Since the total amount of protein in the pulldown was too low to be easily detected, we repeated the experiment with more starting material, in quantities suitable for subsequent mass spectrometry analysis. Unfortunately, even though quality control by western blot promisingly showed similar results, we were not able to detect any difference between the tagged strain and the control when we probed for total protein in the pulldown. This indicates that the amount of SUMOylated proteins purified was too low compared with contaminants. For this reason, we decided to abandon this strategy.

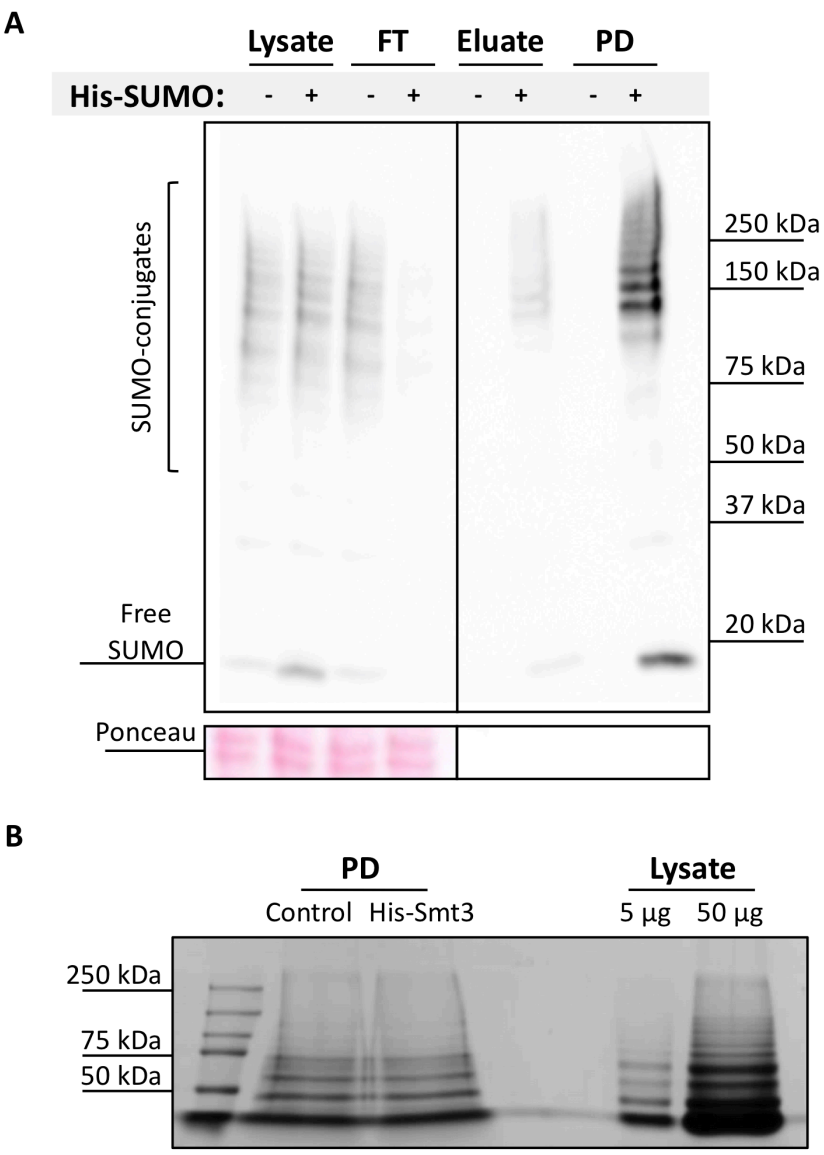

Figure 3.32. His-tag purification of SUMO conjugates

*HIS8-SMT3 cells (Ry7949) and cells expressing wild-type SUMO (Ry7948) were grown in YPD to exponential phase and collected to perform cobalt-affinity purification of His-SUMO conjugates. After the elution step, proteins in the eluate were concentrated by precipitation to obtain the final pulldown. (**A**) 5 mg of lysate was used for the purification. The quality of the purification was assessed by western blot with anti-SUMO. (**B**) 50 mg of lysate was used for the purification. Total protein in the pulldown was detected by Coomassie staining. Known quantities of the lysate were used as a reference. FT, flow-through; PD, pulldown.*

4. Discussion and future directions

Successful chromosome segregation requires the removal of all sorts of cohesion between sister chromatids, including protein complexes (cohesin) and DNA linkages (sister chromatid intertwines or SCIs). If not properly removed, SCIs can break during cell division causing double-strand breaks and jeopardizing genome stability. Although most DNA linkages are removed before mitosis, their complete resolution only occurs concomitantly with chromosome segregation. In this work, we exploited the unique phenotype of *S. cerevisiae cdc5 cdc14* mutant cells to investigate the mechanisms of SCI resolution during mitosis.

In yeast, the simultaneous inactivation of the polo-like kinase Cdc5 and the Cdk-counteracting phosphatase Cdc14 causes cells to arrest after cohesin cleavage, with short bipolar spindles and undivided nuclei (Roccuzzo et al., 2015). Although the main defect of *cdc5 cdc14* cells is in spindle elongation, evidence suggests that these cells are also impaired in sister chromatid separation, due to the presence of unresolved SCIs.

We found that both proteins contribute to the removal of DNA linkages, albeit with different functions. Cdc14 is mainly involved in nucleolar segregation, while Cdc5 seems to act through a more generalized mechanism. Moreover, Cdc14 is specifically required for the processing of recombination intermediates, whereas Cdc5 contributes to the removal of DNA catenanes. The decatenation defect of *cdc5* cells correlates with a dysregulation of the SUMO pathway. Since the polo-like kinase is known to inactivate the SUMO protease Ulp2 in metaphase, this dysregulation determines the lack of SUMOylation of Ulp2 substrates, including Top2. Indeed, we found that Cdc5 controls post-translational modification (PTM) of Top2 during mitosis, particularly its SUMOylation and, possibly, also its phosphorylation. Given the known function of SUMO in the regulation of sister chromatid cohesion, it is tempting to speculate that the hyperactivation of Ulp2 represents the reason behind the sister chromatid separation defect of *cdc5* cells.

4.1. Timing of SCI resolution

In *cdc20* arrested cells, in contrast with *cdc5 cdc14* mutants, ectopic cohesin cleavage induces spindle elongation without forming anaphase bridges (Massari, 2018). This finding

indicates that in metaphase the conditions are set for SCI resolution and points to Cdc5 and/or Cdc14 playing a role in this cell cycle phase. While Cdc5 is known to be active in metaphase, Cdc14 is thought to intervene primarily in anaphase. Consistently, our data suggests that the polo-like kinase is the main contributor to the decatenation defect of *cdc5 cdc14* cells. However, a few studies proposed limited function for Cdc14 in metaphase (Akiyoshi and Biggins, 2010; Taxis et al., 2009; Tomson et al., 2009). This idea is corroborated by our preliminary ChIP-seq experiment, which showed that Top2 binding is altered in *cdc20 cdc14* cells compared to *cdc20* cells (**Figure 3.13**), thus envisioning a metaphase role for the phosphatase in Top2 recruitment as well.

Although the conditions for removing the bulk of DNA linkages are already established in metaphase, several observations suggest that complete SCI resolution is unlikely achieved at this stage. First, this process is inhibited by cohesin complexes (Charbin et al., 2014; Farcas et al., 2011; Mariezcurrena and Uhlmann, 2017). Second, decatenation of the rDNA and replication of certain loci was reported to be completed only during late anaphase (D'Ambrosio et al., 2008a; Ivanova et al., 2020). Finally, Cdc14 activates the resolvase Yen1 at anaphase onset (Blanco et al., 2014; Eissler et al., 2014). To conclude our analysis, we will characterize the role of Cdc5 and Cdc14 in SCI resolution after metaphase. To this aim, we will release *cdc5*, *cdc14*, and *cdc5 cdc14* cells from G1 block in permissive conditions, arrest them in metaphase through nocodazole treatment or Cdc20 depletion, and then release them from metaphase in restrictive conditions for *cdc5* and *cdc14*. To monitor the resolution of SCIs, we will score for the presence of anaphase bridges at the terminal arrest.

4.2. Types of DNA linkages and their resolution

Three types of DNA linkages exist, namely catenanes, unreplicated segments, and recombination intermediates. To identify the source of SCI responsible for the segregation defect of *cdc5 cdc14* cells, we exploited enzymes dedicated to the processing of specific structures, particularly Topoisomerase II, which disentangles DNA catenanes, and Yen1, a nuclease with broad substrate specificity that can target both recombination and late-replication intermediates (Ip et al., 2008; Ölmezer et al., 2016).

Overexpression of cv-TopoII partially rescued both spindle elongation and nuclei division in *cdc5 cdc14* cells, indicating that these cells retain DNA catenanes (**Figure 3.3** and (Massari, 2018)). On the contrary, overexpression of the yeast endogenous Top2 had little to no

effect (Massari, 2018). There are several possible explanations for this discrepancy. First of all, the two proteins may be expressed at different levels. Second, cv-TopoII has higher catalytic activity (Fortune et al., 2001) and may also be less sensitive to condensin inactivation, at least in some contexts. Indeed, overexpression of cv-TopoII can rescue nucleolar segregation in condensin mutants, whereas endogenous Top2 cannot (D'Ambrosio et al., 2008a). Finally, yeast Top2 (but not cv-TopoII) may require an activating step – mediated by Cdc5 or Cdc14 – that is not bypassed by its overexpression, like a change in PTMs. Notably, the main difference between cv-TopoII and eukaryotic topoisomerases is the lack of the regulatory C-terminal domain, which is also the part of the protein that is most targeted by PTMs (Lavrukhin et al., 2000). In the attempt to overcome endogenous Top2 regulation, we previously examined the effects of overexpressing a truncated Top2 enzyme lacking the C-terminal domain, called Top2ΔCTD, and found that it was unable to rescue the *cdc5 cdc14* phenotype (Massari, 2018). Since this result could also be caused by reduced activity or mislocalization of Top2ΔCTD, we are planning to check the behavior of the truncated protein next.

Although our data points to catenanes as the main source of SCIs in *cdc5 cdc14* cells, the observation that ectopic expression of cv-TopoII is not sufficient to fully disentangle the nuclei in these cells (**Figure 3.3** and (Massari, 2018)), raises the possibility that also other types of DNA linkages are present. Cdc5 and Cdc14 are both involved in the resolution of recombination intermediates through dedicated nucleases and Cdc14 is also required to complete DNA replication (Dulev et al., 2009). Cdc5 activates the nuclease Mus81-Mms4 in G2/metaphase while, in anaphase, Cdc14 promotes the activation of Yen1, which serves as a backup mechanism for the removal of persistent DNA linkages (Wild and Matos, 2016). We found that overexpression of Yen1 rescues sister chromatid separation in *cdc14* cells, but not in *cdc5* cells (**Figure 3.2**). This result suggests that, in addition to catenanes, other types of SCIs are likely to be present in *cdc5 cdc14* cells and that their resolution is specifically promoted by the phosphatase Cdc14, whereas the polo-like kinase mainly controls the resolution of catenanes. To understand whether, in *cdc5 cdc14* cells, recombination and late-replication intermediates account for the anaphase bridges that are refractory to Topoisomerase-mediated resolution, we will test simultaneous overexpression of cv-TopoII and Yen1.

4.3. Factors contributing to SCI resolution in mitosis

What is the molecular reason behind the decatenation defect of *cdc5 cdc14* cells? Efficient removal of catenanes by Top2 requires chromosome individualization and separation, meaning cohesin cleavage, DNA condensation, and sister chromatid separation through the mitotic spindle. To understand whether the sister chromatid separation defect of *cdc5 ccd14* is caused by suboptimal conditions for Top2-mediated reaction, we investigated the separate contribution of these three mitotic processes.

4.3.1. Spindle elongation and resolution of SCIs

Treatment with the microtubule-depolymerizing drug nocodazole increases catenation of yeast plasmid and endogenous centromeres, indicating that a bipolar spindle is required for Top2-mediated decatenation (Baxter et al., 2011; Charbin et al., 2014; Mariezcurrena and Uhlmann, 2017). Similarly, anaphase spindle elongation has been proposed to drive the removal of the intertwines that persist through late mitosis, although strong evidence in support of this hypothesis is currently lacking. Consistently, in all our experiments the percentage of cells displaying anaphase bridges decreased as a function of spindle length. There are several possible explanations for the role of the spindle in the resolution of DNA linkages. The most intuitive is that spatial separation of sister chromatids exposes SCIs to the enzymes dedicated to their resolution and biases Top2-mediated reaction toward decatenation (Sen et al., 2016). In addition, the tension imposed by spindle elongation might alter the topology of DNA linkages and favor their recognition and processing. Alternatively, the spindle may act indirectly, through condensin recruitment. Indeed, chromosome attachment to the bipolar spindle triggers the relocalization of condensin from the centromeres to the arms, possibly because the spatial separation of sister centromeres causes the complexes to diffuse away from the locus. Another interesting possibility is that the spindle coordinates the completion of SCI resolution with anaphase progression by acting as a ruler. Upon anaphase onset, the association of Aurora B with the spindle midzone creates a phosphorylation gradient that fades toward the cell poles (Fuller et al., 2008), which controls late mitotic events including anaphase chromosome condensation, spindle disassembly, and mitotic exit (Afonso et al., 2019; Mora-Bermúdez et al., 2007; Neurohr et al., 2011; Rozelle et al., 2011). This mechanism, in addition to the NoCut checkpoint, which also relies on Aurora B at the midzone, avoids trapping and

breaking of the chromosomes during cytokinesis. Consistently, yeast cells divide with longer spindles if condensation is impaired or if the chromosome arm length is increased (D'Ambrosio et al., 2008a; Oliveira et al., 2014).

As highlighted by the *cdc5 cdc14* phenotype (Roccuzzo et al., 2015), both Cdc5 and Cdc14 contribute to spindle elongation and thus, indirectly, to the removal of DNA intertwines. However, the observations that i) *cdc5 cdc14* cells assemble a bipolar spindle (Roccuzzo et al., 2015), ii) forcing spindle elongation is not sufficient to resolve SCIs in these cells (Massari, 2018), and iii) *cdc14* cells are unable to resolve anaphase bridges, despite the spindle reaching full elongation, collectively indicate that spindle elongation is not the only mechanism through which these two proteins promote SCI resolution.

4.3.2. Leftover cohesin

Cdc5-dependent phosphorylation of the Scc1 subunit of the cohesin complex enhances its cleavage by the separase Esp1 (G. Alexandru et al., 2001), while Cdc14-mediated dephosphorylation of the securin Pds1 prompts its fast degradation (Holt et al., 2008). Therefore, one may argue that the sister chromatid separation defect of *cdc5 cdc14* cells may be caused by the incomplete cleavage of cohesin complexes. Although, in these cells, the bulk of cohesin is cleaved (Roccuzzo et al., 2015), and the analysis of sister chromatid separation using fluorescent dots indicates that centromeres lack any type of cohesion (Massari, 2018), some complexes might remain on chromosome arms. The finding that ectopic cohesin cleavage does not improve spindle elongation in *cdc5 cdc14* cells indicates that, even if some cohesin complexes persist, they do not account for the spindle elongation defect (Roccuzzo et al., 2015). However, we do not know whether leftover cohesin accounts for the persistence of SCIs. To rule out this possibility, we will force spindle elongation in *cdc5 cdc14* cells, thus inducing anaphase bridges, and test whether these bridges are reduced by ectopic cohesin cleavage.

4.3.3. Condensin and chromosome compaction

Cdc5 and Cdc14 have both been implicated in condensin activation. Phosphorylation of condensin by Cdc5 increases its DNA supercoiling activity in anaphase (St-Pierre et al., 2009), which in turn was suggested to drive Top2-mediated decatenation. In addition, the polo-like kinase is required to relocalize condensin from centromeres toward chromosome

arms upon anaphase onset, which in turn appears to trigger the analogous relocalization of Top2 (Leonard et al., 2015). On the other hand, Cdc14 is known to promote compaction and decatenation of the rDNA through transcriptional silencing and condensin recruitment to this locus (Clemente-Blanco et al., 2009; D'Amours et al., 2004; Sullivan et al., 2004; Wang et al., 2004). In light of these observations, the idea that condensin is impaired in *cdc5 cdc14* cells appears likely. To address this point, we sought to test whether its overexpression ameliorates sister chromatid separation in these cells, but we were not able to obtain a functional and stable complex with this system. However, although cv-TopoII was reported to function with lower condensin requirements compared to the yeast endogenous enzyme, its overexpression no longer rescues sister chromatid separation in *cdc5 cdc14* mutants if condensin is inactivated, indicating that condensin is at least partially functional in these cells (Massari, 2018). While this result may appear in contrast with the observation that cv-TopoII can rescue nucleolar segregation in condensin mutants (D'Ambrosio et al., 2008a), the enzyme may have different requirements according to the locus and the extent of intertwining. In conclusion, although we cannot completely exclude that condensin malfunction contributes to the sister separation defect of *cdc5 cdc14* cells, it is unlikely to be the main reason behind it.

4.4. How does Cdc5 control catenane resolution?

In *cdc5 cdc14* cells, cohesin is cleaved, condensin is at least partially functional and chromosomes are attached to the bipolar spindle. Hence, none of these factors alone is sufficient to explain the decatenation defect. On the other hand, overexpression of cv-TopoII had a striking effect on these cells. Therefore, we decided to investigate the role of Cdc5 and Cdc14 in promoting Top2 activity. Our data strongly suggests that Top2 acts downstream of Cdc5. The polo-like kinase may act on Top2 directly or indirectly and regulate its localization or activity. We investigated Top2 localization by ChIP-seq and found that the SCI resolution defect of *cdc5* and *cdc14* cells correlates with an altered distribution of the decatenating enzyme on chromatin, although we did not demonstrate causality between the two. In the future, we will also test if Top2 activity is compromised in *cdc5* and *cdc14* cells through *in vitro* decatenation assays.

4.4.1. Directly acting on Top2

Cdc5 could directly regulate Top2 through post-translational modification. In agreement with the literature (Baldwin et al., 2009), we found that Cdc5 promotes Top2 SUMOylation. SUMOylation has been reported to regulate Top2 localization, specifically its recruitment to certain genomic regions, such as the centromeres and the rDNA (Takahashi et al., 2006; Takahashi and Strunnikov, 2008). Interestingly, our ChIP-seq experiment suggests that Top2 binding to some loci, including centromeres, is lost in *cdc5* mutants (**Figure 3.13**). Altogether, this evidence points to the lack of Top2 SUMOylation as the likely reason for the decatenation defect of *cdc5* cells. The fact that the *top2-snm* allele does not increase anaphase bridges argues against this hypothesis. Nevertheless, this result could also be explained by residual SUMOylation of Top2 in the mutant. To address this possibility, we will perform immunoprecipitation of Top2-snm followed by detection of SUMO-conjugates.

In addition to SUMOylation, we collected evidence of direct phosphorylation of Top2 by the polo-like kinase *in vivo*. A caveat of our experiment is that we cannot exclude that this is an off-target effect due to overexpression of the kinase, because, contrary to SUMOylation, we could not detect endogenous Top2 phosphorylation. To address this possibility, we will attempt to detect endogenous Top2 phosphorylation and then test whether, like SUMO, it is dependent on the Polo-like kinase.

Very little is known about Top2 phosphorylation during mitosis. Interestingly, the DNA-binding protein Dpb11/TOPBP1 participates in SCI resolution in mitosis and in the recruitment of Topoisomerase II to anaphase bridges (Germann et al. 2014; Broderick et al. 2015). In human cells, the interaction between the two proteins is mediated by the BRCA1 C Terminus (BRCT) domain of TOPBP1 and the C-terminus of TOP2A (Broderick et al., 2015). Since BRCT domains usually recognize phosphorylated substrates, Cdc5 phosphorylation might guide Dpb11-mediated recruitment of Top2 to anaphase bridges. To test this hypothesis, it would be interesting to investigate if the interaction between Top2 and Dpb11 is conserved in yeast and if it is promoted by Top2 phosphorylation.

4.4.2. The role of the SUMO pathway

Cdc5 impacts Top2 SUMOylation indirectly, through inactivation of the SUMO protease Ulp2 (Baldwin et al., 2009). Ulp2 has long been linked to sister chromatid cohesion and Top2 is only one of the substrates involved in this process (Bachant et al., 2002; Stephens et al., 2015). SUMOylation of condensin and cohesin may also play a role (Mukhopadhyay and Dasso, 2017). For example, Ulp2 inactivation may lead to polySUMOylation and subsequent degradation of cohesin complexes, thus helping SCI resolution (D'Ambrosio and Lavoie, 2014; Psakhye and Branzei, 2021). Moreover, Ycs4 SUMOylation was proposed to direct condensin recruitment to the rDNA and decatenation of this locus (D'Amours et al., 2004). Although our data indicates that none among cohesin cleavage, condensin, and spindle elongation is by itself sufficient to explain the decatenation defect of *cdc5 cdc14* cells, all of them might contribute. In this scenario, the regulation of the SUMO pathway via Cdc5-mediated inactivation of Ulp2 might be at the center of a network promoting Topoisomerase II function. This hypothesis would also explain why *top2-snm* alone is not sufficient to enhance anaphase bridges. In addition to the inactivation of the SUMO protease, other enzymes of the pathway may also be regulated. Interestingly, the SUMO ligase Siz1 is phosphorylated in mitosis and evidence suggests that the responsible kinase may be Cdk1, which targets also Ulp2 (Holt et al., 2009; Johnson and Gupta, 2001). To address the role of the SUMO pathway in the resolution of DNA linkages, we will continue to characterize sister chromatid separation in *ULP2* mutants by monitoring anaphase bridges. As an alternative to the AID system, we will test Ulp2 depletion by shutoff of the galactose-inducible promoter. In the future, it will be interesting to investigate also the real consequences of Ulp2 phosphorylation in mitosis by constructing phospho-mutants.

4.5. Cdc5 and Cdc14 coordinate spindle elongation with the release of sister chromatid cohesion

In addition to the known role of Cdc5 and Cdc14 in cohesin cleavage (Gabriela Alexandru et al., 2001; Holt et al., 2008), our work points to a function in the resolution of DNA intertwines. We propose a model (**Figure 4.1**) in which these two key mitotic regulators direct SCI resolution and coordinate it with spindle elongation, with two purposes. First, spindle elongation assists the removal of residual cohesion between sister chromatids through their physical separation. Additionally, the coordination of the two events helps to

prevent the rupture of DNA bridges and preserve genome stability. Our data suggests that Cdc14 mainly controls the processing of recombination intermediates by Yen1 and the segregation of the nucleolus in late anaphase, while Cdc5 promotes the disentangling of DNA catenanes by the topoisomerase II. The Polo-like kinase may drive Top2 recruitment to specific regions through SUMOylation or phosphorylation. Moreover, Cdc5-mediated inactivation of the SUMO protease Ulp2 triggers SUMOylation of several Ulp2 substrates which contribute to release the cohesion between sister chromatids at the metaphase-to-anaphase transition.

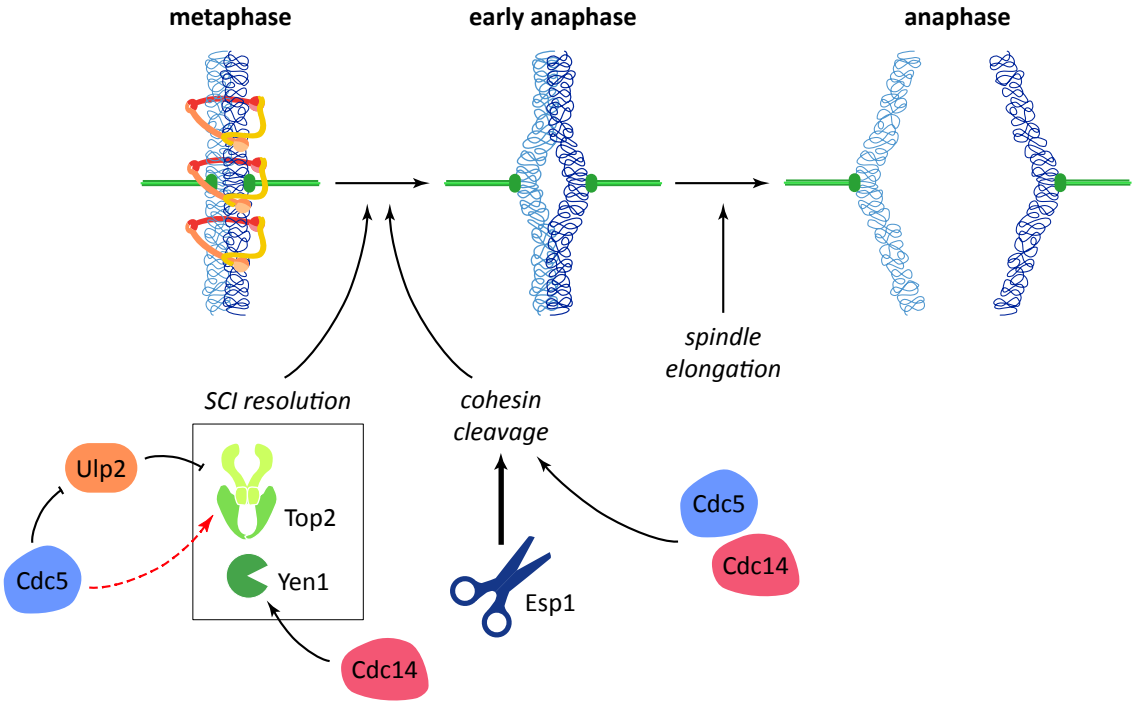

Figure 4.1. Cdc5 and Cdc14 coordinate sister chromatid separation with the resolution of DNA linkages
Red arrow represents our speculation based on this work. The dotted line indicates that we still do not know whether the regulation is direct.

4.6. Simply an unwanted leftover?

Despite the risks posed on genome integrity, DNA linkages normally persist through mitosis, raising the question as to whether they simply cannot be resolved earlier or whether they play an actual function, for example in sister chromatid cohesion. The fact that these structures are a source of cohesion is well established. Evidence suggests that, in certain conditions, the cohesion provided by SCIs can compensate for a lack of cohesin complexes well enough to correctly segregate the chromosomes (Coelho et al., 2008; Wang et al., 2010). Whether this feature is beneficial in a normal cell cycle remains unknown.

Instead, the fact that catenane resolution is subordinate to mitotic processes argues that persistent SCIs are simply an unwanted leftover. While cohesin remains the main source of cohesion, DNA linkages might have an auxiliary role. For example, the level of catenation may control the time of segregation of certain genomic regions. Interestingly, in budding yeast, the timing of decatenation and segregation of the nucleolus is controlled by Cdc14-dependent condensin recruitment at anaphase onset (D'Amours et al., 2004).

From an evolutionary perspective, DNA linkages may have served as the primary source of cohesion before cohesin appeared, as suggested by Clarke and colleagues (Díaz-Martínez et al., 2008). We find this hypothesis intriguing. Bacteria do not possess any protein structure dedicated to the cohesion between sister DNA molecules, although a SMC homolog to eukaryotic condensin is present in many species (Badrinarayanan et al., 2015). This absence is likely due to the fact that, in bacteria, sister chromatid cohesion is not needed, as chromosome segregation and DNA duplication occur simultaneously. On the other hand, in eukaryotes, the genome is more complex and organized in multiple linear chromosomes and DNA replication and mitosis occur at distinct times. Therefore, cells need mechanisms to hold sister chromatids together until all chromosomes can be segregated in a concerted manner, to ensure that the genome is equally distributed between daughter cells. While cohesin likely evolved to satisfy this requirement, SCIs could have had a more prominent role before cohesin appeared. Consistently, while cohesin must be actively loaded on the chromosomes, DNA intertwines, being a byproduct of DNA replication, naturally arise during genome duplication in all organisms.

References

Afonso, O., Castellani, C.M., Cheeseman, L.P., Ferreira, J.G., Orr, B., Ferreira, L.T., Chambers, J.J., Morais-de-Sá, E., Maresca, T.J., Maiato, H., 2019. Spatiotemporal control of mitotic exit during anaphase by an aurora B-Cdk1 crosstalk. eLife 8, e47646. https://doi.org/10.7554/eLife.47646

Agarwal, R., Cohen-Fix, O., 2002. Phosphorylation of the mitotic regulator Pds1/securin by Cdc28 is required for efficient nuclear localization of Esp1/separase. Genes Dev. 16, 1371–1382. https://doi.org/10.1101/gad.971402

Akiyoshi, B., Biggins, S., 2010. Cdc14-dependent dephosphorylation of a kinetochore protein prior to anaphase in Saccharomyces cerevisiae. Genetics 186, 1487–1491. https://doi.org/10.1534/genetics.110.123653

Alexandru, Gabriela, Uhlmann, F., Mechtler, K., Poupart, M.-A., Nasmyth, K., 2001. Phosphorylation of the Cohesin Subunit Scc1 by Polo/Cdc5 Kinase Regulates Sister Chromatid Separation in Yeast. Cell 105, 459–472. https://doi.org/10.1016/S0092-8674(01)00362-2

Alexandru, G., Uhlmann, F., Mechtler, K., Poupart, M.A., Nasmyth, K., 2001. Phosphorylation of the cohesin subunit Scc1 by Polo/Cdc5 kinase regulates sister chromatid separation in yeast. Cell 105, 459–472.

Alexandru, G., Zachariae, W., Schleiffer, A., Nasmyth, K., 1999. Sister chromatid separation and chromosome re-duplication are regulated by different mechanisms in response to spindle damage. EMBO J 18, 2707–2721. https://doi.org/10.1093/emboj/18.10.2707

Alfieri, C., Chang, L., Zhang, Z., Yang, J., Maslen, S., Skehel, M., Barford, D., 2016. Molecular basis of APC/C regulation by the spindle assembly checkpoint. Nature 536, 431–436. https://doi.org/10.1038/nature19083

Almedawar, S., Colomina, N., Bermúdez-López, M., Pociño-Merino, I., Torres-Rosell, J., 2012. A SUMO-Dependent Step during Establishment of Sister Chromatid Cohesion. Current Biology 22, 1576–1581. https://doi.org/10.1016/j.cub.2012.06.046

Amaral, N., Vendrell, A., Funaya, C., Idrissi, F.-Z., Maier, M., Kumar, A., Neurohr, G., Colomina, N., Torres-Rosell, J., Geli, M.-I., Mendoza, M., 2016. The Aurora-B-dependent NoCut checkpoint prevents damage of anaphase bridges after DNA replication stress. Nature Cell Biology 18, 516–526. https://doi.org/10.1038/ncb3343

Amon, A., 2002. Synchronization procedures. Meth. Enzymol. 351, 457–467.

Ampatzidou, E., Irmisch, A., O'Connell, M.J., Murray, J.M., 2006. Smc5/6 is required for repair at collapsed replication forks. Mol. Cell. Biol. 26, 9387–9401. https://doi.org/10.1128/MCB.01335-06

Andrews, E.A., Palecek, J., Sergeant, J., Taylor, E., Lehmann, A.R., Watts, F.Z., 2005. Nse2, a component of the Smc5-6 complex, is a SUMO ligase required for the response to DNA damage. Mol Cell Biol 25, 185–196. https://doi.org/10.1128/MCB.25.1.185-196.2005

Antoniou-Kourounioti, M., Mimmack, M.L., Porter, A.C.G., Farr, C.J., 2019. The Impact of the C-Terminal Region on the Interaction of Topoisomerase II Alpha with Mitotic Chromatin. International Journal of Molecular Sciences 20, 1238. https://doi.org/10.3390/ijms20051238

Arumugam, P., Gruber, S., Tanaka, K., Haering, C.H., Mechtler, K., Nasmyth, K., 2003. ATP

hydrolysis is required for cohesin's association with chromosomes. Curr Biol 13, 1941–1953. https://doi.org/10.1016/j.cub.2003.10.036

Asano, S., Park, J.-E., Sakchaisri, K., Yu, L.-R., Song, S., Supavilai, P., Veenstra, T.D., Lee, K.S., 2005. Concerted mechanism of Swe1/Wee1 regulation by multiple kinases in budding yeast. EMBO J 24, 2194–2204. https://doi.org/10.1038/sj.emboj.7600683

Au, W.-C., Crisp, M.J., DeLuca, S.Z., Rando, O.J., Basrai, M.A., 2008. Altered dosage and mislocalization of histone H3 and Cse4p lead to chromosome loss in Saccharomyces cerevisiae. Genetics 179, 263–275. https://doi.org/10.1534/genetics.108.088518

Azuma, Y., Arnaoutov, A., Dasso, M., 2003. SUMO-2/3 regulates topoisomerase II in mitosis. J. Cell Biol. 163, 477–487. https://doi.org/10.1083/jcb.200304088

Azzam, R., Chen, S.L., Shou, W., Mah, A.S., Alexandru, G., Nasmyth, K., Annan, R.S., Carr, S.A., Deshaies, R.J., 2004. Phosphorylation by cyclin B-Cdk underlies release of mitotic exit activator Cdc14 from the nucleolus. Science 305, 516–519. https://doi.org/10.1126/science.1099402

Bachant, J., Alcasabas, A., Blat, Y., Kleckner, N., Elledge, S.J., 2002. The SUMO-1 Isopeptidase Smt4 Is Linked to Centromeric Cohesion through SUMO-1 Modification of DNA Topoisomerase II. Molecular Cell 9, 1169–1182. https://doi.org/10.1016/S1097-2765(02)00543-9

Badrinarayanan, A., Le, T.B.K., Laub, M.T., 2015. Bacterial Chromosome Organization and Segregation. Annual Review of Cell and Developmental Biology 31, 171–199. https://doi.org/10.1146/annurev-cellbio-100814-125211

Baldwin, M., Bachant, J., 2009. Top2 SUMO conjugation in yeast cell lysates. Methods Mol. Biol. 582, 209–219. https://doi.org/10.1007/978-1-60761-340-4_16

Baldwin, M.L., Julius, J.A., Tang, X., Wang, Y., Bachant, J., 2009. The yeast SUMO isopeptidase Smt4/Ulp2 and the polo kinase Cdc5 act in an opposing fashion to regulate sumoylation in mitosis and cohesion at centromeres. Cell Cycle 8, 3406–3419. https://doi.org/10.4161/cc.8.20.9911

Bardin, A.J., Visintin, R., Amon, A., 2000. A mechanism for coupling exit from mitosis to partitioning of the nucleus. Cell 102, 21–31. https://doi.org/10.1016/s0092-8674(00)00007-6

Barefield, C., Karlseder, J., 2012. The BLM helicase contributes to telomere maintenance through processing of late-replicating intermediate structures. Nucleic Acids Res. 40, 7358–7367. https://doi.org/10.1093/nar/gks407

Batty, P., Gerlich, D.W., 2019. Mitotic Chromosome Mechanics: How Cells Segregate Their Genome. Trends in Cell Biology. https://doi.org/10.1016/j.tcb.2019.05.007

Baumann, C., Körner, R., Hofmann, K., Nigg, E.A., 2007. PICH, a centromere-associated SNF2 family ATPase, is regulated by Plk1 and required for the spindle checkpoint. Cell 128, 101–114. https://doi.org/10.1016/j.cell.2006.11.041

Baxter, J., Diffley, J.F.X., 2008. Topoisomerase II inactivation prevents the completion of DNA replication in budding yeast. Mol. Cell 30, 790–802. https://doi.org/10.1016/j.molcel.2008.04.019

Baxter, J., Sen, N., Martínez, V.L., Carandini, M.E.M.D., Schvartzman, J.B., Diffley, J.F.X., Aragón, L., 2011. Positive Supercoiling of Mitotic DNA Drives Decatenation by Topoisomerase II in Eukaryotes. Science 331, 1328–1332.

https://doi.org/10.1126/science.1201538

Benzi, G., Piatti, S., 2020. Killing two birds with one stone: how budding yeast Mps1 controls chromosome segregation and spindle assembly checkpoint through phosphorylation of a single kinetochore protein. Curr Genet 66, 1037–1044. https://doi.org/10.1007/s00294-020-01091-x

Bermejo, R., Doksani, Y., Capra, T., Katou, Y.-M., Tanaka, H., Shirahige, K., Foiani, M., 2007. Top1- and Top2-mediated topological transitions at replication forks ensure fork progression and stability and prevent DNA damage checkpoint activation. Genes Dev. 21, 1921–1936. https://doi.org/10.1101/gad.432107

Bermúdez-López, M., Ceschia, A., de Piccoli, G., Colomina, N., Pasero, P., Aragón, L., Torres-Rosell, J., 2010. The Smc5/6 complex is required for dissolution of DNA-mediated sister chromatid linkages. Nucleic Acids Res 38, 6502–6512. https://doi.org/10.1093/nar/gkq546

Biggins, S., Murray, A.W., 2001. The budding yeast protein kinase Ipl1/Aurora allows the absence of tension to activate the spindle checkpoint. Genes Dev. 15, 3118–3129. https://doi.org/10.1101/gad.934801

Bishop, A.C., Ubersax, J.A., Petsch, D.T., Matheos, D.P., Gray, N.S., Blethrow, J., Shimizu, E., Tsien, J.Z., Schultz, P.G., Rose, M.D., Wood, J.L., Morgan, D.O., Shokat, K.M., 2000. A chemical switch for inhibitor-sensitive alleles of any protein kinase. Nature 407, 395–401. https://doi.org/10.1038/35030148

Blanco, M.G., Matos, J., Rass, U., Ip, S.C.Y., West, S.C., 2010. Functional overlap between the structure-specific nucleases Yen1 and Mus81-Mms4 for DNA-damage repair in S. cerevisiae. DNA Repair 9, 394–402. https://doi.org/10.1016/j.dnarep.2009.12.017

Blanco, M.G., Matos, J., West, S.C., 2014. Dual control of Yen1 nuclease activity and cellular localization by Cdk and Cdc14 prevents genome instability. Mol. Cell 54, 94–106. https://doi.org/10.1016/j.molcel.2014.02.011

Blat, Y., Kleckner, N., 1999. Cohesins bind to preferential sites along yeast chromosome III, with differential regulation along arms versus the centric region. Cell 98, 249–259.

Blecher-Gonen, R., Barnett-Itzhaki, Z., Jaitin, D., Amann-Zalcenstein, D., Lara-Astiaso, D., Amit, I., 2013. High-throughput chromatin immunoprecipitation for genome-wide mapping of in vivo protein-DNA interactions and epigenomic states. Nat Protoc 8, 539–554. https://doi.org/10.1038/nprot.2013.023

Bloom, J., Cross, F.R., 2007. Multiple levels of cyclin specificity in cell-cycle control. Nat Rev Mol Cell Biol 8, 149–160. https://doi.org/10.1038/nrm2105

Botchkarev, V.V., Garabedian, M.V., Lemos, B., Paulissen, E., Haber, J.E., 2017. The budding yeast Polo-like kinase localizes to distinct populations at centrosomes during mitosis. Mol Biol Cell 28, 1011–1020. https://doi.org/10.1091/mbc.E16-05-0324

Botchkarev, V.V., Rossio, V., Yoshida, S., 2014. The budding yeast Polo-like kinase Cdc5 is released from the nucleus during anaphase for timely mitotic exit. Cell Cycle 13, 3260–3270. https://doi.org/10.4161/15384101.2014.953882

Boveri, T., 2008. Concerning the Origin of Malignant Tumours by Theodor Boveri. Translated and annotated by Henry Harris. Journal of Cell Science 121, 1–84. https://doi.org/10.1242/jcs.025742

Branzei, D., Sollier, J., Liberi, G., Zhao, X., Maeda, D., Seki, M., Enomoto, T., Ohta, K., Foiani, M., 2006. Ubc9- and Mms21-Mediated Sumoylation Counteracts Recombinogenic Events

at Damaged Replication Forks. Cell 127, 509–522. https://doi.org/10.1016/j.cell.2006.08.050

Branzei, D., Vanoli, F., Foiani, M., 2008. SUMOylation regulates Rad18-mediated template switch. Nature 456, 915–920. https://doi.org/10.1038/nature07587

Broderick, R., Nieminuszczy, J., Blackford, A.N., Winczura, A., Niedzwiedz, W., 2015. TOPBP1 recruits TOP2A to ultra-fine anaphase bridges to aid in their resolution. Nat Commun 6, 6572. https://doi.org/10.1038/ncomms7572

Bustamante, C., Smith, S.B., Liphardt, J., Smith, D., 2000. Single-molecule studies of DNA mechanics. Curr. Opin. Struct. Biol. 10, 279–285. https://doi.org/10.1016/s0959-440x(00)00085-3

Bylebyl, G.R., Belichenko, I., Johnson, E.S., 2003. The SUMO isopeptidase Ulp2 prevents accumulation of SUMO chains in yeast. J. Biol. Chem. 278, 44113–44120. https://doi.org/10.1074/jbc.M308357200

Care, R.S., Trevethick, J., Binley, K.M., Sudbery, P.E., 1999. The MET3 promoter: a new tool for Candida albicans molecular genetics. Mol Microbiol 34, 792–798. https://doi.org/10.1046/j.1365-2958.1999.01641.x

Cebrián, J., Castán, A., Martínez, V., Kadomatsu-Hermosa, M.J., Parra, C., Fernández-Nestosa, M.J., Schaerer, C., Hernández, P., Krimer, D.B., Schvartzman, J.B., 2015. Direct Evidence for the Formation of Precatenanes during DNA Replication. J. Biol. Chem. 290, 13725–13735. https://doi.org/10.1074/jbc.M115.642272

Cejka, P., Plank, J.L., Dombrowski, C.C., Kowalczykowski, S.C., 2012. Decatenation of DNA by the S. cerevisiae Sgs1-Top3-Rmi1 and RPA complex: a mechanism for disentangling chromosomes. Mol. Cell 47, 886–896. https://doi.org/10.1016/j.molcel.2012.06.032

Chan, C.S., Botstein, D., 1993. Isolation and characterization of chromosome-gain and increase-in-ploidy mutants in yeast. Genetics 135, 677–691. https://doi.org/10.1093/genetics/135.3.677

Chan, K.-L., Gligoris, T., Upcher, W., Kato, Y., Shirahige, K., Nasmyth, K., Beckouët, F., 2013. Pds5 promotes and protects cohesin acetylation. Proc Natl Acad Sci U S A 110, 13020–13025. https://doi.org/10.1073/pnas.1306900110

Chan, K.-L., North, P.S., Hickson, I.D., 2007. BLM is required for faithful chromosome segregation and its localization defines a class of ultrafine anaphase bridges. EMBO J. 26, 3397–3409. https://doi.org/10.1038/sj.emboj.7601777

Chan, K.L., Palmai-Pallag, T., Ying, S., Hickson, I.D., 2009. Replication stress induces sister-chromatid bridging at fragile site loci in mitosis. Nat. Cell Biol. 11, 753–760. https://doi.org/10.1038/ncb1882

Chan, Y.W., Fugger, K., West, S.C., 2018. Unresolved recombination intermediates lead to ultra-fine anaphase bridges, chromosome breaks and aberrations. Nat. Cell Biol. 20, 92–103. https://doi.org/10.1038/s41556-017-0011-1

Chan, Y.W., West, S.C., 2018. A new class of ultrafine anaphase bridges generated by homologous recombination. Cell Cycle 17, 2101–2109. https://doi.org/10.1080/15384101.2018.1515555

Chan, Y.W., West, S.C., 2014. Spatial control of the GEN1 Holliday junction resolvase ensures genome stability. Nat Commun 5, 4844. https://doi.org/10.1038/ncomms5844

Chang, Y.-C., Oram, M.K., Bielinsky, A.-K., 2021. SUMO-Targeted Ubiquitin Ligases and Their

Functions in Maintaining Genome Stability. Int J Mol Sci 22, 5391. https://doi.org/10.3390/ijms22105391

Chao, W.C.H., Murayama, Y., Muñoz, S., Costa, A., Uhlmann, F., Singleton, M.R., 2015. Structural Studies Reveal the Functional Modularity of the Scc2-Scc4 Cohesin Loader. Cell Rep 12, 719–725. https://doi.org/10.1016/j.celrep.2015.06.071

Charbin, A., Bouchoux, C., Uhlmann, F., 2014. Condensin aids sister chromatid decatenation by topoisomerase II. Nucleic Acids Res. 42, 340–348. https://doi.org/10.1093/nar/gkt882

Charles, J.F., Jaspersen, S.L., Tinker-Kulberg, R.L., Hwang, L., Szidon, A., Morgan, D.O., 1998. The Polo-related kinase Cdc5 activates and is destroyed by the mitotic cyclin destruction machinery in S. cerevisiae. Curr Biol 8, 497–507. https://doi.org/10.1016/s0960-9822(98)70201-5

Cheng, C.-H., Lo, Y.-H., Liang, S.-S., Ti, S.-C., Lin, F.-M., Yeh, C.-H., Huang, H.-Y., Wang, T.-F., 2006. SUMO modifications control assembly of synaptonemal complex and polycomplex in meiosis of Saccharomyces cerevisiae. Genes Dev 20, 2067–2081. https://doi.org/10.1101/gad.1430406

Cheng, L., Hunke, L., Hardy, C.F., 1998. Cell cycle regulation of the Saccharomyces cerevisiae polo-like kinase cdc5p. Mol Cell Biol 18, 7360–7370. https://doi.org/10.1128/mcb.18.12.7360

Ciosk, R., Shirayama, M., Shevchenko, Anna, Tanaka, T., Toth, A., Shevchenko, Andrej, Nasmyth, K., 2000. Cohesin's Binding to Chromosomes Depends on a Separate Complex Consisting of Scc2 and Scc4 Proteins. Molecular Cell 5, 243–254. https://doi.org/10.1016/S1097-2765(00)80420-7

Ciosk, R., Zachariae, W., Michaelis, C., Shevchenko, A., Mann, M., Nasmyth, K., 1998. An ESP1/PDS1 Complex Regulates Loss of Sister Chromatid Cohesion at the Metaphase to Anaphase Transition in Yeast. Cell 93, 1067–1076. https://doi.org/10.1016/S0092-8674(00)81211-8

Clarke, D.J., Johnson, R.T., Downes, C.S., 1993. Topoisomerase II inhibition prevents anaphase chromatid segregation in mammalian cells independently of the generation of DNA strand breaks. J. Cell. Sci. 105 (Pt 2), 563–569.

Clemente-Blanco, A., Mayán-Santos, M., Schneider, D.A., Machín, F., Jarmuz, A., Tschochner, H., Aragón, L., 2009. Cdc14 inhibits transcription by RNA polymerase I during anaphase. Nature 458, 219–222. https://doi.org/10.1038/nature07652

Clemente-Blanco, A., Sen, N., Mayan-Santos, M., Sacristán, M.P., Graham, B., Jarmuz, A., Giess, A., Webb, E., Game, L., Eick, D., Bueno, A., Merkenschlager, M., Aragón, L., 2011. Cdc14 phosphatase promotes segregation of telomeres through repression of RNA polymerase II transcription. Nature Cell Biology 13, 1450–1456. https://doi.org/10.1038/ncb2365

Coelho, P.A., Queiroz-Machado, J., Carmo, A.M., Moutinho-Pereira, S., Maiato, H., Sunkel, C.E., 2008. Dual Role of Topoisomerase II in Centromere Resolution and Aurora B Activity. PLOS Biology 6, e207. https://doi.org/10.1371/journal.pbio.0060207

Cohen-Fix, O., Peters, J.M., Kirschner, M.W., Koshland, D., 1996. Anaphase initiation in Saccharomyces cerevisiae is controlled by the APC-dependent degradation of the anaphase inhibitor Pds1p. Genes Dev. 10, 3081–3093. https://doi.org/10.1101/gad.10.24.3081

Corbett, K.D., 2017. Molecular Mechanisms of Spindle Assembly Checkpoint Activation and Silencing, in: Black, B.E. (Ed.), Centromeres and Kinetochores: Discovering the Molecular

Mechanisms Underlying Chromosome Inheritance, Progress in Molecular and Subcellular Biology. Springer International Publishing, Cham, pp. 429–455. https://doi.org/10.1007/978-3-319-58592-5_18

Cuijpers, S.A.G., Vertegaal, A.C.O., 2018. Guiding Mitotic Progression by Crosstalk between Post-translational Modifications. Trends in Biochemical Sciences 43, 251–268. https://doi.org/10.1016/j.tibs.2018.02.004

Cuylen, S., Metz, J., Haering, C.H., 2011. Condensin structures chromosomal DNA through topological links. Nat. Struct. Mol. Biol. 18, 894–901. https://doi.org/10.1038/nsmb.2087

Cuylen, S., Metz, J., Hruby, A., Haering, C.H., 2013. Entrapment of chromosomes by condensin rings prevents their breakage during cytokinesis. Dev. Cell 27, 469–478. https://doi.org/10.1016/j.devcel.2013.10.018

D'Ambrosio, C., Kelly, G., Shirahige, K., Uhlmann, F., 2008a. Condensin-Dependent rDNA Decatenation Introduces a Temporal Pattern to Chromosome Segregation. Current Biology 18, 1084–1089. https://doi.org/10.1016/j.cub.2008.06.058

D'Ambrosio, C., Schmidt, C.K., Katou, Y., Kelly, G., Itoh, T., Shirahige, K., Uhlmann, F., 2008b. Identification of cis-acting sites for condensin loading onto budding yeast chromosomes. Genes Dev. 22, 2215–2227. https://doi.org/10.1101/gad.1675708

D'Ambrosio, L.M., Lavoie, B.D., 2014. Pds5 prevents the PolySUMO-dependent separation of sister chromatids. Curr Biol 24, 361–371. https://doi.org/10.1016/j.cub.2013.12.038

D'Amours, D., Stegmeier, F., Amon, A., 2004. Cdc14 and Condensin Control the Dissolution of Cohesin-Independent Chromosome Linkages at Repeated DNA. Cell 117, 455–469. https://doi.org/10.1016/S0092-8674(04)00413-1

Daniloski, Z., Bisht, K.K., McStay, B., Smith, S., 2019. Resolution of human ribosomal DNA occurs in anaphase, dependent on tankyrase 1, condensin II, and topoisomerase IIα. Genes Dev. 33, 276–281. https://doi.org/10.1101/gad.321836.118

D'Aquino, K.E., Monje-Casas, F., Paulson, J., Reiser, V., Charles, G.M., Lai, L., Shokat, K.M., Amon, A., 2005. The protein kinase Kin4 inhibits exit from mitosis in response to spindle position defects. Mol Cell 19, 223–234. https://doi.org/10.1016/j.molcel.2005.06.005

Darieva, Z., Bulmer, R., Pic-Taylor, A., Doris, K.S., Geymonat, M., Sedgwick, S.G., Morgan, B.A., Sharrocks, A.D., 2006. Polo kinase controls cell-cycle-dependent transcription by targeting a coactivator protein. Nature 444, 494–498. https://doi.org/10.1038/nature05339

Dasso, M., 2008. Emerging roles of the SUMO pathway in mitosis. Cell Div 3, 5. https://doi.org/10.1186/1747-1028-3-5

Davidson, I.F., Bauer, B., Goetz, D., Tang, W., Wutz, G., Peters, J.-M., 2019. DNA loop extrusion by human cohesin. Science 366, 1338–1345. https://doi.org/10.1126/science.aaz3418

Dawlaty, M.M., Malureanu, L., Jeganathan, K.B., Kao, E., Sustmann, C., Tahk, S., Shuai, K., Grosschedl, R., van Deursen, J.M., 2008. Resolution of sister centromeres requires RanBP2-mediated SUMOylation of topoisomerase IIalpha. Cell 133, 103–115. https://doi.org/10.1016/j.cell.2008.01.045

De Antoni, A., Pearson, C.G., Cimini, D., Canman, J.C., Sala, V., Nezi, L., Mapelli, M., Sironi, L., Faretta, M., Salmon, E.D., Musacchio, A., 2005. The Mad1/Mad2 complex as a template for Mad2 activation in the spindle assembly checkpoint. Curr. Biol. 15, 214–225.

https://doi.org/10.1016/j.cub.2005.01.038

De Piccoli, G., Cortes-Ledesma, F., Ira, G., Torres-Rosell, J., Uhle, S., Farmer, S., Hwang, J.-Y., Machin, F., Ceschia, A., McAleenan, A., Cordon-Preciado, V., Clemente-Blanco, A., Vilella-Mitjana, F., Ullal, P., Jarmuz, A., Leitao, B., Bressan, D., Dotiwala, F., Papusha, A., Zhao, X., Myung, K., Haber, J.E., Aguilera, A., Aragón, L., 2006. Smc5–Smc6 mediate DNA double-strand-break repair by promoting sister-chromatid recombination. Nat Cell Biol 8, 1032–1034. https://doi.org/10.1038/ncb1466

De Wulf, P., Montani, F., Visintin, R., 2009. Protein phosphatases take the mitotic stage. Curr Opin Cell Biol 21, 806–815. https://doi.org/10.1016/j.ceb.2009.08.003

Díaz-Martínez, L.A., Giménez-Abián, J.F., Clarke, D.J., 2008. Chromosome cohesion - rings, knots, orcs and fellowship. J. Cell. Sci. 121, 2107–2114. https://doi.org/10.1242/jcs.029132

DiNardo, S., Voelkel, K., Sternglanz, R., 1984. DNA topoisomerase II mutant of Saccharomyces cerevisiae: topoisomerase II is required for segregation of daughter molecules at the termination of DNA replication. Proc. Natl. Acad. Sci. U.S.A. 81, 2616–2620. https://doi.org/10.1073/pnas.81.9.2616

Dong, K.C., Berger, J.M., 2007. Structural basis for gate-DNA recognition and bending by type IIA topoisomerases. Nature 450, 1201–1205. https://doi.org/10.1038/nature06396

Doughty, T.W., Arsenault, H.E., Benanti, J.A., 2016. Levels of Ycg1 Limit Condensin Function during the Cell Cycle. PLoS Genet 12, e1006216. https://doi.org/10.1371/journal.pgen.1006216

Duda, H., Arter, M., Gloggnitzer, J., Teloni, F., Wild, P., Blanco, M.G., Altmeyer, M., Matos, J., 2016. A Mechanism for Controlled Breakage of Under-replicated Chromosomes during Mitosis. Dev. Cell 39, 740–755. https://doi.org/10.1016/j.devcel.2016.11.017

Dulev, S., de Renty, C., Mehta, R., Minkov, I., Schwob, E., Strunnikov, A., 2009. Essential global role of CDC14 in DNA synthesis revealed by chromosome underreplication unrecognized by checkpoints in cdc14 mutants. Proc Natl Acad Sci U S A 106, 14466–14471. https://doi.org/10.1073/pnas.0900190106

Edgerton, H., Johansson, M., Keifenheim, D., Mukherjee, S., Chacón, J.M., Bachant, J., Gardner, M.K., Clarke, D.J., 2016. A noncatalytic function of the topoisomerase II CTD in Aurora B recruitment to inner centromeres during mitosis. J Cell Biol 213, 651–664. https://doi.org/10.1083/jcb.201511080

Eeftens, J.M., Bisht, S., Kerssemakers, J., Kschonsak, M., Haering, C.H., Dekker, C., 2017. Real-time detection of condensin-driven DNA compaction reveals a multistep binding mechanism. EMBO J. 36, 3448–3457. https://doi.org/10.15252/embj.201797596

Eissler, C.L., Mazón, G., Powers, B.L., Savinov, S.N., Symington, L.S., Hall, M.C., 2014. The Cdk/cDc14 module controls activation of the Yen1 holliday junction resolvase to promote genome stability. Mol. Cell 54, 80–93. https://doi.org/10.1016/j.molcel.2014.02.012

Elia, A.E.H., Cantley, L.C., Yaffe, M.B., 2003. Proteomic screen finds pSer/pThr-binding domain localizing Plk1 to mitotic substrates. Science 299, 1228–1231. https://doi.org/10.1126/science.1079079

Elmore, Z.C., Donaher, M., Matson, B.C., Murphy, H., Westerbeck, J.W., Kerscher, O., 2011. Sumo-dependent substrate targeting of the SUMO protease Ulp1. BMC Biol 9, 74. https://doi.org/10.1186/1741-7007-9-74

Espert, A., Uluocak, P., Bastos, R.N., Mangat, D., Graab, P., Gruneberg, U., 2014. PP2A-B56

opposes Mps1 phosphorylation of Knl1 and thereby promotes spindle assembly checkpoint silencing. J Cell Biol 206, 833–842. https://doi.org/10.1083/jcb.201406109

Fachinetti, D., Bermejo, R., Cocito, A., Minardi, S., Katou, Y., Kanoh, Y., Shirahige, K., Azvolinsky, A., Zakian, V.A., Foiani, M., 2010. Replication termination at eukaryotic chromosomes is mediated by Top2 and occurs at genomic loci containing pausing elements. Mol. Cell 39, 595–605. https://doi.org/10.1016/j.molcel.2010.07.024

Falquet, B., Rass, U., 2019. Structure-Specific Endonucleases and the Resolution of Chromosome Underreplication. Genes (Basel) 10. https://doi.org/10.3390/genes10030232

Farcas, A.-M., Uluocak, P., Helmhart, W., Nasmyth, K., 2011. Cohesin's concatenation of sister DNAs maintains their intertwining. Mol. Cell 44, 97–107. https://doi.org/10.1016/j.molcel.2011.07.034

Finardi, A., Massari, L.F., Visintin, R., 2020. Anaphase Bridges: Not All Natural Fibers Are Healthy. Genes (Basel) 11. https://doi.org/10.3390/genes11080902

Fortune, J.M., Lavrukhin, O.V., Gurnon, J.R., Van Etten, J.L., Lloyd, R.S., Osheroff, N., 2001. Topoisomerase II from Chlorella Virus PBCV-1 Has an Exceptionally High DNA Cleavage Activity*. Journal of Biological Chemistry 276, 24401–24408. https://doi.org/10.1074/jbc.M101693200

Francisco, L., Wang, W., Chan, C.S., 1994. Type 1 protein phosphatase acts in opposition to IpL1 protein kinase in regulating yeast chromosome segregation. Mol Cell Biol 14, 4731–4740. https://doi.org/10.1128/mcb.14.7.4731-4740.1994

Fraschini, R., D'Ambrosio, C., Venturetti, M., Lucchini, G., Piatti, S., 2006. Disappearance of the budding yeast Bub2-Bfa1 complex from the mother-bound spindle pole contributes to mitotic exit. J Cell Biol 172, 335–346. https://doi.org/10.1083/jcb.200507162

Freeman, L., Aragon-Alcaide, L., Strunnikov, A., 2000. The Condensin Complex Governs Chromosome Condensation and Mitotic Transmission of Rdna. Journal of Cell Biology 149, 811–824. https://doi.org/10.1083/jcb.149.4.811

Fuller, B.G., Lampson, M.A., Foley, E.A., Rosasco-Nitcher, S., Le, K.V., Tobelmann, P., Brautigan, D.L., Stukenberg, P.T., Kapoor, T.M., 2008. Midzone activation of aurora B in anaphase produces an intracellular phosphorylation gradient. Nature 453, 1132–1136. https://doi.org/10.1038/nature06923

Gaillard, H., García-Muse, T., Aguilera, A., 2015. Replication stress and cancer. Nature Reviews Cancer 15, 276–289. https://doi.org/10.1038/nrc3916

Gallo-Fernández, M., Saugar, I., Ortiz-Bazán, M.Á., Vázquez, M.V., Tercero, J.A., 2012. Cell cycle-dependent regulation of the nuclease activity of Mus81-Eme1/Mms4. Nucleic Acids Res. 40, 8325–8335. https://doi.org/10.1093/nar/gks599

Gandhi, R., Gillespie, P.J., Hirano, T., 2006. Human Wapl is a cohesin-binding protein that promotes sister-chromatid resolution in mitotic prophase. Curr. Biol. 16, 2406–2417. https://doi.org/10.1016/j.cub.2006.10.061

Ganem, N.J., Pellman, D., 2012. Linking abnormal mitosis to the acquisition of DNA damage. J. Cell Biol. 199, 871–881. https://doi.org/10.1083/jcb.201210040

Ganji, M., Shaltiel, I.A., Bisht, S., Kim, E., Kalichava, A., Haering, C.H., Dekker, C., 2018. Real-time imaging of DNA loop extrusion by condensin. Science 360, 102–105. https://doi.org/10.1126/science.aar7831

García-Luis, J., Machín, F., 2014. Mus81-Mms4 and Yen1 resolve a novel anaphase bridge

formed by noncanonical Holliday junctions. Nature Communications 5, 1–11. https://doi.org/10.1038/ncomms6652

Garner, E., Kim, Y., Lach, F.P., Kottemann, M.C., Smogorzewska, A., 2013. Human GEN1 and the SLX4-associated nucleases MUS81 and SLX1 are essential for the resolution of replication-induced Holliday junctions. Cell Rep 5, 207–215. https://doi.org/10.1016/j.celrep.2013.08.041

Germann, S.M., Schramke, V., Pedersen, R.T., Gallina, I., Eckert-Boulet, N., Oestergaard, V.H., Lisby, M., 2014. TopBP1/Dpb11 binds DNA anaphase bridges to prevent genome instability. J Cell Biol 204, 45–59. https://doi.org/10.1083/jcb.201305157

Gibcus, J.H., Samejima, K., Goloborodko, A., Samejima, I., Naumova, N., Nuebler, J., Kanemaki, M.T., Xie, L., Paulson, J.R., Earnshaw, W.C., Mirny, L.A., Dekker, J., 2018. A pathway for mitotic chromosome formation. Science 359. https://doi.org/10.1126/science.aao6135

Gligoris, T.G., Scheinost, J.C., Bürmann, F., Petela, N., Chan, K.-L., Uluocak, P., Beckouët, F., Gruber, S., Nasmyth, K., Löwe, J., 2014. Closing the cohesin ring: structure and function of its Smc3-kleisin interface. Science 346, 963–967. https://doi.org/10.1126/science.1256917

Glynn, E.F., Megee, P.C., Yu, H.-G., Mistrot, C., Unal, E., Koshland, D.E., DeRisi, J.L., Gerton, J.L., 2004. Genome-wide mapping of the cohesin complex in the yeast Saccharomyces cerevisiae. PLoS Biol. 2, E259. https://doi.org/10.1371/journal.pbio.0020259

Granot, D., Snyder, M., 1991. Segregation of the nucleolus during mitosis in budding and fission yeast. Cell Motil Cytoskeleton 20, 47–54. https://doi.org/10.1002/cm.970200106

Grigaitis, R., Ranjha, L., Wild, P., Kasaciunaite, K., Ceppi, I., Kissling, V., Henggeler, A., Susperregui, A., Peter, M., Seidel, R., Cejka, P., Matos, J., 2020. Phosphorylation of the RecQ Helicase Sgs1/BLM Controls Its DNA Unwinding Activity during Meiosis and Mitosis. Developmental Cell 53, 706-723.e5. https://doi.org/10.1016/j.devcel.2020.05.016

Gritenaite, D., Princz, L.N., Szakal, B., Bantele, S.C.S., Wendeler, L., Schilbach, S., Habermann, B.H., Matos, J., Lisby, M., Branzei, D., Pfander, B., 2014. A cell cycle-regulated Slx4-Dpb11 complex promotes the resolution of DNA repair intermediates linked to stalled replication. Genes Dev. 28, 1604–1619. https://doi.org/10.1101/gad.240515.114

Guacci, V., Hogan, E., Koshland, D., 1994. Chromosome condensation and sister chromatid pairing in budding yeast. Journal of Cell Biology 125, 517–530. https://doi.org/10.1083/jcb.125.3.517

Guacci, V., Koshland, D., Strunnikov, A., 1997. A Direct Link between Sister Chromatid Cohesion and Chromosome Condensation Revealed through the Analysis of MCD1 in S. cerevisiae. Cell 91, 47–57. https://doi.org/10.1016/S0092-8674(01)80008-8

Haering, C.H., Farcas, A.-M., Arumugam, P., Metson, J., Nasmyth, K., 2008. The cohesin ring concatenates sister DNA molecules. Nature 454, 297–301. https://doi.org/10.1038/nature07098

Harmon, F.G., DiGate, R.J., Kowalczykowski, S.C., 1999. RecQ helicase and topoisomerase III comprise a novel DNA strand passage function: a conserved mechanism for control of DNA recombination. Mol. Cell 3, 611–620. https://doi.org/10.1016/s1097-2765(00)80354-8

Hartwell, L.H., Weinert, T.A., 1989. Checkpoints: controls that ensure the order of cell cycle events. Science 246, 629–634. https://doi.org/10.1126/science.2683079

Hassler, M., Shaltiel, I.A., Haering, C.H., 2018. Towards a Unified Model of SMC Complex Function. Curr. Biol. 28, R1266–R1281. https://doi.org/10.1016/j.cub.2018.08.034

Higashi, T.L., Eickhoff, P., Sousa, J.S., Locke, J., Nans, A., Flynn, H.R., Snijders, A.P., Papageorgiou, G., O'Reilly, N., Chen, Z.A., O'Reilly, F.J., Rappsilber, J., Costa, A., Uhlmann, F., 2020. A Structure-Based Mechanism for DNA Entry into the Cohesin Ring. Molecular Cell 79, 917-933.e9. https://doi.org/10.1016/j.molcel.2020.07.013

Holm, C., Goto, T., Wang, J.C., Botstein, D., 1985. DNA topoisomerase II is required at the time of mitosis in yeast. Cell 41, 553–563.

Holt, L.J., Krutchinsky, A.N., Morgan, D.O., 2008. Positive feedback sharpens the anaphase switch. Nature 454, 353–357. https://doi.org/10.1038/nature07050

Holt, L.J., Tuch, B.B., Villén, J., Johnson, A.D., Gygi, S.P., Morgan, D.O., 2009. Global analysis of Cdk1 substrate phosphorylation sites provides insights into evolution. Science 325, 1682–1686. https://doi.org/10.1126/science.1172867

Hornig, N.C.D., Knowles, P.P., McDonald, N.Q., Uhlmann, F., 2002. The Dual Mechanism of Separase Regulation by Securin. Current Biology 12, 973–982. https://doi.org/10.1016/S0960-9822(02)00847-3

Houchmandzadeh, B., Marko, J.F., Chatenay, D., Libchaber, A., 1997. Elasticity and structure of eukaryote chromosomes studied by micromanipulation and micropipette aspiration. J. Cell Biol. 139, 1–12. https://doi.org/10.1083/jcb.139.1.1

Hu, F., Wang, Y., Liu, D., Li, Y., Qin, J., Elledge, S.J., 2001. Regulation of the Bub2/Bfa1 GAP Complex by Cdc5 and Cell Cycle Checkpoints. Cell 107, 655–665. https://doi.org/10.1016/S0092-8674(01)00580-3

Hwang, L.H., Lau, L.F., Smith, D.L., Mistrot, C.A., Hardwick, K.G., Hwang, E.S., Amon, A., Murray, A.W., 1998. Budding yeast Cdc20: a target of the spindle checkpoint. Science 279, 1041–1044.

Ip, S.C.Y., Rass, U., Blanco, M.G., Flynn, H.R., Skehel, J.M., West, S.C., 2008. Identification of Holliday junction resolvases from humans and yeast. Nature 456, 357–361. https://doi.org/10.1038/nature07470

Ira, G., Malkova, A., Liberi, G., Foiani, M., Haber, J.E., 2003. Srs2 and Sgs1-Top3 suppress crossovers during double-strand break repair in yeast. Cell 115, 401–411. https://doi.org/10.1016/s0092-8674(03)00886-9

Irmisch, A., Ampatzidou, E., Mizuno, K., O'Connell, M.J., Murray, J.M., 2009. Smc5/6 maintains stalled replication forks in a recombination-competent conformation. EMBO J. 28, 144–155. https://doi.org/10.1038/emboj.2008.273

Ivanova, T., Maier, M., Missarova, A., Ziegler-Birling, C., Dam, M., Gomar-Alba, M., Carey, L.B., Mendoza, M., 2020. Budding yeast complete DNA synthesis after chromosome segregation begins. Nat Commun 11, 2267. https://doi.org/10.1038/s41467-020-16100-3

Izawa, D., Pines, J., 2015. The mitotic checkpoint complex binds a second CDC20 to inhibit active APC/C. Nature 517, 631–634. https://doi.org/10.1038/nature13911

Jaspersen, S.L., Charles, J.F., Tinker-Kulberg, R.L., Morgan, D.O., 1998. A late mitotic regulatory network controlling cyclin destruction in Saccharomyces cerevisiae. Mol. Biol. Cell 9, 2803–2817.

Jaspersen, S.L., Morgan, D.O., 2000. Cdc14 activates cdc15 to promote mitotic exit in budding yeast. Curr Biol 10, 615–618. https://doi.org/10.1016/s0960-9822(00)00491-7

Jeppsson, K., Carlborg, K.K., Nakato, R., Berta, D.G., Lilienthal, I., Kanno, T., Lindqvist, A., Brink, M.C., Dantuma, N.P., Katou, Y., Shirahige, K., Sjögren, C., 2014. The chromosomal association of the Smc5/6 complex depends on cohesion and predicts the level of sister chromatid entanglement. PLoS Genet. 10, e1004680. https://doi.org/10.1371/journal.pgen.1004680

Johnson, E.S., Blobel, G., 1999. Cell Cycle–Regulated Attachment of the Ubiquitin-Related Protein Sumo to the Yeast Septins. Journal of Cell Biology 147, 981–994. https://doi.org/10.1083/jcb.147.5.981

Johnson, E.S., Gupta, A.A., 2001. An E3-like Factor that Promotes SUMO Conjugation to the Yeast Septins. Cell 106, 735–744. https://doi.org/10.1016/S0092-8674(01)00491-3

Kakui, Y., Uhlmann, F., 2018. SMC complexes orchestrate the mitotic chromatin interaction landscape. Curr Genet 64, 335–339. https://doi.org/10.1007/s00294-017-0755-y

Kanno, T., Berta, D.G., Sjögren, C., 2015. The Smc5/6 Complex Is an ATP-Dependent Intermolecular DNA Linker. Cell Rep 12, 1471–1482. https://doi.org/10.1016/j.celrep.2015.07.048

Kapanidou, M., Curtis, N.L., Bolanos-Garcia, V.M., 2017. Cdc20: At the Crossroads between Chromosome Segregation and Mitotic Exit. Trends in Biochemical Sciences 42, 193–205. https://doi.org/10.1016/j.tibs.2016.12.001

Kegel, A., Betts-Lindroos, H., Kanno, T., Jeppsson, K., Ström, L., Katou, Y., Itoh, T., Shirahige, K., Sjögren, C., 2011. Chromosome length influences replication-induced topological stress. Nature 471, 392–396. https://doi.org/10.1038/nature09791

Kelly, A.E., Funabiki, H., 2009. Correcting aberrant kinetochore microtubule attachments: an Aurora B-centric view. Current Opinion in Cell Biology, Cell structure and dynamics 21, 51–58. https://doi.org/10.1016/j.ceb.2009.01.004

Khmelinskii, A., Lawrence, C., Roostalu, J., Schiebel, E., 2007. Cdc14-regulated midzone assembly controls anaphase B. J Cell Biol 177, 981–993. https://doi.org/10.1083/jcb.200702145

Kilmartin, J.V., Adams, A.E., 1984. Structural rearrangements of tubulin and actin during the cell cycle of the yeast Saccharomyces. J Cell Biol 98, 922–933. https://doi.org/10.1083/jcb.98.3.922

Kim, E., Kerssemakers, J., Shaltiel, I.A., Haering, C.H., Dekker, C., 2020. DNA-loop extruding condensin complexes can traverse one another. Nature 579, 438–442. https://doi.org/10.1038/s41586-020-2067-5

Kim, Y., Shi, Z., Zhang, H., Finkelstein, I.J., Yu, H., 2019. Human cohesin compacts DNA by loop extrusion. Science 366, 1345–1349. https://doi.org/10.1126/science.aaz4475

Kimura, K., Hirano, T., 1997. ATP-dependent positive supercoiling of DNA by 13S condensin: a biochemical implication for chromosome condensation. Cell 90, 625–634. https://doi.org/10.1016/s0092-8674(00)80524-3

Kimura, K., Rybenkov, V.V., Crisona, N.J., Hirano, T., Cozzarelli, N.R., 1999. 13S Condensin Actively Reconfigures DNA by Introducing Global Positive Writhe: Implications for Chromosome Condensation. Cell 98, 239–248. https://doi.org/10.1016/S0092-8674(00)81018-1

Kinoshita, E., Kinoshita-Kikuta, E., Koike, T., 2009. Separation and detection of large phosphoproteins using Phos-tag SDS-PAGE. Nat Protoc 4, 1513–1521.

https://doi.org/10.1038/nprot.2009.154

Kitada, K., Johnson, A.L., Johnston, L.H., Sugino, A., 1993. A multicopy suppressor gene of the Saccharomyces cerevisiae G1 cell cycle mutant gene dbf4 encodes a protein kinase and is identified as CDC5. Mol Cell Biol 13, 4445–4457. https://doi.org/10.1128/mcb.13.7.4445-4457.1993

König, C., Maekawa, H., Schiebel, E., 2010. Mutual regulation of cyclin-dependent kinase and the mitotic exit network. J Cell Biol 188, 351–368. https://doi.org/10.1083/jcb.200911128

Kosugi, S., Hasebe, M., Tomita, M., Yanagawa, H., 2009. Systematic identification of cell cycle-dependent yeast nucleocytoplasmic shuttling proteins by prediction of composite motifs. Proc. Natl. Acad. Sci. U.S.A. 106, 10171–10176. https://doi.org/10.1073/pnas.0900604106

Krenn, V., Musacchio, A., 2015. The Aurora B Kinase in Chromosome Bi-Orientation and Spindle Checkpoint Signaling. Front Oncol 5, 225. https://doi.org/10.3389/fonc.2015.00225

Kueng, S., Hegemann, B., Peters, B.H., Lipp, J.J., Schleiffer, A., Mechtler, K., Peters, J.-M., 2006. Wapl Controls the Dynamic Association of Cohesin with Chromatin. Cell 127, 955–967. https://doi.org/10.1016/j.cell.2006.09.040

Lavoie, B.D., Hogan, E., Koshland, D., 2004. In vivo requirements for rDNA chromosome condensation reveal two cell-cycle-regulated pathways for mitotic chromosome folding. Genes Dev. 18, 76–87. https://doi.org/10.1101/gad.1150404

Lavrukhin, O.V., Fortune, J.M., Wood, T.G., Burbank, D.E., Van Etten, J.L., Osheroff, N., Lloyd, R.S., 2000. Topoisomerase II from Chlorella virus PBCV-1. Characterization of the smallest known type II topoisomerase. J Biol Chem 275, 6915–6921. https://doi.org/10.1074/jbc.275.10.6915

Lawrimore, J., Aicher, J.K., Hahn, P., Fulp, A., Kompa, B., Vicci, L., Falvo, M., Taylor, R.M., Bloom, K., 2016. ChromoShake: a chromosome dynamics simulator reveals that chromatin loops stiffen centromeric chromatin. MBoC 27, 153–166. https://doi.org/10.1091/mbc.E15-08-0575

Lawrimore, J., Doshi, A., Friedman, B., Yeh, E., Bloom, K., 2018. Geometric partitioning of cohesin and condensin is a consequence of chromatin loops. Mol Biol Cell 29, 2737–2750. https://doi.org/10.1091/mbc.E18-02-0131

Lawrimore, J., Vasquez, P.A., Falvo, M.R., Taylor, R.M., II, Vicci, L., Yeh, E., Forest, M.G., Bloom, K., 2015. DNA loops generate intracentromere tension in mitosis. Journal of Cell Biology 210, 553–564. https://doi.org/10.1083/jcb.201502046

Lazar-Stefanita, L., Scolari, V.F., Mercy, G., Muller, H., Guérin, T.M., Thierry, A., Mozziconacci, J., Koszul, R., 2017. Cohesins and condensins orchestrate the 4D dynamics of yeast chromosomes during the cell cycle. EMBO J. 36, 2684–2697. https://doi.org/10.15252/embj.201797342

Le Beau, M.M., Rassool, F.V., Neilly, M.E., Espinosa, R., Glover, T.W., Smith, D.I., McKeithan, T.W., 1998. Replication of a common fragile site, FRA3B, occurs late in S phase and is delayed further upon induction: implications for the mechanism of fragile site induction. Hum. Mol. Genet. 7, 755–761. https://doi.org/10.1093/hmg/7.4.755

Le, T.T., Gao, X., Park, S. ha, Lee, J., Inman, J.T., Lee, J.H., Killian, J.L., Badman, R.P., Berger, J.M., Wang, M.D., 2019. Synergistic Coordination of Chromatin Torsional Mechanics and

Topoisomerase Activity. Cell 179, 619-631.e15. https://doi.org/10.1016/j.cell.2019.09.034

Lee, J.H., Berger, J.M., 2019. Cell Cycle-Dependent Control and Roles of DNA Topoisomerase II. Genes (Basel) 10. https://doi.org/10.3390/genes10110859

Lee, K.S., Park, J.-E., Asano, S., Park, C.J., 2005. Yeast polo-like kinases: functionally conserved multitask mitotic regulators. Oncogene 24, 217–229. https://doi.org/10.1038/sj.onc.1208271

Lengronne, A., Katou, Y., Mori, S., Yokobayashi, S., Kelly, G.P., Itoh, T., Watanabe, Y., Shirahige, K., Uhlmann, F., 2004. Cohesin relocation from sites of chromosomal loading to places of convergent transcription. Nature 430, 573–578. https://doi.org/10.1038/nature02742

Leonard, J., Sen, N., Torres, R., Sutani, T., Jarmuz, A., Shirahige, K., Aragón, L., 2015. Condensin Relocalization from Centromeres to Chromosome Arms Promotes Top2 Recruitment during Anaphase. Cell Reports 13, 2336–2344. https://doi.org/10.1016/j.celrep.2015.11.041

Li, H., Wang, Y., Liu, X., 2008. Plk1-dependent phosphorylation regulates functions of DNA topoisomerase IIalpha in cell cycle progression. J. Biol. Chem. 283, 6209–6221. https://doi.org/10.1074/jbc.M709007200

Li, S., Yue, Z., Tanaka, T.U., 2017. Smc3 Deacetylation by Hos1 Facilitates Efficient Dissolution of Sister Chromatid Cohesion during Early Anaphase. Molecular Cell 68, 605-614.e4. https://doi.org/10.1016/j.molcel.2017.10.009

Li, S.-J., Hochstrasser, M., 2003. The Ulp1 SUMO isopeptidase: distinct domains required for viability, nuclear envelope localization, and substrate specificity. J Cell Biol 160, 1069–1081. https://doi.org/10.1083/jcb.200212052

Li, S.-J., Hochstrasser, M., 2000. The Yeast ULP2 (SMT4) Gene Encodes a Novel Protease Specific for the Ubiquitin-Like Smt3 Protein. Mol Cell Biol 20, 2367–2377.

Li, S.J., Hochstrasser, M., 1999. A new protease required for cell-cycle progression in yeast. Nature 398, 246–251. https://doi.org/10.1038/18457

Li, Y., Stewart, N.K., Berger, A.J., Vos, S., Schoeffler, A.J., Berger, J.M., Chait, B.T., Oakley, M.G., 2010. Escherichia coli condensin MukB stimulates topoisomerase IV activity by a direct physical interaction. Proc. Natl. Acad. Sci. U.S.A. 107, 18832–18837. https://doi.org/10.1073/pnas.1008678107

Liberi, G., Maffioletti, G., Lucca, C., Chiolo, I., Baryshnikova, A., Cotta-Ramusino, C., Lopes, M., Pellicioli, A., Haber, J.E., Foiani, M., 2005. Rad51-dependent DNA structures accumulate at damaged replication forks in sgs1 mutants defective in the yeast ortholog of BLM RecQ helicase. Genes Dev. 19, 339–350. https://doi.org/10.1101/gad.322605

Lieberman-Aiden, E., van Berkum, N.L., Williams, L., Imakaev, M., Ragoczy, T., Telling, A., Amit, I., Lajoie, B.R., Sabo, P.J., Dorschner, M.O., Sandstrom, R., Bernstein, B., Bender, M.A., Groudine, M., Gnirke, A., Stamatoyannopoulos, J., Mirny, L.A., Lander, E.S., Dekker, J., 2009. Comprehensive Mapping of Long-Range Interactions Reveals Folding Principles of the Human Genome. Science 326, 289–293. https://doi.org/10.1126/science.1181369

Lindroos, H.B., Ström, L., Itoh, T., Katou, Y., Shirahige, K., Sjögren, C., 2006. Chromosomal Association of the Smc5/6 Complex Reveals that It Functions in Differently Regulated Pathways. Molecular Cell 22, 755–767. https://doi.org/10.1016/j.molcel.2006.05.014

Litwin, I., Wysocki, R., 2018. New insights into cohesin loading. Curr Genet 64, 53–61.

https://doi.org/10.1007/s00294-017-0723-6

Liu, D., Vader, G., Vromans, M.J.M., Lampson, M.A., Lens, S.M.A., 2009. Sensing chromosome bi-orientation by spatial separation of aurora B kinase from kinetochore substrates. Science 323, 1350–1353. https://doi.org/10.1126/science.1167000

Liu, D., Vleugel, M., Backer, C.B., Hori, T., Fukagawa, T., Cheeseman, I.M., Lampson, M.A., 2010. Regulated targeting of protein phosphatase 1 to the outer kinetochore by KNL1 opposes Aurora B kinase. J Cell Biol 188, 809–820. https://doi.org/10.1083/jcb.201001006

Liu, Y., Cussiol, J.R., Dibitetto, D., Sims, J.R., Twayana, S., Weiss, R.S., Freire, R., Marini, F., Pellicioli, A., Smolka, M.B., 2017. TOPBP1Dpb11 plays a conserved role in homologous recombination DNA repair through the coordinated recruitment of 53BP1Rad9. J. Cell Biol. 216, 623–639. https://doi.org/10.1083/jcb.201607031

London, N., Ceto, S., Ranish, J.A., Biggins, S., 2012. Phosphoregulation of Spc105 by Mps1 and PP1 regulates Bub1 localization to kinetochores. Curr Biol 22, 900–906. https://doi.org/10.1016/j.cub.2012.03.052

Longtine, M.S., McKenzie, A., Demarini, D.J., Shah, N.G., Wach, A., Brachat, A., Philippsen, P., Pringle, J.R., 1998. Additional modules for versatile and economical PCR-based gene deletion and modification in Saccharomyces cerevisiae. Yeast 14, 953–961. https://doi.org/10.1002/(SICI)1097-0061(199807)14:10<953::AID-YEA293>3.0.CO;2-U

Lopez-Serra, L., Kelly, G., Patel, H., Stewart, A., Uhlmann, F., 2014. The Scc2–Scc4 complex acts in sister chromatid cohesion and transcriptional regulation by maintaining nucleosome-free regions. Nat Genet 46, 1147–1151. https://doi.org/10.1038/ng.3080

Losada, A., Hirano, M., Hirano, T., 1998. Identification of Xenopus SMC protein complexes required for sister chromatid cohesion. Genes Dev 12, 1986–1997.

Losada, A., Hirano, T., 2001. Intermolecular DNA interactions stimulated by the cohesin complex in vitro: Implications for sister chromatid cohesion. Current Biology 11, 268–272. https://doi.org/10.1016/S0960-9822(01)00066-5

Luo, X., Fang, G., Coldiron, M., Lin, Y., Yu, H., Kirschner, M.W., Wagner, G., 2000. Structure of the Mad2 spindle assembly checkpoint protein and its interaction with Cdc20. Nat Struct Biol 7, 224–229. https://doi.org/10.1038/73338

Luo, X., Tang, Z., Xia, G., Wassmann, K., Matsumoto, T., Rizo, J., Yu, H., 2004. The Mad2 spindle checkpoint protein has two distinct natively folded states. Nat Struct Mol Biol 11, 338–345. https://doi.org/10.1038/nsmb748

Maeshima, K., Matsuda, T., Shindo, Y., Imamura, H., Tamura, S., Imai, R., Kawakami, S., Nagashima, R., Soga, T., Noji, H., Oka, K., Nagai, T., 2018. A Transient Rise in Free Mg2+ Ions Released from ATP-Mg Hydrolysis Contributes to Mitotic Chromosome Condensation. Curr Biol 28, 444-451.e6. https://doi.org/10.1016/j.cub.2017.12.035

Mah, A.S., Jang, J., Deshaies, R.J., 2001. Protein kinase Cdc15 activates the Dbf2-Mob1 kinase complex. Proc Natl Acad Sci U S A 98, 7325–7330. https://doi.org/10.1073/pnas.141098998

Manthei, K.A., Keck, J.L., 2013. The BLM dissolvasome in DNA replication and repair. Cell. Mol. Life Sci. 70, 4067–4084. https://doi.org/10.1007/s00018-013-1325-1

Manzoni, R., Montani, F., Visintin, C., Caudron, F., Ciliberto, A., Visintin, R., 2010. Oscillations in Cdc14 release and sequestration reveal a circuit underlying mitotic exit. J. Cell Biol. 190, 209–222. https://doi.org/10.1083/jcb.201002026

Mariezcurrena, A., Uhlmann, F., 2017. Observation of DNA intertwining along authentic budding yeast chromosomes. Genes Dev. 31, 2151–2161. https://doi.org/10.1101/gad.305557.117

Massari, L.F., 2018. Complete resolution of sister chromatid intertwines requires the Polo-like kinase Cdc5 and the phosphatase Cdc14 in budding yeast. (Doctoral dissertation), University of Milan. https://doi.org/10.13130/massari-lucia-francesca_phd2018-03-26

Matos, J., Blanco, M.G., Maslen, S., Skehel, J.M., West, S.C., 2011. Regulatory control of the resolution of DNA recombination intermediates during meiosis and mitosis. Cell 147, 158–172. https://doi.org/10.1016/j.cell.2011.08.032

Matos, J., Blanco, M.G., West, S.C., 2013. Cell-cycle kinases coordinate the resolution of recombination intermediates with chromosome segregation. Cell Rep 4, 76–86. https://doi.org/10.1016/j.celrep.2013.05.039

Mazón, G., Symington, L.S., 2013. Mph1 and Mus81-Mms4 prevent aberrant processing of mitotic recombination intermediates. Mol. Cell 52, 63–74. https://doi.org/10.1016/j.molcel.2013.09.007

McAleenan, A., Cordon-Preciado, V., Clemente-Blanco, A., Liu, I.-C., Sen, N., Leonard, J., Jarmuz, A., Aragón, L., 2012. SUMOylation of the α-kleisin subunit of cohesin is required for DNA damage-induced cohesion. Curr Biol 22, 1564–1575. https://doi.org/10.1016/j.cub.2012.06.045

McClintock, B., 1941. The Stability of Broken Ends of Chromosomes in Zea Mays. Genetics 26, 234–282.

Megee, P.C., Mistrot, C., Guacci, V., Koshland, D., 1999. The centromeric sister chromatid cohesion site directs Mcd1p binding to adjacent sequences. Mol. Cell 4, 445–450.

Mendoza, M., Norden, C., Durrer, K., Rauter, H., Uhlmann, F., Barral, Y., 2009. A mechanism for chromosome segregation sensing by the NoCut checkpoint. Nat. Cell Biol. 11, 477–483. https://doi.org/10.1038/ncb1855

Menolfi, D., Delamarre, A., Lengronne, A., Pasero, P., Branzei, D., 2015. Essential Roles of the Smc5/6 Complex in Replication through Natural Pausing Sites and Endogenous DNA Damage Tolerance. Mol. Cell 60, 835–846. https://doi.org/10.1016/j.molcel.2015.10.023

Michaelis, C., Ciosk, R., Nasmyth, K., 1997. Cohesins: Chromosomal Proteins that Prevent Premature Separation of Sister Chromatids. Cell 91, 35–45. https://doi.org/10.1016/S0092-8674(01)80007-6

Minocherhomji, S., Ying, S., Bjerregaard, V.A., Bursomanno, S., Aleliunaite, A., Wu, W., Mankouri, H.W., Shen, H., Liu, Y., Hickson, I.D., 2015. Replication stress activates DNA repair synthesis in mitosis. Nature 528, 286–290. https://doi.org/10.1038/nature16139

Mishra, P.K., Ciftci-Yilmaz, S., Reynolds, D., Au, W.-C., Boeckmann, L., Dittman, L.E., Jowhar, Z., Pachpor, T., Yeh, E., Baker, R.E., Hoyt, M.A., D'Amours, D., Bloom, K., Basrai, M.A., 2016. Polo kinase Cdc5 associates with centromeres to facilitate the removal of centromeric cohesin during mitosis. Mol Biol Cell 27, 2286–2300. https://doi.org/10.1091/mbc.E16-01-0004

Mohl, D.A., Huddleston, M.J., Collingwood, T.S., Annan, R.S., Deshaies, R.J., 2009. Dbf2-Mob1 drives relocalization of protein phosphatase Cdc14 to the cytoplasm during exit from mitosis. J Cell Biol 184, 527–539. https://doi.org/10.1083/jcb.200812022

Montpetit, B., Hazbun, T.R., Fields, S., Hieter, P., 2006. Sumoylation of the budding yeast

kinetochore protein Ndc10 is required for Ndc10 spindle localization and regulation of anaphase spindle elongation. J. Cell Biol. 174, 653–663. https://doi.org/10.1083/jcb.200605019

Mora-Bermúdez, F., Gerlich, D., Ellenberg, J., 2007. Maximal chromosome compaction occurs by axial shortening in anaphase and depends on Aurora kinase. Nat. Cell Biol. 9, 822–831. https://doi.org/10.1038/ncb1606

Morales, C., Losada, A., 2018. Establishing and dissolving cohesion during the vertebrate cell cycle. Current Opinion in Cell Biology, Cell Nucleus 52, 51–57. https://doi.org/10.1016/j.ceb.2018.01.010

Morawska, M., Ulrich, H.D., 2013. An expanded tool kit for the auxin-inducible degron system in budding yeast. Yeast 30, 341–351. https://doi.org/10.1002/yea.2967

Moudry, P., Watanabe, K., Wolanin, K.M., Bartkova, J., Wassing, I.E., Watanabe, S., Strauss, R., Troelsgaard Pedersen, R., Oestergaard, V.H., Lisby, M., Andújar-Sánchez, M., Maya-Mendoza, A., Esashi, F., Lukas, J., Bartek, J., 2016. TOPBP1 regulates RAD51 phosphorylation and chromatin loading and determines PARP inhibitor sensitivity. J Cell Biol 212, 281–288. https://doi.org/10.1083/jcb.201507042

Mukhopadhyay, D., Dasso, M., 2017. The SUMO Pathway in Mitosis. Adv. Exp. Med. Biol. 963, 171–184. https://doi.org/10.1007/978-3-319-50044-7_10

Mullen, J.R., Kaliraman, V., Ibrahim, S.S., Brill, S.J., 2001. Requirement for three novel protein complexes in the absence of the Sgs1 DNA helicase in Saccharomyces cerevisiae. Genetics 157, 103–118.

Mundbjerg, K., Jørgensen, S.W., Fredsøe, J., Nielsen, I., Pedersen, J.M., Bentsen, I.B., Lisby, M., Bjergbaek, L., Andersen, A.H., 2015. Top2 and Sgs1-Top3 Act Redundantly to Ensure rDNA Replication Termination. PLoS Genet 11. https://doi.org/10.1371/journal.pgen.1005697

Murayama, Y., Uhlmann, F., 2015. DNA Entry into and Exit out of the Cohesin Ring by an Interlocking Gate Mechanism. Cell 163, 1628–1640. https://doi.org/10.1016/j.cell.2015.11.030

Murayama, Y., Uhlmann, F., 2014. Biochemical reconstitution of topological DNA binding by the cohesin ring. Nature 505, 367–371. https://doi.org/10.1038/nature12867

Musacchio, A., 2015. The Molecular Biology of Spindle Assembly Checkpoint Signaling Dynamics. Current Biology 25, R1002–R1018. https://doi.org/10.1016/j.cub.2015.08.051

Naim, V., Rosselli, F., 2009. The FANC pathway and BLM collaborate during mitosis to prevent micro-nucleation and chromosome abnormalities. Nat. Cell Biol. 11, 761–768. https://doi.org/10.1038/ncb1883

Navadgi-Patil, V.M., Burgers, P.M., 2008. Yeast DNA replication protein Dpb11 activates the Mec1/ATR checkpoint kinase. J. Biol. Chem. 283, 35853–35859. https://doi.org/10.1074/jbc.M807435200

Negrini, S., Gorgoulis, V.G., Halazonetis, T.D., 2010. Genomic instability — an evolving hallmark of cancer. Nat Rev Mol Cell Biol 11, 220–228. https://doi.org/10.1038/nrm2858

Neurohr, G., Naegeli, A., Titos, I., Theler, D., Greber, B., Díez, J., Gabaldón, T., Mendoza, M., Barral, Y., 2011. A Midzone-Based Ruler Adjusts Chromosome Compaction to Anaphase Spindle Length. Science 332, 465–468. https://doi.org/10.1126/science.1201578

Nezi, L., Rancati, G., De Antoni, A., Pasqualato, S., Piatti, S., Musacchio, A., 2006.

Accumulation of Mad2–Cdc20 complex during spindle checkpoint activation requires binding of open and closed conformers of Mad2 in Saccharomyces cerevisiae. Journal of Cell Biology 174, 39–51. https://doi.org/10.1083/jcb.200602109

Ng, T.M., Waples, W.G., Lavoie, B.D., Biggins, S., 2009. Pericentromeric sister chromatid cohesion promotes kinetochore biorientation. Mol. Biol. Cell 20, 3818–3827. https://doi.org/10.1091/mbc.e09-04-0330

Nishimura, K., Fukagawa, T., Takisawa, H., Kakimoto, T., Kanemaki, M., 2009. An auxin-based degron system for the rapid depletion of proteins in nonplant cells. Nature Methods 6, 917–922. https://doi.org/10.1038/nmeth.1401

Norden, C., Mendoza, M., Dobbelaere, J., Kotwaliwale, C.V., Biggins, S., Barral, Y., 2006. The NoCut pathway links completion of cytokinesis to spindle midzone function to prevent chromosome breakage. Cell 125, 85–98. https://doi.org/10.1016/j.cell.2006.01.045

Ocampo-Hafalla, M., Muñoz, S., Samora, C.P., Uhlmann, F., 2016. Evidence for cohesin sliding along budding yeast chromosomes. Open Biol 6, 150178. https://doi.org/10.1098/rsob.150178

Ohkuni, K., Takahashi, Y., Fulp, A., Lawrimore, J., Au, W.-C., Pasupala, N., Levy-Myers, R., Warren, J., Strunnikov, A., Baker, R.E., Kerscher, O., Bloom, K., Basrai, M.A., 2016. SUMO-targeted ubiquitin ligase (STUbL) Slx5 regulates proteolysis of centromeric histone H3 variant Cse4 and prevents its mislocalization to euchromatin. MBoC 27, 1500–1510. https://doi.org/10.1091/mbc.E15-12-0827

Oliveira, R.A., Kotadia, S., Tavares, A., Mirkovic, M., Bowlin, K., Eichinger, C.S., Nasmyth, K., Sullivan, W., 2014. Centromere-Independent Accumulation of Cohesin at Ectopic Heterochromatin Sites Induces Chromosome Stretching during Anaphase. PLOS Biology 12, e1001962. https://doi.org/10.1371/journal.pbio.1001962

Ölmezer, G., Levikova, M., Klein, D., Falquet, B., Fontana, G.A., Cejka, P., Rass, U., 2016. Replication intermediates that escape Dna2 activity are processed by Holliday junction resolvase Yen1. Nature Communications 7, 13157. https://doi.org/10.1038/ncomms13157

Paldi, F., Alver, B., Robertson, D., Schalbetter, S.A., Kerr, A., Kelly, D.A., Baxter, J., Neale, M.J., Marston, A.L., 2020. Convergent genes shape budding yeast pericentromeres. Nature 582, 119–123. https://doi.org/10.1038/s41586-020-2244-6

Palozola, K.C., Donahue, G., Liu, H., Grant, G.R., Becker, J.S., Cote, A., Yu, H., Raj, A., Zaret, K.S., 2017. Mitotic transcription and waves of gene reactivation during mitotic exit. Science 358, 119–122. https://doi.org/10.1126/science.aal4671

Park, C.J., Park, J.-E., Karpova, T.S., Soung, N.-K., Yu, L.-R., Song, S., Lee, K.H., Xia, X., Kang, E., Dabanoglu, I., Oh, D.-Y., Zhang, J.Y., Kang, Y.H., Wincovitch, S., Huffaker, T.C., Veenstra, T.D., McNally, J.G., Lee, K.S., 2008. Requirement for the budding yeast polo kinase Cdc5 in proper microtubule growth and dynamics. Eukaryot Cell 7, 444–453. https://doi.org/10.1128/EC.00283-07

Pedersen, R.T., Kruse, T., Nilsson, J., Oestergaard, V.H., Lisby, M., 2015. TopBP1 is required at mitosis to reduce transmission of DNA damage to G1 daughter cells. J. Cell Biol. 210, 565–582. https://doi.org/10.1083/jcb.201502107

Peeper, D.S., Parker, L.L., Ewen, M.E., Toebes, M., Hall, F.L., Xu, M., Zantema, A., van der Eb, A.J., Piwnica-Worms, H., 1993. A- and B-type cyclins differentially modulate substrate specificity of cyclin-cdk complexes. EMBO J 12, 1947–1954.

Peplowska, K., Wallek, A.U., Storchova, Z., 2014. Sgo1 Regulates Both Condensin and

Ipl1/Aurora B to Promote Chromosome Biorientation. PLOS Genetics 10, e1004411. https://doi.org/10.1371/journal.pgen.1004411

Pereira, G., Manson, C., Grindlay, J., Schiebel, E., 2002. Regulation of the Bfa1p-Bub2p complex at spindle pole bodies by the cell cycle phosphatase Cdc14p. J Cell Biol 157, 367–379. https://doi.org/10.1083/jcb.200112085

Peters, J.-M., 2006. The anaphase promoting complex/cyclosome: a machine designed to destroy. Nat. Rev. Mol. Cell Biol. 7, 644–656. https://doi.org/10.1038/nrm1988

Petsalaki, E., Zachos, G., 2019. Building bridges between chromosomes: novel insights into the abscission checkpoint. Cell. Mol. Life Sci. 76, 4291–4307. https://doi.org/10.1007/s00018-019-03224-z

Piatti, S., Venturetti, M., Chiroli, E., Fraschini, R., 2006. The spindle position checkpoint in budding yeast: the motherly care of MEN. Cell Division 1, 2. https://doi.org/10.1186/1747-1028-1-2

Pines, J., 2011. Cubism and the cell cycle: the many faces of the APC/C. Nat Rev Mol Cell Biol 12, 427–438. https://doi.org/10.1038/nrm3132

Piskadlo, E., Tavares, A., Oliveira, R.A., 2017. Metaphase chromosome structure is dynamically maintained by condensin I-directed DNA (de)catenation. Elife 6. https://doi.org/10.7554/eLife.26120

Pommier, Y., Sun, Y., Huang, S.N., Nitiss, J.L., 2016. Roles of eukaryotic topoisomerases in transcription, replication and genomic stability. Nature Reviews Molecular Cell Biology 17, 703–721. https://doi.org/10.1038/nrm.2016.111

Potapova, T.A., Unruh, J.R., Yu, Z., Rancati, G., Li, H., Stampfer, M.R., Gerton, J.L., 2019. Superresolution microscopy reveals linkages between ribosomal DNA on heterologous chromosomes. J. Cell Biol. 218, 2492–2513. https://doi.org/10.1083/jcb.201810166

Prado, F., 2018. Homologous Recombination: To Fork and Beyond. Genes (Basel) 9. https://doi.org/10.3390/genes9120603

Primorac, I., Weir, J.R., Chiroli, E., Gross, F., Hoffmann, I., van Gerwen, S., Ciliberto, A., Musacchio, A., 2013. Bub3 reads phosphorylated MELT repeats to promote spindle assembly checkpoint signaling. Elife 2, e01030. https://doi.org/10.7554/eLife.01030

Psakhye, I., Branzei, D., 2021. SMC complexes are guarded by the SUMO protease Ulp2 against SUMO-chain-mediated turnover. Cell Rep 36, 109485. https://doi.org/10.1016/j.celrep.2021.109485

Psakhye, I., Castellucci, F., Branzei, D., 2019. SUMO-Chain-Regulated Proteasomal Degradation Timing Exemplified in DNA Replication Initiation. Molecular Cell 76, 632-645.e6. https://doi.org/10.1016/j.molcel.2019.08.003

Puddu, F., Granata, M., Di Nola, L., Balestrini, A., Piergiovanni, G., Lazzaro, F., Giannattasio, M., Plevani, P., Muzi-Falconi, M., 2008. Phosphorylation of the budding yeast 9-1-1 complex is required for Dpb11 function in the full activation of the UV-induced DNA damage checkpoint. Mol. Cell. Biol. 28, 4782–4793. https://doi.org/10.1128/MCB.00330-08

Queralt, E., Lehane, C., Novak, B., Uhlmann, F., 2006. Downregulation of PP2A(Cdc55) phosphatase by separase initiates mitotic exit in budding yeast. Cell 125, 719–732. https://doi.org/10.1016/j.cell.2006.03.038

Rattner, J.B., Hendzel, M.J., Furbee, C.S., Muller, M.T., Bazett-Jones, D.P., 1996. Topoisomerase II alpha is associated with the mammalian centromere in a cell cycle- and

species-specific manner and is required for proper centromere/kinetochore structure. J. Cell Biol. 134, 1097–1107. https://doi.org/10.1083/jcb.134.5.1097

Renshaw, M.J., Ward, J.J., Kanemaki, M., Natsume, K., Nédélec, F.J., Tanaka, T.U., 2010. Condensins Promote Chromosome Recoiling during Early Anaphase to Complete Sister Chromatid Separation. Developmental Cell 19, 232–244. https://doi.org/10.1016/j.devcel.2010.07.013

Ribeiro, S.A., Gatlin, J.C., Dong, Y., Joglekar, A., Cameron, L., Hudson, D.F., Farr, C.J., McEwen, B.F., Salmon, E.D., Earnshaw, W.C., Vagnarelli, P., 2009. Condensin Regulates the Stiffness of Vertebrate Centromeres. MBoC 20, 2371–2380. https://doi.org/10.1091/mbc.e08-11-1127

Ribet, D., Boscaini, S., Cauvin, C., Siguier, M., Mostowy, S., Echard, A., Cossart, P., 2017. SUMOylation of human septins is critical for septin filament bundling and cytokinesis. J Cell Biol 216, 4041–4052. https://doi.org/10.1083/jcb.201703096

Riou, G., Delain, E., 1969. Electron microscopy of the circular kinetoplastic DNA from Trypanosoma cruzi: occurrence of catenated forms. Proc. Natl. Acad. Sci. U.S.A. 62, 210–217. https://doi.org/10.1073/pnas.62.1.210

Robellet, X., Thattikota, Y., Wang, F., Wee, T.-L., Pascariu, M., Shankar, S., Bonneil, É., Brown, C.M., D'Amours, D., 2015. A high-sensitivity phospho-switch triggered by Cdk1 governs chromosome morphogenesis during cell division. Genes Dev. 29, 426–439. https://doi.org/10.1101/gad.253294.114

Roccuzzo, M., 2013. Regulation of chromosome segregation by conserved phosphatase Cdc14 and kinase Cdc5. (Doctoral dissertation), University of Milan.

Roccuzzo, M., Visintin, C., Tili, F., Visintin, R., 2015. FEAR-mediated activation of Cdc14 is the limiting step for spindle elongation and anaphase progression. Nat. Cell Biol. 17, 251–261. https://doi.org/10.1038/ncb3105

Rolef Ben-Shahar, T., Heeger, S., Lehane, C., East, P., Flynn, H., Skehel, M., Uhlmann, F., 2008. Eco1-dependent cohesin acetylation during establishment of sister chromatid cohesion. Science 321, 563–566. https://doi.org/10.1126/science.1157774

Ross, K.E., Cohen-Fix, O., 2004. A role for the FEAR pathway in nuclear positioning during anaphase. Dev Cell 6, 729–735. https://doi.org/10.1016/s1534-5807(04)00128-5

Rozelle, D.K., Hansen, S.D., Kaplan, K.B., 2011. Chromosome passenger complexes control anaphase duration and spindle elongation via a kinesin-5 brake. J. Cell Biol. 193, 285–294. https://doi.org/10.1083/jcb.201011002

Russell, B., Bhattacharyya, S., Keirsey, J., Sandy, A., Grierson, P., Perchiniak, E., Kavecansky, J., Acharya, S., Groden, J., 2011. Chromosome breakage is regulated by the interaction of the BLM helicase and topoisomerase IIalpha. Cancer Res. 71, 561–571. https://doi.org/10.1158/0008-5472.CAN-10-1727

Rybenkov, V.V., Vologodskii, A.V., Cozzarelli, N.R., 1997. The effect of ionic conditions on the conformations of supercoiled DNA. II. Equilibrium catenation. J. Mol. Biol. 267, 312–323. https://doi.org/10.1006/jmbi.1996.0877

Ryu, H., Yoshida, M.M., Sridharan, V., Kumagai, A., Dunphy, W.G., Dasso, M., Azuma, Y., 2015. SUMOylation of the C-terminal domain of DNA topoisomerase IIα regulates the centromeric localization of Claspin. Cell Cycle 14, 2777–2784. https://doi.org/10.1080/15384101.2015.1066537

Ryu, H.-Y., Wilson, N.R., Mehta, S., Hwang, S.S., Hochstrasser, M., 2016. Loss of the SUMO protease Ulp2 triggers a specific multichromosome aneuploidy. Genes Dev. 30, 1881–1894. https://doi.org/10.1101/gad.282194.116

Saka, Y., Sutani, T., Yamashita, Y., Saitoh, S., Takeuchi, M., Nakaseko, Y., Yanagida, M., 1994. Fission yeast cut3 and cut14, members of a ubiquitous protein family, are required for chromosome condensation and segregation in mitosis. EMBO J. 13, 4938–4952.

Sakchaisri, K., Asano, S., Yu, L.-R., Shulewitz, M.J., Park, C.J., Park, J.-E., Cho, Y.-W., Veenstra, T.D., Thorner, J., Lee, K.S., 2004. Coupling morphogenesis to mitotic entry. Proc Natl Acad Sci U S A 101, 4124–4129. https://doi.org/10.1073/pnas.0400641101

Sanchez, Y., Bachant, J., Wang, H., Hu, F., Liu, D., Tetzlaff, M., Elledge, S.J., 1999. Control of the DNA damage checkpoint by chk1 and rad53 protein kinases through distinct mechanisms. Science 286, 1166–1171. https://doi.org/10.1126/science.286.5442.1166

Sanchez, Y., Desany, B.A., Jones, W.J., Liu, Q., Wang, B., Elledge, S.J., 1996. Regulation of RAD53 by the ATM-like kinases MEC1 and TEL1 in yeast cell cycle checkpoint pathways. Science 271, 357–360. https://doi.org/10.1126/science.271.5247.357

Sansregret, L., Swanton, C., 2017. The Role of Aneuploidy in Cancer Evolution. Cold Spring Harb Perspect Med 7, a028373. https://doi.org/10.1101/cshperspect.a028373

Santaguida, S., Amon, A., 2015. Short- and long-term effects of chromosome mis-segregation and aneuploidy. Nat Rev Mol Cell Biol 16, 473–485. https://doi.org/10.1038/nrm4025

Sarangapani, K.K., Asbury, C.L., 2014. Catch and release: how do kinetochores hook the right microtubules during mitosis? Trends in Genetics 30, 150–159. https://doi.org/10.1016/j.tig.2014.02.004

Sarbajna, S., Davies, D., West, S.C., 2014. Roles of SLX1-SLX4, MUS81-EME1, and GEN1 in avoiding genome instability and mitotic catastrophe. Genes Dev. 28, 1124–1136. https://doi.org/10.1101/gad.238303.114

Sarlós, K., Biebricher, A.S., Bizard, A.H., Bakx, J.A.M., Ferreté-Bonastre, A.G., Modesti, M., Paramasivam, M., Yao, Q., Peterman, E.J.G., Wuite, G.J.L., Hickson, I.D., 2018. Reconstitution of anaphase DNA bridge recognition and disjunction. Nature Structural & Molecular Biology 25, 868–876. https://doi.org/10.1038/s41594-018-0123-8

Schalbetter, S.A., Goloborodko, A., Fudenberg, G., Belton, J.-M., Miles, C., Yu, M., Dekker, J., Mirny, L., Baxter, J., 2017. SMC complexes differentially compact mitotic chromosomes according to genomic context. Nat. Cell Biol. 19, 1071–1080. https://doi.org/10.1038/ncb3594

Schalbetter, S.A., Mansoubi, S., Chambers, A.L., Downs, J.A., Baxter, J., 2015. Fork rotation and DNA precatenation are restricted during DNA replication to prevent chromosomal instability. Proc. Natl. Acad. Sci. U.S.A. 112, E4565-4570. https://doi.org/10.1073/pnas.1505356112

Schimmang, T., Tollervey, D., Kern, H., Frank, R., Hurt, E.C., 1989. A yeast nucleolar protein related to mammalian fibrillarin is associated with small nucleolar RNA and is essential for viability. EMBO J 8, 4015–4024.

Schwartz, E.K., Wright, W.D., Ehmsen, K.T., Evans, J.E., Stahlberg, H., Heyer, W.-D., 2012. Mus81-Mms4 functions as a single heterodimer to cleave nicked intermediates in recombinational DNA repair. Mol Cell Biol 32, 3065–3080. https://doi.org/10.1128/MCB.00547-12

Schweiggert, J., Stevermann, L., Panigada, D., Kammerer, D., Liakopoulos, D., 2016. Regulation of a Spindle Positioning Factor at Kinetochores by SUMO-Targeted Ubiquitin Ligases. Developmental Cell 36, 415–427. https://doi.org/10.1016/j.devcel.2016.01.011

Sczaniecka, M., Feoktistova, A., May, K.M., Chen, J.-S., Blyth, J., Gould, K.L., Hardwick, K.G., 2008. The spindle checkpoint functions of Mad3 and Mad2 depend on a Mad3 KEN box-mediated interaction with Cdc20-anaphase-promoting complex (APC/C). J Biol Chem 283, 23039–23047. https://doi.org/10.1074/jbc.M803594200

Sen, N., Leonard, J., Torres, R., Garcia-Luis, J., Palou-Marin, G., Aragón, L., 2016. Physical Proximity of Sister Chromatids Promotes Top2-Dependent Intertwining. Molecular Cell 64, 134–147. https://doi.org/10.1016/j.molcel.2016.09.007

Seufert, W., Futcher, B., Jentsch, S., 1995. Role of a ubiquitin-conjugating enzyme in degradation of S- and M-phase cyclins. Nature 373, 78–81. https://doi.org/10.1038/373078a0

Seufert, Wolfgang, Futcher, B., Jentsch, S., 1995. Role of a ubiquitin-conjugating enzyme in degradation of S- and M-phase cyclins. Nature 373, 78. https://doi.org/10.1038/373078a0

Shepperd, L.A., Meadows, J.C., Sochaj, A.M., Lancaster, T.C., Zou, J., Buttrick, G.J., Rappsilber, J., Hardwick, K.G., Millar, J.B.A., 2012. Phosphodependent recruitment of Bub1 and Bub3 to Spc7/KNL1 by Mph1 kinase maintains the spindle checkpoint. Curr Biol 22, 891–899. https://doi.org/10.1016/j.cub.2012.03.051

Shintomi, K., Inoue, F., Watanabe, H., Ohsumi, K., Ohsugi, M., Hirano, T., 2017. Mitotic chromosome assembly despite nucleosome depletion in Xenopus egg extracts. Science 356, 1284–1287. https://doi.org/10.1126/science.aam9702

Shintomi, K., Takahashi, T.S., Hirano, T., 2015. Reconstitution of mitotic chromatids with a minimum set of purified factors. Nature Cell Biology 17, 1014–1023. https://doi.org/10.1038/ncb3187

Shirayama, M., Zachariae, W., Ciosk, R., Nasmyth, K., 1998. The Polo-like kinase Cdc5p and the WD-repeat protein Cdc20p/fizzy are regulators and substrates of the anaphase promoting complex in Saccharomyces cerevisiae. EMBO J 17, 1336–1349. https://doi.org/10.1093/emboj/17.5.1336

Shogren-Knaak, M., Ishii, H., Sun, J.-M., Pazin, M.J., Davie, J.R., Peterson, C.L., 2006. Histone H4-K16 acetylation controls chromatin structure and protein interactions. Science 311, 844–847. https://doi.org/10.1126/science.1124000

Shou, W., Azzam, R., Chen, S.L., Huddleston, M.J., Baskerville, C., Charbonneau, H., Annan, R.S., Carr, S.A., Deshaies, R.J., 2002. Cdc5 influences phosphorylation of Net1 and disassembly of the RENT complex. BMC Mol Biol 3, 3. https://doi.org/10.1186/1471-2199-3-3

Shou, W., Seol, J.H., Shevchenko, A., Baskerville, C., Moazed, D., Chen, Z.W., Jang, J., Shevchenko, A., Charbonneau, H., Deshaies, R.J., 1999. Exit from mitosis is triggered by Tem1-dependent release of the protein phosphatase Cdc14 from nucleolar RENT complex. Cell 97, 233–244. https://doi.org/10.1016/s0092-8674(00)80733-3

Shyian, M., Albert, B., Zupan, A.M., Ivanitsa, V., Charbonnet, G., Dilg, D., Shore, D., 2019. Fork pausing complex engages topoisomerases at the replisome. Genes Dev. https://doi.org/10.1101/gad.331868.119

Sivakumar, S., Gorbsky, G.J., 2015. Spatiotemporal regulation of the anaphase-promoting complex in mitosis. Nat Rev Mol Cell Biol 16, 82–94. https://doi.org/10.1038/nrm3934

Skibbens, R.V., 2019. Condensins and cohesins – one of these things is not like the other! J Cell Sci 132, jcs220491. https://doi.org/10.1242/jcs.220491

Snead, J.L., Sullivan, M., Lowery, D.M., Cohen, M.S., Zhang, C., Randle, D.H., Taunton, J., Yaffe, M.B., Morgan, D.O., Shokat, K.M., 2007. A coupled chemical-genetic and bioinformatic approach to Polo-like kinase pathway exploration. Chem Biol 14, 1261–1272. https://doi.org/10.1016/j.chembiol.2007.09.011

Song, S., Grenfell, T.Z., Garfield, S., Erikson, R.L., Lee, K.S., 2000. Essential function of the polo box of Cdc5 in subcellular localization and induction of cytokinetic structures. Mol Cell Biol 20, 286–298. https://doi.org/10.1128/MCB.20.1.286-298.2000

Song, S., Lee, K.S., 2001. A novel function of Saccharomyces cerevisiae CDC5 in cytokinesis. J Cell Biol 152, 451–469. https://doi.org/10.1083/jcb.152.3.451

Spell, R.M., Holm, C., 1994. Nature and distribution of chromosomal intertwinings in Saccharomyces cerevisiae. Mol. Cell. Biol. 14, 1465–1476. https://doi.org/10.1128/mcb.14.2.1465

Stead, K., Aguilar, C., Hartman, T., Drexel, M., Meluh, P., Guacci, V., 2003. Pds5p regulates the maintenance of sister chromatid cohesion and is sumoylated to promote the dissolution of cohesion. J. Cell Biol. 163, 729–741. https://doi.org/10.1083/jcb.200305080

Stegmeier, F., Amon, A., 2004. Closing mitosis: the functions of the Cdc14 phosphatase and its regulation. Annu. Rev. Genet. 38, 203–232. https://doi.org/10.1146/annurev.genet.38.072902.093051

Stegmeier, F., Visintin, R., Amon, A., 2002. Separase, polo kinase, the kinetochore protein Slk19, and Spo12 function in a network that controls Cdc14 localization during early anaphase. Cell 108, 207–220.

Stephens, A.D., Haase, J., Vicci, L., Taylor, R.M., Bloom, K., 2011. Cohesin, condensin, and the intramolecular centromere loop together generate the mitotic chromatin spring. J. Cell Biol. 193, 1167–1180. https://doi.org/10.1083/jcb.201103138

Stephens, A.D., Snider, C.E., Bloom, K., 2015. The SUMO deconjugating peptidase Smt4 contributes to the mechanism required for transition from sister chromatid arm cohesion to sister chromatid pericentromere separation. Cell Cycle 14, 2206–2218. https://doi.org/10.1080/15384101.2015.1046656

St-Pierre, J., Douziech, M., Bazile, F., Pascariu, M., Bonneil, É., Sauvé, V., Ratsima, H., D'Amours, D., 2009. Polo Kinase Regulates Mitotic Chromosome Condensation by Hyperactivation of Condensin DNA Supercoiling Activity. Molecular Cell 34, 416–426. https://doi.org/10.1016/j.molcel.2009.04.013

Strick, T.R., Kawaguchi, T., Hirano, T., 2004. Real-Time Detection of Single-Molecule DNA Compaction by Condensin I. Current Biology 14, 874–880. https://doi.org/10.1016/j.cub.2004.04.038

Ström, L., Lindroos, H.B., Shirahige, K., Sjögren, C., 2004. Postreplicative recruitment of cohesin to double-strand breaks is required for DNA repair. Mol Cell 16, 1003–1015. https://doi.org/10.1016/j.molcel.2004.11.026

Strunnikov, A.V., Hogan, E., Koshland, D., 1995. SMC2, a Saccharomyces cerevisiae gene essential for chromosome segregation and condensation, defines a subgroup within the SMC family. Genes Dev. 9, 587–599.

Stuchinskaya, T., Mitchenall, L.A., Schoeffler, A.J., Corbett, K.D., Berger, J.M., Bates, A.D.,

Maxwell, A., 2009. How do type II topoisomerases use ATP hydrolysis to simplify DNA topology beyond equilibrium? Investigating the relaxation reaction of nonsupercoiling type II topoisomerases. J. Mol. Biol. 385, 1397–1408. https://doi.org/10.1016/j.jmb.2008.11.056

Su, X.B., Wang, M., Schaffner, C., Nerusheva, O.O., Clift, D., Spanos, C., Kelly, D.A., Tatham, M., Wallek, A., Wu, Y., Rappsilber, J., Jeyaprakash, A.A., Storchova, Z., Hay, R.T., Marston, A.L., 2021. SUMOylation stabilizes sister kinetochore biorientation to allow timely anaphase. Journal of Cell Biology 220. https://doi.org/10.1083/jcb.202005130

Sudakin, V., Ganoth, D., Dahan, A., Heller, H., Hershko, J., Luca, F.C., Ruderman, J.V., Hershko, A., 1995. The cyclosome, a large complex containing cyclin-selective ubiquitin ligase activity, targets cyclins for destruction at the end of mitosis. Mol Biol Cell 6, 185–197. https://doi.org/10.1091/mbc.6.2.185

Sullivan, M., Higuchi, T., Katis, V.L., Uhlmann, F., 2004. Cdc14 Phosphatase Induces rDNA Condensation and Resolves Cohesin-Independent Cohesion during Budding Yeast Anaphase. Cell 117, 471–482. https://doi.org/10.1016/S0092-8674(04)00415-5

Sullivan, M., Morgan, D.O., 2007. Finishing mitosis, one step at a time. Nat Rev Mol Cell Biol 8, 894–903. https://doi.org/10.1038/nrm2276

Sumner, A.T., 1996. The distribution of topoisomerase II on mammalian chromosomes. Chromosome Res 4, 5–14. https://doi.org/10.1007/BF02254938

Sun, Z., Fay, D.S., Marini, F., Foiani, M., Stern, D.F., 1996. Spk1/Rad53 is regulated by Mec1-dependent protein phosphorylation in DNA replication and damage checkpoint pathways. Genes Dev 10, 395–406. https://doi.org/10.1101/gad.10.4.395

Sundin, O., Varshavsky, A., 1981. Arrest of segregation leads to accumulation of highly intertwined catenated dimers: dissection of the final stages of SV40 DNA replication. Cell 25, 659–669. https://doi.org/10.1016/0092-8674(81)90173-2

Sundin, O., Varshavsky, A., 1980. Terminal stages of SV40 DNA replication proceed via multiply intertwined catenated dimers. Cell 21, 103–114. https://doi.org/10.1016/0092-8674(80)90118-x

Sunkel, C.E., Glover, D.M., 1988. polo, a mitotic mutant of Drosophila displaying abnormal spindle poles. J Cell Sci 89 (Pt 1), 25–38.

Szakal, B., Branzei, D., 2013. Premature Cdk1/Cdc5/Mus81 pathway activation induces aberrant replication and deleterious crossover. EMBO J. 32, 1155–1167. https://doi.org/10.1038/emboj.2013.67

Takahashi, Y., Iwase, M., Konishi, M., Tanaka, M., Toh-e, A., Kikuchi, Y., 1999. Smt3, a SUMO-1 Homolog, Is Conjugated to Cdc3, a Component of Septin Rings at the Mother-Bud Neck in Budding Yeast. Biochemical and Biophysical Research Communications 259, 582–587. https://doi.org/10.1006/bbrc.1999.0821

Takahashi, Y., Kahyo, T., Toh-E, A., Yasuda, H., Kikuchi, Y., 2001. Yeast Ull1/Siz1 is a novel SUMO1/Smt3 ligase for septin components and functions as an adaptor between conjugating enzyme and substrates. J Biol Chem 276, 48973–48977. https://doi.org/10.1074/jbc.M109295200

Takahashi, Y., Mizoi, J., Toh-E, A., Kikuchi, Y., 2000. Yeast Ulp1, an Smt3-specific protease, associates with nucleoporins. J Biochem 128, 723–725. https://doi.org/10.1093/oxfordjournals.jbchem.a022807

Takahashi, Y., Strunnikov, A., 2008. In vivo modeling of polysumoylation uncovers targeting of Topoisomerase II to the nucleolus via optimal level of SUMO modification. Chromosoma 117, 189–198. https://doi.org/10.1007/s00412-007-0137-1

Takahashi, Y., Yong-Gonzalez, V., Kikuchi, Y., Strunnikov, A., 2006. SIZ1/SIZ2 control of chromosome transmission fidelity is mediated by the sumoylation of topoisomerase II. Genetics 172, 783–794. https://doi.org/10.1534/genetics.105.047167

Tanaka, S., Umemori, T., Hirai, K., Muramatsu, S., Kamimura, Y., Araki, H., 2007. CDK-dependent phosphorylation of Sld2 and Sld3 initiates DNA replication in budding yeast. Nature 445, 328–332. https://doi.org/10.1038/nature05465

Tanaka, T.U., Cosma, M.P., Wirth, K., Nasmyth, K., 1999. Identification of Cohesin Association Sites at Centromeres and along Chromosome Arms. Cell 98, 847–858. https://doi.org/10.1016/S0092-8674(00)81518-4

Tanaka, T.U., Fuchs, J., Loidl, J., Nasmyth, K., 2000. Cohesin ensures bipolar attachment of microtubules to sister centromeres and resists their precocious separation. Nat Cell Biol 2, 492–499. https://doi.org/10.1038/35019529

Tanaka, T.U., Rachidi, N., Janke, C., Pereira, G., Galova, M., Schiebel, E., Stark, M.J.R., Nasmyth, K., 2002. Evidence that the Ipl1-Sli15 (Aurora kinase-INCENP) complex promotes chromosome bi-orientation by altering kinetochore-spindle pole connections. Cell 108, 317–329.

Tang, Z., Bharadwaj, R., Li, B., Yu, H., 2001. Mad2-Independent Inhibition of APCCdc20 by the Mitotic Checkpoint Protein BubR1. Developmental Cell 1, 227–237. https://doi.org/10.1016/S1534-5807(01)00019-3

Taxis, C., Stier, G., Spadaccini, R., Knop, M., 2009. Efficient protein depletion by genetically controlled deprotection of a dormant N-degron. Molecular Systems Biology 5, 267. https://doi.org/10.1038/msb.2009.25

Taylor, A.M., Shih, J., Ha, G., Gao, G.F., Zhang, X., Berger, A.C., Schumacher, S.E., Wang, C., Hu, H., Liu, Jianfang, Lazar, A.J., Caesar-Johnson, S.J., Demchok, J.A., Felau, I., Kasapi, M., Ferguson, M.L., Hutter, C.M., Sofia, H.J., Tarnuzzer, R., Wang, Z., Yang, L., Zenklusen, J.C., Zhang, J. (Julia), Chudamani, S., Liu, Jia, Lolla, L., Naresh, R., Pihl, T., Sun, Q., Wan, Y., Wu, Y., Cho, J., DeFreitas, T., Frazer, S., Gehlenborg, N., Getz, G., Heiman, D.I., Kim, J., Lawrence, M.S., Lin, P., Meier, S., Noble, M.S., Saksena, G., Voet, D., Zhang, Hailei, Bernard, B., Chambwe, N., Dhankani, V., Knijnenburg, T., Kramer, R., Leinonen, K., Liu, Y., Miller, M., Reynolds, S., Shmulevich, I., Thorsson, V., Zhang, W., Akbani, R., Broom, B.M., Hegde, A.M., Ju, Z., Kanchi, R.S., Korkut, A., Li, J., Liang, H., Ling, S., Liu, W., Lu, Y., Mills, G.B., Ng, K.-S., Rao, A., Ryan, M., Wang, Jing, Weinstein, J.N., Zhang, J., Abeshouse, A., Armenia, J., Chakravarty, D., Chatila, W.K., Bruijn, I. de, Gao, J., Gross, B.E., Heins, Z.J., Kundra, R., La, K., Ladanyi, M., Luna, A., Nissan, M.G., Ochoa, A., Phillips, S.M., Reznik, E., Sanchez-Vega, F., Sander, C., Schultz, N., Sheridan, R., Sumer, S.O., Sun, Y., Taylor, B.S., Wang, Jioajiao, Zhang, Hongxin, Anur, P., Peto, M., Spellman, P., Benz, C., Stuart, J.M., Wong, C.K., Yau, C., Hayes, D.N., Parker, J.S., Wilkerson, M.D., Ally, A., Balasundaram, M., Bowlby, R., Brooks, D., Carlsen, R., Chuah, E., Dhalla, N., Holt, R., Jones, S.J.M., Kasaian, K., Lee, D., Ma, Y., Marra, M.A., Mayo, M., Moore, R.A., Mungall, A.J., Mungall, K., Robertson, A.G., Sadeghi, S., Schein, J.E., Sipahimalani, P., Tam, A., Thiessen, N., Tse, K., Wong, T., Berger, A.C., Beroukhim, R., Cherniack, A.D., Cibulskis, C., Gabriel, S.B., Gao, G.F., Ha, G., Meyerson, M., Schumacher, S.E., Shih, J., Kucherlapati, M.H., Kucherlapati, R.S., Baylin, S., Cope, L., Danilova, L., Bootwalla, M.S., Lai, P.H., Maglinte, D.T., Berg, D.J.V.D., Weisenberger, D.J., Auman, J.T., Balu, S., Bodenheimer, T., Fan, C., Hoadley, K.A., Hoyle, A.P., Jefferys, S.R.,

Jones, C.D., Meng, S., Mieczkowski, P.A., Mose, L.E., Perou, A.H., Perou, C.M., Roach, J., Shi, Y., Simons, J.V., Skelly, T., Soloway, M.G., Tan, D., Veluvolu, U., Fan, H., Hinoue, T., Laird, P.W., Shen, H., Zhou, W., Bellair, M., Chang, K., Covington, K., Creighton, C.J., Dinh, H., Doddapaneni, H., Donehower, L.A., Drummond, J., Gibbs, R.A., Glenn, R., Hale, W., Han, Y., Hu, J., Korchina, V., Lee, S., Lewis, L., Li, W., Liu, X., Morgan, M., Morton, D., Muzny, D., Santibanez, J., Sheth, M., Shinbrot, E., Wang, L., Wang, M., Wheeler, D.A., Xi, L., Zhao, F., Hess, J., Appelbaum, E.L., Bailey, M., Cordes, M.G., Ding, L., Fronick, C.C., Fulton, L.A., Fulton, R.S., Kandoth, C., Mardis, E.R., McLellan, M.D., Miller, C.A., Schmidt, H.K., Wilson, R.K., Crain, D., Curley, E., Gardner, J., Lau, K., Mallery, D., Morris, S., Paulauskis, J., Penny, R., Shelton, C., Shelton, T., Sherman, M., Thompson, E., Yena, P., Bowen, J., Gastier-Foster, J.M., Gerken, M., Leraas, K.M., Lichtenberg, T.M., Ramirez, N.C., Wise, L., Zmuda, E., Corcoran, N., Costello, T., Hovens, C., Carvalho, A.L., Carvalho, A.C. de, Fregnani, J.H., Longatto-Filho, A., Reis, R.M., Scapulatempo-Neto, C., Silveira, H.C.S., Vidal, D.O., Burnette, A., Eschbacher, J., Hermes, B., Noss, A., Singh, R., Anderson, M.L., Castro, P.D., Ittmann, M., Huntsman, D., Kohl, B., Le, X., Thorp, R., Andry, C., Duffy, E.R., Lyadov, V., Paklina, O., Setdikova, G., Shabunin, A., Tavobilov, M., McPherson, C., Warnick, R., Berkowitz, R., Cramer, D., Feltmate, C., Horowitz, N., Kibel, A., Muto, M., Raut, C.P., Malykh, A., Barnholtz-Sloan, J.S., Barrett, W., Devine, K., Fulop, J., Ostrom, Q.T., Shimmel, K., Wolinsky, Y., Sloan, A.E., Rose, A.D., Giuliante, F., Goodman, M., Karlan, B.Y., Hagedorn, C.H., Eckman, J., Harr, J., Myers, J., Tucker, K., Zach, L.A., Deyarmin, B., Hu, H., Kvecher, L., Larson, C., Mural, R.J., Somiari, S., Vicha, A., Zelinka, T., Bennett, J., Iacocca, M., Rabeno, B., Swanson, P., Latour, M., Lacombe, L., Têtu, B., Bergeron, A., McGraw, M., Staugaitis, S.M., Chabot, J., Hibshoosh, H., Sepulveda, A., Su, T., Wang, T., Potapova, O., Voronina, O., Desjardins, L., Mariani, O., Roman-Roman, S., Sastre, X., Stern, M.-H., Cheng, F., Signoretti, S., Berchuck, A., Bigner, D., Lipp, E., Marks, J., McCall, S., McLendon, R., Secord, A., Sharp, A., Behera, M., Brat, D.J., Chen, A., Delman, K., Force, S., Khuri, F., Magliocca, K., Maithel, S., Olson, J.J., Owonikoko, T., Pickens, A., Ramalingam, S., Shin, D.M., Sica, G., Meir, E.G.V., Zhang, Hongzheng, Eijckenboom, W., Gillis, A., Korpershoek, E., Looijenga, L., Oosterhuis, W., Stoop, H., Kessel, K.E. van, Zwarthoff, E.C., Calatozzolo, C., Cuppini, L., Cuzzubbo, S., DiMeco, F., Finocchiaro, G., Mattei, L., Perin, A., Pollo, B., Chen, C., Houck, J., Lohavanichbutr, P., Hartmann, A., Stoehr, C., Stoehr, R., Taubert, H., Wach, S., Wullich, B., Kycler, W., Murawa, D., Wiznerowicz, M., Chung, K., Edenfield, W.J., Martin, J., Baudin, E., Bubley, G., Bueno, R., Rienzo, A.D., Richards, W.G., Kalkanis, S., Mikkelsen, T., Noushmehr, H., Scarpace, L., Girard, N., Aymerich, M., Campo, E., Giné, E., Guillermo, A.L., Bang, N.V., Hanh, P.T., Phu, B.D., Tang, Y., Colman, H., Evason, K., Dottino, P.R., Martignetti, J.A., Gabra, H., Juhl, H., Akeredolu, T., Stepa, S., Hoon, D., Ahn, K., Kang, K.J., Beuschlein, F., Breggia, A., Birrer, M., Bell, D., Borad, M., Bryce, A.H., Castle, E., Chandan, V., Cheville, J., Copland, J.A., Farnell, M., Flotte, T., Giama, N., Ho, T., Kendrick, M., Kocher, J.-P., Kopp, K., Moser, C., Nagorney, D., O'Brien, D., O'Neill, B.P., Patel, T., Petersen, G., Que, F., Rivera, M., Roberts, L., Smallridge, R., Smyrk, T., Stanton, M., Thompson, R.H., Torbenson, M., Yang, J.D., Zhang, L., Brimo, F., Ajani, J.A., Gonzalez, A.M.A., Behrens, C., Bondaruk, J., Broaddus, R., Czerniak, B., Esmaeli, B., Fujimoto, J., Gershenwald, J., Guo, C., Lazar, A.J., Logothetis, C., Meric-Bernstam, F., Moran, C., Ramondetta, L., Rice, D., Sood, A., Tamboli, P., Thompson, T., Troncoso, P., Tsao, A., Wistuba, I., Carter, C., Haydu, L., Hersey, P., Jakrot, V., Kakavand, H., Kefford, R., Lee, K., Long, G., Mann, G., Quinn, M., Saw, R., Scolyer, R., Shannon, K., Spillane, A., Stretch, J., Synott, M., Thompson, J., Wilmott, J., Al-Ahmadie, H., Chan, T.A., Ghossein, R., Gopalan, A., Levine, D.A., Reuter, V., Singer, S., Singh, B., Tien, N.V., Broudy, T., Mirsaidi, C., Nair, P., Drwiega, P., Miller, J., Smith, J., Zaren, H., Park, J.-W., Hung, N.P., Kebebew, E., Linehan, W.M., Metwalli, A.R., Pacak, K., Pinto, P.A., Schiffman, M., Schmidt, L.S., Vocke, C.D., Wentzensen, N., Worrell, R., Yang, H., Moncrieff, M., Goparaju, C., Melamed, J., Pass,

H., Botnariuc, N., Caraman, I., Cernat, M., Chemencedji, I., Clipca, A., Doruc, S., Gorincioi, G., Mura, S., Pirtac, M., Stancul, I., Tcaciuc, D., Albert, M., Alexopoulou, I., Arnaout, A., Bartlett, J., Engel, J., Gilbert, S., Parfitt, J., Sekhon, H., Thomas, G., Rassl, D.M., Rintoul, R.C., Bifulco, C., Tamakawa, R., Urba, W., Hayward, N., Timmers, H., Antenucci, A., Facciolo, F., Grazi, G., Marino, M., Merola, R., Krijger, R. de, Gimenez-Roqueplo, A.-P., Piché, A., Chevalier, S., McKercher, G., Birsoy, K., Barnett, G., Brewer, C., Farver, C., Naska, T., Pennell, N.A., Raymond, D., Schilero, C., Smolenski, K., Williams, F., Morrison, C., Borgia, J.A., Liptay, M.J., Pool, M., Seder, C.W., Junker, K., Omberg, L., Dinkin, M., Manikhas, G., Alvaro, D., Bragazzi, M.C., Cardinale, V., Carpino, G., Gaudio, E., Chesla, D., Cottingham, S., Dubina, M., Moiseenko, F., Dhanasekaran, R., Becker, K.-F., Janssen, K.-P., Slotta-Huspenina, J., Abdel-Rahman, M.H., Aziz, D., Bell, S., Cebulla, C.M., Davis, A., Duell, R., Elder, J.B., Hilty, J., Kumar, B., Lang, J., Lehman, N.L., Mandt, R., Nguyen, P., Pilarski, R., Rai, K., Schoenfield, L., Senecal, K., Wakely, P., Hansen, P., Lechan, R., Powers, J., Tischler, A., Grizzle, W.E., Sexton, K.C., Kastl, A., Henderson, J., Porten, S., Waldmann, J., Fassnacht, M., Asa, S.L., Schadendorf, D., Couce, M., Graefen, M., Huland, H., Sauter, G., Schlomm, T., Simon, R., Tennstedt, P., Olabode, O., Nelson, M., Bathe, O., Carroll, P.R., Chan, J.M., Disaia, P., Glenn, P., Kelley, R.K., Landen, C.N., Phillips, J., Prados, M., Simko, J., Smith-McCune, K., VandenBerg, S., Roggin, K., Fehrenbach, A., Kendler, A., Sifri, S., Steele, R., Jimeno, A., Carey, F., Forgie, I., Mannelli, M., Carney, M., Hernandez, B., Campos, B., Herold-Mende, C., Jungk, C., Unterberg, A., Deimling, A. von, Bossler, A., Galbraith, J., Jacobus, L., Knudson, M., Knutson, T., Ma, D., Milhem, M., Sigmund, R., Godwin, A.K., Madan, R., Rosenthal, H.G., Adebamowo, C., Adebamowo, S.N., Boussioutas, A., Beer, D., Giordano, T., Mes-Masson, A.-M., Saad, F., Bocklage, T., Landrum, L., Mannel, R., Moore, K., Moxley, K., Postier, R., Walker, J., Zuna, R., Feldman, M., Valdivieso, F., Dhir, R., Luketich, J., Pinero, E.M.M., Quintero-Aguilo, M., Carlotti, C.G., Santos, J.S.D., Kemp, R., Sankarankuty, A., Tirapelli, D., Catto, J., Agnew, K., Swisher, E., Creaney, J., Robinson, B., Shelley, C.S., Godwin, E.M., Kendall, S., Shipman, C., Bradford, C., Carey, T., Haddad, A., Moyer, J., Peterson, L., Prince, M., Rozek, L., Wolf, G., Bowman, R., Fong, K.M., Yang, I., Korst, R., Rathmell, W.K., Fantacone-Campbell, J.L., Hooke, J.A., Kovatich, A.J., Shriver, C.D., DiPersio, J., Drake, B., Govindan, R., Heath, S., Ley, T., Tine, B.V., Westervelt, P., Rubin, M.A., Lee, J.I., Aredes, N.D., Mariamidze, A., Cherniack, A.D., Beroukhim, R., Meyerson, M., 2018. Genomic and Functional Approaches to Understanding Cancer Aneuploidy. Cancer Cell 33, 676-689.e3. https://doi.org/10.1016/j.ccell.2018.03.007

Terakawa, T., Bisht, S., Eeftens, J.M., Dekker, C., Haering, C.H., Greene, E.C., 2017. The condensin complex is a mechanochemical motor that translocates along DNA. Science 358, 672–676. https://doi.org/10.1126/science.aan6516

Thu, Y.M., Van Riper, S.K., Higgins, L., Zhang, T., Becker, J.R., Markowski, T.W., Nguyen, H.D., Griffin, T.J., Bielinsky, A.K., 2016. Slx5/Slx8 Promotes Replication Stress Tolerance by Facilitating Mitotic Progression. Cell Rep 15, 1254–1265. https://doi.org/10.1016/j.celrep.2016.04.017

Tipton, A.R., Wang, K., Link, L., Bellizzi, J.J., Huang, H., Yen, T., Liu, S.-T., 2011. BUBR1 and closed MAD2 (C-MAD2) interact directly to assemble a functional mitotic checkpoint complex. J Biol Chem 286, 21173–21179. https://doi.org/10.1074/jbc.M111.238543

Titos, I., Ivanova, T., Mendoza, M., 2014. Chromosome length and perinuclear attachment constrain resolution of DNA intertwines. J. Cell Biol. 206, 719–733. https://doi.org/10.1083/jcb.201404039

Tomson, B.N., D'Amours, D., Adamson, B.S., Aragon, L., Amon, A., 2006. Ribosomal DNA transcription-dependent processes interfere with chromosome segregation. Mol. Cell. Biol.

26, 6239–6247. https://doi.org/10.1128/MCB.00693-06

Tomson, B.N., Rahal, R., Reiser, V., Monje-Casas, F., Mekhail, K., Moazed, D., Amon, A., 2009. Regulation of Spo12 phosphorylation and its essential role in the FEAR network. Curr. Biol. 19, 449–460. https://doi.org/10.1016/j.cub.2009.02.024

Torres-Rosell, J., De Piccoli, G., Cordon-Preciado, V., Farmer, S., Jarmuz, A., Machin, F., Pasero, P., Lisby, M., Haber, J.E., Aragón, L., 2007. Anaphase Onset Before Complete DNA Replication with Intact Checkpoint Responses. Science 315, 1411–1415. https://doi.org/10.1126/science.1134025

Torres-Rosell, J., Machín, F., Farmer, S., Jarmuz, A., Eydmann, T., Dalgaard, J.Z., Aragón, L., 2005. SMC5 and SMC6 genes are required for the segregation of repetitive chromosome regions. Nat Cell Biol 7, 412–419. https://doi.org/10.1038/ncb1239

Torres-Rosell, J., Machín, F., Jarmuz, A., Aragón, L., 2004. Nucleolar segregation lags behind the rest of the genome and requires Cdc14p activation by the FEAR network. Cell Cycle 3, 496–502.

Uemura, T., Ohkura, H., Adachi, Y., Morino, K., Shiozaki, K., Yanagida, M., 1987. DNA topoisomerase II is required for condensation and separation of mitotic chromosomes in S. pombe. Cell 50, 917–925. https://doi.org/10.1016/0092-8674(87)90518-6

Uemura, T., Tanagida, M., 1986. Mitotic spindle pulls but fails to separate chromosomes in type II DNA topoisomerase mutants: uncoordinated mitosis. EMBO J 5, 1003–1010.

Uemura, T., Yanagida, M., 1984. Isolation of type I and II DNA topoisomerase mutants from fission yeast: single and double mutants show different phenotypes in cell growth and chromatin organization. EMBO J 3, 1737–1744.

Uhlmann, F., 2016. SMC complexes: from DNA to chromosomes. Nat Rev Mol Cell Biol 17, 399–412. https://doi.org/10.1038/nrm.2016.30

Uhlmann, F., Lottspeich, F., Nasmyth, K., 1999. Sister-chromatid separation at anaphase onset is promoted by cleavage of the cohesin subunit Scc1. Nature 400, 37–42. https://doi.org/10.1038/21831

Uhlmann, F., Wernic, D., Poupart, M.-A., Koonin, E.V., Nasmyth, K., 2000. Cleavage of Cohesin by the CD Clan Protease Separin Triggers Anaphase in Yeast. Cell 103, 375–386. https://doi.org/10.1016/S0092-8674(00)00130-6

Umbreit, N.T., Zhang, C.-Z., Lynch, L.D., Blaine, L.J., Cheng, A.M., Tourdot, R., Sun, L., Almubarak, H.F., Judge, K., Mitchell, T.J., Spektor, A., Pellman, D., 2020. Mechanisms generating cancer genome complexity from a single cell division error. Science 368. https://doi.org/10.1126/science.aba0712

Unal, E., Arbel-Eden, A., Sattler, U., Shroff, R., Lichten, M., Haber, J.E., Koshland, D., 2004. DNA damage response pathway uses histone modification to assemble a double-strand break-specific cohesin domain. Mol Cell 16, 991–1002. https://doi.org/10.1016/j.molcel.2004.11.027

Unal, E., Heidinger-Pauli, J.M., Kim, W., Guacci, V., Onn, I., Gygi, S.P., Koshland, D.E., 2008. A molecular determinant for the establishment of sister chromatid cohesion. Science 321, 566–569. https://doi.org/10.1126/science.1157880

van de Pasch, L.A.L., Miles, A.J., Nijenhuis, W., Brabers, N.A.C.H., van Leenen, D., Lijnzaad, P., Brown, M.K., Ouellet, J., Barral, Y., Kops, G.J.P.L., Holstege, F.C.P., 2013. Centromere binding and a conserved role in chromosome stability for SUMO-dependent ubiquitin

ligases. PLoS ONE 8, e65628. https://doi.org/10.1371/journal.pone.0065628

van der Horst, A., Lens, S.M.A., 2014. Cell division: control of the chromosomal passenger complex in time and space. Chromosoma 123, 25–42. https://doi.org/10.1007/s00412-013-0437-6

Varela, E., Shimada, K., Laroche, T., Leroy, D., Gasser, S.M., 2009. Lte1, Cdc14 and MEN-controlled Cdk inactivation in yeast coordinate rDNA decompaction with late telophase progression. EMBO J 28, 1562–1575. https://doi.org/10.1038/emboj.2009.111

Vas, A.C.J., Andrews, C.A., Kirkland Matesky, K., Clarke, D.J., 2007. In Vivo Analysis of Chromosome Condensation in Saccharomyces cerevisiae. Mol Biol Cell 18, 557–568. https://doi.org/10.1091/mbc.E06-05-0454

Verzijlbergen, K.F., Nerusheva, O.O., Kelly, D., Kerr, A., Clift, D., de Lima Alves, F., Rappsilber, J., Marston, A.L., 2014. Shugoshin biases chromosomes for biorientation through condensin recruitment to the pericentromere. eLife 3, e01374. https://doi.org/10.7554/eLife.01374

Visintin, R., Craig, K., Hwang, E.S., Prinz, S., Tyers, M., Amon, A., 1998. The phosphatase Cdc14 triggers mitotic exit by reversal of Cdk-dependent phosphorylation. Mol. Cell 2, 709–718.

Visintin, R., Hwang, E.S., Amon, A., 1999. Cfi1 prevents premature exit from mitosis by anchoring Cdc14 phosphatase in the nucleolus. Nature 398, 818–823. https://doi.org/10.1038/19775

Visintin, R., Prinz, S., Amon, A., 1997. CDC20 and CDH1: a family of substrate-specific activators of APC-dependent proteolysis. Science 278, 460–463.

Visintin, R., Stegmeier, F., Amon, A., 2003. The role of the polo kinase Cdc5 in controlling Cdc14 localization. Mol. Biol. Cell 14, 4486–4498. https://doi.org/10.1091/mbc.E03-02-0095

Vos, S.M., Tretter, E.M., Schmidt, B.H., Berger, J.M., 2011. All tangled up: how cells direct, manage and exploit topoisomerase function. Nat. Rev. Mol. Cell Biol. 12, 827–841. https://doi.org/10.1038/nrm3228

Waizenegger, I.C., Hauf, S., Meinke, A., Peters, J.-M., 2000. Two Distinct Pathways Remove Mammalian Cohesin from Chromosome Arms in Prophase and from Centromeres in Anaphase. Cell 103, 399–410. https://doi.org/10.1016/S0092-8674(00)00132-X

Wang, B.-D., Yong-Gonzalez, V., Strunnikov, A.V., 2004. Cdc14p/FEAR pathway controls segregation of nucleolus in S. cerevisiae by facilitating condensin targeting to rDNA chromatin in anaphase. Cell Cycle 3, 960–967. https://doi.org/10.4161/cc.3.7.1003

Wang, L.H.-C., Mayer, B., Stemmann, O., Nigg, E.A., 2010. Centromere DNA decatenation depends on cohesin removal and is required for mammalian cell division. J Cell Sci 123, 806–813. https://doi.org/10.1242/jcs.058255

Wang, L.H.-C., Schwarzbraun, T., Speicher, M.R., Nigg, E.A., 2008. Persistence of DNA threads in human anaphase cells suggests late completion of sister chromatid decatenation. Chromosoma 117, 123–135. https://doi.org/10.1007/s00412-007-0131-7

Wang, Y., Ng, T.-Y., 2006. Phosphatase 2A negatively regulates mitotic exit in Saccharomyces cerevisiae. Mol Biol Cell 17, 80–89. https://doi.org/10.1091/mbc.e04-12-1109

Watt, P.M., Louis, E.J., Borts, R.H., Hickson, I.D., 1995. Sgs1: A eukaryotic homolog of E. coil

RecQ that interacts with topoisomerase II in vivo and is required for faithful chromosome segregation. Cell 81, 253–260. https://doi.org/10.1016/0092-8674(95)90335-6

Wechsler, T., Newman, S., West, S.C., 2011. Aberrant chromosome morphology in human cells defective for Holliday junction resolution. Nature 471, 642–646. https://doi.org/10.1038/nature09790

Wei-Shan, H., Amit, V.C., Clarke, D.J., 2019. Cell cycle regulation of condensin Smc4. Oncotarget 10, 263–276. https://doi.org/10.18632/oncotarget.26467

West, R.W., Yocum, R.R., Ptashne, M., 1984. Saccharomyces cerevisiae GAL1-GAL10 divergent promoter region: location and function of the upstream activating sequence UASG. Mol Cell Biol 4, 2467–2478. https://doi.org/10.1128/mcb.4.11.2467-2478.1984

Wild, P., Matos, J., 2016. Cell cycle control of DNA joint molecule resolution. Current Opinion in Cell Biology, Cell nucleus 40, 74–80. https://doi.org/10.1016/j.ceb.2016.02.018

Wilkins, B.J., Rall, N.A., Ostwal, Y., Kruitwagen, T., Hiragami-Hamada, K., Winkler, M., Barral, Y., Fischle, W., Neumann, H., 2014. A cascade of histone modifications induces chromatin condensation in mitosis. Science 343, 77–80. https://doi.org/10.1126/science.1244508

Wyatt, H.D.M., Laister, R.C., Martin, S.R., Arrowsmith, C.H., West, S.C., 2017. The SMX DNA Repair Tri-nuclease. Mol. Cell 65, 848-860.e11. https://doi.org/10.1016/j.molcel.2017.01.031

Wyatt, H.D.M., Sarbajna, S., Matos, J., West, S.C., 2013. Coordinated actions of SLX1-SLX4 and MUS81-EME1 for Holliday junction resolution in human cells. Mol. Cell 52, 234–247. https://doi.org/10.1016/j.molcel.2013.08.035

Wyatt, H.D.M., West, S.C., 2014. Holliday junction resolvases. Cold Spring Harb Perspect Biol 6, a023192. https://doi.org/10.1101/cshperspect.a023192

Xu, S., Huang, H.K., Kaiser, P., Latterich, M., Hunter, T., 2000. Phosphorylation and spindle pole body localization of the Cdc15p mitotic regulatory protein kinase in budding yeast. Curr Biol 10, 329–332. https://doi.org/10.1016/s0960-9822(00)00382-1

Yamagishi, Y., Yang, C.-H., Tanno, Y., Watanabe, Y., 2012. MPS1/Mph1 phosphorylates the kinetochore protein KNL1/Spc7 to recruit SAC components. Nat Cell Biol 14, 746–752. https://doi.org/10.1038/ncb2515

Yellman, C.M., Burke, D.J., 2006. The role of Cdc55 in the spindle checkpoint is through regulation of mitotic exit in Saccharomyces cerevisiae. Mol Biol Cell 17, 658–666. https://doi.org/10.1091/mbc.e05-04-0336

Yoshida, M.M., Ting, L., Gygi, S.P., Azuma, Y., 2016. SUMOylation of DNA topoisomerase IIα regulates histone H3 kinase Haspin and H3 phosphorylation in mitosis. J Cell Biol 213, 665–678. https://doi.org/10.1083/jcb.201511079

Yoshida, S., Kono, K., Lowery, D.M., Bartolini, S., Yaffe, M.B., Ohya, Y., Pellman, D., 2006. Polo-like kinase Cdc5 controls the local activation of Rho1 to promote cytokinesis. Science 313, 108–111. https://doi.org/10.1126/science.1126747

Yoshida, S., Toh-e, A., 2002. Budding yeast Cdc5 phosphorylates Net1 and assists Cdc14 release from the nucleolus. Biochem Biophys Res Commun 294, 687–691. https://doi.org/10.1016/S0006-291X(02)00544-2

Zechiedrich, E.L., Cozzarelli, N.R., 1995. Roles of topoisomerase IV and DNA gyrase in DNA unlinking during replication in Escherichia coli. Genes Dev. 9, 2859–2869. https://doi.org/10.1101/gad.9.22.2859

Zegerman, P., Diffley, J.F.X., 2007. Phosphorylation of Sld2 and Sld3 by cyclin-dependent kinases promotes DNA replication in budding yeast. Nature 445, 281–285. https://doi.org/10.1038/nature05432

Zhang, J., Shi, X., Li, Y., Kim, B.-J., Jia, J., Huang, Z., Yang, T., Fu, X., Jung, S.Y., Wang, Y., Zhang, P., Kim, S.-T., Pan, X., Qin, J., 2008. Acetylation of Smc3 by Eco1 is required for S phase sister chromatid cohesion in both human and yeast. Mol. Cell 31, 143–151. https://doi.org/10.1016/j.molcel.2008.06.006

Zhiteneva, A., Bonfiglio, J.J., Makarov, A., Colby, T., Vagnarelli, P., Schirmer, E.C., Matic, I., Earnshaw, W.C., 2017. Mitotic post-translational modifications of histones promote chromatin compaction in vitro. Open Biol 7, 170076. https://doi.org/10.1098/rsob.170076

Acknowledgments

Clearly, I want to thank Rosella Visintin for supervising me during these four years and all the SEMM PhD school staff for giving me this opportunity. I thank the AIRC foundation very much and Mr. Gerosa for the fellowship “Luigi, Antonietta and Gabriele Gerosa”. I extremely thank Daniel Fernandez-Perez of Pasini lab for the analysis of ChIP-seq data. I also would like to thank my advisors, Susanna Chiocca and Dimitris Liakopoulos, for their utmost scientific suggestions. Finally, I thank Ivan Psakhye and all Branzei lab for reagents.

I thank the Visintin lab members for their help, advices, and support inside and outside the lab. Special thanks to Eng. Alessandro Vetere for his help with the analysis of anaphase bridges.